THE UNIVERSITY
of EDINBURGH

Boronic acid speciation in Suzuki-Miyaura cross–coupling

THE UNIVERSITY *of* EDINBURGH

Katherine Geogheghan

Doctor of Philosophy

University of Edinburgh

2018

Declaration

I declare that the work in this thesis was carried by me under the supervision of Prof. Guy Lloyd-Jones FRS and is in accordance with the requirements of the University of Edinburgh. This work is original, except where indicated by special reference in the text, and no part of the dissertation has been previously submitted for any other academic award.

Signed …….

Date ……

Abstract

Since its discovery in 1979, the Suzuki-Miyaura (SM) reaction has become one of the most widely utilised tools for carbon-carbon bond formation. The palladium catalysed coupling of an organoboron and organohalide compounds proceeds through a three-stage mechanism of oxidative addition, transmetalation and reductive elimination. The transmetalation of boronic acids to a palladium(II) complex has been widely studied. However, very little is known about the transmetalation of boronic esters, which are commonly used as an alternative to unstable boronic acids. Whether these species undergo direct transmetalation or prior hydrolysis to the boronic acid under SM conditions remains unknown. This research aimed to elucidate the mechanism of this cross-coupling process.

Initial results under typical SM conditions created a biphasic reaction, promoted by the inorganic base and solvent composition, and showed that the boronic esters and corresponding boronic acid couple at the same absolute rate. This is thought to be a consequence of the formation of a biphasic mixture, rendering phase transfer the turnover-limiting step. The conditions were thus adapted to maintain a monophasic system using an organic soluble base, 2-*tert*-butyl-1,1,3,3-tetramethylguanidine, enabling the focus to be transmetalation as the turnover-limiting step. These new conditions show a significant difference in both reaction rate and induction period when using a boronic ester compared to the corresponding boronic acid.

The use of guanidine was also shown to have an interesting effect on the boronic acid/ester species by ^{19}F and ^{11}B NMR. Further studies found the use of guanidine to create a boronate species, with this species being an aryl trihydroxyboronate or the hydroxyl“ate”-complex of the boronic ester, depending on the presence of diol in the system. Formation of a boronate species was found to be crucial for efficient cross-coupling. When testing weaker bases, unable to form a boronate species, poor SM cross-coupling conversion was found using the newly developed phosphine-free guanidine conditions, showing the importance of the boronate species under these conditions. The results suggest that depending on the strength of base used, the pathway of transmetalation pathway can be switched, between the boronate pathway and the oxo-palladium pathway, under the specific conditions developed.

Lay Summary

The ability to join two simple compounds (starting materials) together to form complex products is called cross-coupling, and is invaluable in both industry and academia. A common method is to carry out this process is to use a palladium catalyst. Research into this area won the 2010 Nobel Prize in Chemistry, shared between three reactions; the Heck reaction, the Negishi reaction and the Suzuki-Miyaura reaction. From the three, research into the Suzuki-Miyaura reaction has flourished, as it offers mild conditions and the ability to coupling a wide range of compounds. Studies into how the process occurs have also been carried out and offer insight to the intricate details of the reaction, but despite extensive research, there still remain puzzles to be solved.

Typically, the Suzuki-Miyaura reaction is carried out in solution split into two phases, because of the use of an inorganic base. This research has developed conditions that does not cause phase separation, by using an organic base, keeping everything together in one homogenous solution. This has allowed in-depth study of the different compounds present throughout the reaction, and study of how the addition of extra compounds, such as alcohols, affect the reaction at hand.

Acknowledgements

Firstly, I would like to thank Professor Guy Lloyd-Jones for his advice, support and patience over the course of my PhD. His insight and guidance has been invaluable and I am incredibly grateful for the opportunity to be part of such a talented group.

I have been lucky enough to work with a fantastic group of wonderful and interesting individuals. Firstly, I would like to thank Team Boron, for taking me in when I joined the group and their continued support and friendship over the years; Dr Nick Taylor, Dr Paul Cox, Dr Jorge Gonzalez, Dr Alba Collado. Our meetings made all the difference to shaping my research and my confidence. Thanks to all Lloyd-Jones members, past and present; Dr Liam Ball, Dr Carl Poree, Dr Ruth Dooley, Dr Rob Cox, Dr Joe Tate, Dr Tom Corrie, Dr Alex Cresswell, Matthew Robinson, Dr Marc Reid, Dr Eric Keske, Magdalene Teh, Ariana Jones, Eduardo Nieto, Dr Craig Johnston, Alex Pagett, Dr Tom West, Dr Chris Nottingham, Dr Yuya Orito, Veronica Forcina, Harvey Dale and Hannah Hayes.

I would like to thank the McKeown group, for welcoming me with open arms as an honorary member and offering a sanctuary in times of need. I am truly grateful to all of you for helping me out.

I would like to thank my industrial supervisor Dr David Blakemore, and Pfizer, for valuable input and support throughout the project. Thanks to all the people at the University of Edinburgh that keep the department running, in particular Juraj Bella and Lorna Murray in the NMR facility.

Most importantly, I would like to thank my family, who have encouraged and believed in me every step of the way. Thank you for always looking after me and the hundreds of hours of phone calls over the years. Particularly to my mum and dad, for always welcoming me home, visiting me and looking out for me. And to my grandparents, for their continued love and support in everything I do. It means the world.

And finally Richard Kirk, for his love, guidance and unwavering confidence in me. He has been my rock for many years, though ups and downs and adventures together. You have kept me sane and kept me going, and I do not think I could have done this without you. Thank you for making this journey so wonderful.

Contents

Abbreviations

18-crown-6	1,4,7,10,13,16-hexaoxacyclooctadecane
Ar	Aryl
n-Bu	Butyl
n-BuLi	*n*-Butyllithium
t-Bu	Tertiary butyl
$CDCl_3$	Deuterated chloroform
DABCO	1,4-Diazabicyclo[2.2.2]octane
DBU	1,8-Diazabicyclo[5.4.0]undec-7-ene
DCM	Dichloromethane
DFT	Density functional theory
DMAP	4-Dimethylaminopyridine
DMAN (‘proton sponge’)	1,8-Bis(dimethyl-amino)naphthalene
DMSO	Dimethyl sulfoxide
Et	Ethyl
EtOH	Ethanol
ESI-MS	Electrospray ionization mass spectrometry
Me	Methyl
MeOH	Methanol
MIDA	*N*-methylimidodiacetic acid
m.p.	Melting point
MS	Mass spectrometry
MTBD	7-Methyl-1,5,7-triazabicyclo[4.4.0]dec-5-ene
NMR	Nuclear magnetic resonance

OMe	Ethoxy
Ph	Phenyl
PPh_3	Triphenylphosphine
RDS	Rate determining step
SM	Suzuki-Miyaura
THF	Tetrahydrofuran
TMG	1,1,3,3-Tetramethylguanidine **13**

Chapter 1

Introduction

1.1. Cross-coupling reactions

To form a carbon-carbon bond is one of the most useful techniques available to synthetic chemists.[1] A cross-coupling reaction generally refers to substitution of an aryl, vinyl or alkyl halide or pseudohalide with a nucleophile using a metal catalyst. The ability to form biaryls (Ar-Ar') is extremely important as they are predominant in natural products, and the pharmaceutical and agrochemical industries.[2]

There are a wide range of coupling reactions dating as early as the Wurtz homocoupling in 1855, **Scheme 1.1.1**.[3] The first example of a nickel/palladium catalysed cross-coupling with organic halides was the Kumada coupling, reported in 1972, **Scheme 1.1.1**.[4,5] Since then many other coupling reactions have been discovered allowing for an ever increasing scope of starting materials and creating a more diverse range of available products, **Scheme 1.1.2**.

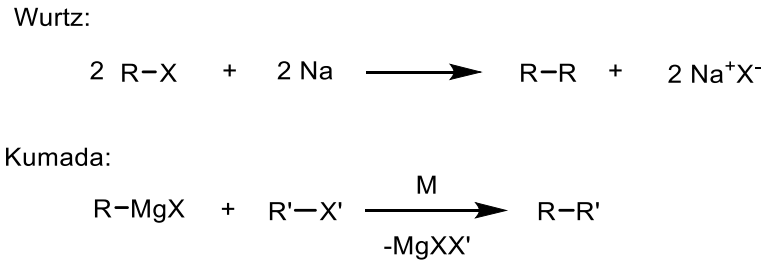

Scheme 1.1.1 – Wurtz and Kumada couplings

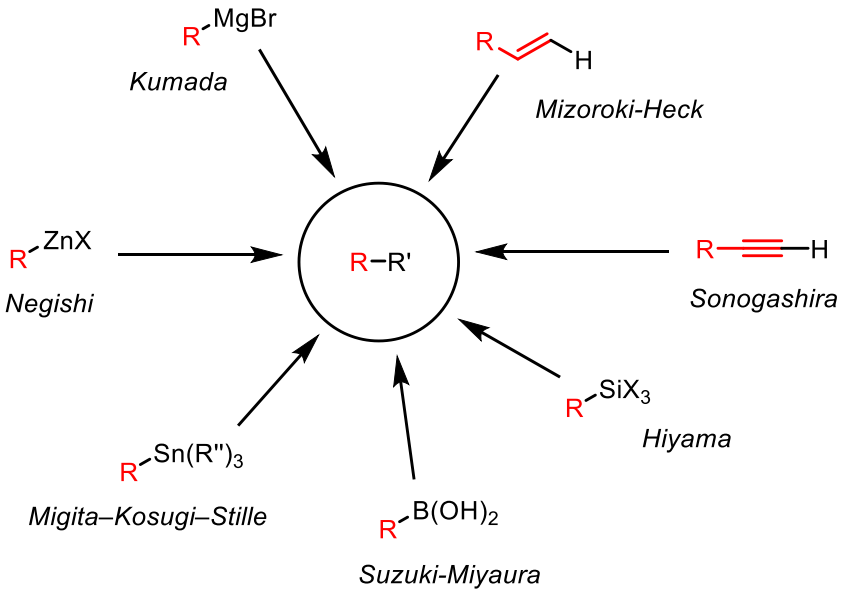

Scheme 1.1.2 – Range of different cross-coupling reactions

Palladium catalysts have been shown to be very effective, with the utility of these reactions demonstrated by the awarding of a Nobel Prize in Chemistry in 2010 to Richard F. Heck, Ei-ichi Negishi and Akira Suzuki, for the development of palladium catalysed cross-coupling reactions.[6] Advances in recent years have vastly improved the reaction scope and practicality, bringing metal-catalysed cross-coupling into the everyday repertoire of an organic chemist.

1.2. Suzuki-Miyaura

One of the most efficient and well known cross-coupling reactions is the Suzuki-Miyaura (SM) reaction, first published in 1979 by Norio Miyaura, Kinji Yamada, and Akira Suzuki.[7] This palladium catalysed coupling is carried out in the presence of base, to combine an organoboron and organohalide species to form a biaryl through the formation of a new C–C bond. **Scheme 1.2.1**.

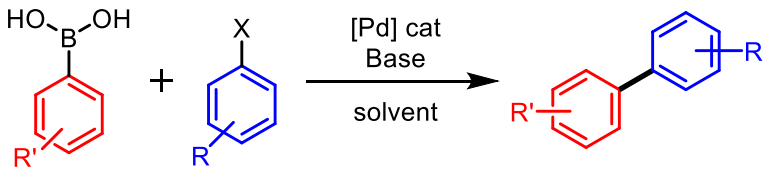

Scheme 1.2.1 – Generic SM cross-coupling reaction to form a biaryl

While other couplings such as Negishi,[8,9] Stille[9,10] and Himaya[11] can form C–C bonds, the SM reaction provides several advantages and research into this coupling has grown dramatically over recent decades.[12] The popularity of this cross-coupling is due to its exceptional functional group tolerance, relatively benign starting materials and by-products, high chemoselectivity and scalability.[13–17] Toxicity issues are a concern with other couplings, such as the Stille reaction which uses toxic tin reagents, giving a major drawback in terms of scalability.[9] The SM reaction has also been shown to be both air and moisture tolerant, as well as being able to couple at low temperatures and in a range of solvents, including water, giving it the advantage of mild reaction conditions.[16,18]

Recent advances have enabled the coupling of challenging reagents, such as aryl chlorides[19] and sterically hindered substrates,[20] as well as creating milder reaction conditions, by lowering catalyst loading and temperature.[21–25]

1.2.1. Boronic acids

The most commonly used SM organoboron reagents are boronic acids, which are often commercially available or relatively easy to synthesise and isolate, and generally air and moisture stable.[9,17,26] The use of boronic acids also aids purification of the cross-coupling product, as the by-product, boric acid, can be easily removed by aqueous base extraction.[9]

While the use of organoboron reagents offers several advantages, it also gives this reaction its major disadvantages – decomposition to unwanted side products.[16] Due to the vacant p-orbital on the boron, **Fig 1.2.1**, boronic acids often decompose *in situ*, giving varying amounts of protodeboronation, as just one example. The different side products will be discussed further in **Section 1.2.3**. Boronic acids have high affinity of water due to this vacant p-orbital, forming an equilibrium between the boronic acid and a tetrahedral boronate species with the release of a hydronium ion (H^+), **Scheme 1.2.2**.

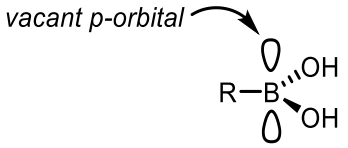

Fig 1.2.1 – Trigonal planar structure of boronic acids, with vacant p-orbital

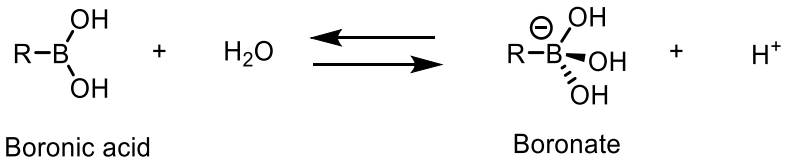

Scheme 1.2.2 – Boronate formation

Another issue with boronic acids is that they exist in equilibrium with the trimeric cyclic anhydride boroxine, **Scheme 1.2.3**.[27] This makes it difficult to determine the relative amounts of boronic acid/boroxine in a mixture, so the common solution is to add excess boronic acid to ensure full conversion of the aryl halide, but this is extremely inefficient. Boronic acid derivatives offer a solution to this problem and will be discussed further in **Section 1.2.4**.

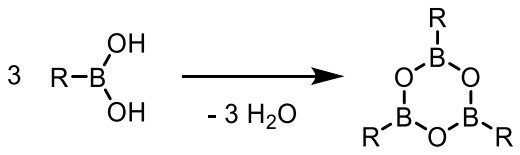

Scheme 1.2.3 – Boronic acid/boroxine equilibrium

A study of the relative reactivity of different aromatic boronic acids found electron-donating groups in the *para*-position to be more reactive, **Scheme 1.2.4, Fig 1.2.2**.[26] This is explained by the fact that increasing the electron-donating ability of the *para*-substituent increases the nucleophilicity of the boronic acid, making it more reactive toward SM cross-coupling.[28]

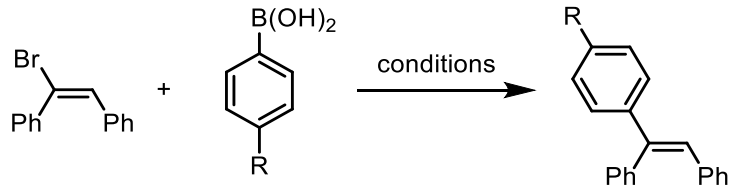

Scheme 1.2.4 – Study of substituent effects on SM cross-coupling of (*E*)-bromostilbene with phenyl boronic acids. R = OMe, Me, H, Cl, CF_3. Conditions = 1 equiv. (*E*)-bromostilbene, 1 equiv. boronic acid, 1.5 equiv. tetradecane, 1:1 methanol/THF, 2 equiv. KOH, 0.5 mol% $Pd(OAc)_2$ (0.5 mol%)/PPh_3 (1 mol%), 25 °C.

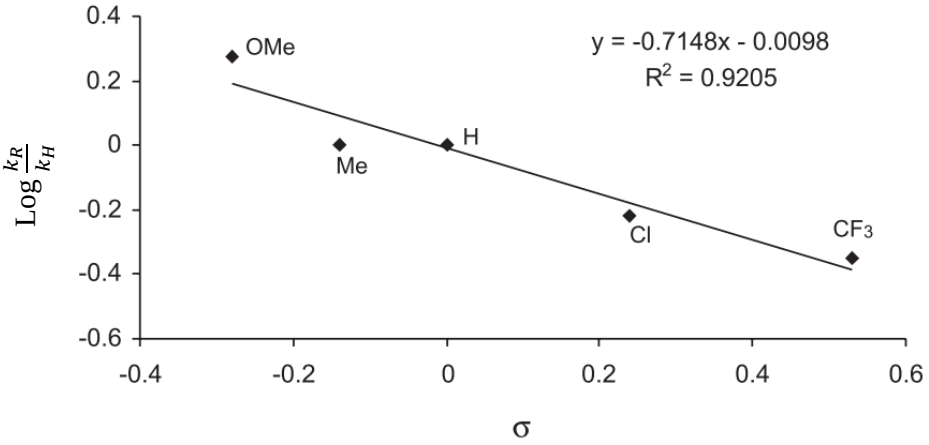

Fig 1.2.2 – Study of substituent effects on SM cross-coupling of (*E*)-bromostilbene with phenyl boronic acids, **Scheme 1.2.4**.

1.2.2. Mechanism

The general mechanism of the SM reaction involves three major steps in the catalytic cycle; oxidative addition (OA), transmetalation (TM) and reductive elimination (RE), **Scheme 1.2.5**. These reactions are often carried out with a palladium (II) pre-catalyst,[29] due to their increased stability relative to palladium(0) catalysts which can undergo decomposition when stored, making *in situ* catalyst activation to a palladium(0) species the first step of the reaction. The true mechanism of the SM reaction has been an area of controversy for many years and remains so to this day.[30–32] While the oxidative addition and reductive elimination steps, which are

present in several other couplings, have been reasonably well studied the debate continues as to how the transmetalation step of the cycle occurs. The difficulty in determining the true mechanism is also due to the dependence of different variables in the reaction, such as solvent, substrates and palladium ligands/phosphines. Each variable can greatly affect the most favoured mechanism, as various pathways have been shown to be possible.[29]

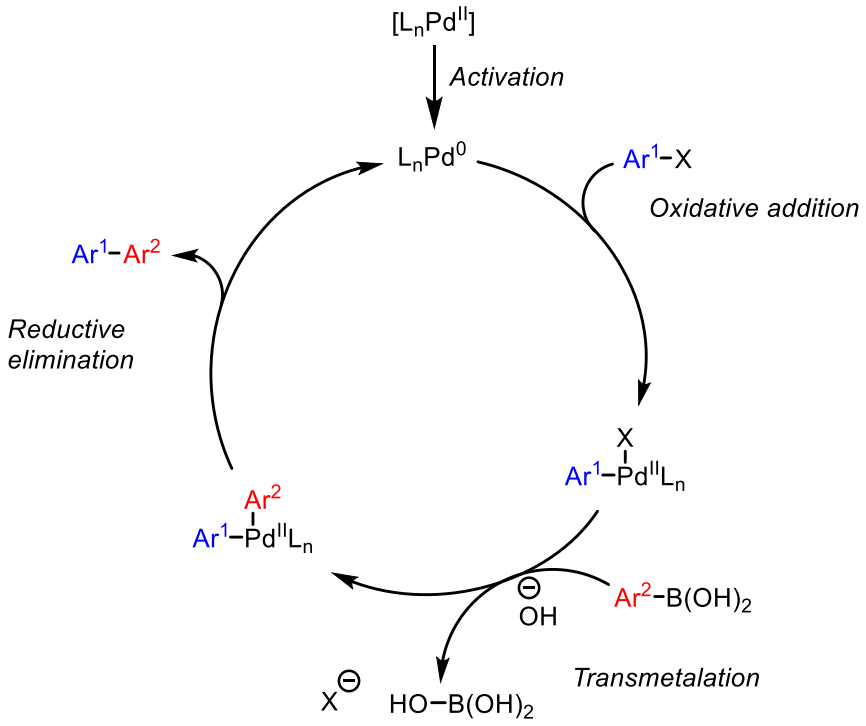

Scheme 1.2.5 – General mechanism for SM cross-coupling reaction

1.2.2.1. Catalyst

The active catalyst is generally assumed to be a 14-electron Pd^0L_2 species, with common ligands being phosphines.[15] The number of ligands on palladium throughout the system has been studied using DFT calculations on a simple catalyst system, $Pd(PH_3)_2$.[29] This study showed that all steps in the cycle of a diphosphine system and monophosphine system have low energy barriers, so are all feasible processes at room temperature, or with minimal heating. The preferred pathway will depend on variables such as ligand, solvent, and substrate. A diphosphine system is likely for chelating ligands, whereas a monophosphine system is likely for bulky phosphines. However, as all steps for both processes can occur and provide points where the two can inter-cross between a monophosphine and diphosphine system, either by loss or gain of a phosphine ligand, the mechanism is likely a mixture of both pathways.

1.2.2.2. Oxidative Addition

In the OA step, the C–X bond of the aryl halide is broken and the palladium is oxidised, generating a palladium(II) intermediate. Depending on the conditions and reagents used, the OA step of the cycle is known to be the rate determining step (RDS).[1,33] For aryl chloride in particular, OA is thought to be the RDS, however for aryl bromide and iodides it may not be the case.[34] The bond dissociation enthalpy of the aryl halide is proportional to the ease of OA: I > OTf > Br >> Cl, hence why this step is likely rate limiting for aryl chlorides. OA can be promoted by the addition of electron-withdrawing substituents to the aryl halide, weakening the C-X bond, or by using electron-rich ligands to create an electron-rich catalyst.

Two main mechanisms have been proposed for OA, **Scheme 1.2.6**.[1] The first involves simultaneous formation of both new bonds to palladium, Pd–C and Pd–X, in the transition state *via* a concerted pathway. The second is a dissociative process, where the carbon is first attacked by palladium, creating a cationic species, followed by recombination of the two charged species.

A DFT study has found theoretical evidence for the dissociative route in solution, when studying a palladium centre containing bidentate phosphines.[35] Schoeneback *et al*. also conducted a DFT study and report finding the concerted transition state in polar solvents, disproving earlier suggestions that the concerted transition states would not exist in solution.[36] Studies on how the structure of the phosphine ligand affect OA found that hindered phosphines ($P(1\text{-nathyl})_3$) promote a concerted mechanism, whereas less hindered phosphines (PPh_3) favour the dissociative route.[1,37]

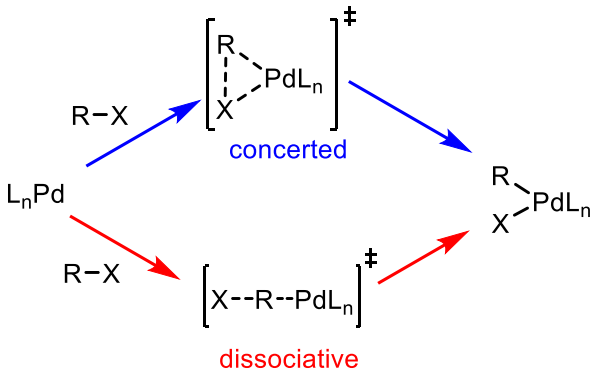

Scheme 1.2.6 – Two proposed reaction pathways for OA

OA of an organic halide to a Pd^0L_2 species produces a *cis* complex.[29] It is often assumed that this complex undergoes isomerisation to the *trans* isomer prior to TM. However, a computational study by Maseras *et al.* in 2006 showed the *trans* TM pathway to have a higher energy barrier than the *cis*, in a system where palladium contained two phosphine ligands, **Scheme 1.2.7**.[29] While the system studied used model phosphine ligands lacking steric bulk, it does suggest that the *trans* diphosphine species may not be the reactive species in all cases.

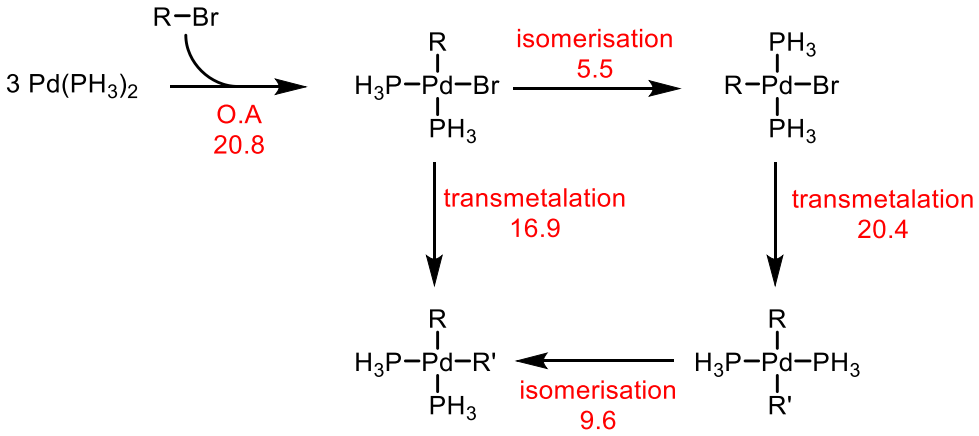

Scheme 1.2.7 – Proposed mechanism for OA with two phosphine ligands, with energy barriers shown in kcal/mol

1.2.2.3. Transmetalation

The TM step is where the organic moiety is transferred from boron to palladium, and can also be the RDS of the reaction.[38] Organoboron reagents are reported to undergo rapid transmetalation, and while this offers another advantage to this powerful reaction, it has made elucidating the dominant pathway an on-going puzzle.[39] TM involves a three-coordinate boron species which undergoes association with a fourth ligand to generate a four-coordinate complex. Depending on the source of this fourth ligand, there are two possible pathways by which transmetalation can occur; the oxo-palladium pathway and the boronate pathway, **Scheme 1.2.8**.[14,17,38–40,32,41,42,31]

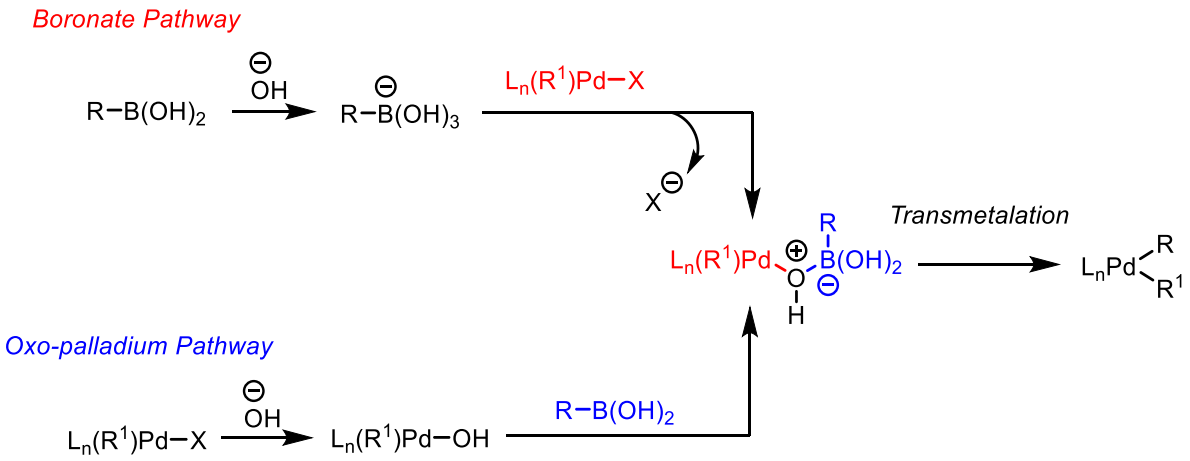

Scheme 1.2.8 – Two TM pathways

The boronate pathway involves hydroxide ion association to the three-coordinate boronic acid species to generate a boronate complex, which could then react with the organopalladium(II) species to generate a Pd-O-B linked intermediate. In the alternative route, the halide ligand on the palladium is exchanged for a hydroxide ligand to form an oxo-palladium species, which can then act as a Lewis base toward the neutral three-coordinate boron species, generating the same Pd-O-B linked intermediate.

Both pathways depend on the role of the base. The presence of base, usually inorganic, has been shown to be critical for efficient coupling, but the precise role of the base is still unclear.[1,14,26,29,34,40,32,41,42]. Three roles of the base have been reported: formation of the oxo-palladium species, formation of the boronate species, and promotion of reductive elimination.[34,38,42,43] While promotion of reductive elimination is always advantageous, only one of the other two roles will lead to productive catalysis, either the oxo-palladium species or the boronate species, but not both.

As both pathways form the same intermediate, the kinetically active boron and palladium intermediates must be found to determine the dominate pathway. But these species are often at very low relative concentrations, making detection difficult, giving rise to many conflicting studies.[32]

Boronate pathway

An early study by Canary *et al.* used electrospray ionisation mass spectrometry (ESI-MS) to study the catalytic intermediates from a series of SM coupling reactions, **Scheme 1.2.9**.[44] This study observed pyridyl palladium(II) complexes in two forms, $[(pyrH)Pd(PPh_3)_2Br]^+$ or $[(pyr)Pd(PPh_3)_2]^+$, as well as the biaryl palladium(II) species, $[(pyrH)(R_1R_2C_6H_3)Pd(PPh_3)_2]^+$. The corresponding oxo-palladium species were not observed. Not only does this study confirm the presences of key intermediates, it also shows that TM is not the turnover limiting step in the reaction. If this were the case, the predominant intermediate detected would be from the oxidative addition step, yet the post-transmetalation biaryl palladium species is observed.

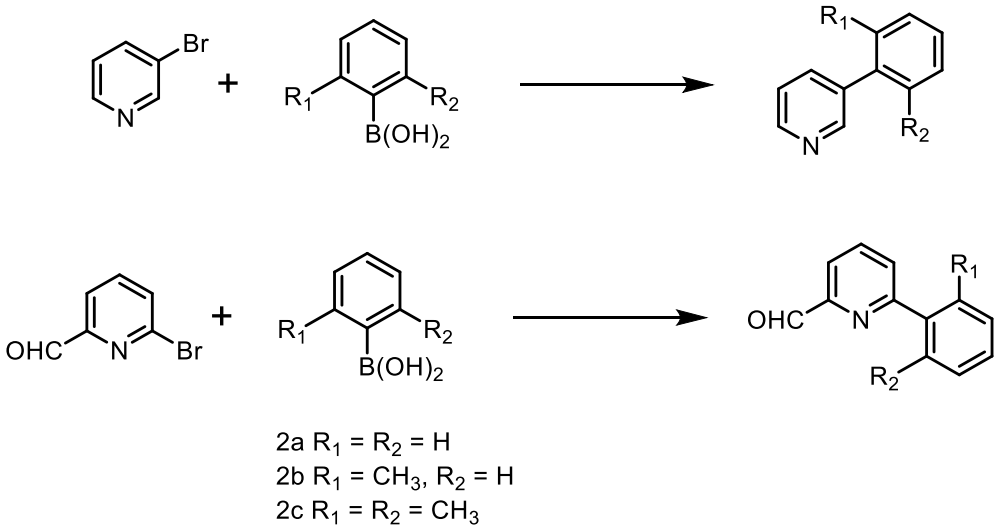

Scheme 1.2.9 – ESI-MS study by Canary *et al*. To a stirred solution of 3.9 x 10^{-4} mol aryl halide and 1.2 x 10^{-5} $Pd(PPh_3)_4$ in 2 mL toluene, 1 mL of 2 M Na_2CO_3 and 4.8 x 10^{-4} mol aryl boronic acid in 0.5 mL methanol was added. Carried out under nitrogen, in an oil bath at 80 °C with vigorous stirring.[44]

A 2005 paper from Maseras *et al*. investigated the different TM pathways, as well as the mechanism without the addition of base, of SM cross-couplings involving vinyl groups using DFT calculations.[14] The first path investigated was the direct reaction between the boronic acid and palladium halide without the addition of base, **Scheme 1.2.10 – Path 0**. The energy profile showed the direct transmetalation to be too energy demanding to occur without the addition of base, with an uphill, endothermic reaction profile and an energetic difference of 31.6 kcal/mol between reactants and products. Investigation into the formation of the organoboronate species, **Scheme 1.2.10 – Path A**, found the formation of the organoboronate species, from boronic acid and base, to be practically barrierless – only 2.7 kcal/mol. The

reaction of this organoboronate species with the palladium halide was then found to be a feasible mechanism, with facile replacement of the halide by the boronate species in the coordination sphere of the catalyst. Looking at the oxo-palladium pathway, **Scheme 1.2.10 – Path B**, found that the base was unable to directly replace the halide in the coordination sphere of the catalyst. An alternative path where the base binds to a phosphine ligand first, then migrates to the palladium centre with release of halide was suggested and found to be viable computationally. However, this pathway would produce large amounts of phosphine oxidation, which is not observed in SM couplings experimentally. The final path investigated is the reaction from a preformed oxo-palladium species, without addition of base, **Scheme 1.2.10 – Path C**, which shows coupling to occur. But despite the efficiency of **Path C**, it does not support the oxo-palladium pathway (**Path B**), as **Path C** starts with an oxo ligand in the catalyst coordination sphere, allowing facile bond formation with the boronic acid. Hydroxide is unable to directly replace the halide to form the necessary oxo-palladium species, **Path B**. Therefore, this study concludes the main catalytic pathway must be **Path A**.

Further theoretical research into aryl coupling, more commonly used experimentally, gave similar results to that of vinyl coupling; that without base the reaction does not occur, and when base is present, it reacts first with the boronic acid – the boronate pathway, **Path A**.[15]

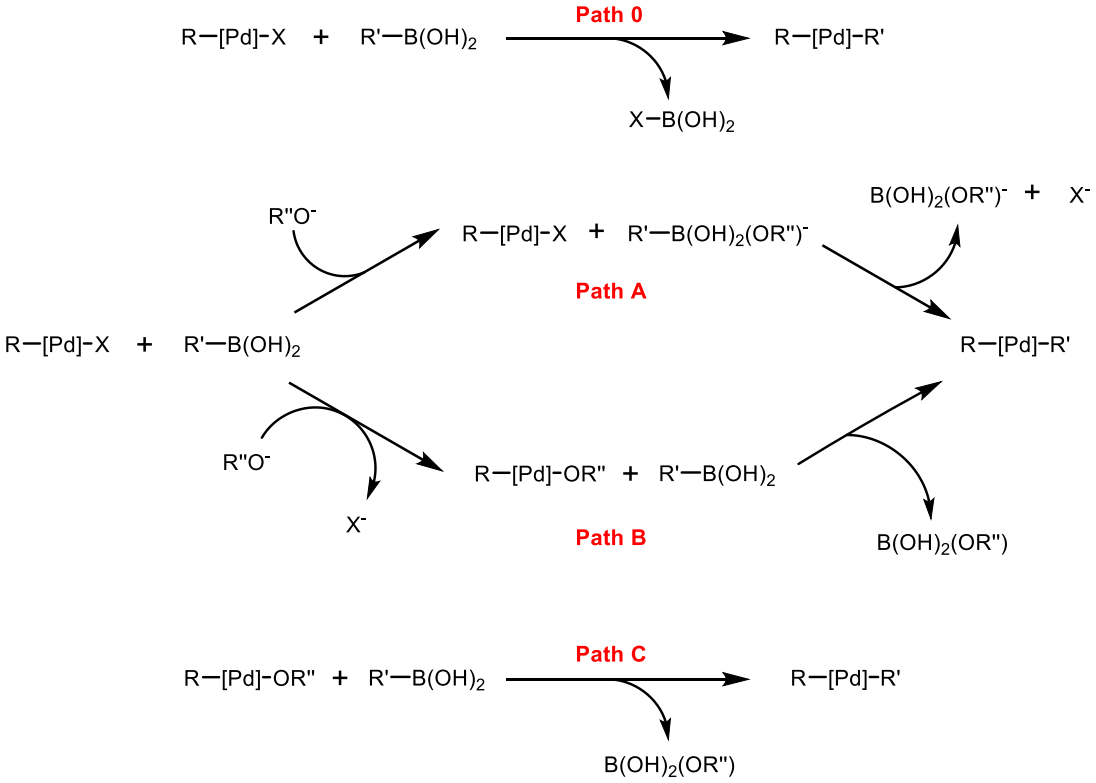

Scheme 1.2.10 – Different pathways investigated by Maseras.[14,15] Path 0 – direct reaction between the boronic acid and palladium halide without the addition of base. Path A – boronate pathway. Path B – oxo-palladium pathway. Path C – reaction of a preformed oxo-palladium complex with boronic acid.

Monteiro *et al*. also used ESI-MS to probe the intermediates in the SM reaction, specifically looking at the nature of the boron species before, during, and after the reaction.[26] Boronate species were found to form during the reaction, **Fig 1.2.3**, which the authors claim as evidence for the boronate pathway. However, the formation of these species does not definitively prove that the boronate is the reactive transmetalation species.

Organoboron	Species detected during reaction
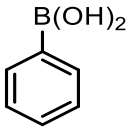	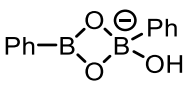 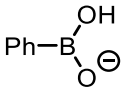

Fig 1.2.3 – Species found by ESI-MS in the reaction of organoboron (0.30 mmol) with (*E*)-bromostilbene (0.25 mmol), KOH (0.5 mmol), $Pd(OAc)_2$ (1.25 µmol), PPh_3 (2.5 µmol), MeOH (1.5 mL), THF (1.5 mL), 25 °C – dilution with water/acetonitrile mixture

Oxo-palladium pathway

Amatore and Jutand investigated the SM reaction using electrochemical techniques, starting from *trans*-[ArPdX$(PPh_3)_2$] complex – the product from OA, **Scheme 1.2.11**.[34] The base was found to have three roles in the reaction, two of which are productive; the formation of a reactive [ArPd(OH)$(PPh_3)_2$] species and unexpected acceleration of the RE step, and a competing negative role; the formation of an unreactive boronate species. The TM of [ArPd(OH)$(PPh_3)_2$] was found to be the RDS. This work also showed that high amounts of base do not necessarily promote greater reaction rates, as a result of the competing unreactive boronate formation.

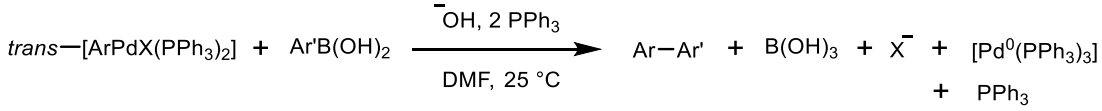

Scheme 1.2.11 – System studied by Amatore and Jutand

Hartwig *et al.* studied the TM step by looking at the relative rates of two separate stoichiometric reactions; isolated arylpalladium hydroxo complex and boronic acid in one case and isolated arylpalladium halide complex with trihydroxyborate in the other, **Scheme 1.2.12**.[38] At room temperature, both reactions were found to reach high yields within minutes. The temperature was therefore lowered (−40 °C) and the observed rate constants calculated, using ^{31}P NMR for the oxo-palladium pathway and activation parameters for the boronate pathway. The oxo-palladium pathway was found to have an observed rate constant of 2.4 x 10^{-3} s^{-1}, in comparison to a rate constant of 1.7 x 10^{-7} s^{-1} for the boronate pathway. This large difference in rate constants is reported to strongly support the oxo-palladium pathway as the main path for TM in the SM coupling. However, the point is made that this study represents a

system with a weak base, potassium carbonate, but if the base used was sufficiently strong, the boronate pathway could become competitive.

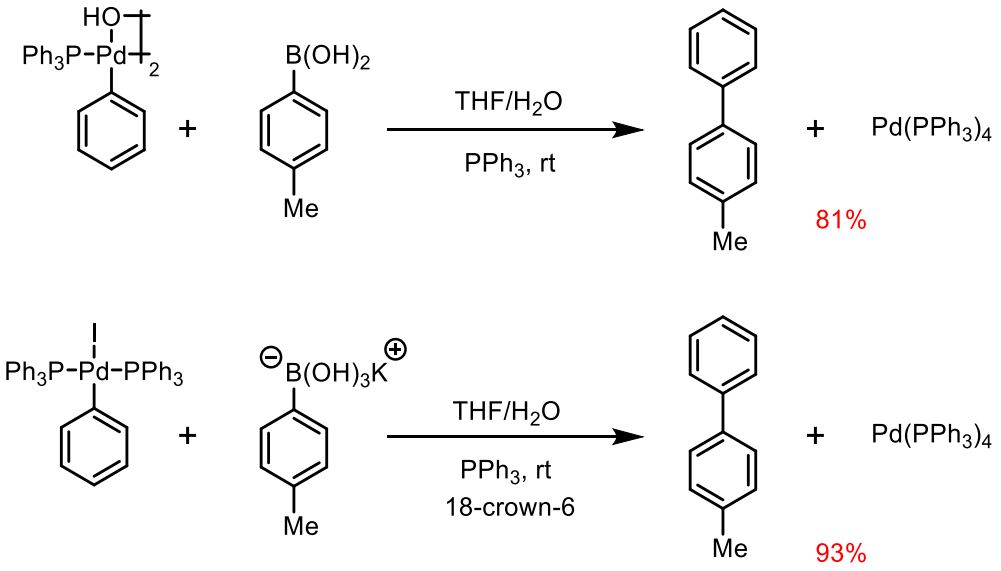

Scheme 1.2.12 – Two reactions studied by Hartwig *et al*. 50:1 THF/water

The debate as to which pathway occurs continues and is a difficult problem to solve as it is very dependent on specific reaction conditions. Both pathways have been shown to occur, using different methods and techniques, so the two may be competitive.[1]

While studies over the years have investigated the two pathways of transmetalation, the key intermediate containing the Pd-O-B linkage had not yet been observed or characterized. Recent advances by Denmark *et al.* have found evidence for the elusive transmetalation intermediates, using low temperature, rapid injection NMR spectroscopy and kinetic studies.[17,30]

Three key intermediates were found, all of which contain the Pd-O-B linkage.[17] The first was the formation of tricoordinate boron palladium(II) complex **A** via three independent routes, **Scheme 1.2.13**. The second was a tetracoordinate boron complex **B**, which required the use of a monoligated palladium complex to remove steric hinderance and allow saturation of the boron, **Scheme 1.2.14**. And the third was tetracoordinate boron complex **C**, formed from the reaction of complex **B** with boronic acid, **Scheme 1.2.15**. All species were then studied for their ability to undergo cross-coupling, and all were found to form the desired product, showing both tetracoordinate and tricoordinate examples are able to undergo efficient transmetalation.

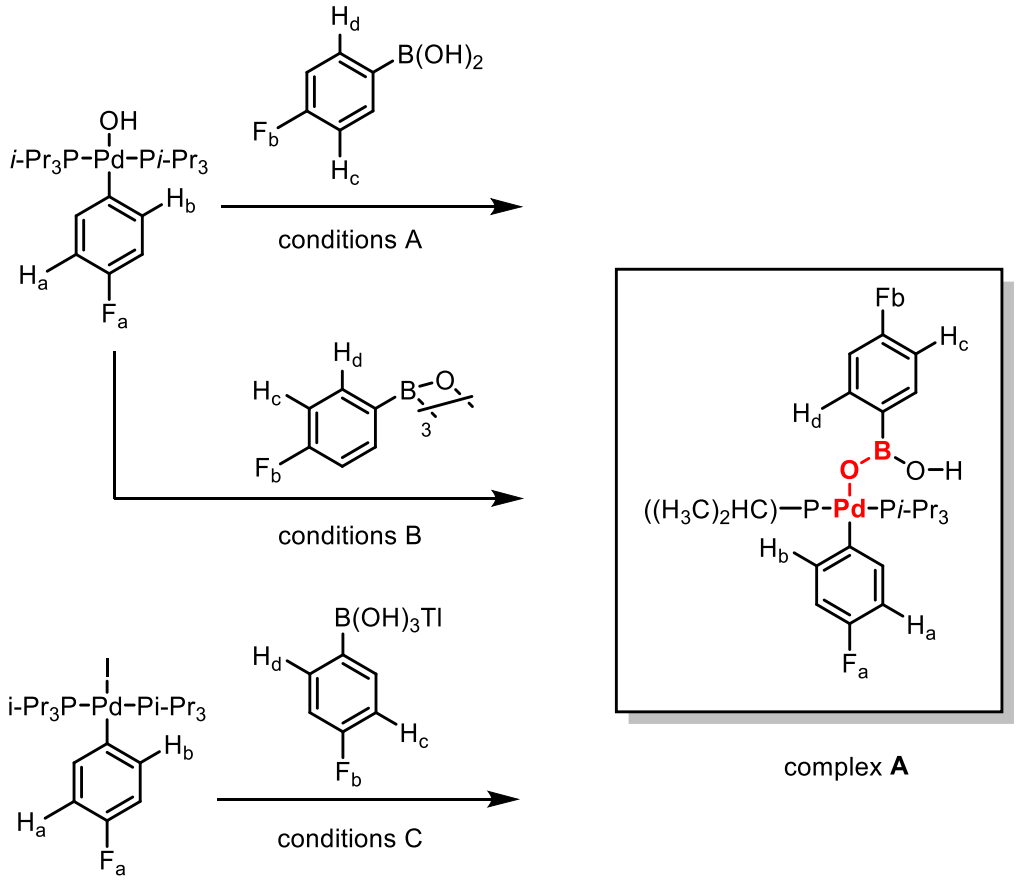

Scheme 1.2.13 – Formation of complex **A** – tricoordinate boron palladium(II) complex containing a Pd-O-B linkage. Conditions A: 1 equiv. boronic acid, −78 °C then −30 °C, 3h, 2 equiv. *i*-Pr_3P, THF-d_8, 100% conversion. Conditions B: 0.33 equiv. boroxine, −78 °C then −60 °C, 36h, 2 equiv. *i*-Pr_3P, THF-d_8, 50% conversion. Conditions C: 3 equiv. boronate, 1 equiv. dibenzo-22-crown-6, −78 °C then −30 °C, 3h, 1 equiv. *i*-Pr_3P, THF, 10% conversion.

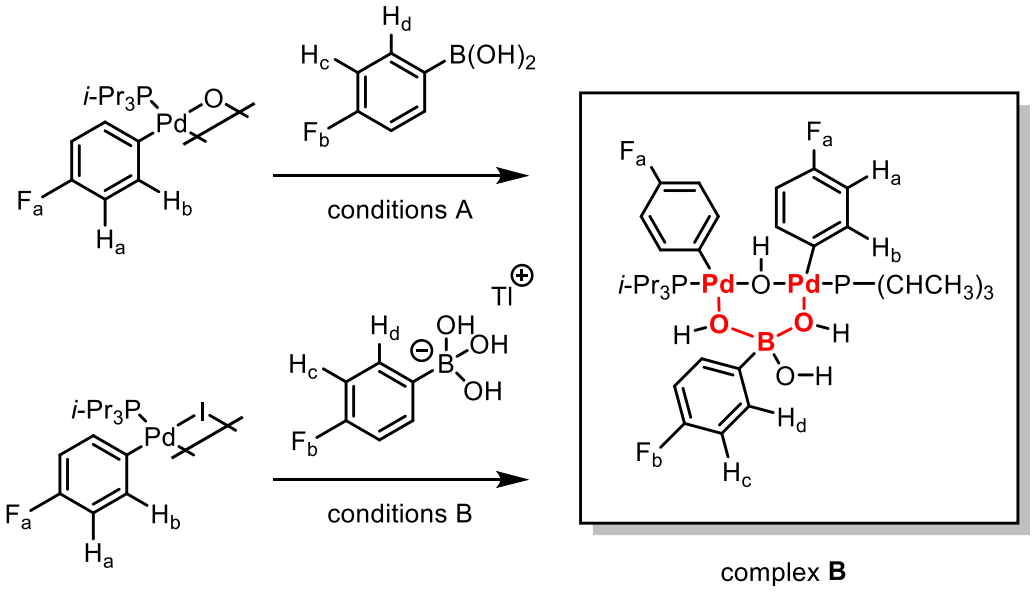

Scheme 1.2.14 – Formation of complex **B** – tetracoordinate boron complex. Conditions A: 1, 2 or 4 equiv. boronic acid, THF-d_8, −78 °C to −60 °C then −100 °C, 100% conversion. Conditions B: 3 equiv. boronate, THF-d_8, −78 °C to −50 °C for 1h then −100 °C, approx. 50% conversion.

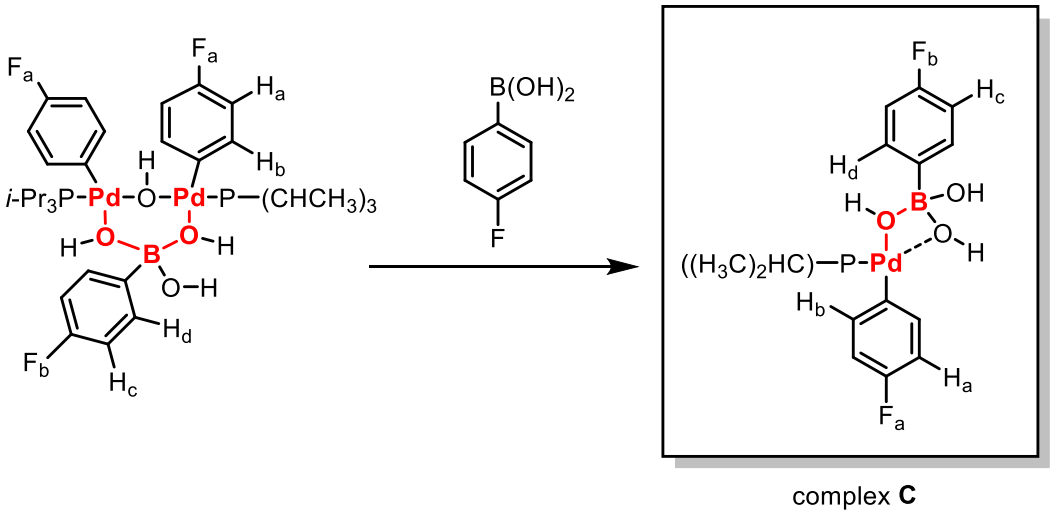

Scheme 1.2.15 – Formation of complex **C** – tetracoordinate boron complex. Conditions: 1 equiv. boronic acid, rapid injection CH_3OH, THF-d_8, −60 °C, 100% conversion,

1.2.2.4. Reductive elimination

To complete the catalytic cycle, generate the desired product and return to a Pd^0 species, reductive elimination must occur, **Scheme 1.2.16**. Isomerisation of the *trans* isomer to the *cis* is reported to occur prior to reductive elimination.[1,29,44] Base has been shown to promote the RE step, by addition of OH^- as a fifth ligand to the bis-aryl palladium complex, **Scheme 1.2.17**.[34] This negates the isomerisation to the *cis* complex, which is thermodynamically uphill.

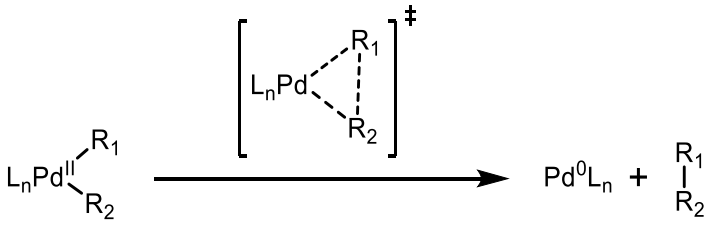

Scheme 1.2.16 – Concerted mechanism for RE

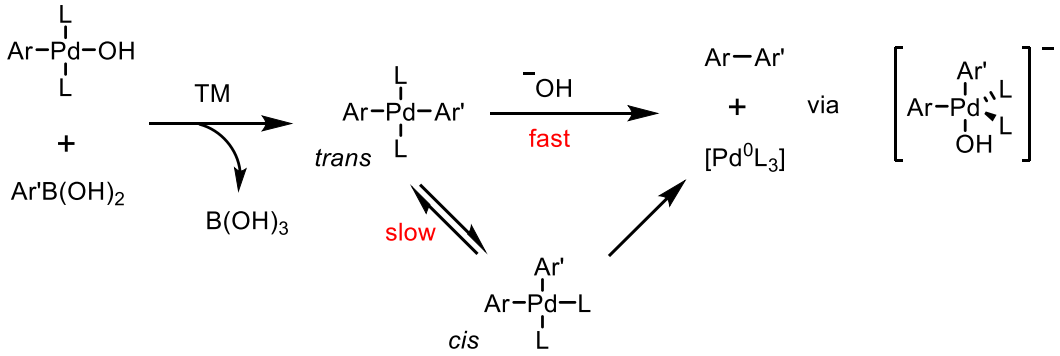

Scheme 1.2.17 – Base promoted RE

1.2.3. Side reactions

Protodeboronation, oxidative homocoupling and oxidation of the boronic acid are the major side reactions that plague SM couplings, all deriving from the boronic acid species, **Fig 1.2.4**.[16] Boronic acid homocoupling can also occur from pre-catalyst activation, **Scheme 1.2.18**. Side product formation creates several issues, such as difficulty in isolating the desired product, lower yield, and a waste of valuable starting material. The side products formed also have the potential to act as a catalyst poison, causing further damage to the reaction. Catalyst decomposition and protodehalogenation of the organohalide can also occur, and the varying degrees of side product formation depend heavily on the reaction conditions and starting components.

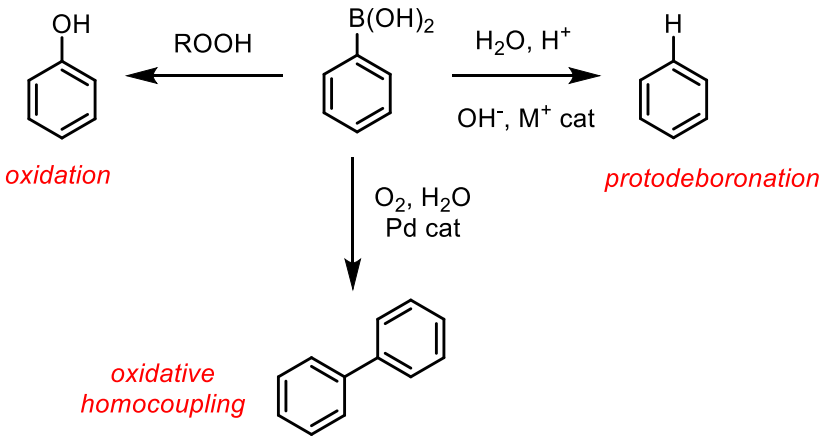

Fig 1.2.4 – The three common side products in the SM coupling, formed from the arylboronic acid

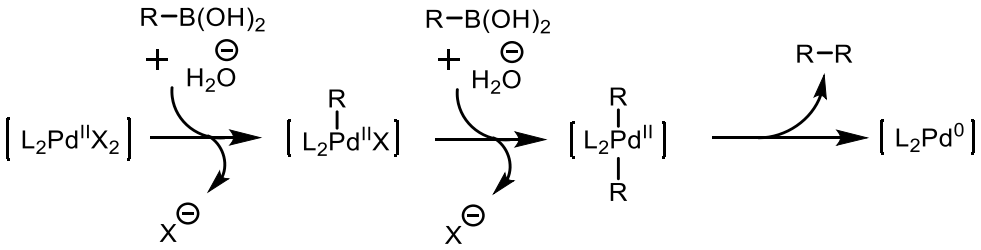

Scheme 1.2.18 – Reductive activation of Pd(II) pre-catalyst, consuming 2 equiv. boronic acid and forming boronic acid homocoupled side product and a Pd(0) species

1.2.3.1. Protodeboronation

One of the major side reactions in SM couplings is protodeboronation, **Scheme 1.2.19**. This is where the boron of the boronic acid is replaced by a proton, forming Ar-H and boric acid. This reaction was studied by Kuivila in the early 1960s, before the wide-spread use of the SM coupling.[45–48] Kuivila measured the protodeboronation of a range of boronic acids in aqueous buffers at 90 °C, and analysed the pH-rate profiles (between pH 1.0 and 6.7) to distinguish the different pathways in operation, finding there to be a base-catalysed and an acid-catalysed pathway, **Scheme 1.2.20**. Kuivila also studied the effects of a range of metal ions on the rate of protodeboronation of 2,6-dimethoxybenzeneboronic acid, and found all the metals studied to increase the rate of reaction with copper giving the fastest rate and nickel giving the slowest: copper(I1) > lead(I1) > silver ≥ cadmium > zinc > cobalt(I1) > magnesium > nickel(I1).[49]

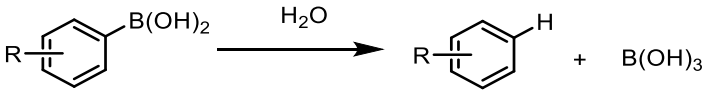

Scheme 1.2.19 – Protodeboronation

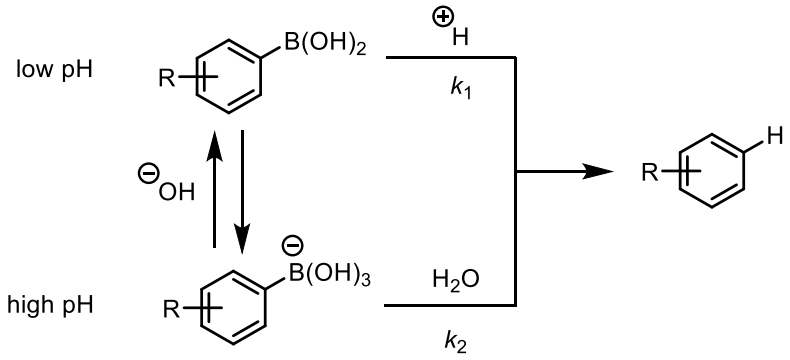

Scheme 1.2.20 – Kuivila pathways for protodeboronation of aryl boronic acids. Acid-catalysed (k_1) and base-catalysed (k_2) pathways

Typical SM reaction are carried out in basic conditions, but as Kuivila had only studied protodeboronation of a limited pH region, a detailed study at high pH was needed. Recently Lloyd-Jones *et al*. conducted in-depth studies of the protodeboronation of a wide range of boronic acids at pH range 1-13 and found, using both experimental and theoretical data, that five different pathways can occur; acid-catalysed, base-catalysed, uncatalysed, autocatalysis, and disproportionation, **Scheme 1.2.21**.[50] Reaction variables, such as pH and temperature, have a huge effect on the rate of protodeboronation. Lloyd-Jones *et al*. have also carried out a detailed kinetic study of the base-catalysed protodeboronation of 30 different arylboronic acid, using NMR, stopped-flow IR, and quenched-flow techniques, providing further insight into this reaction process, **Scheme 1.2.22**.[51]

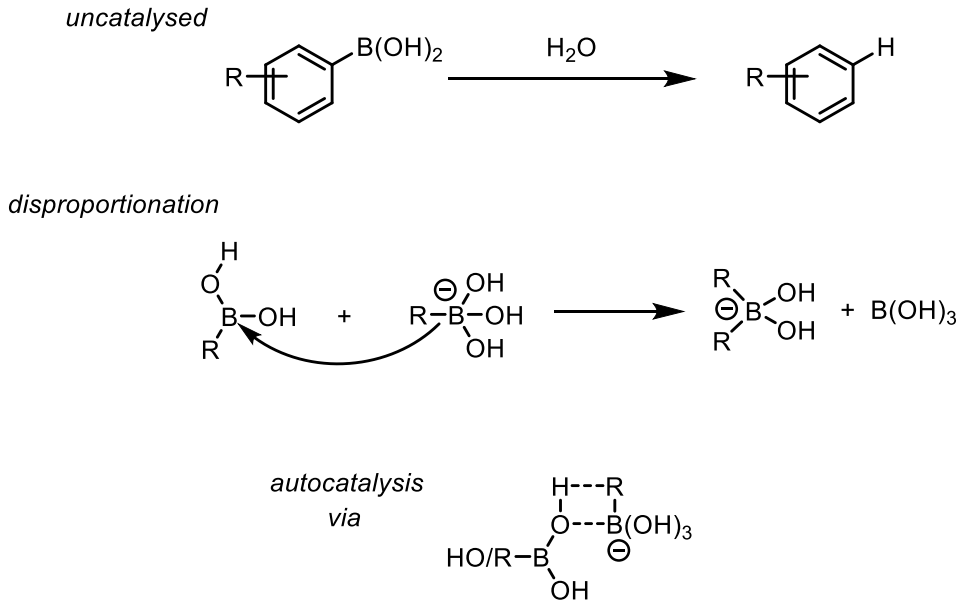

Scheme 1.2.21 – Protodeboronation pathways[50]

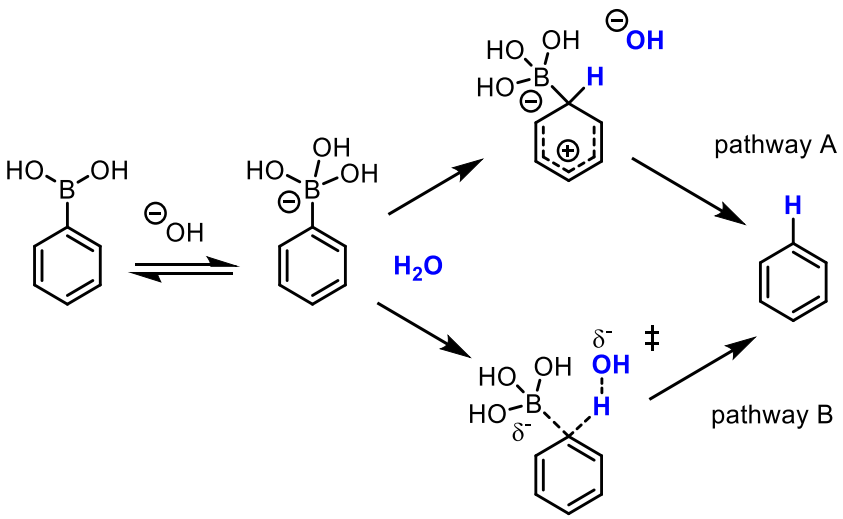

Scheme 1.2.22 – Base-catalysed protodeboronation of arylboronic acid *via* a stepwise (pathway A) or concerted (pathway B) mechanism[51]

It is common to use a large excess of boronic acids in SM coupling to reach a high conversion despite competing side reactions, but this is not an ideal solution. Significant amounts of research have been carried out to find ways to minimise protodeboronation.

Catalyst acceleration, often by ligand tuning, is one method to minimise protodeboronation. Several studies have been carried out in this area, offering advancements by achieving coupling of unstable boronic acids and increasing rates for TM and RE; reducing the competitive protodeboronation.[52–57] An alternative method is to use an additive to increase the efficiency of TM of the boronic acid, with silver oxide and copper salts being two examples.[16,39,58–67] A third method is to "mask" the boronic acid group and will be covered in more detail in **Section 1.2.4**.

1.2.3.2. Oxidation

Many boronic acids are stable in air and water due to the large activation energy required to undergo oxidation with atmospheric oxygen or water.[68] However, oxidation can occur with oxidants such as hydrogen peroxide, which readily oxidise the boronic acid to the corresponding alcohol.[69] Oxidation can also occur from hydroperoxides, formed in unstabilised (inhibitor-free) ethereal solvents, such as THF, which are commonly used in SM reactions, **Scheme 1.2.23**.[16,70]. These hydroperoxides can then oxidise boronic acids, forming alcohol (phenol), **Scheme 1.2.24**. The use of anaerobic techniques can minimise this side reaction, or the use of stabilisers, such as butylated hydroxytoluene (BHT) in THF for example, to stop the formation of hydroperoxides.[16]

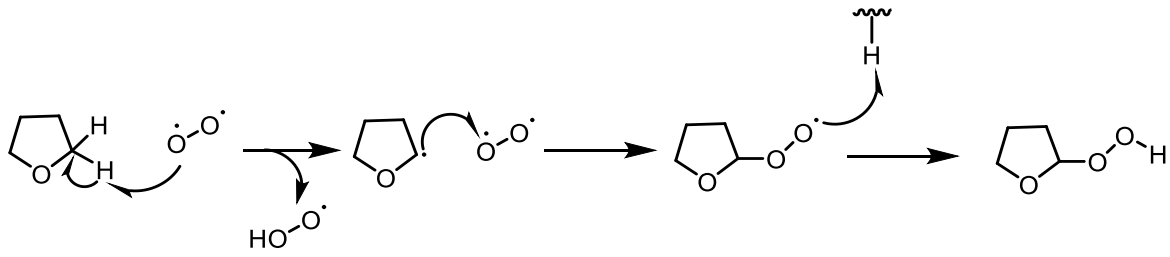

Scheme 1.2.23 – Formation of peroxides in THF

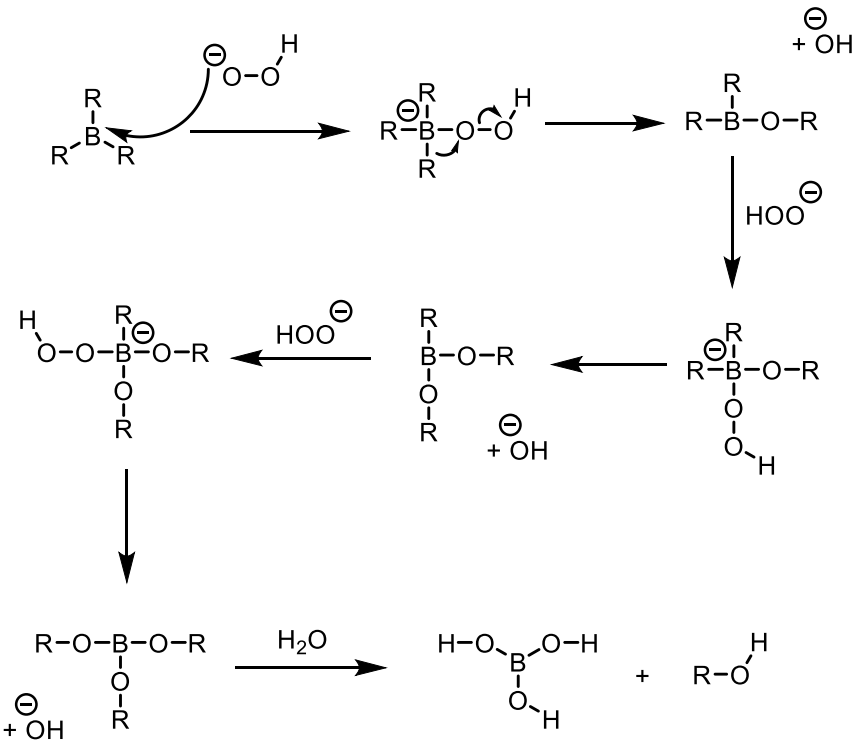

Scheme 1.2.24 – Hydroboration-oxidation mechanism for the formation of phenol from boronic acids

Boronic acid oxidative homocoupling is the other oxidative process that consumes boronic acid starting material. This process is palladium catalysed, and so is in competition with the desired SM cross-coupling.[71] This process starts with a Pd(0) species reacting with atmospheric oxygen to generate a peroxo complex, which can then react with boronic acid to form a new Pd(II) peroxo species. This species can then undergo transmetalation with a second equivalent of boronic acid, followed by reductive elimination to form the homocoupled product, **Scheme 1.2.25**.[71,72] This cycle also forms peroxide, which can oxidise a third molecule of boronic acid to its corresponding alcohol. So, this palladium catalysed cycle forms both boronic acid homocoupling and boronic acid oxidation. Anaerobic techniques can reduce the formation of these side products.[16]

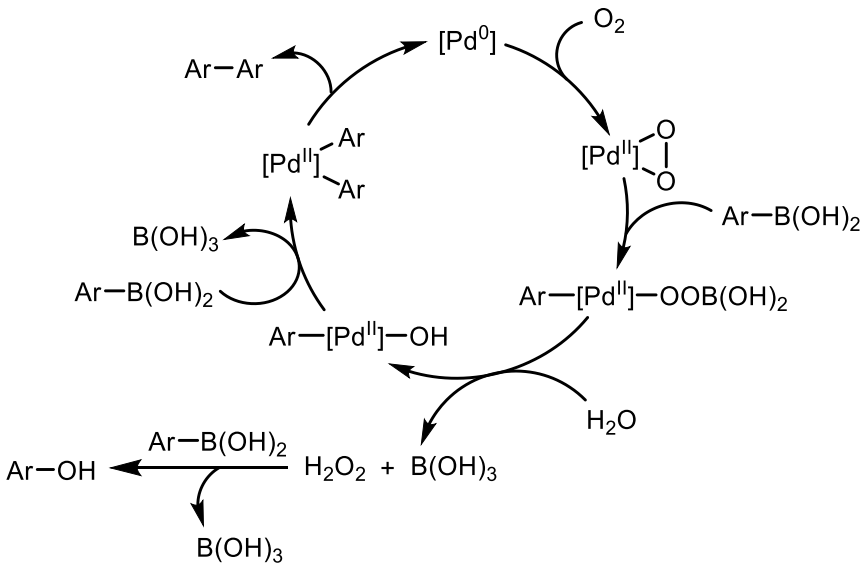

Scheme 1.2.25 – Palladium catalysed oxidative homocoupling competing with SM cross-coupling

1.2.4. Boronic acid derivatives

To minimise side product formation, a common technique is to use boronic acid derivatives, which also allow the coupling of unstable boronic acids. Standout examples are MIDA boronates, potassium organotrifluoroborates and boronic esters, **Fig 1.2.5**.

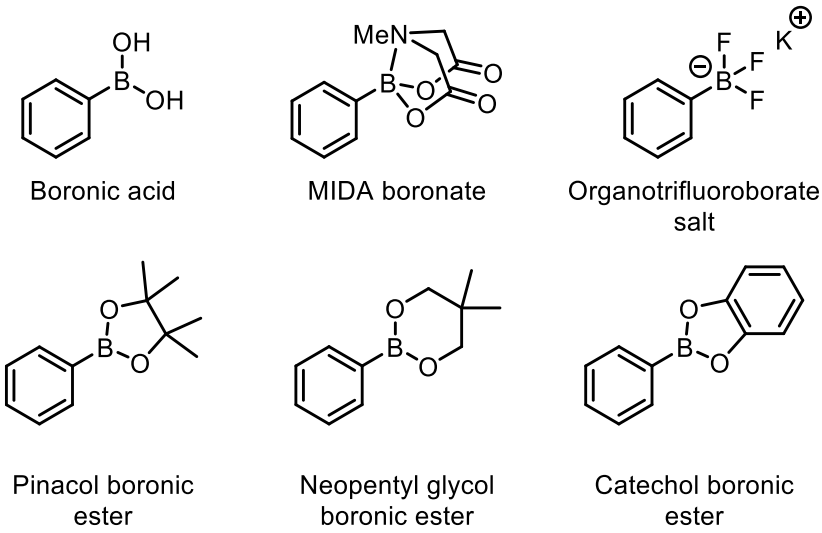

Fig 1.2.5 – Common organoboron reagents for SM cross-coupling

The hydrolysis of MIDA boronates[73] and potassium organotrifluoroborates[74] has been well studied and found that both reagents undergo *in situ* hydrolysis to release the boronic acid, which can then undergo TM in the SM catalytic cycle. The key advantage is the ability to control the release of the boronic acid depending on the reaction conditions.[16] This allows the amount of free reactive boronic acid to be controlled, therefore minimising side reactions.

1.2.4.1. MIDA boronates

The original MIDA study was carried out by Burke *et al.*, providing a method of synthesising these masked boronate reagents, as well as demonstrating their *in situ* hydrolysis and cross-coupling ability.[75] This class of compound has internal coordination between the vacant p-orbital and the nitrogen lone pair, giving rise to a tetrahedral boron species. MIDA boronates can be synthesised by either refluxing the boronic acid with the MIDA ligand under Dean-Stark conditions or, for unstable heterocyclic boronic acids, starting with the corresponding aryl halide undergoing a lithium halogen exchange, followed by treatment with triisopropylborate and quench with MIDA, **Scheme 1.2.26**.[76]

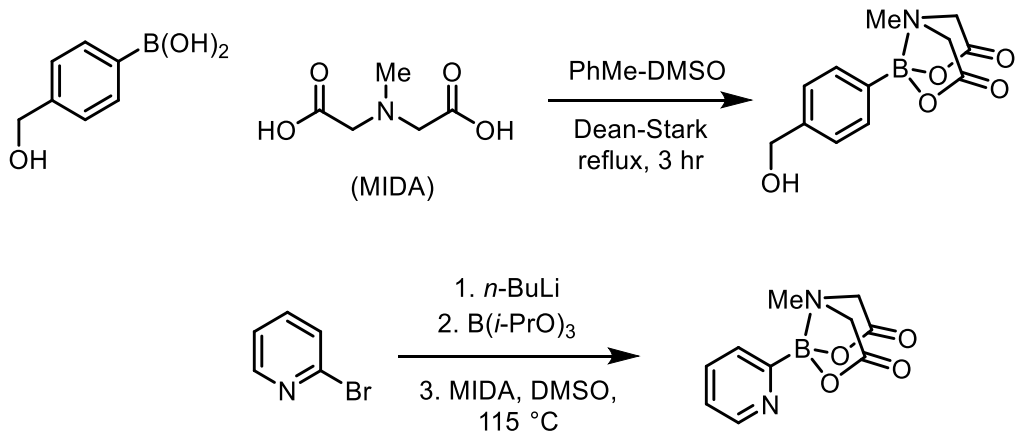

Scheme 1.2.26 – MIDA boronate formation

Typical basic SM conditions allow the MIDA ligand to be cleaved from the boron centre, releasing the free boronic acid to undergo TM. Reaction conditions, such as base, temperature and solvent, must all be carefully chosen to keep the concentration of free, reactive boronic acid low, to reduce side reactions, i.e. slow release.[16] A detailed study of the slow release of MIDA boronates was reported by Lloyd-Jones *et al*. who found two distinct mechanisms for the hydrolysis; a neutral pathway and a base mediated pathway, with the latter having a rate

more than three orders of magnitude faster than the neutral pathway, therefore highly relevant for SM reaction which are commonly carried out in very basic conditions, **Scheme 1.2.27**.[73]

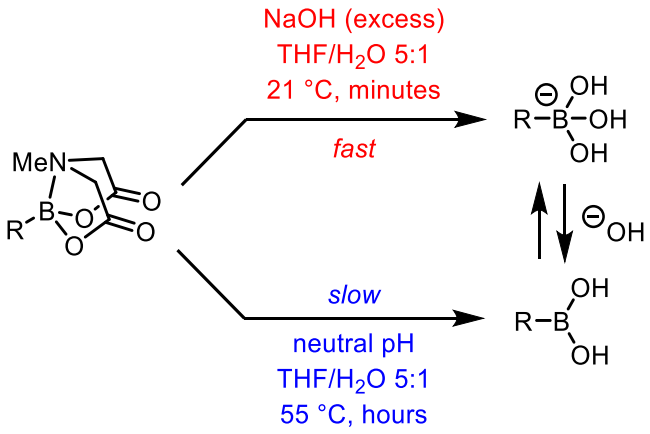

Scheme 1.2.27 – MIDA boronate hydrolysis

1.2.4.2. Potassium organotrifluoroborates

Research into this class of compounds was originally carried out by Genet and Molander.[27,77] Genet *et al*. found that potassium organotrifluoroborates gave consistently better yields in comparison to the corresponding boronic acid.[77] The synthesis of potassium organotrifluoroborates involves the addition of KHF_2 to the corresponding boronic acid in methanol at room temperature.[18,78,79] The products precipitate out of the reaction and are air and moisture stable.[18] Mechanistic studies carried out by Lloyd-Jones *et al*. found two pathways for hydrolysis; acid-catalysed and direct, **Scheme 1.2.28**, and the rate of hydrolysis to be dependent on substituent type.[74,80] This study also revealed the partial phase splitting, therefore vessel shape, size and stirring rate, to have an effect on hydrolysis, which is important in the context of SM reaction which are commonly carried out in biphasic conditions.[74]

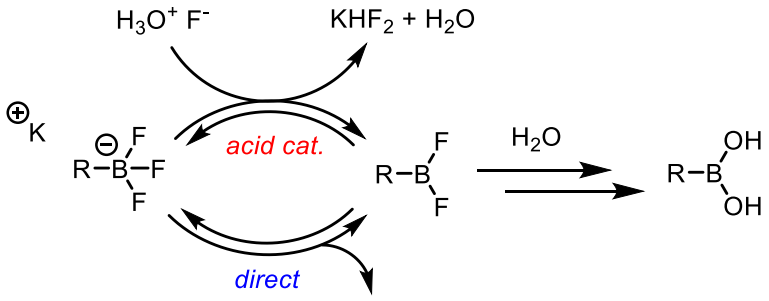

Scheme 1.2.28 – Organotrifluoroborates hydrolysis

1.2.4.3. Boronic esters

Boronic esters, with bulky and electron-rich ligands, reduce the Lewis acidity at the boron centre, giving the ester increased stability relative to the corresponding boronic acid. Boronic esters are monomeric, so do not form aggregates which can be an issue when using boronic acids. Pinacol esters in particular have become a key reagent in synthetic applications, aided by being commercially available.[57,65] A straightforward method for the synthesis of boronic esters is *via* esterification of the boronic acid with the corresponding diol, **Scheme 1.2.29**.[70,81] The use of Dean-Stark conditions drives the formation of boronic ester, by azeotropic removal of water to limit the reverse reaction of boronic ester hydrolysis. An alternative method for the formation of pinacol esters is Miyaura borylation, **Scheme 1.2.30**.[82]

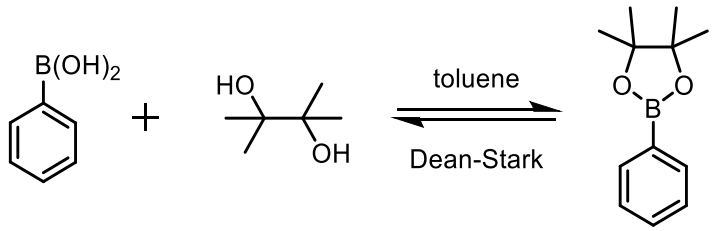

Scheme 1.2.29 – Formation of pinacol ester *via* esterification of the boronic acid

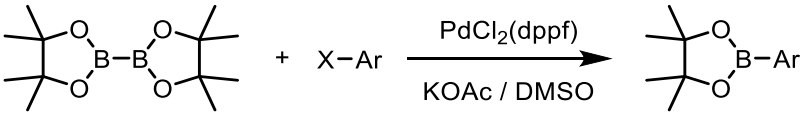

Scheme 1.2.30 – Miyaura borylation reaction

Watson *et al*. recently developed a method to synthesize complex boronic pinacol esters, using a chemoselectively controlled reaction between a pinacol ester and MIDA boronate, **Scheme 1.2.31**.[43,83] This strategy has then been employed in the synthesis of functionalised phenols,[84] and in the chemoselective SM cross-coupling, allowing the formation of two new C–C bonds in a single transformation, **Scheme 1.2.32**.[85]

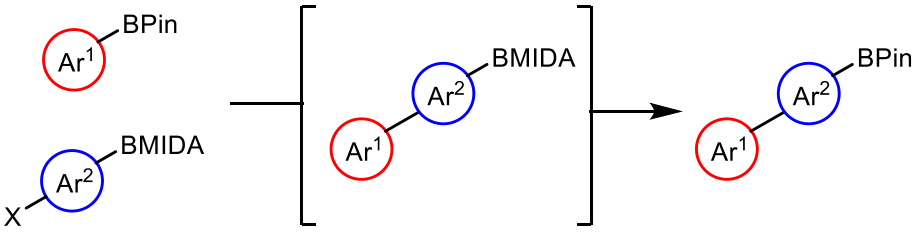

Scheme 1.2.31 – Synthesis of pinacol esters by controlled speciation. X = halogen.

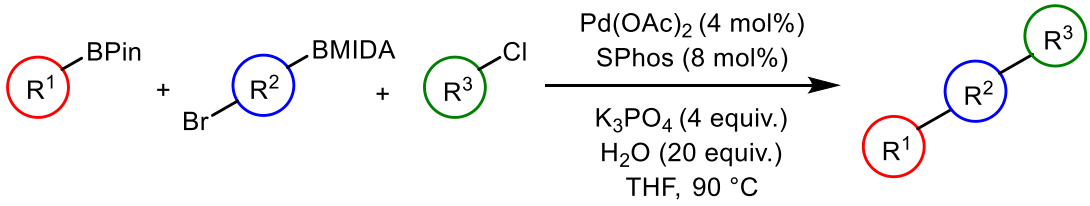

Scheme 1.2.32 – Chemoselective tandem SM cross-coupling

Further discussion of boronic esters can be found in **Chapter 2.**

1.3. Aims of the project

While studies into the SM reaction, especially the mechanism of transmetalation for boronic acids, has gained a lot of interest over recent years with numerous studies, key parts of the mechanism of this now indispensable reaction remain unknown. A common solution to the use of unstable boronic acids is to use a masked boronic acid. But while the mechanism of MIDA boronates and potassium organotrifluoroborates has been well studied,[73,74] the true pathway for the SM cross-coupling of boronic esters remains unknown, **Scheme 1.3.1**. Specifically, whether these species undergo direct transmetalation or prior hydrolysis to the boronic acid under SM conditions remains unknown. This research aims to elucidate the mechanism of this valuable cross-coupling process.

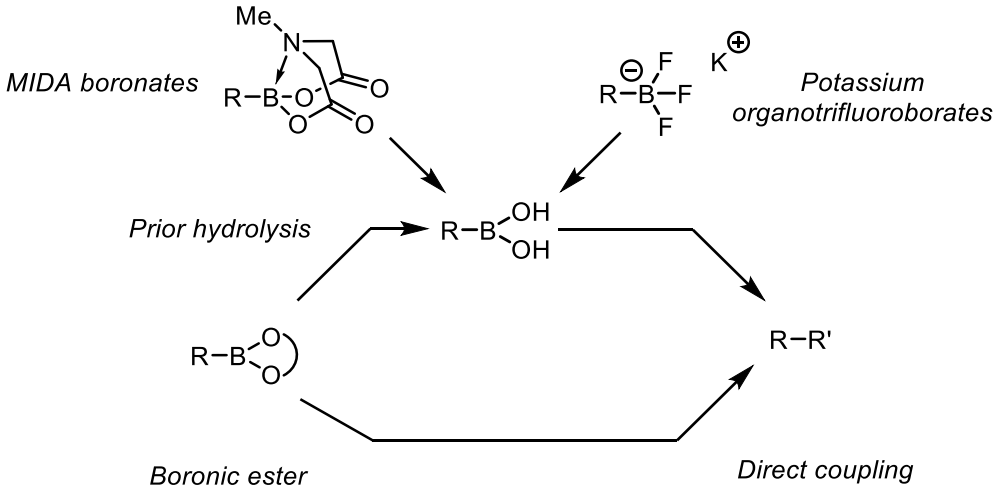

Scheme 1.3.1 – Elucidating the cross-coupling of boronic acid derivatives

1.4. References

(1) García-Melchor, M.; Braga, A. A. C.; Lledós, A.; Ujaque, G.; Maseras, F. *Acc. Chem. Res.* **2013**, *46* (11), 2626–2634.

(2) Li, H.; Johansson Seechurn, C. C. C.; Colacot, T. J. *ACS Catal.* **2012**, *2* (6), 1147–1164.

(3) Wurtz, A. *Ann. der Chemie und Pharm.* **1855**, *96* (3), 364–375.

(4) Tamao, K.; Sumitani, K.; Kumada, M. *J. Am. Chem. Soc.* **1972**, *94* (12), 4374–4376.

(5) Corriu, R. J. P.; Masse, J. P. *J. Chem. Soc. Chem. Commun.* **1972**, No. 3, 144.

(6) http://nobelprize.org/nobel_prizes/chemistry/laureates/2010/.

(7) Miyaura, N.; Yamada, K.; Suzuki, A. *Tetrahedron Lett.* **1979**, *20* (36), 3437–3440.

(8) King, A. O.; Okukado, N.; Negishi, E. *J. Chem. Soc. Chem. Commun.* **1977**, No. 19, 683.

(9) King, A. O.; Yasuda, N. In *Organometallics in Process Chemistry*; **2004**; Vol. 6, pp 205–245.

(10) Stille, J. K. *Angewandte Chem International Edition in English*. June **1986**, pp 508–524.

(11) Hatanaka, Y.; Hiyama, T. *J. Org. Chem.* **1988**, *53* (4), 918–920.

(12) "Suzuki-Miyaura." *SciFinder*.

(13) Kotha, S.; Lahiri, K.; Kashinath, D. *Tetrahedron* **2002**, *58* (48), 9633–9695.

(14) Braga, A. A. C.; Morgon, N. H.; Ujaque, G.; Maseras, F. *J. Am. Chem. Soc.* **2005**, *127* (25), 9298–9307.

(15) Braga, A. a. C.; Morgon, N. H.; Ujaque, G.; Lledós, A.; Maseras, F. *J. Organomet. Chem.* **2006**, *691* (21), 4459–4466.

(16) Lennox, A. J. J.; Lloyd-Jones, G. C. *Isr. J. Chem.* **2010**, *50* (5–6), 664–674.

(17) Thomas, A. A.; Denmark, S. E. *Science (80-.).* **2016**, *352* (6283), 329–332.

(18) Batey, R. A.; Quach, T. D. *Tetrahedron Lett.* **2001**, *42* (52), 9099–9103.

(19) Littke, A. F.; Fu, G. C. *Angew. Chem Int. Ed.* **2002**, *41* (22), 4176–4211.

(20) Altenhoff, G.; Goddard, R.; Lehmann, C. W.; Glorius, F. *J. Am. Chem. Soc.* **2004**, *126* (46), 15195–15201.

(21) Zim, D.; Gruber, A. S.; Ebeling, G.; Dupont, J.; Monteiro, A. L. *Org. Lett.* **2000**, *2* (18), 2881–2884.

(22) Littke, A. F.; Dai, C.; Fu, G. C. *J. Am. Chem. Soc.* **2000**, *122* (17), 4020–4028.

(23) Wolfe, J. P.; Buchwald, S. L. *Angew. Chem Int. Ed.* **1999**, *38* (16), 2413–2416.

(24) Wolfe, J. P.; Singer, R. A.; Yang, B. H.; Buchwald, S. L. *J. Am. Chem. Soc.* **1999**, *121* (41), 9550–9561.

(25) Fihri, A.; Luart, D.; Len, C.; Solhy, A.; Chevrin, C.; Polshettiwar, V. *Dalt. Trans.* **2011**, *40* (13), 3116.

(26) Nunes, C. M.; Monteiro, A. L. *J. Braz. Chem. Soc.* **2007**, *18* (7), 1443–1447.

(27) Molander, G. A.; Ellis, N. *Acc. Chem. Res.* **2007**, *40* (4), 275–286.

(28) Feeney, K.; Berionni, G.; Mayr, H.; Aggarwal, V. K. *Org. Lett.* **2015**, *17* (11), 2614–2617.

(29) Braga, A. A. C.; Ujaque, G.; Maseras, F. *Organometallics* **2006**, *25* (15), 3647–3658.

(30) Thomas, A. A.; Wang, H.; Zahrt, A. F.; Denmark, S. E. *J. Am. Chem. Soc.* **2017**, *139*

(10), 3805–3821.

(31) Ortuño, M. a.; Lledós, A.; Maseras, F.; Ujaque, G. *ChemCatChem* **2014**, *6* (11), 3132–3138.

(32) Lennox, A. J. J.; Lloyd-Jones, G. C. *Angew. Chem Int. Ed.* **2013**, *52* (29), 7362–7370.

(33) Espino, G.; Kurbangalieva, A.; Brown, J. M. *Chem. Commun.* **2007**, *17* (17), 1742–1744.

(34) Amatore, C.; Jutand, A.; Le Duc, G. *Chem. - A Eur. J.* **2011**, *17* (8), 2492–2503.

(35) Senn, H. M.; Ziegler, T. *Organometallics* **2004**, *23* (12), 2980–2988.

(36) Lyngvi, E.; Schoenebeck, F. *Tetrahedron* **2013**, *69* (27–28), 5715–5718.

(37) Mollar, C.; Besora, M.; Maseras, F.; Asensio, G.; Medio-Simón, M. *Chem. - A Eur. J.* **2010**, *16* (45), 13390–13397.

(38) Carrow, B. P.; Hartwig, J. F. *J. Am. Chem. Soc.* **2011**, *133* (7), 2116–2119.

(39) Lennox, A. J. J.; Lloyd-Jones, G. C. *Chem. Soc. Rev.* **2014**, *43* (1), 412–443.

(40) Lima, C. F. R. a. C.; Rodrigues, A. S. M. C.; Silva, V. L. M.; Silva, A. M. S.; Santos, L. M. N. B. F. *ChemCatChem* **2014**, *6*, 1291–1302.

(41) Hofer, M.; Gomez-Bengoa, E.; Nevado, C. *Organometallics* **2014**, *33* (6), 1328–1332.

(42) Schmidt, A. F.; Kurokhtina, A. A.; Larina, E. V. *Russ. J. Gen. Chem.* **2011**, *81* (7), 1573–1574.

(43) Fyfe, J. W. B.; Seath, C. P.; Watson, A. J. B. *Angew. Chem Int. Ed.* **2014**, *53* (45), 12077–12080.

(44) Aliprantis, A. O.; Canary, J. W. *J. Am. Chem. Soc.* **1994**, *116* (15), 6985–6986.

(45) Kuivila, H. G.; Nahabedian, K. V. *J. Am. Chem. Soc.* **1961**, *83* (9), 2159–2163.

(46) Kuivila, H. G.; Nahabedian, K. V. *J. Am. Chem. Soc.* **1961**, *83* (9), 2164–2166.

(47) Nahabedian, K. V.; Kuivila, H. G. *J. Am. Chem. Soc.* **1961**, *83* (9), 2167–2174.

(48) Kuivila, H. G.; Reuwer Jr., J. F.; Mangravite, J. A. *Can. J. Chem.* **1963**, *41* (12), 3081–3090.

(49) Kuivila, H. G.; Reuwer, J. F.; Mangravite, J. A. *J. Am. Chem. Soc.* **1964**, *86* (13), 2666–

2670.

(50) Cox, P. A.; Leach, A. G.; Campbell, A. D.; Lloyd-Jones, G. C. *J. Am. Chem. Soc.* **2016**, *138* (29), 9145–9157.

(51) Cox, P. A.; Reid, M.; Leach, A. G.; Campbell, A. D.; King, E. J.; Lloyd-Jones, G. C. *J. Am. Chem. Soc.* **2017**, *139* (37), 13156–13165.

(52) Martin, R.; Buchwald, S. L. *Acc. Chem. Res.* **2008**, *41* (11), 1461–1473.

(53) Billingsley, K. L.; Anderson, K. W.; Buchwald, S. L. *Angew. Chem Int. Ed.* **2006**, *45* (21), 3484–3488.

(54) Billingsley, K.; Buchwald, S. L. *J. Am. Chem. Soc.* **2007**, *129* (11), 3358–3366.

(55) Kinzel, T.; Zhang, Y.; Buchwald, S. L. *J. Am. Chem. Soc.* **2010**, *132* (40), 14073–14075.

(56) Kudo, N.; Perseghini, M.; Fu, G. C. *Angew. Chem Int. Ed.* **2006**, *45* (8), 1282–1284.

(57) Yang, D. X.; Colletti, S. L.; Wu, K.; Song, M.; Li, G. Y.; Shen, H. C. *Org. Lett.* **2009**, *11* (2), 381–384.

(58) Dick, G. R.; Woerly, E. M.; Burke, M. D. *Angew. Chem Int. Ed.* **2012**, *51* (11), 2667–2672.

(59) Sakashita, S.; Takizawa, M.; Sugai, J.; Ito, H.; Yamamoto, Y. *Org. Lett.* **2013**, *15* (17), 4308–4311.

(60) Zhou, M.-B.; Wei, W.-T.; Xie, Y.-X.; Lei, Y.; Li, J.-H. *J. Org. Chem.* **2010**, *75* (16), 5635–5642.

(61) Nishihara, Y.; Onodera, H.; Osakada, K. *Chem. Commun.* **2004**, No. 2, 192–193.

(62) Korenaga, T.; Kosaki, T.; Fukumura, R.; Ema, T.; Sakai, T. *Org. Lett.* **2005**, *7* (22), 4915–4917.

(63) Adonin, N. Y.; Babushkin, D. E.; Parmon, V. N.; Bardin, V. V.; Kostin, G. A.; Mashukov, V. I.; Frohn, H.-J. *Tetrahedron* **2008**, *64* (25), 5920–5924.

(64) Leconte, N.; Keromnes-Wuillaume, A.; Suzenet, F.; Guillaumet, G. *Synlett* **2007**, *2007* (2), 204–210.

(65) Deng, J. Z.; Paone, D. V.; Ginnetti, A. T.; Kurihara, H.; Dreher, S. D.; Weissman, S.

A.; Stauffer, S. R.; Burgey, C. S. *Org. Lett.* **2009**, *11* (2), 345–347.

(66) Zou, G.; Reddy, Y. K.; Falck, J. R. *Tetrahedron Lett.* **2001**, *42* (41), 7213–7215.

(67) Chen, J.; Cammers-Goodwin, A. *Tetrahedron Lett.* **2003**, *44* (7), 1503–1506.

(68) Sana, M.; Leroy, G.; Wilante, C. *Organometallics* **1991**, *10* (1), 264–270.

(69) Contreras-Celedón, C. A.; Chacón-García, L.; Lira-Corral, N. J. *J. Chem.* **2014**, *2014*, 1–5.

(70) Hall, D. G. In *Boronic Acids*; Wiley-VCH Verlag GmbH & Co. KGaA: Weinheim, Germany, 2011; pp 1–133.

(71) Adamo, C.; Amatore, C.; Ciofini, I.; Jutand, A.; Lakmini, H. *J. Am. Chem. Soc.* **2006**, *128* (21), 6829–6836.

(72) Lakmini, H.; Ciofini, I.; Jutand, A.; Amatore, C.; Adamo, C. *J. Phys. Chem. A* **2008**, *112* (50), 12896–12903.

(73) Gonzalez, J. A.; Ogba, O. M.; Morehouse, G. F.; Rosson, N.; Houk, K. N.; Leach, A. G.; Cheong, P. H.-Y.; Burke, M. D.; Lloyd-Jones, G. C. *Nat. Chem.* **2016**, *8* (11), 1067–1075.

(74) Lennox, A. J. J.; Lloyd-Jones, G. C. *J. Am. Chem. Soc.* **2012**, *134* (17), 7431–7441.

(75) Gillis, E. P.; Burke, M. D. *Aldrichimica Acta.* **2009**, *42* (1), 17–27.

(76) Dick, G. R.; Knapp, D. M.; Gillis, E. P.; Burke, M. D. *Org. Lett.* **2010**, *12* (10), 2314–2317.

(77) Darses, S.; Genêt, J.-P.; Brayer, J.-L.; Demoute, J.-P. *Tetrahedron Lett.* **1997**, *38* (25), 4393–4396.

(78) Vedejs, E.; Chapman, R. W.; Fields, S. C.; Lin, S.; Schrimpf, M. R. *J. Org. Chem.* **1995**, *60* (10), 3020–3027.

(79) Lennox, A. J. J.; Lloyd-Jones, G. C. *Angew. Chem Int. Ed.* **2012**, *51* (37), 9385–9388.

(80) Butters, M.; Harvey, J. N.; Jover, J.; Lennox, A. J.; Lloyd-Jones, G. C.; Murray, P. M. *Angew. Chem Int. Ed. - Int. Ed.* **2010**, *49* (30), 5156–5160.

(81) Zhang, N.; Hoffman, D. J.; Gutsche, N.; Gupta, J.; Percec, V. *J. Org. Chem.* **2012**, *77* (14), 5956–5964.

(82) Ishiyama, T.; Murata, M.; Miyaura, N. *J. Org. Chem.* **1995**, *60* (23), 7508–7510.

(83) Fyfe, J. W. B.; Valverde, E.; Seath, C. P.; Kennedy, A. R.; Redmond, J. M.; Anderson, N. A.; Watson, A. J. B. *Chem. - A Eur. J.* **2015**, *21* (24), 8951–8964.

(84) Molloy, J. J.; Law, R. P.; Fyfe, J. W. B.; Seath, C. P.; Hirst, D. J.; Watson, A. J. B. *Org. Biomol. Chem.* **2015**, *13* (10), 3093–3102.

(85) Fyfe, J. W. B.; Fazakerley, N. J.; Watson, A. J. B. *Angew. Chem Int. Ed.* **2017**, *56* (5), 1249–1253.

Chapter 2

Boronic Esters

2.1. Overview

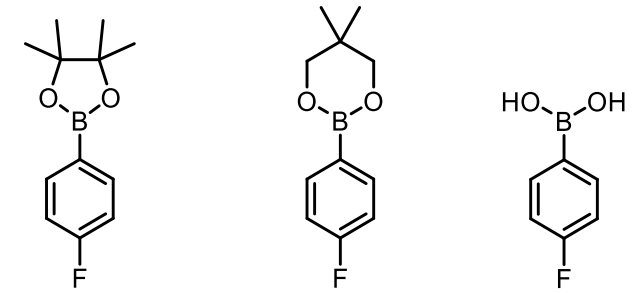

Fig 2.1.1 – The two boronic esters **1/2** and corresponding boronic acid **3** investigated in this study

The two boronic esters, **1** & **2 Fig 2.1.1**, chosen for this study were made using literature procedures[1,2] and have both been previously used in SM cross-coupling reactions.[3] Previous investigations by Hartwig *et al*. used the esters to investigate the two different transmetalation pathways, **Scheme 2.1.1**.[4] Path A shows the reaction of a palladium halide species with aryltrihydroxyborate, and path B is the reaction between an isolated hydroxyl palladium species and boronic acids, $ArB(OH)_2$, and esters, $ArB(OR)_2$. It was found that both pathways form the desired product. Further investigation into Path B using boronic esters showed the pinacol ester **1** to react much slower (1.5 hr) in comparison to the neopentyl glycol ester **2** (< 2 min), **Scheme 2.1.2**. It is interesting to note that when using the corresponding boronic acid **3** in this study, it was found to react as quickly as the neopentyl glycol ester **2**, < 2 min.

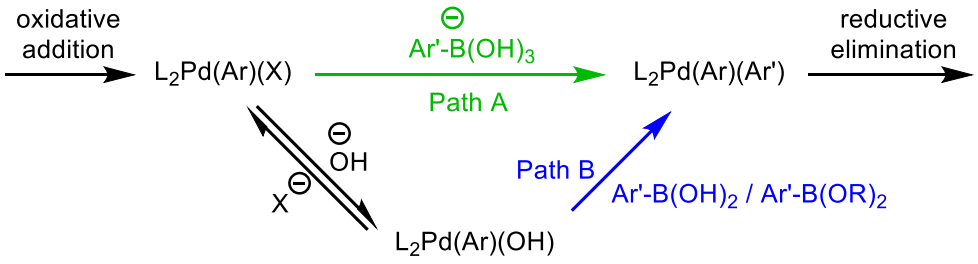

Scheme 2.1.1 – Two transmetalation pathways investigated

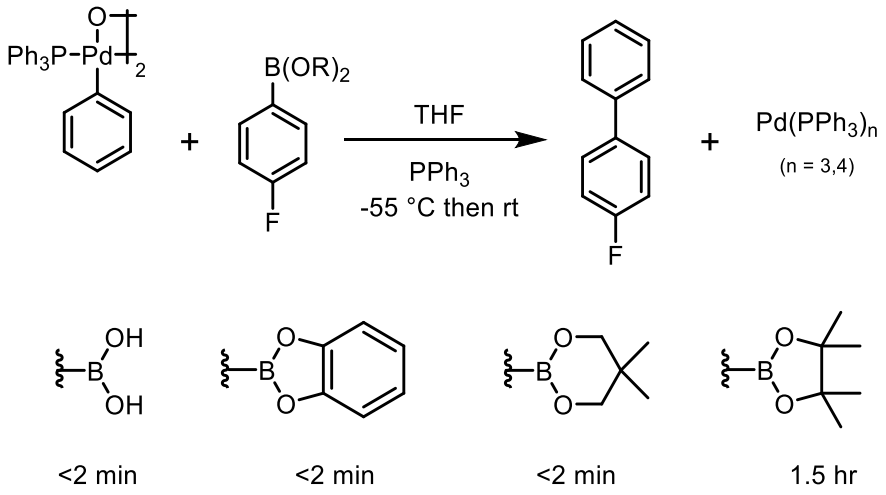

Scheme 2.1.2 – Path B

The stability of the boronic esters has also been studied by Roy and Brown in 2006, by monitoring the rate of transesterification with ethylene glycol phenylboronic ester, **Scheme 2.1.3**.[5] It was found that both the pinacol and neopentyl glycol diol produce thermodynamically stable boronic esters, but at very different rates. The neopentyl glycol ester was found to undergo 85% transesterification in 0.1 hour, compared to the pinacol ester taking 94 hours to reach 87.8% transesterification. This infers that while both esters are stable, there is a much lower barrier to form the neopentyl glycol ester, hence the faster transesterification rate.

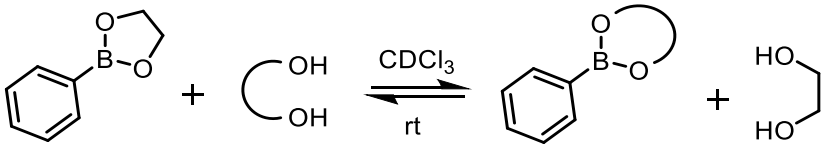

Scheme 2.1.3 – General scheme for transesterification study

A study of the reactivity of a pinacol ester and a neopentyl glycol ester found the overall reactivity to be 5 times higher for the neopentyl glycol ester (4-methoxyphenyl neopentylglycolboronate) compared to the pinacol ester (4-methoxyphenyl pinacolboronate), when studying the kinetics of the cross-coupling with methyl 4-((methylsulfonyl)oxy)-benzoate, **Scheme 2.1.4**.[3] Further studies of nickel-catalysed cross-coupling reactions of aryl boron-based nucleophiles with methyl 4-((methylsulfonyl)oxy)benzoate found that 4-methoxyphenylboronic acid gave the highest efficiency of the nucleophiles studies. But the

drawbacks to the use of boronic acids is their *in situ* decomposition and the presence of dimers and trimers, compared to monomeric boronic esters with increased stability.

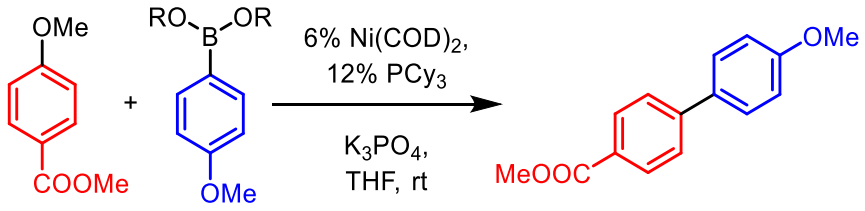

Scheme 2.1.4 – Kinetic studies of the cross-coupling of 4-methoxyphenyl neopentylglycolboronate and 4-methoxyphenyl pinacolboronate. Aryl mesylate (1 equiv.), aryl boronate (1 equiv.), K_3PO_4 (3 equiv.)

Aggarwal *et al.* have also studied the reactivity of different boronate complexes.[6] They also find the neopentyl glycol ester to be more reactive than the pinacol ester, reporting over 100-fold difference between the two, when looking at the reactivity of the esters with benzhydryliums, **Scheme 2.1.5**.

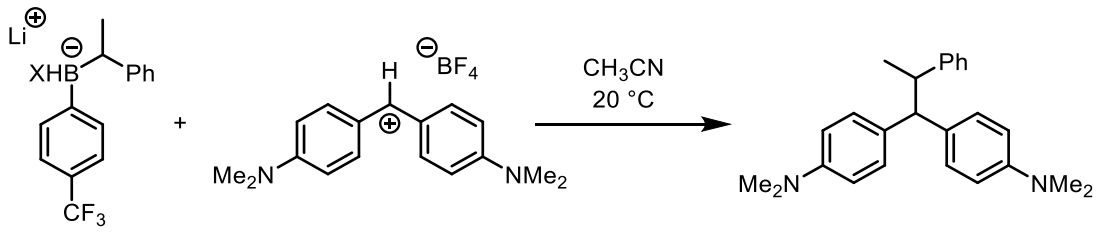

Scheme 2.1.5 – Reaction between lithium boronate complexes with $Ar_2CH^+BF_4$ (benzhydryliums). X = pinacol, second-order rate constant k_2 = 1.34 x 10^1. X = neopentyl glycol, second-order rate constant k_2 = 1.86 x 10^3.

Marder, Radius *et al*. have studied the reactivity of a slightly wider range of boronic esters, including the pinacol (pin) and neopentyl glycol (neop), in addition to ethyleneglycol (eg) and catechol (cat).[7] The nickel-catalysed SM cross-coupling of the boronates with polyfluorinated arenes showed the ethyleneglycol and neopentyl glycol to give the highest yields, **Fig 2.1.2**.

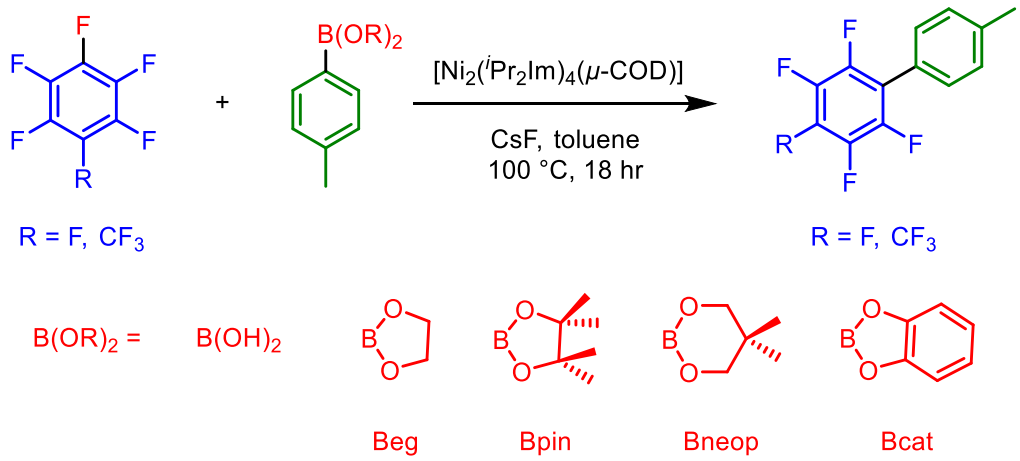

	Ar-F	Yield (%)
p-tolyl boronic acid	C_6F_6	10[a]
p-tolyl-Beg	C_6F_6	95
p-tolyl-Bneop	C_6F_6	84
p-tolyl-Bpin	C_6F_6	8
p-tolyl-Bcat	C_6F_6	6
p-tolyl boronic acid	CF_3-C_6F_6	97[a]
p-tolyl-Beg	CF_3-C_6F_6	100
p-tolyl-Bneop	CF_3-C_6F_6	96
p-tolyl-Bpin	CF_3-C_6F_6	47
p-tolyl-Bcat	CF_3-C_6F_6	6

Fig 2.1.2 – Nickel-catalysed SM cross-coupling of boronic acid/esters with polyfluorinated arenes. $[Ni_2(^iPr_2Im)_4(\mu\text{-COD})]$ (5 mol%), *p*-tolyl-$B(OR)_2$ (0.2 mmol), polyfluorinated arene (C_6F_6 0.4 mmol; CF_3-C_6F_6 0.2 mmol), CsF (0.2 mmol), 2 mL toluene, 100 °C, 18 h. Gas chromatography yields based on boronic acid/ester using $C_{12}H_{26}$ as an internal standard. [a] = K_2CO_3 (0.6 mmol) employed as the base

Watson *et al*. have recently investigated the reactivity of boronic acids and pinacol esters in independent and competition reactions.[8] The reactivity of phenyl boronic acid and the corresponding phenyl pinacol ester were found to be comparable, giving the same initial rate and comparable reaction profiles. However, in a competition reaction between *p*-tolylboronic acid and phenyl pinacol ester, the boronic acid was found to far outcompete the ester, **Scheme 2.1.6**. The conditions developed deliberately inhibit ester hydrolysis to the boronic acid and maintain a homogenous solution. The selective coupling of the boronic acid over the pinacol

ester was tested with a range of coupling partners and found to be highly selective. In addition, if a second aryl bromide is added to the reaction mixture after the initial coupling, the unreacted pinacol ester then undergoes cross-coupling, to produce varied coupling products in one pot, **Scheme 2.1.7**. The method was then further tested and found to allow chemoselective tandem SM cross-coupling, **Scheme 2.1.8**. This required a more active catalyst system, to allow the coupling of the aryl chloride, but was shown to work well for a range of aryl and heteroaryl boron species.

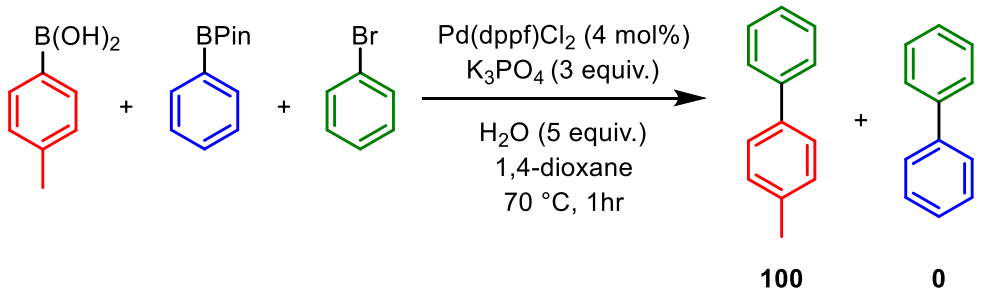

Scheme 2.1.6 – Competition reaction between p-tolylboronic acid (1 equiv.) and phenyl pinacol ester (1 equiv.) with phenyl bromide (1 equiv.). Selective coupling of the boronic acid. Determined by HPLC analysis

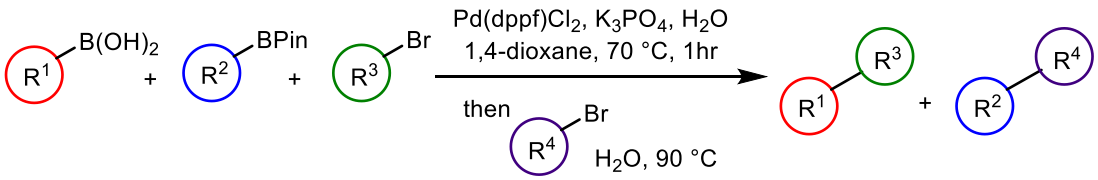

Scheme 2.1.7 – Sequential SM cross-coupling

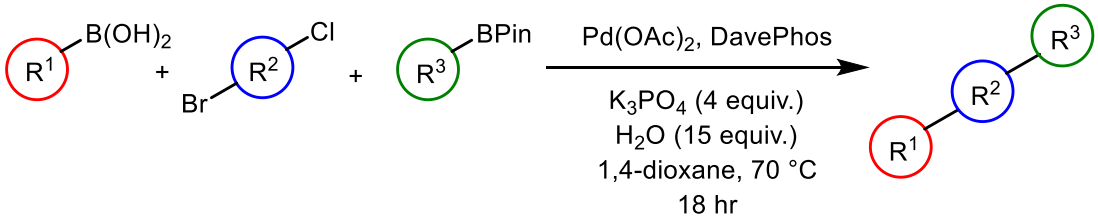

Scheme 2.1.8 – Chemoselective tandem SM cross-coupling

2.2. Hydrolysis

2.2.1. Pinacol Ester

The hydrolysis of the pinacol ester **1** in 10:1 THF/water was investigated using ^{19}F NMR and was found to have a rate of 1.15 x 10^{-5} M min^{-1}, **Scheme 2.2.1**, **Graph 2.2.1**. The final equilibrium position was found to be 35:65 pinacol ester to boronic acid after 24 hours.

The addition of 1 equivalent of an inorganic base (K_2CO_3) was found to increase the rate of hydrolysis to 5.24 x 10^{-5} M min^{-1} and generate a final equilibrium ratio of 40:60 pinacol ester to boronic acid after 24 hours, **Graph 2.2.1**. To determine whether phase separation occurred in the system, leading to potential loss of total fluorine signal, the experiment was carried out using an internal standard (1-fluoronaphthalene) to monitor the hydrolysis, and total ^{19}F concentration present. This study showed the concentration to remain constant throughout, confirming all species present are being monitored.

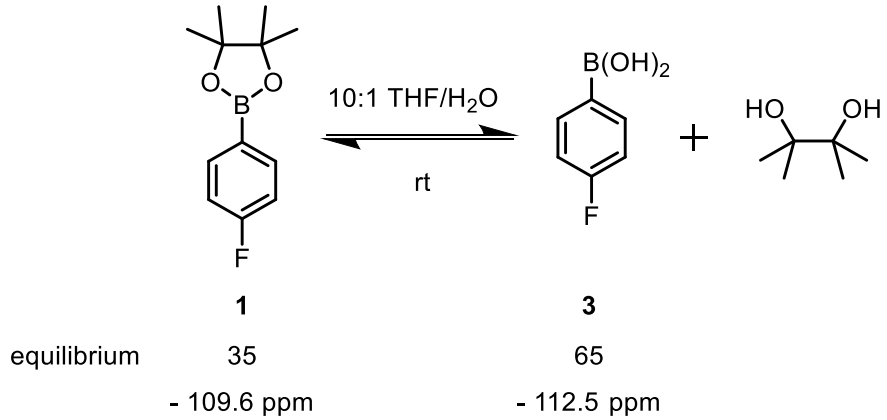

Scheme 2.2.1 – Pinacol ester **1** (0.04 M) hydrolysis monitored by ^{19}F NMR with 1-fluoronaphthalene as an internal standard.

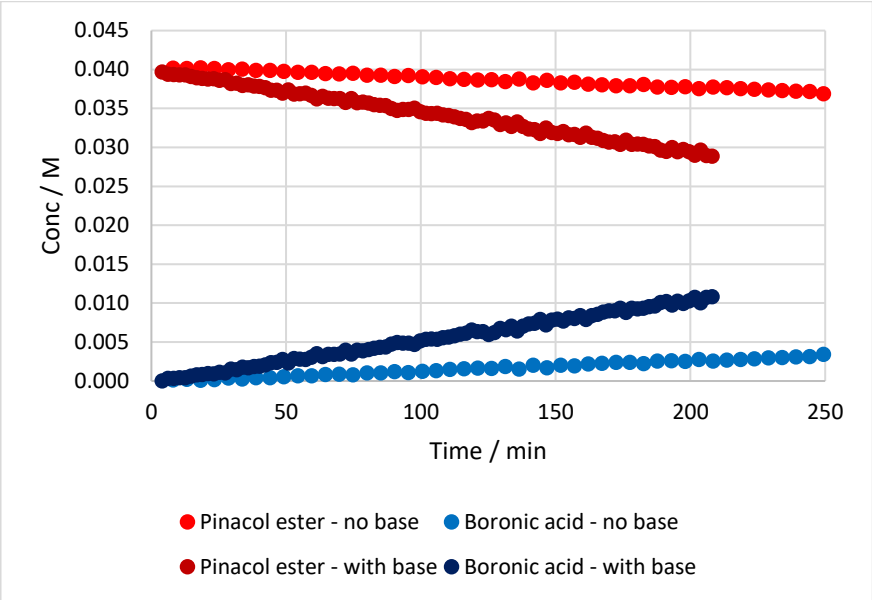

Graph 2.2.1 – Comparison of hydrolysis of pinacol ester **1** (0.04 M) in 10:1 THF/water with 1 equiv. K_2CO_3 and without base. Monitored by ^{19}F NMR with 1-fluoronaphthalene as an internal standard, 300 K.

The backward equilibrium reaction, **Scheme 2.2.1**, of the boronic acid **3** with 1 equivalent pinacol in 10:1 THF/water was also investigated, as the rate of this reaction will be important for competition coupling reactions using a pinacol ester **1** and a boronic acid **3**, **Graph 2.2.2**. An initial quantity of pinacol ester **1** is formed (0.0059 M) as a result of the reaction between the boronic acid **3** and pinacol in the solid phase before the addition of solvent. This reaction created a final equilibrium ratio of 65:35 boronic acid to pinacol ester after 24 hours. The rate of ester formation is 7.83 x 10^{-6} M min^{-1}, which shows the hydrolysis of the pinacol ester **1** (1.15 x 10^{-5} M min^{-1}) to be faster than the formation of pinacol ester from boronic acid **3** and pinacol.

$$k_{eq} = \frac{forward}{backward} = 0.68$$

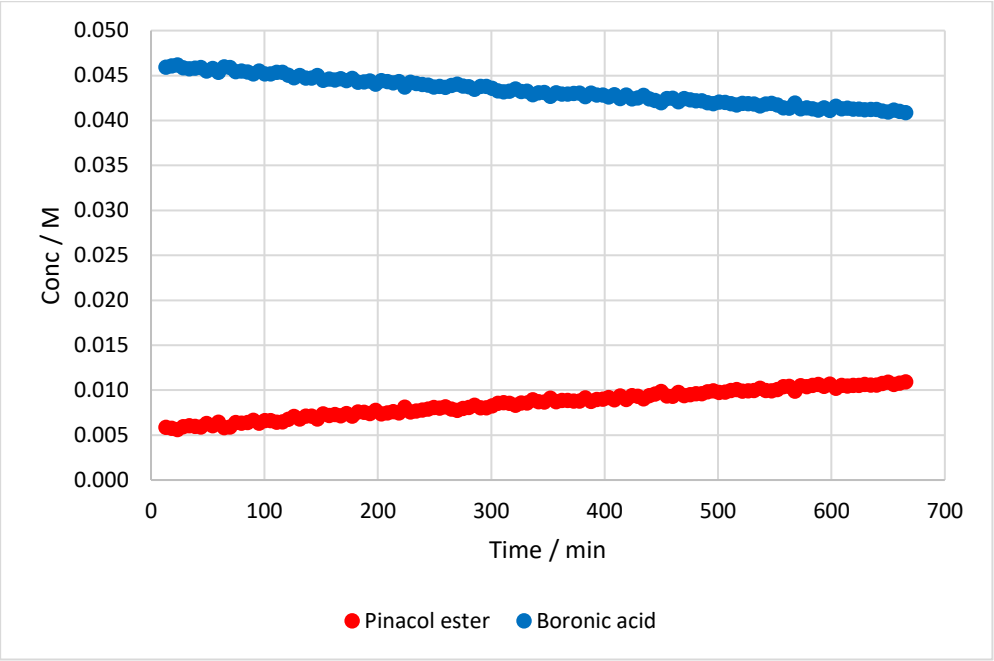

Graph 2.2.2 – Reaction of boronic acid **3** and pinacol alcohol (1:1) in 10:1 THF/water. Monitored by ^{19}F NMR with 1-fluoronaphthalene as an internal standard, 300 K.

2.1.1. Neopentyl Glycol Ester

The hydrolysis of the neopentyl glycol ester **2** in 10:1 THF/water was investigated using ^{19}F NMR and found to be extremely fast in comparison to the pinacol ester **1**, **Scheme 2.2.2**, **Graph 2.2.3**. Equilibrium between the boronic acid **3** and glycol ester **2** had been reached within 10 minutes and found to lie in favour of the boronic acid, creating a ratio of 75:25 boronic acid to glycol ester.

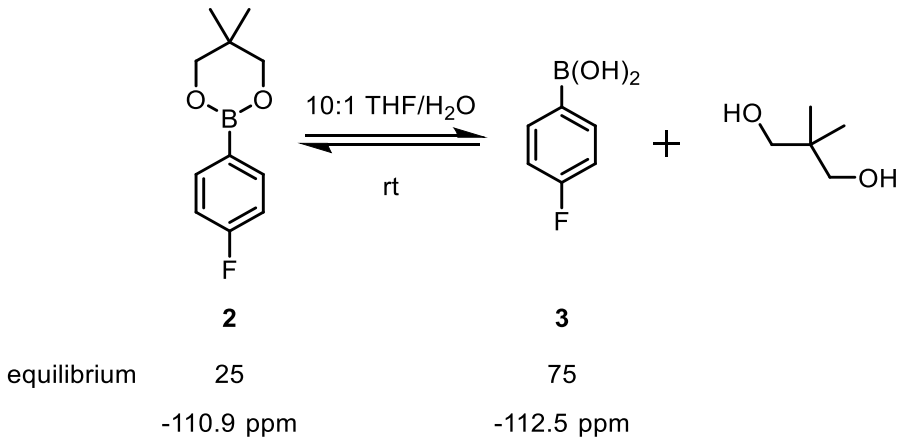

Scheme 2.2.2 – Neopentyl glycol ester **2** (0.04 M) hydrolysis monitored by ^{19}F NMR with 1-fluoronaphthalene as an internal standard.

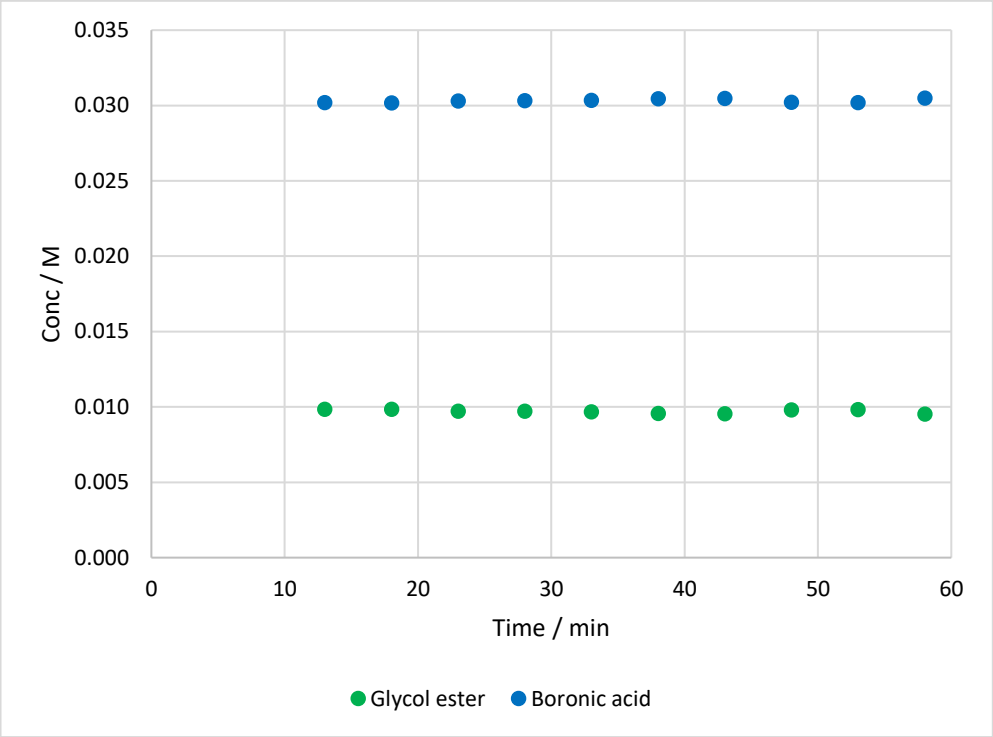

Graph 2.2.3 – Hydrolysis of neopentyl glycol ester **2** (0.04 M) in 10:1 THF/water. Monitored by ^{19}F NMR with 1-fluoronaphthalene as an internal standard, 300 K.

When the neopentyl glycol ester **2** hydrolysis was repeated with 1 equivalent of inorganic base, K_2CO_3, the equilibrium was obtained in 10 minutes, but shifted to 65:35 boronic acid to glycol ester. This experiment was carried out using an internal standard (1-fluoronaphthalene), to rule

out potential phase separation or micelle formation issues and ensure the total fluorine concentration remained constant throughout.

In addition, the reaction of the boronic acid **3** and neopentyl glycol in 10:1 THF/water was monitored, and also found to be very fast, less than 10 minutes was required to give to the same equilibrium position as starting with the glycol ester **2**, 25% glycol ester and 75% boronic acid.

2.3. Conclusion

The two boronic esters, **1** & **2**, have very different rates of hydrolysis, allowing for the study of how hydrolysis affects cross-coupling. The results also agree with the previous literature[5], that the pinacol ester **1** is more stable than the neopentyl glycol ester **2**, hence having a much slower rate of hydrolysis.

2.4. References

(1) Lennox, A. J. J.; Lloyd-Jones, G. C. *Angew. Chem Int. Ed.* **2012**, *51* (37), 9385–9388.

(2) Wilson, D. A.; Wilson, C. J.; Moldoveanu, C.; Resmerita, A.-M.; Corcoran, P.; Hoang, L. M.; Rosen, B. M.; Percec, V. *J. Am. Chem. Soc.* **2010**, *132* (6), 1800–1801.

(3) Zhang, N.; Hoffman, D. J.; Gutsche, N.; Gupta, J.; Percec, V. *J. Org. Chem.* **2012**, *77* (14), 5956–5964.

(4) Carrow, B. P.; Hartwig, J. F. *J. Am. Chem. Soc.* **2011**, *133* (7), 2116–2119.

(5) Roy, C. D.; Brown, H. C. *J. Organomet. Chem.* **2007**, *692* (4), 784–790.

(6) Feeney, K.; Berionni, G.; Mayr, H.; Aggarwal, V. K. *Org. Lett.* **2015**, *17* (11), 2614–2617.

(7) Zhou, J.; Berthel, J. H. J.; Kuntze-Fechner, M. W.; Friedrich, A.; Marder, T. B.; Radius, U. J. Org. Chem. **2016**, 81 (13), 5789–5794.

(8) Fyfe, J. W. B.; Fazakerley, N. J.; Watson, A. J. B. *Angew. Chem Int. Ed.* **2017**, *56* (5), 1249–1253.

Chapter 3

Coupling with an inorganic base

3.1. Aims of the chapter

This chapter gives the preliminary results of the investigation into Suzuki-Miyaura cross-coupling using an inorganic base, and compares the reactivity of a boronic acid and two boronic esters. This work also reveals the importance of reaction conditions and phase separation, which altered the desired focus of this study.

3.2. Initial studies

Initial studies began with the Suzuki-Miyaura (SM) cross-coupling of 4-fluorophenylboronic acid **3** with 1,3-bis(trifluoromethyl)-5-bromobenzene **4** in a 1:1 ratio, with three equivalents of an inorganic base (potassium carbonate) at 55 °C, **Scheme 3.2.1**. The reaction was carried out in a 10:1 mixture of THF/water, respectively, using 1 mol% of bis(triphenylphosphine)-palladium(II) dichloride, $(Ph_3P)_2PdCl_2$, as a pre-catalyst. This literature reaction was chosen as it had previously been studied in detail for the corresponding reaction with potassium organotrifluoroborates.[1] The reagents chosen allow the reaction to be easily monitored by ^{19}F NMR, as the starting materials, desired product **5** and side products all have distinct fluorine peaks with no overlap, **Fig 3.2.1**.

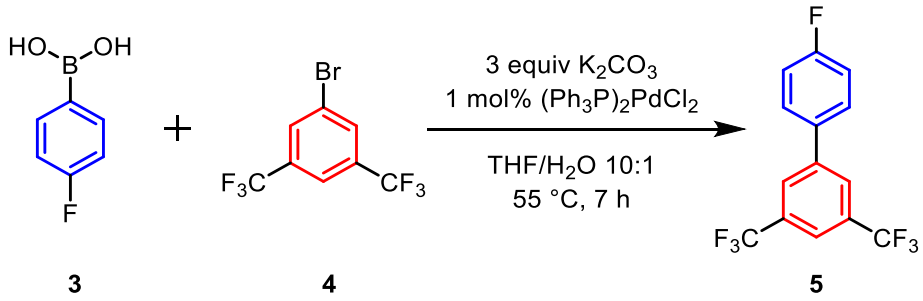

Scheme 3.2.1 – SM reaction of 4-fluorophenylboronic acid **3** (1 equiv.) with 1,3-bis(trifluoromethyl)-5-bromobenzene **4** (1 equiv.) monitored over 7 hours by ^{19}F NMR with 1-fluoronaphthalene as an internal standard.

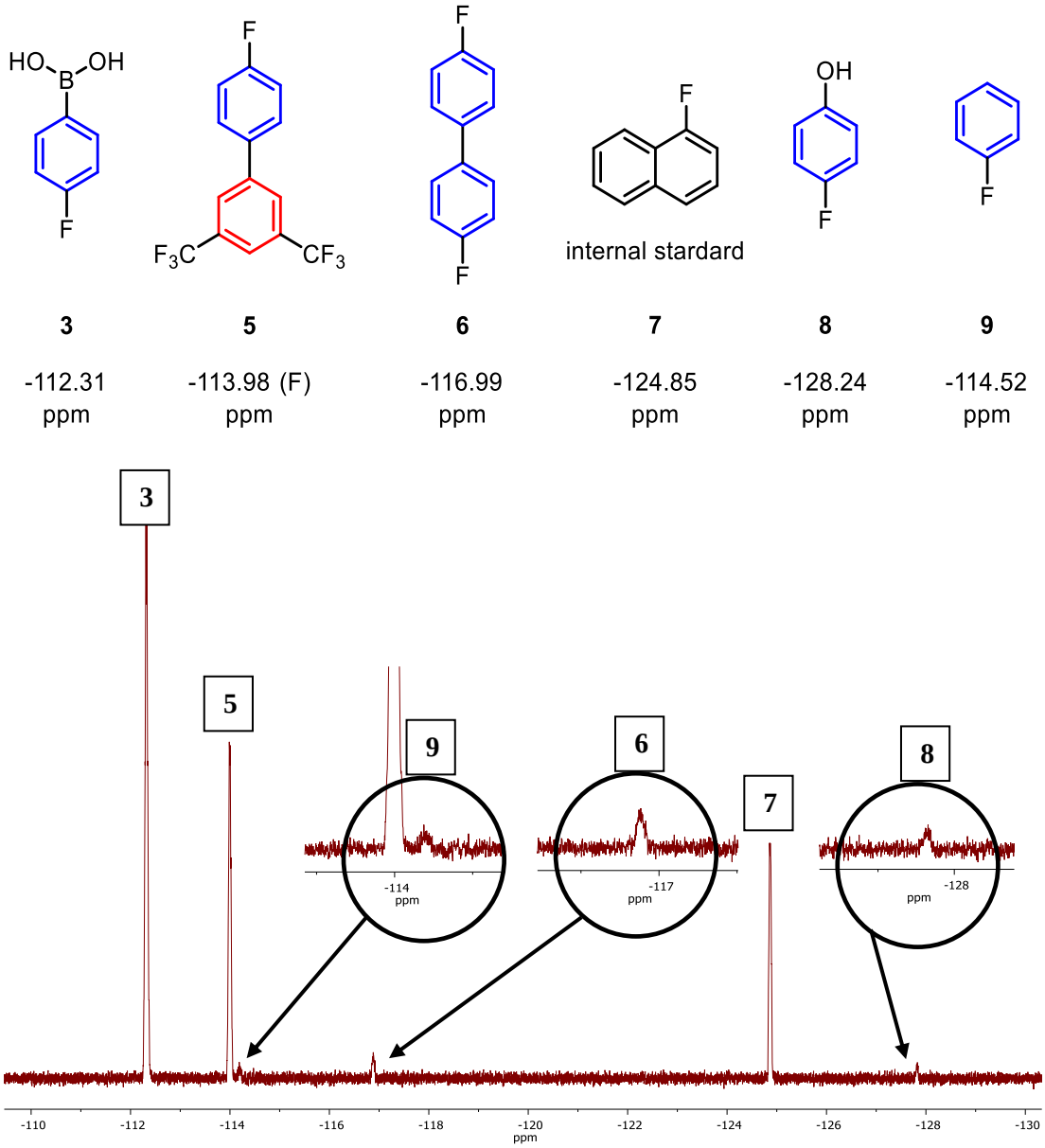

Fig 3.2.1 – ^{19}F NMR spectrum of the boronic acid region of the SM reaction of 4-fluorophenylboronic acid **3** (0.04 M) with 1,3-bis(trifluoromethyl)-5-bromobenzene **4** (0.04 M) with 1-fluoronaphthalene **7** as an internal standard, with inserts for fluorobenzene **9** −114.52 ppm, boronic acid homocoupling **6** −116.99 ppm, and fluorophenol **8** −128.24 ppm.

The THF/water ratio of 10:1 and the amount of inorganic base, potassium carbonate, used creates a biphasic system. The boronic acid, aryl bromide and palladium catalyst are predominant in the organic phase, while the boronate formed during the reaction is highly water soluble so it is found in the aqueous phase, along with the hydroxide ions generated by the base, **Fig 3.2.2**.[2]

This was confirmed by looking at a 1:1 THF/water mixture with 5 equivalents of potassium carbonate relative to the boronic acid and analysing the THF layer and water layer separately by ^{11}B NMR, **Fig 3.2.3**. The water layer contained only boronate (5.91 ppm) whereas the THF layer contained solely boronic acid **3** (22.46 ppm).

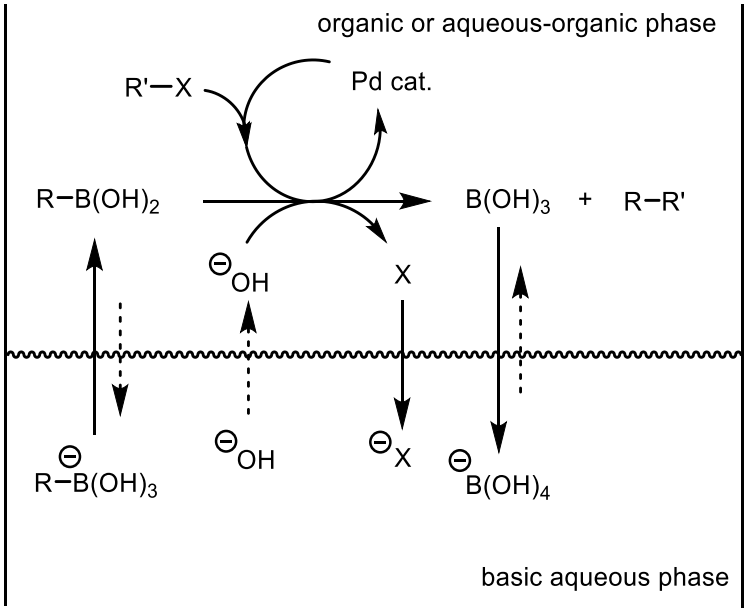

Fig 3.2.2 – Representation of a biphasic mixture, showing different species present in the aqueous-organic phase (lower pH) and the basic aqueous phase (high pH). The aqueous phase acts as a reservoir of base, as well as containing the halide and boron salts formed during the reaction.[2]

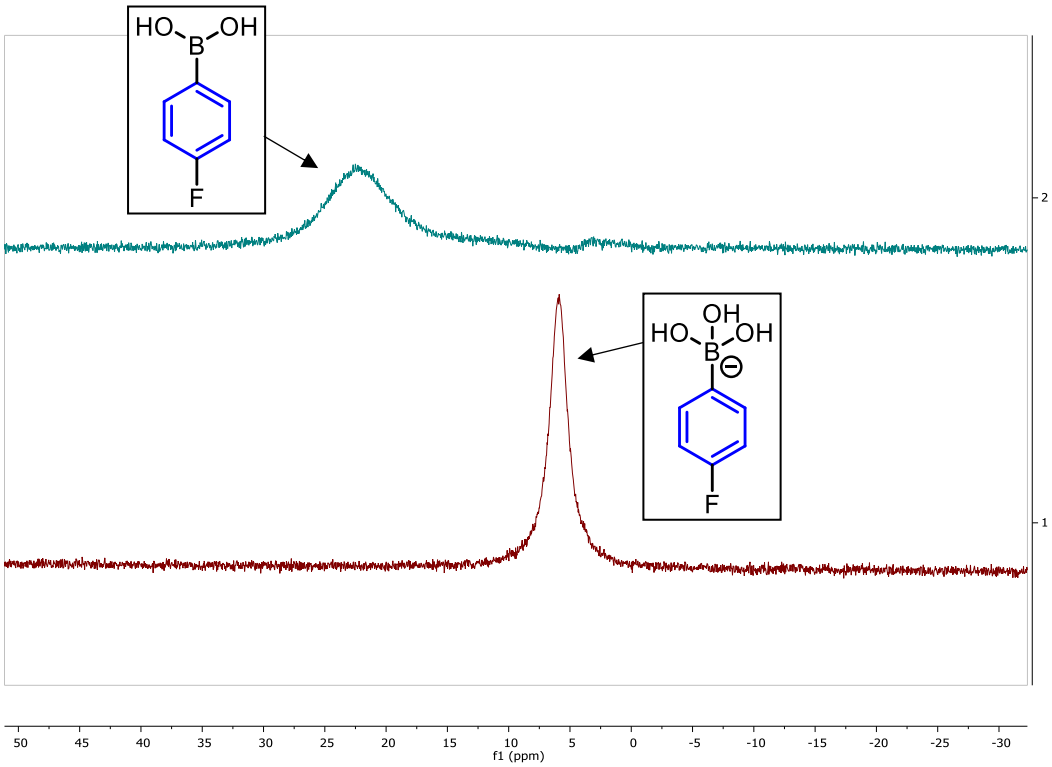

Fig 3.2.3 – THF layer containing boronic acid **3** 22.46 ppm (top spectrum) and water layer containing boronate 5.91 ppm (bottom spectrum) analysed by ^{11}B NMR, 300K.

3.2.1. General reaction profile

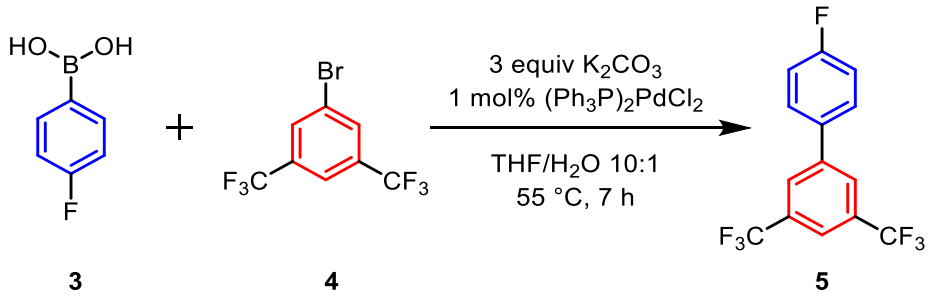

Scheme 3.2.1 – SM reaction of 4-fluorophenylboronic acid **3** (1 equiv.) with 1,3-bis(trifluoromethyl)-5-bromobenzene **4** (1 equiv.) monitored over 7 hours and analysed by ^{19}F NMR with 1-fluoronaphthalene as an internal standard.

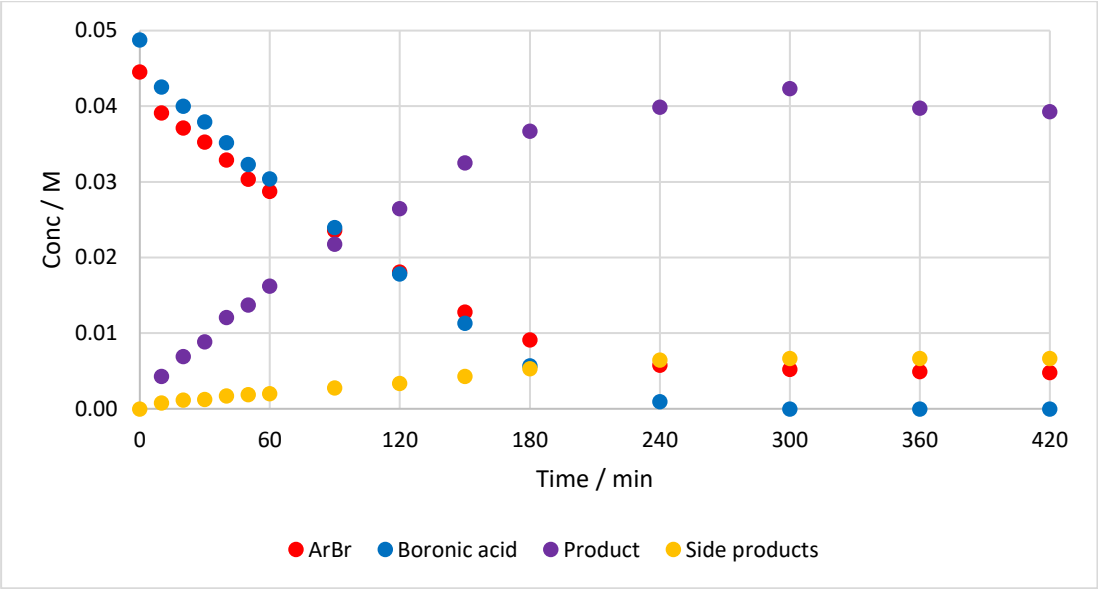

Graph 3.2.1 – SM coupling profile of 4-fluorophenylboronic acid **3** (0.049 M) with 1,3-bis(trifluoromethyl)-5-bromobenzene **4** (0.045 M) sampled ex situ over 7 hours and analysed by ^{19}F NMR with 1-fluoronaphthalene as an internal standard. Side products = boronic acid homocoupling **6** and boronic acid oxidation **8**. (Procedure B)

The general reaction profile for the 4-fluorophenylboronic acid **3** SM cross-coupling, **Scheme 3.2.1**, is shown in **Graph 3.2.1**. The boronic acid **3** and the aryl halide **4** were found to be consumed at similar rates over the first three hours – boronic acid **3** = 2.26 x 10^{-4} M min^{-1}, aryl halide **4** = 1.88 x 10^{-4} M min^{-1}, and the reaction reached completion after approximately 5 hours. The starting concentration of boronic acid **3** was found to be consistent but slightly higher than expected, i.e. it should be 0.04 M but starting concentration in **Graph 3.2.1** is 0.049 M. This is due to the fact that the majority of the boronic acid **3** being added to the reaction mixture is actually boroxine, confirmed by elemental analysis, **Fig 3.2.4**. Despite this increased concentration, the boronic acid **3** is fully consumed, as it also undergoes side product formation throughout the reaction, leaving a small amount (less than 0.005 M) of aryl halide **4** unreacted at the end of the reaction.

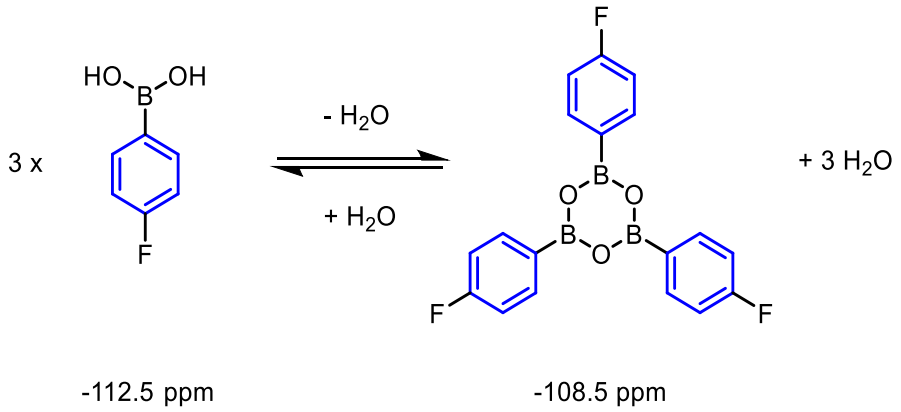

Element	Carbon / %	Hydrogen / %
Expected for boronic acid **3**	51.50	4.32
Found	58.65	2.97
Boroxine	59.12	3.31

Fig 3.2.4 – Elemental analysis results for the 4-fluorophenylboronic acid **3**

3.2.1.1. Side products

There are several side products formed during a SM cross-coupling reaction, **Fig 3.2.5**. Three of the four shown below are formed from the boronic acid **3**, which can undergo homocoupling to form a biaryl **6** (−116.99 ppm), or oxidation to form a phenol **8** (fluorophenol = −128.24 ppm). The boronic acid **3** can also undergo protodeboronation, resulting in the formation of fluorobenzene **9** (−114.52 ppm). The other side product is protodebromination of the aryl bromide **10** (−63.42 ppm).[3–5] Side products are discussed further in **Chapter 1, Section 1.2.3**.

Boronic acid homocoupling	Fluorophenol	Protodeboronation	Protodebromination
6	**8**	**9**	**10**
-116.99 ppm	-128.24 ppm	-114.52 ppm	-63.42 ppm

Fig 3.2.5 – Side products of the SM reaction of 4-fluorophenylboronic acid **3** with 1,3-bis(trifluoromethyl)-5-bromobenzene **4** and ^{19}F NMR chemical shifts

The two main side products formed throughout the reaction are from boronic acid homocoupling **6** and oxidation **8**. Early studies of the SM reaction did not form fluorobenzene **9** from protodeboronation, only later studies discussed in **Chapter 4**, and even then the amount of protodeboronation was minimal (~1%). The amount of protodebromination **10** in the reaction is also minimal (less than 1%) and traces of this material are found in the aryl halide **4** starting material. Small amounts are formed during the reaction, but due to its chemical shift (−63.42 ppm), between the aryl halide **4** (−63.48 ppm) and product peak **5** (−63.29 ppm), it can be difficult to monitor, **Fig 3.2.6**.

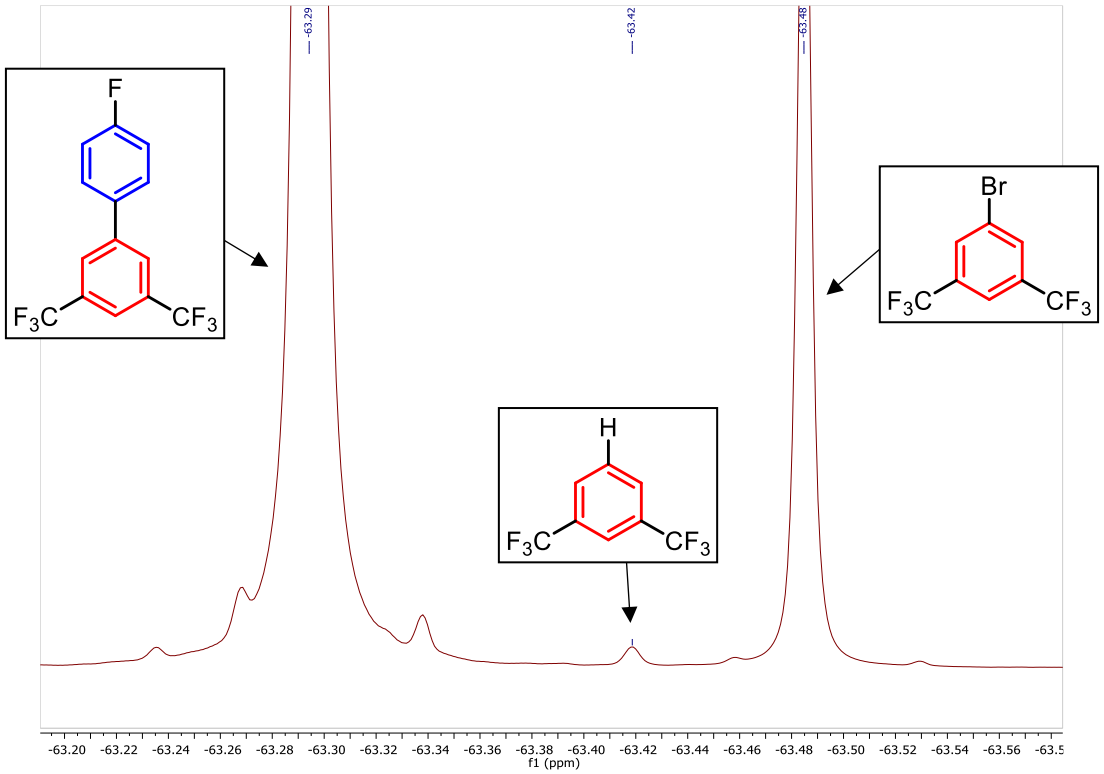

Fig 3.2.6 – ^{19}F NMR spectrum of the trifluoromethyl region of the SM coupling of 4-fluorophenylboronic acid **3** (0.04 M) with 1,3-bis(trifluoromethyl)-5-bromobenzene **4** (0.04 M) with 1-fluoronaphthalene as an internal standard

3.2.2. Scale effects

Originally, the reaction was carried out on a 0.2 mmol scale (5 mL) to allow samples (0.5 mL) to be taken every hour, for 7 hours, to monitor the progress of the reaction. In order to determine the initial rate of reaction the first hour needed to be studied in more depth, so the reaction was adapted to a 0.4 mmol scale (10 mL) to allow for more aliquots to be taken. The

change in the rate of reaction is negligible as a result of the change in the scale; initial rates, 0.2 mmol = 1.68 x 10^{-4} M min^{-1}, 0.4 mmol = 1.69 x 10^{-4} M min^{-1}, **Graph 3.2.2**.

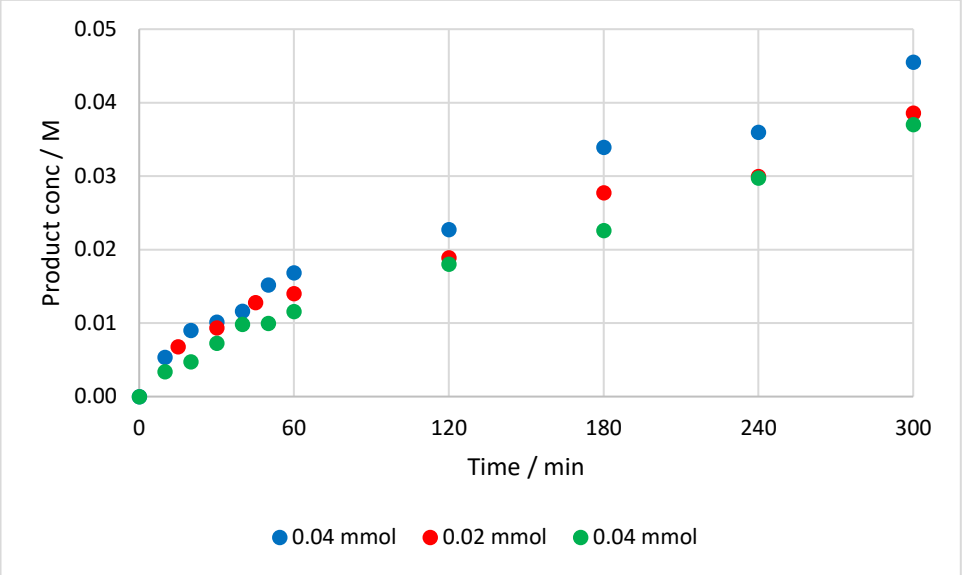

Graph 3.2.2 – Product **5** formation for the SM reaction of 4-fluorophenylboronic acid **3** (0.04 M) with 1,3-bis(trifluoromethyl)-5-bromobenzene **4** (0.04 M) sampled over 5 hours and analysed by ^{19}F NMR with 1-fluoronaphthalene as an internal standard. Three separate reactions sampled – two at 0.4 mmol and one at 0.2 mmol. (Procedure A)

3.2.3. Reaction variables

It is reported in the literature that rates for biphasic reactions can often be affected by stirring rate and vessel size.[2,6] To investigate the importance of these variables, reactions usually carried out at 750 rpm stirring in a 30 mL Schleck flask (20 mm diameter) were compared to those carried out at 250 rpm stirring in a 30 mL Schlenk flask (20 mm diameter) and at 750 rpm stirring in a 25 mL round bottom flask (RBF), **Graph 3.2.3**. All reactions were carried out with the same size stirrer bar.

The reduction of stirring rate gave a considerable drop in the rate of reaction, 2.82 x 10^{-4} M min^{-1} for 750 rpm compared to 6.50 x 10^{-5} M min^{-1} for 250 rpm, as expected for a biphasic reaction where phase transfer is important, **Graph 3.2.3**. A faster stirring rate would increase the exchange and interaction of the two phases, therefore, increasing the rate of reaction.

When the reaction was carried out in an RBF (750 rpm), the rate of reaction was also found to decrease considerably to 9.00 x 10^{-5} M min^{-1}, **Graph 3.2.3**.

To establish whether reaction aliquots continue to react in the NMR tube, a sample was taken and monitored via NMR with the probe pre-heated to 55 °C, then compared to a reaction being stirred and sampled periodically. It was found that the rate of reaction of the sample in the NMR was much slower compared to the standard reaction being stirred in a Schlenk flask, **Graph 3.2.3**. This shows that while the reaction aliquot does continue to react it does so at a much slower rate, 5.00 x 10^{-5} M min^{-1}, providing further evidence of the importance of mixing the biphasic solution.

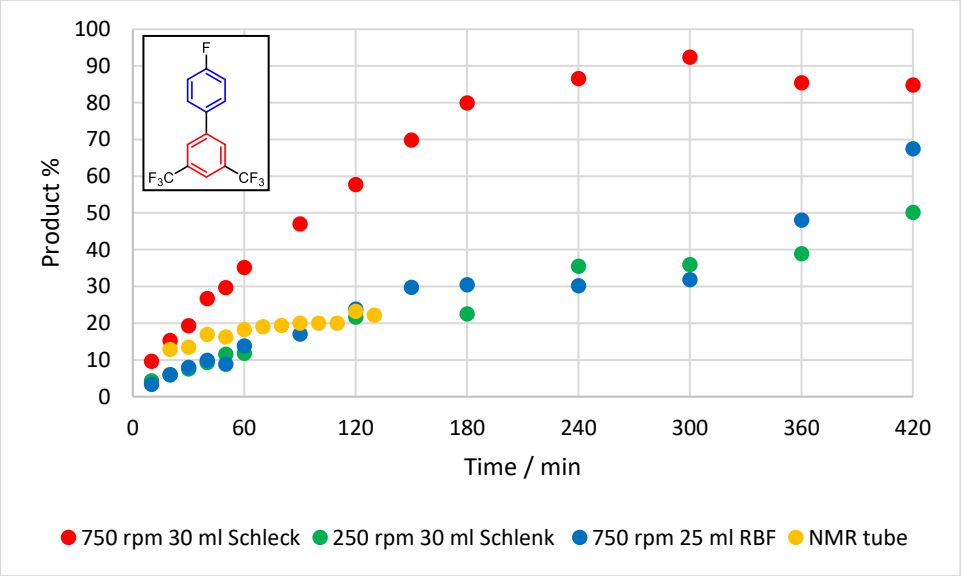

Graph 3.2.3 – Product **5** formation for the SM reaction of 4-fluorophenylboronic acid **3** (0.04 M) with 1,3-bis(trifluoromethyl)-5-bromobenzene **4** (0.04 M) sampled over 7 hours and analysed by ^{19}F NMR with 1-fluoronaphthalene as an internal standard. Impact of changing stirring rate/vessel size

	Initial rate / M min^{-1}	% product **5** conversion	% total side products	% BA homocoupling **6**	% fluorophenol **8**
750 rpm 30 mL Schlenk flask	2.82 x 10^{-4}	85	14	7	7
250 rpm 30 mL Schlenk flask	6.50 x 10^{-5}	50	4	2	2
750 rpm 25 mL RBF	9.00 x 10^{-5}	66	12	6	6
NMR tube (3 hours)	5.00 x 10^{-5}	22	5	2.5	2.5

Fig 3.2.7 – Impact of changing stirring rate/vessel size in the SM reaction of 4-fluorophenylboronic acid **3** (0.04 M) with 1,3-bis(trifluoromethyl)-5-bromobenzene **4** (0.04 M) sampled over 7 hours by ^{19}F NMR with 1-fluoronaphthalene as an internal standard. (Graphs – Appendix 8.3.1)

3.3. Boronic acid vs boronic esters

3.3.1. Pinacol ester

The SM cross-coupling reaction of the pinacol ester **1**, **Scheme 3.3.1**, is shown in **Graph 3.3.1**. In addition to monitoring the product **5** formation, the *in situ* hydrolysis of the ester **1** can be followed, **Graph 3.3.1 insert**. This shows only small amounts of the boronic acid **3** is formed during the reaction, and the ester **1** is fully consumed after 3 hours.

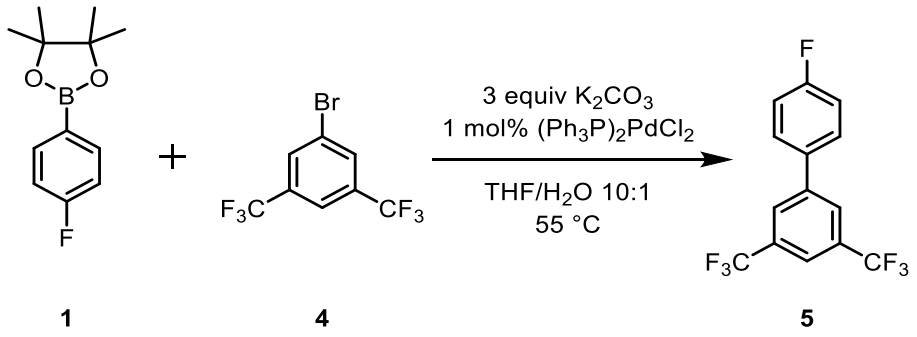

1 **4** **5**

Scheme 3.3.1 – SM reaction of pinacol ester **1** (1 equiv.) with 1,3-bis(trifluoromethyl)-5-bromobenzene **4** (1 equiv.) monitored over 7 hours and analysed by ^{19}F NMR with 1-fluoronaphthalene as an internal standard.

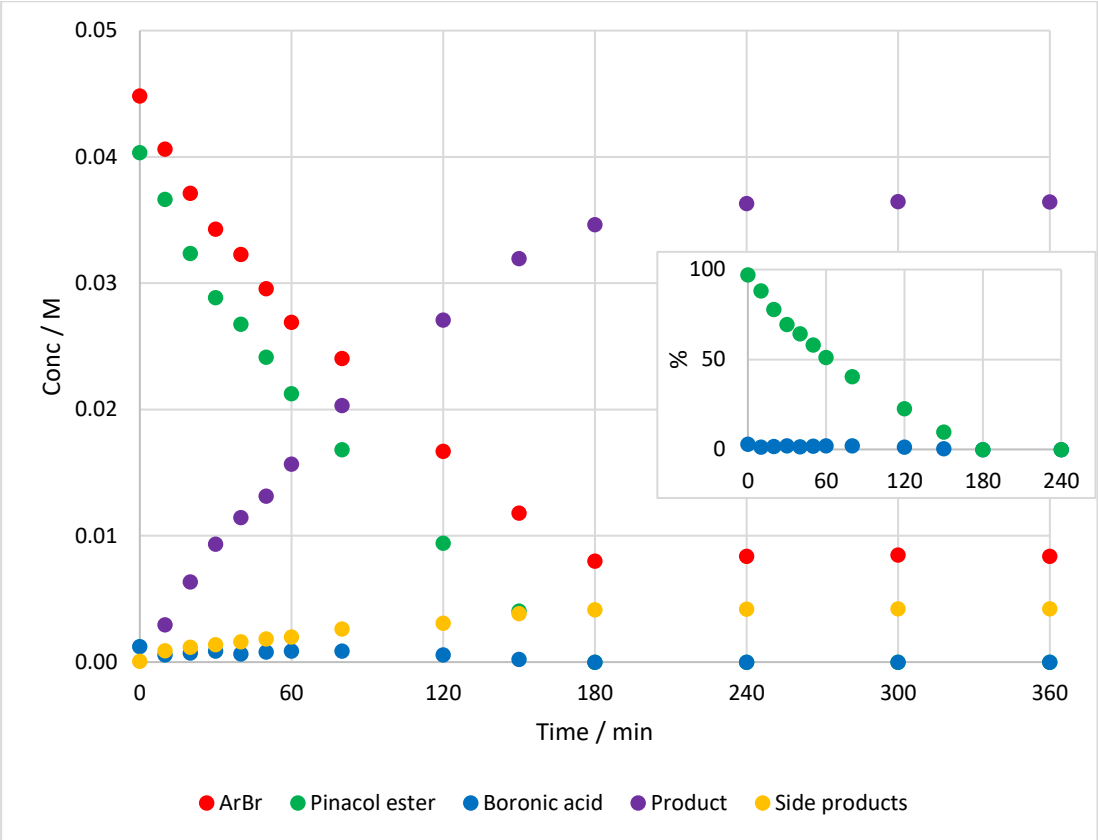

Graph 3.3.1 – SM coupling profile of pinacol ester **1** (0.04 M) with 1,3-bis(trifluoromethyl)-5-bromobenzene **4** (0.045 M) sampled over 7 hours and analysed by ^{19}F NMR with 1-fluoronaphthalene as an internal standard. Insert graph shows *in situ* hydrolysis of pinacol ester **1**. (Procedure B)

3.3.2. Neopentyl glycol ester

The SM cross-coupling reaction of the neopentyl glycol ester **2** under the standard coupling condition, **Scheme 3.3.2**, is shown in **Graph 3.3.2**. In addition to monitoring the product **5** formation, the *in situ* hydrolysis of the ester **2** can be followed, **Graph 3.3.2 insert**. The t0 sample shows a large amount of boronic acid **3** is present, due to the rapid hydrolysis of the glycol ester **2**. The first reaction sample then shows an increase in the amount of glycol ester present, relative to the t0 sample. This indicates that the two boron species present in the reaction are being consumed at different rates, by either SM coupling or ester hydrolysis, which affects the ester to acid ratio throughout the reaction. Following the reaction, both the boronic acid **3** and glycol ester **2** decrease over time until fully consumed at 3 hours.

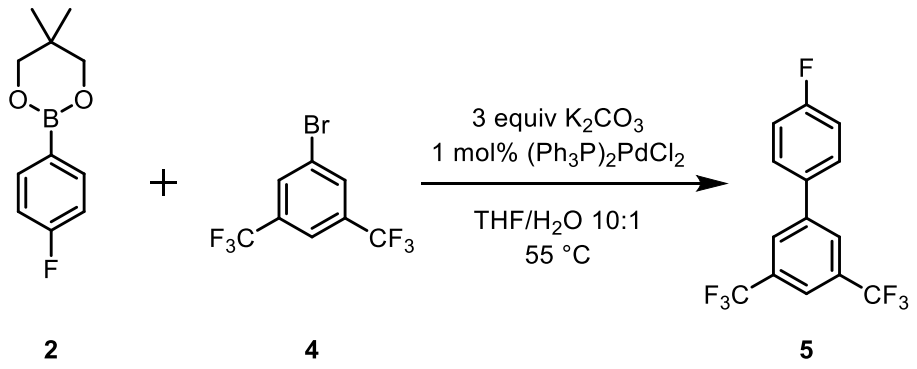

2 **4** **5**

Scheme 3.3.2 – SM reaction of neopentyl glycol ester **2** (1 equiv.) with 1,3-bis(trifluoromethyl)-5-bromobenzene **4** (1 equiv.) monitored over 7 hours and analysed by ^{19}F NMR with 1-fluoronaphthalene as an internal standard.

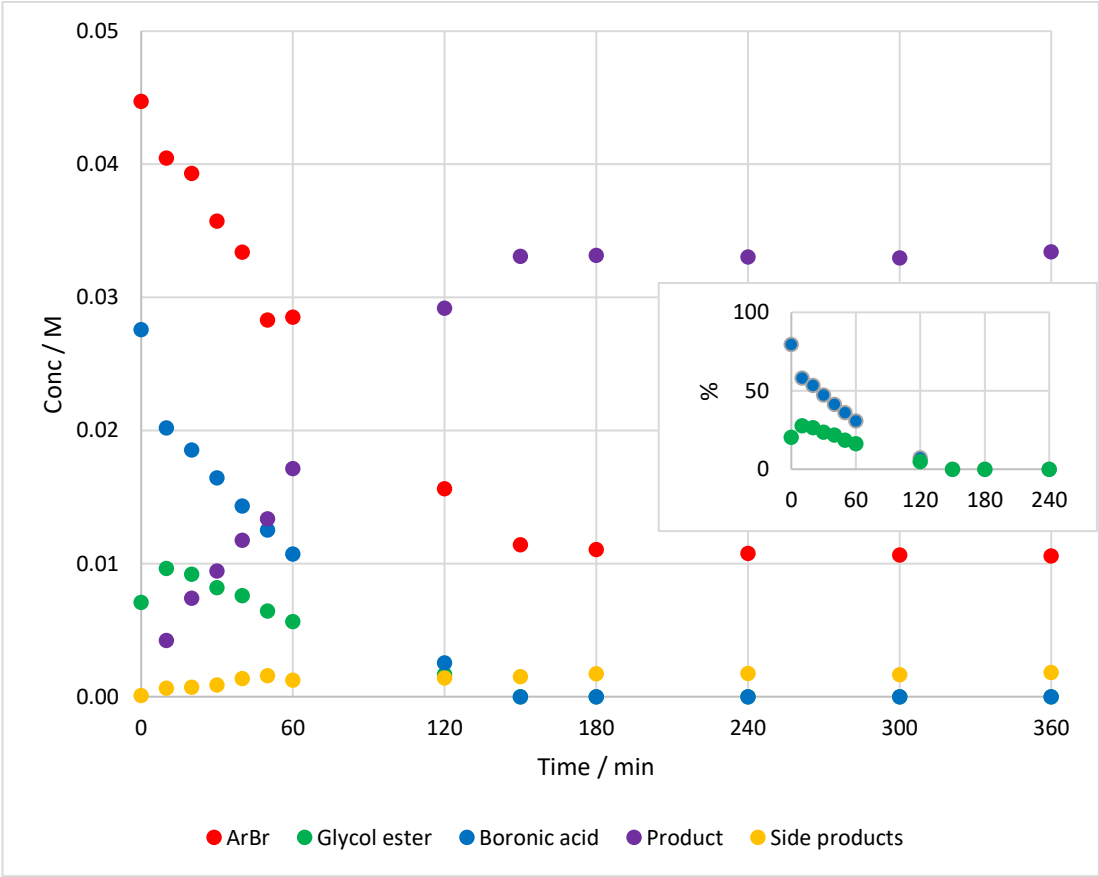

Graph 3.3.2 – SM coupling profile of neopentyl glycol ester **2** (0.035 M) with 1,3-bis(trifluoromethyl)-5-bromobenzene **4** (0.045 M) sampled over 7 hours and analysed by ^{19}F NMR with 1-fluoronaphthalene as an internal standard. Insert graph shows *in situ* hydrolysis of neopentyl glycol ester **2**. (Procedure B)

3.3.3. Comparison

The initial rate of coupling for the three different reactions is comparable; boronic acid = 1.90 x 10^{-4} M min^{-1}, pinacol ester = 1.86 x 10^{-4} M min^{-1}, glycol ester = 2.08 x 10^{-4} M min^{-1}, **Graph 3.3.3**. All three reactions reach a product generation of ~85% after 4 hours, **Graph 3.3.4**. Despite the different rates of hydrolysis between the two esters studied, this does not affect the rate of cross-coupling, as the turnover-limiting step is phase-transfer for all three reactions.

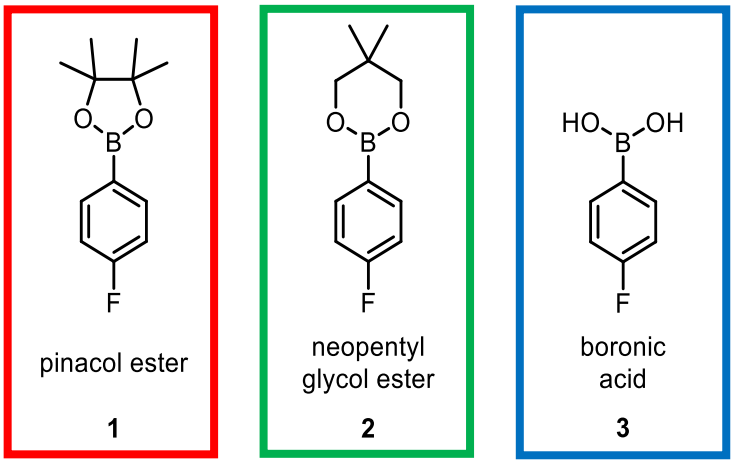

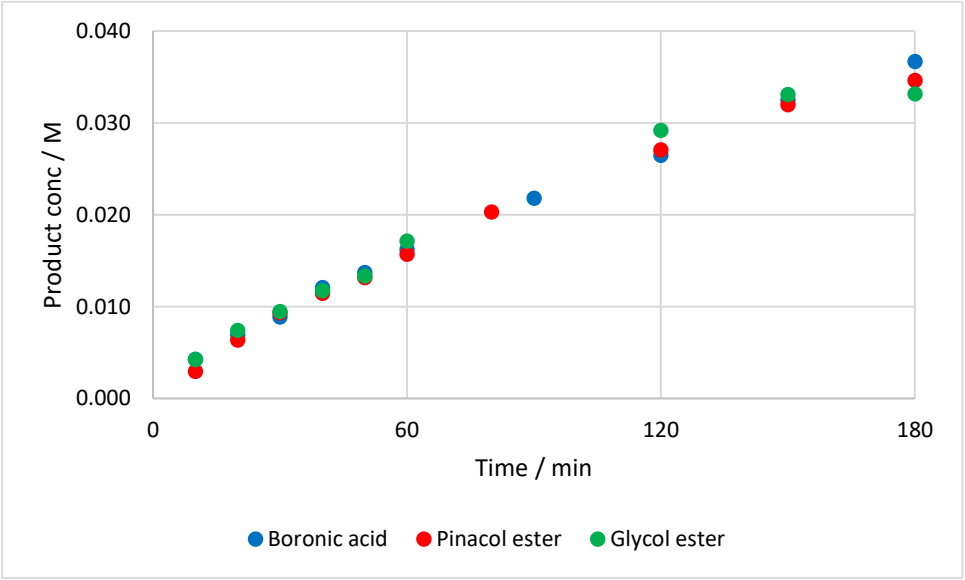

Graph 3.3.3 – Product **5** concentration for the SM cross-coupling of boronic acid **3**/ester **1**/**2** (0.04 M) with 1,3-bis(trifluoromethyl)-5-bromobenzene **4** (0.04 M) sampled and analysed by ^{19}F NMR with 1-fluoronaphthalene as an internal standard.

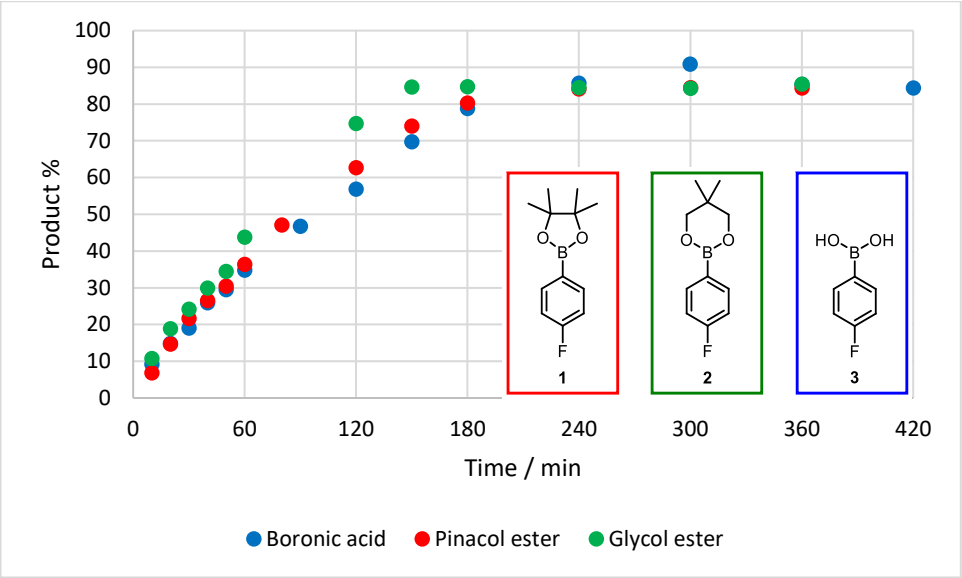

Graph 3.3.4 – Product **5** percentage for the SM cross-coupling of boronic acid **3**/ester **1**/**2** (0.04 M) with 1,3-bis(trifluoromethyl)-5-bromobenzene **4** (0.04 M) sampled and analysed by ^{19}F NMR with 1-fluoronaphthalene as an internal standard.

While the reactions give the same rate of product conversion, the three do differ in terms of the amount of side products produced throughout the reaction, **Graph 3.3.5**. The two major side products formed result from boronic acid homocoupling **6** and boronic acid oxidation to fluorophenol **8**. The boronic acid **3** reaction produces the most side products, 20%, followed by the pinacol ester **1**, 15%. The neopentyl glycol ester **2** reaction produces the least amount of side products of the three, 7%.

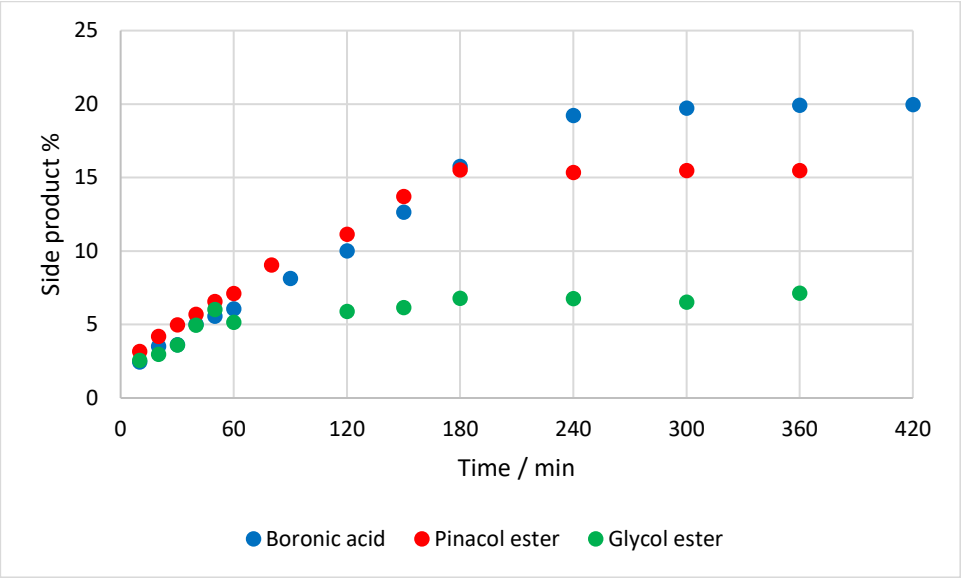

Graph 3.3.5 – Side product (**6** & **8**) formation comparison from the SM cross-coupling of boronic acid **3**/ester **1**/**2** (0.04 M) with 1,3-bis(trifluoromethyl)-5-bromobenzene **4** (0.04 M) sampled and analysed by ^{19}F NMR with 1-fluoronaphthalene as an internal standard. (Individual side product formation graphs – Appendix 8.3.2)

3.4. Conclusion

The fact that the boronic acid **3** reaction and two ester **1**/**2** reactions all give the same rate of coupling is likely a consequence of phase-separation, rendering phase transfer the turnover-limiting process. The fact that reaction rate is dependent to stirring rate supports this hypothesis. To be able to study transmetalation, the conditions need to be adapted to maintain a homogenous system using an alternative organic soluble base.

3.5. References

(1) Butters, M.; Harvey, J. N.; Jover, J.; Lennox, A. J. J.; Lloyd-Jones, G. C.; Murray, P. M. *Angew. Chem Int. Ed.* **2010**, *49* (30), 5156–5160.

(2) Lennox, A. J. J.; Lloyd-Jones, G. C. *Angew. Chem Int. Ed.* **2013**, *52* (29), 7362–7370.

(3) Labre, F.; Gimbert, Y.; Bannwarth, P.; Olivero, S.; Duñach, E.; Chavant, P. Y. *Org. Lett.* **2014**, *16* (9), 2366–2369.

(4) Laulhé, S.; Blackburn, J. M.; Roizen, J. L. *Chem. Commun.* **2017**, *53* (53), 7270–7273.

(5) Jedinák, L.; Zátopková, R.; Zemánková, H.; Šustková, A.; Cankař, P. *J. Org. Chem.* **2017**, *82* (1), 157–169.

(6) Lennox, A. J. J.; Lloyd-Jones, G. C. *J. Am. Chem. Soc.* **2012**, *134* (17), 7431–7441.

Chapter 4

The search for homogeneous, reproducible conditions

4.1. Background

While the SM reaction is typically carried out using an inorganic base, there are reports using organic bases instead, with the most common organic base tested being triethylamine. The use of triethylamine does not always give efficient coupling when compared to an inorganic base, reportedly due to precipitation of palladium black and/or decomposition of the boronic acid starting material.[1–5] A study by Wang *et al.* on the coupling of 4-nitrochlorobenzene and phenylboronic acid found that triethylamine gave only trace amounts of SM cross-coupled product, while potassium carbonate, an inorganic base, gave 90% yield.[6] DMAP (4-dimethylaminopyridine), another organic base, was also tested in this study and found to be completely inactive. Sajiki *et al.* found triethylamine to give a 45% yield, sodium carbonate to give 98% yield, while DABCO (1,4-diazabicyclo[2.2.2]octane) yielded no product, when studying the coupling of 4-nitrobromobenzene and phenyl boronic acid.[7] However, high yields (85%) have been shown for SM cross-coupling of 4-iodoanisole with phenyl boronic acid, carried out using triethylamine in water with Stilbazo as a ligand, **Fig 4.1.1**.[8]

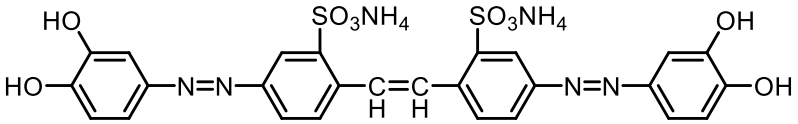

Fig 4.1.1 – The structure of Stilbazo

Despite the lack of reactivity shown when using DABCO as a base, it has been successfully utilised as a ligand for SM cross-coupling. Li *et al.* investigated the copper iodide catalysed SM cross-coupling of 1-iodoanisole and phenylboronic acid, using caesium carbonate as a base, and found the addition of DABCO as a ligand (20 mol%) improved yield, from 78% to 98%. However, the addition of triethylamine as a ligand (20 mol%) seems to have a detrimental effect, reducing the yield to 66%.[9] Further studies by Li *et al.* in 2007 report copper iodide catalysed SM and Sonogashira cross-coupling reactions using DABCO as a ligand.[10] Without DABCO, the coupling of 2-phenylvinyl iodide and phenyl boric acid using caesium carbonate as a base reaches 63% yield. With the addition of DABCO (20 mol%), the yield increases to 83%.

4.1.1. Superbases

Superbases are defined as being stronger than a 'proton sponge' (DMAN – 1,8-bis(dimethyl-amino)naphthalene); have an absolute proton affinity larger than 245.3 kcal mol^{-1} and gas phase basicity over 239 kcal mol^{-1}.[11]

Common organic bases have a number of issues limiting their use in Pd-catalysed couplings, such as catalyst inhibition, lack of basicity, or decomposition.[12] A 2015 study by Dreher *et al.* explored the use of organic superbases as an alternative to common organic and inorganic bases, providing a strong base while being sterically hindered, limiting catalyst inhibition.[12] The use of superbases was thought to potentially provide a number of key advantages; they would not form Lewis or Brønsted acidic counterion by-products, they would be soluble in a wide range of organic solvents allowing potential homogeneous conditions, there would be opportunity to tune steric and electric properties.

This study investigated the use of four commercially available organic superbases in the reaction between 3-bromopyridine and seven different nucleophiles, including a pinacol boronic ester for SM cross-coupling, **Scheme 4.1.1**. The phosphazene, P_2Et, showed the greatest reactivity of the bases tested, while DBU gave the lowest reactivity of the four.

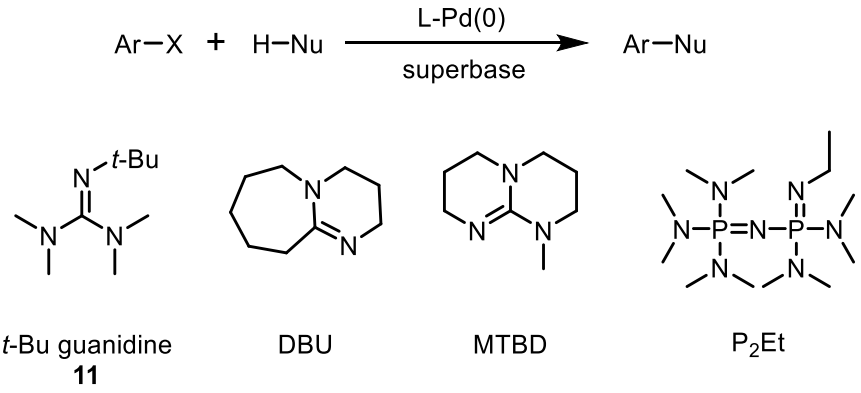

Scheme 4.1.1 – Pd-catalysed cross-coupling reactions using organic superbases

4.1.2. Use as a ligand

In addition to use as a base, some superbases have been shown to be advantageous when used as a ligand in SM cross-couplings. In 2007, Zhang *et al* reported the use of guanidine as a ligand in a palladium acetate-catalysed room temperature SM cross-coupling reaction using potassium carbonate as a base, testing nine different guanidines, **Scheme 4.1.2**.[13] The addition of all of the guanidines studied gave improved reactivity in comparison to the ligand-free

reaction, **Fig 4.1.2**. A complex of palladium acetate with 2-*n*-butyl-1,1,3,3-tetramethylguanidine was formed, isolated, and tested for its activity in a range of SM couplings. It was found to work well at low loadings (0.001 – 2 mol%) and at room temperature, with the exception of aryl chlorides which required higher temperatures (80 °C).

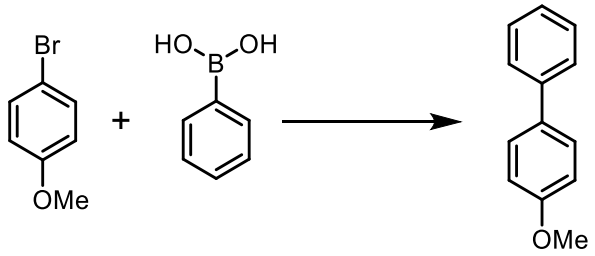

Scheme 4.1.2 – SM coupling. 1.5 mol% $Pd(OAc)_2$, 3.0-6.0 mol% ligand, 1.0 mmol 4-bromoanisole, 1.2 mmol phenylboronic acid, 3.0 mmol K_2CO_3, 3.0 mL CH_3CN, 80 °C, 2 hours.

Ligand	Yield (%)	Ligand	Yield (%)
None	42%	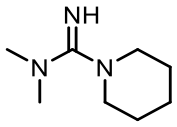	80%
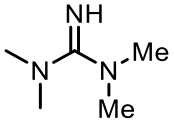	74%	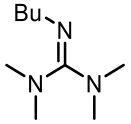	99%
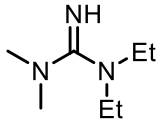	78%	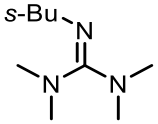	100%
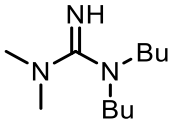	81%	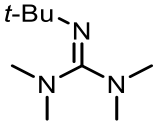	100%
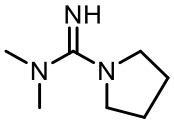	83%	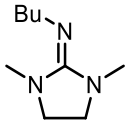	98%

Fig 4.1.2 – Isolated yields from reaction shown in **Scheme 4.1.2**

4.2. Aims of the study

This chapter reports our search to find homogenous SM conditions to facilitate the study of the transmetalation step of the catalytic cycle by ^{19}F NMR. These conditions will then be used to study the difference in reactivity between a boronic acid and two boronic esters. Organic bases will be tested and compared to the more commonly used inorganic bases. In addition, a range of boronic acids and aryl halides will be tested to explore the generality of the newly developed reaction.

4.3. Initial results

4.3.1. General profile

Previous work within our research group showed 2-*tert*-butyl-1,1,3,3-tetramethylguanidine (guanidine **11**) to work well as a base in SM cross-coupling. This is supported by literature,[12,13] and so was the first organic base investigated in this study, **Scheme 4.3.1**. The reaction was monitored by ^{19}F NMR, and a large increase in rate was found by switching the base from potassium carbonate to guanidine **11**. The guanidine **11** reaction was complete within 10 minutes (first spectrum) and was found to give higher conversion with reduced side products, **Graph 4.3.1 & 4.3.2**. The use of guanidine **11** gave product conversion of 98% after 20 minutes compared to 85% after 4 hours with potassium carbonate. Using potassium carbonate the amount of side products obtained at the end of the reaction was 20% (boronic acid homocoupling **6** and oxidation **8**), compared to the guanidine **11** reaction which only produces 3%. There is no fluorophenol **8** formed in the guanidine **11** reaction under these conditions and vastly reduced amounts of the boronic acid homocoupling product **6**.

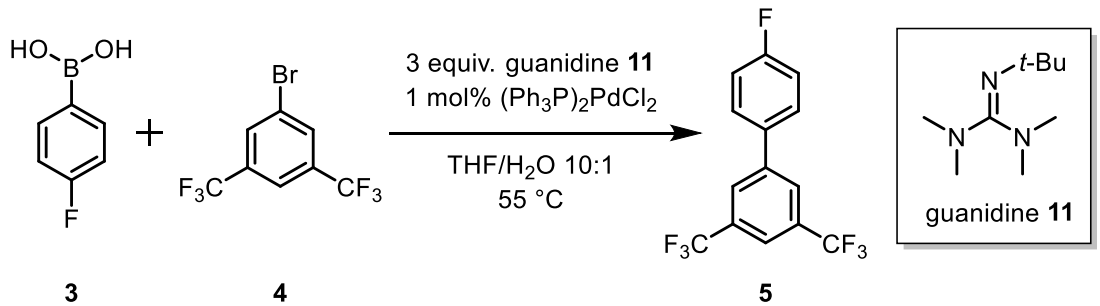

3 -112.7 ppm

4 -63.5 ppm

5 -114.1 ppm / -63.3 ppm

Scheme 4.3.1 – SM cross-coupling of boronic acid **3** (1 equiv.) with 1,3-bis(trifluoromethyl)-5-bromobenzene **4** (1 equiv.) monitored by ^{19}F NMR with 1-fluoronaphthalene as an internal standard, showing ^{19}F NMR chemical shifts

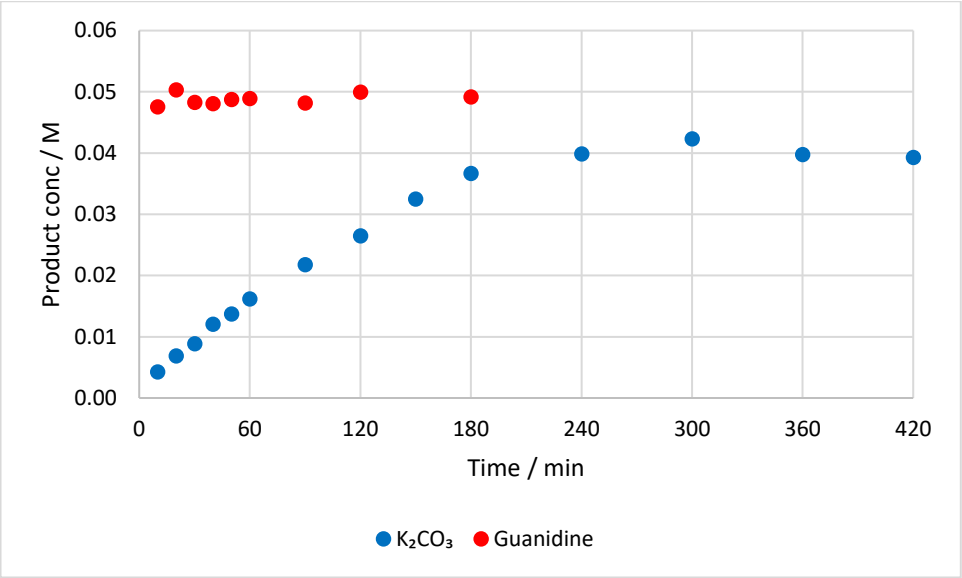

Graph 4.3.1 – Product formation **5** in the SM cross-coupling of boronic acid **3** (0.05 M) with 1,3-bis(trifluoromethyl)-5-bromobenzene **4** (0.05 M) monitored by ^{19}F NMR with 1-fluoronaphthalene as an internal standard. Comparison of the use of potassium carbonate vs guanidine **11** (Procedure B & D)

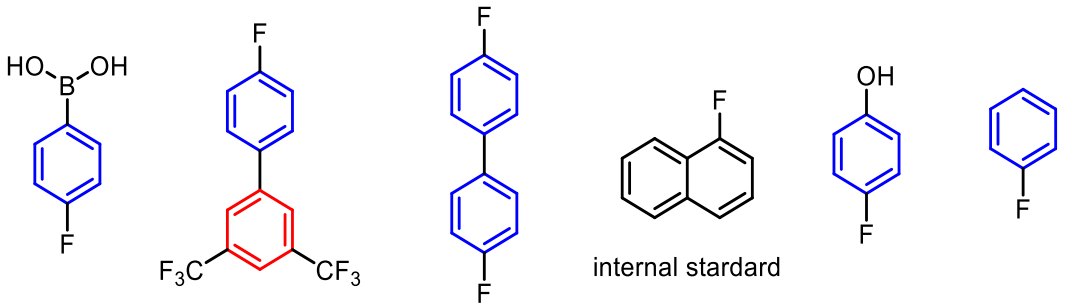

3	**5**	**6**	**7**	**8**	**9**
-112.31 ppm	-113.98 (F) ppm	-116.99 ppm	-124.85 ppm	-128.24 ppm	-114.52 ppm

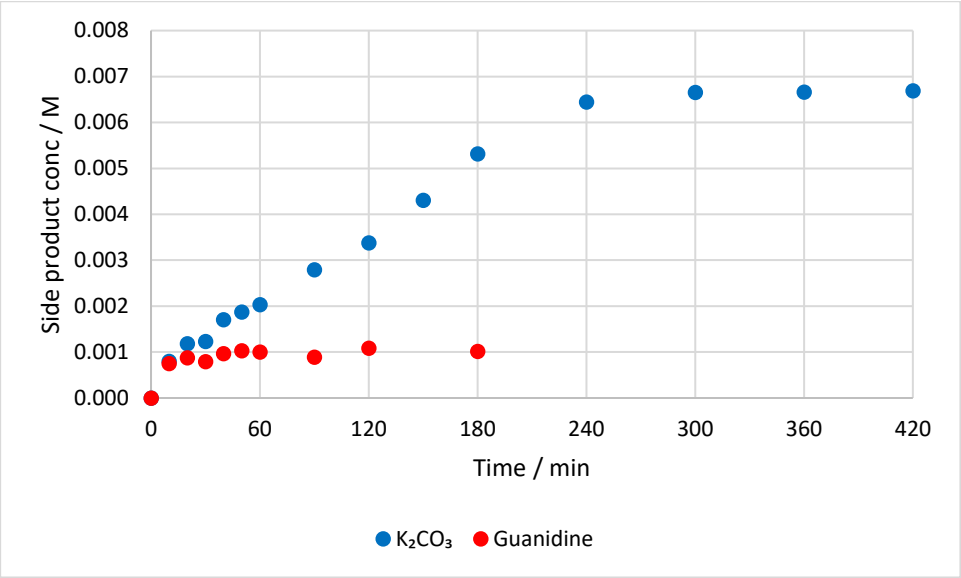

Graph 4.3.2 – Side product formation in the SM cross-coupling of boronic acid **3** (0.05 M) with 1,3-bis(trifluoromethyl)-5-bromobenzene **4** (0.05 M) monitored by ^{19}F NMR with 1-fluoronaphthalene as an internal standard. Comparison of the use of potassium carbonate vs guanidine **11**

To be able to monitor the initial stage of the reaction in more detail the temperature was lowered from 55 °C to 23 °C, **Scheme 4.3.2**, **Graph 4.3.3**. This change in conditions gave a similar rate of reaction as potassium carbonate at 55 °C, (initial rates: K_2CO_3 55 °C = 1.90 x 10^{-4} M min^{-1}, guanidine **11** 23 °C = 1.49 x 10^{-4} M min^{-1}) but the reduction in side product formation was maintained, **Graph 4.3.3**.

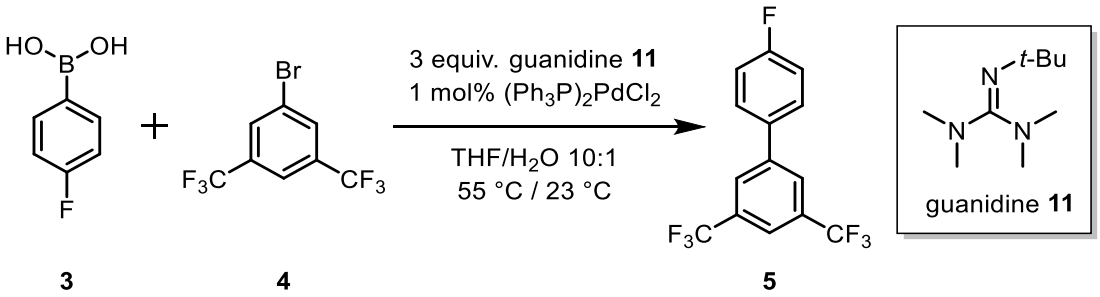

3 **4** **5**

Scheme 4.3.2 – SM cross-coupling of boronic acid **3** (1 equiv.) with 1,3-bis(trifluoromethyl)-5-bromobenzene **4** (1 equiv.) monitored by ^{19}F NMR with 1-fluoronaphthalene as an internal standard.

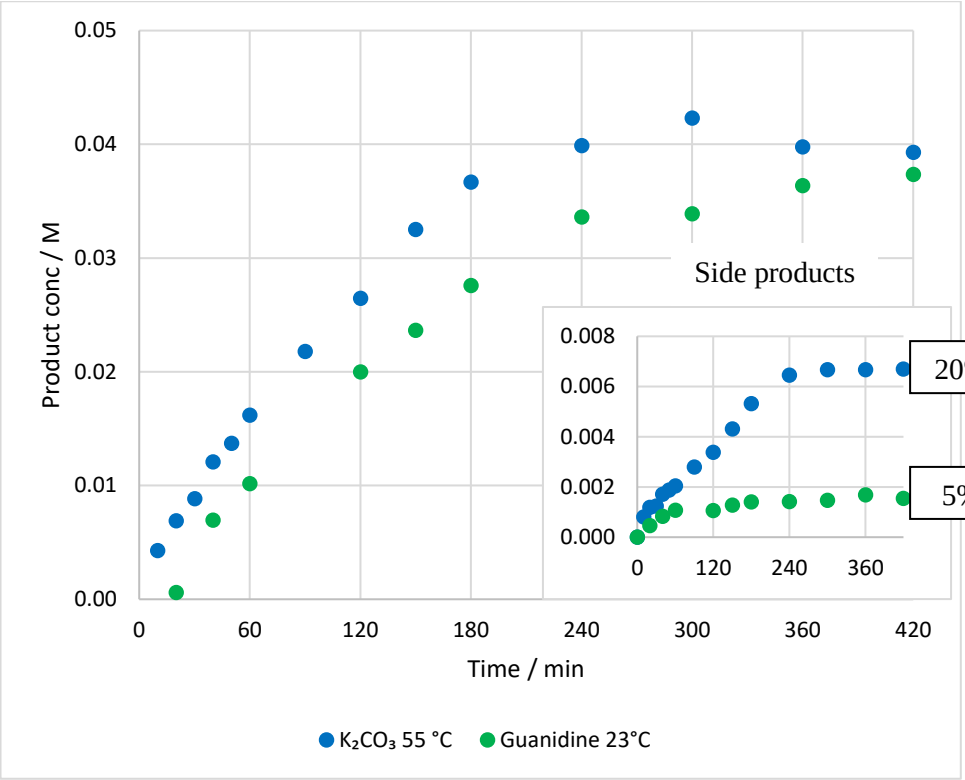

Graph 4.3.3 – Product **5** formation in the SM cross-coupling of boronic acid **3** (0.05 M) with 1,3-bis(trifluoromethyl)-5-bromobenzene **4** (0.04 M) monitored by ^{19}F NMR with 1-fluoronaphthalene as an internal standard. Comparison of potassium carbonate at 55 °C vs guanidine **11** at 23 °C. Insert graph shows side product formation. (Procedure B & D)

Lowering the temperature of the guanidine **11** reaction also revealed a large loss in total fluorine concentration by ^{19}F NMR, compared to a t_0 sample without base, using 1-fluoronaphthalene as an internal standard, **Graph 4.3.4**. By having both starting materials labelled with fluorine, all products formed and starting material consumed should be observed and tracked by ^{19}F NMR. But at the first data point (20 minutes) the total signal present in the sample was representative of only of 51% of the total concentration. The "missing" signal was attributed to have originated form the boronic acid **3**, as this was the only peak to be significantly affected by the addition of guanidine **11**, **Fig 4.3.1**. As the reaction reaches completion, the total signal increases, as the unseen boronic acid **3** is consumed and product **5** is formed, and all other peaks are unaffected by the presence of guanidine **11**. Furthermore, the use of guanidine **11** creates a new peak at −121 ppm, which has been assigned to a boronate complex, **Scheme 4.3.3**, and will be discussed in more detail in **Chapter 5 – Boronate formation**.

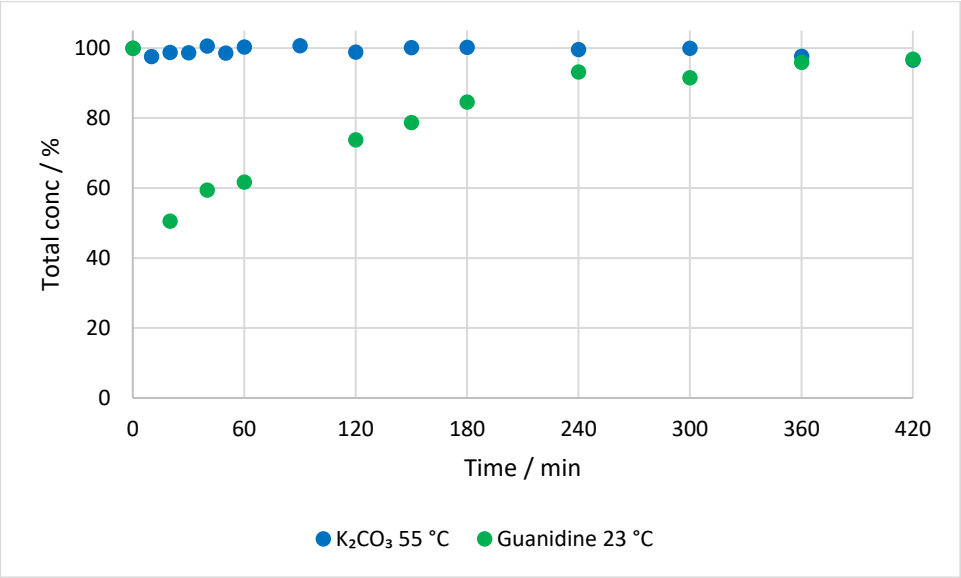

Graph 4.3.4 – Total detected concentration (^{19}F) in the SM cross-coupling of boronic acid **3** (0.05 M) with 1,3-bis(trifluoromethyl)-5-bromobenzene **4** (0.04 M) monitored by NMR with 1-fluoronaphthalene as an internal standard. Comparison of potassium carbonate at 55 °C vs guanidine **11** at 23 °C

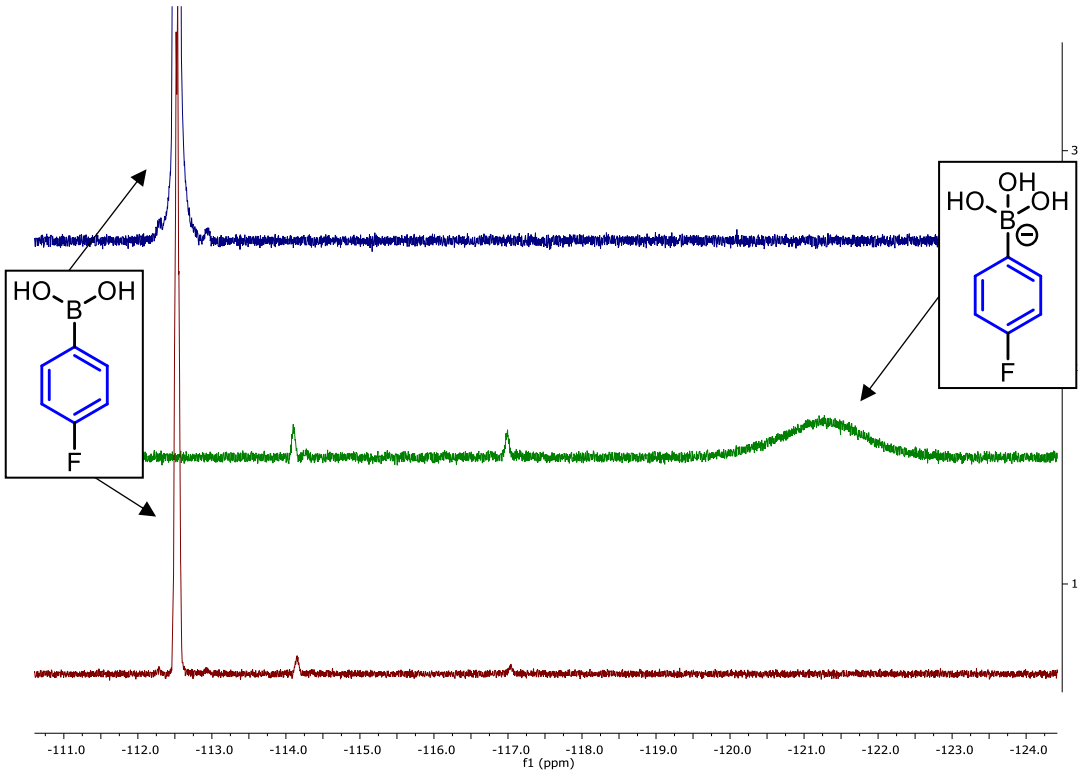

Fig 4.3.1 – Boronic acid region of SM cross-coupling of boronic acid **3** (0.05 M) with 1,3-bis(trifluoromethyl)-5-bromobenzene **4** (0.04 M). ^{19}F NMR with 1-fluoronaphthalene as an internal standard (−125 ppm). Top spectrum before addition of guanidine **11** shows boronic acid **3** signal −112 ppm. Middle spectrum after addition of guanidine **11** shows boronate signal −121 ppm, and additional peaks at −114 ppm and −117 ppm (discussed in **Chapter 5**). Bottom spectrum after acetic acid quench shows boronic acid **3** signal −112 ppm.

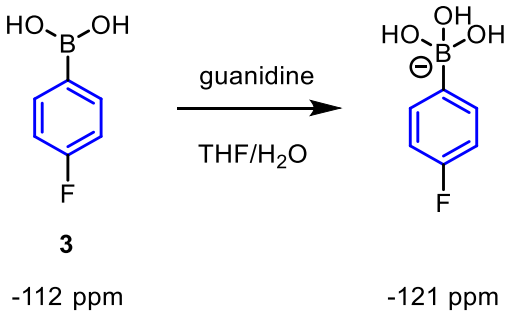

Scheme 4.3.3 – Boronate formation

Quenching the boronate

Given the broadening of the boronic acid **3** to boronate peak, the amount of starting material in the reaction could not be followed. However, quenching with glacial acetic acid allowed the boronic acid **3** signal to be monitored. This quench also ensured the sample was representative of a specific time point and allowed for all components of the reaction to be monitored, **Graph 4.3.5**.

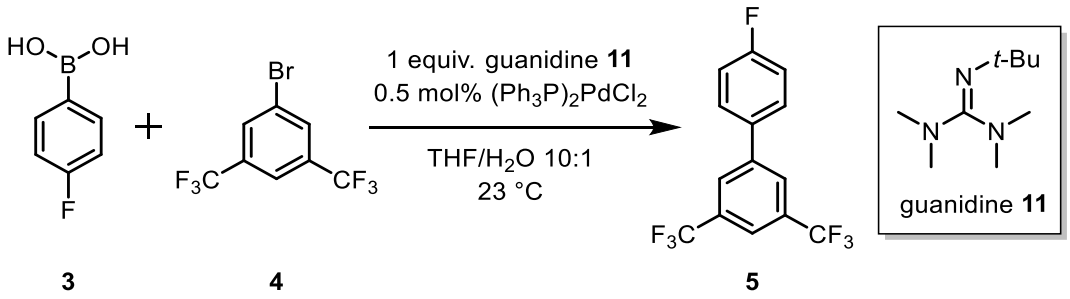

3 **4** **5**

Scheme 4.3.4 – SM cross-coupling of boronic acid **3** (1 equiv.) with 1,3-bis(trifluoromethyl)-5-bromobenzene **4** (1 equiv.) monitored by ^{19}F NMR with 1-fluoronaphthalene as an internal standard.

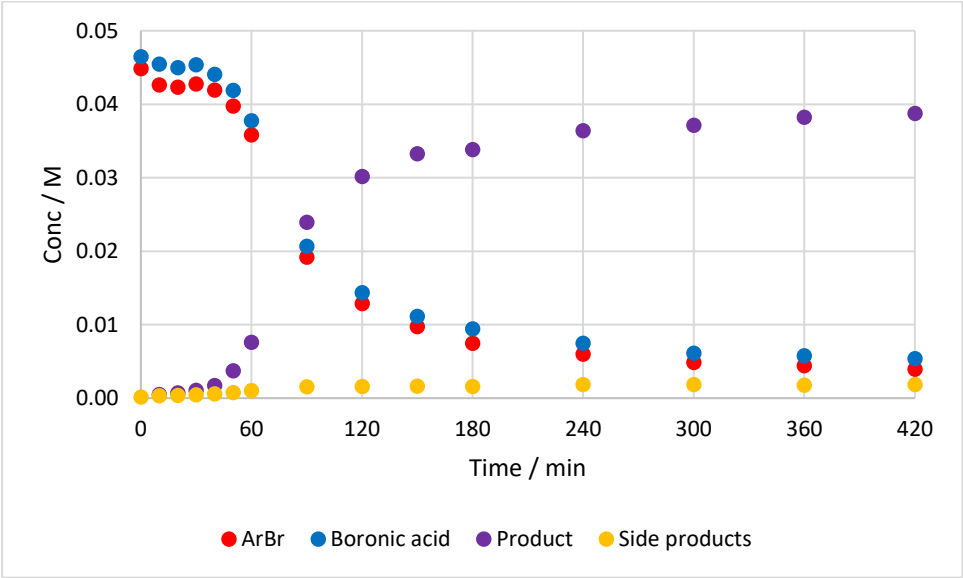

Graph 4.3.5 – SM cross-coupling of boronic acid **3** (0.047 M) with 1,3-bis(trifluoromethyl)-5-bromobenzene **4** (0.045 M) monitored by ^{19}F NMR with 1-fluoronaphthalene as an internal standard (Procedure E)

4.3.2. Homogenous system

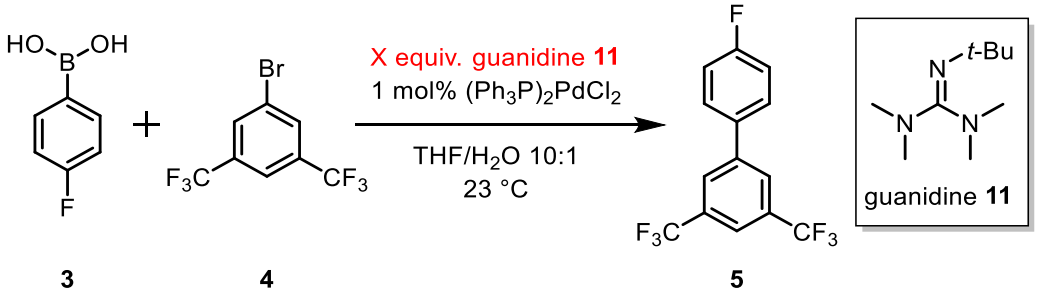

3 **4** **5**

Scheme 4.3.5 – SM cross-coupling of boronic acid **3** (1 equiv.) with 1,3-bis(trifluoromethyl)-5-bromobenzene **4** (1 equiv.) monitored by ^{19}F NMR with 1-fluoronaphthalene as an internal standard.

While the use of guanidine **11** had greatly reduced side product formation, it was found that three equivalents, relative to the boronic acid **3**, still created a biphasic reaction mixture. If all the other components of the reaction are mixed together in 10:1 THF/water, the solution is homogenous. It is only upon addition of the base, guanidine **11**, that a phase separation occurs. To be able to study the transmetalation step of the reaction a homogeneous system was needed, which could be achieved by lowing the concentration of guanidine **11** used, **Scheme 4.3.5**. Lowering the guanidine **11** was found to increase the rate of reaction, **Graph 4.3.6**. Reactions using one or two equivalents were found to give similar rate of reaction, while the reaction using half an equivalent gave the fastest rate, but only reached 50% conversion. But while lowering the base increased the rate of product formation, reactions employing 0.5 or 1 equiv. guanidine **11** produced more side products, now including the formation of fluorophenol **8**, **Fig 4.3.2**.

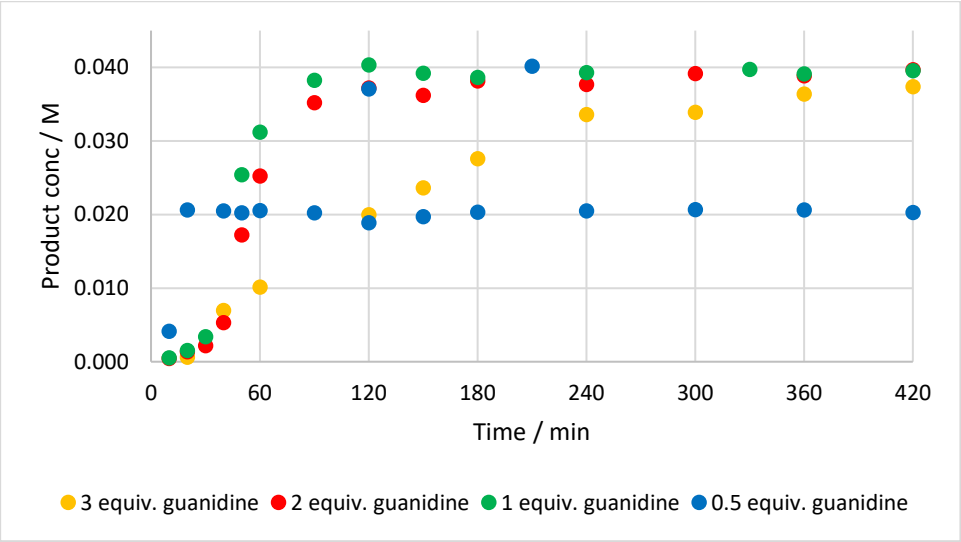

Graph 4.3.6 – Product **5** formation in the SM cross-coupling of boronic acid **3** (0.04 M) with 1,3-bis(trifluoromethyl)-5-bromobenzene **4** (0.04 M) using different equivalents of guanidine, monitored by ^{19}F NMR with 1-fluoronaphthalene as an internal standard. (Procedure D)

Equiv. guanidine	% Product **5**	% total side products	% boronic acid homocoupling **6**	% fluorophenol **8**
3	88%	6%	6%	0%
2	88%	4%	4%	0%
1	85%	7%	4%	3%
0.5	45%	5%	3%	2%

Fig 4.3.2 – Product **5** and side product conversion after 7 hours, in the SM cross-coupling of boronic acid **3** (0.04 M) with 1,3-bis(trifluoromethyl)-5-bromobenzene **4** (0.04 M) using different equivalents of guanidine **11**, monitored by ^{19}F NMR with 1-fluoronaphthalene as an internal standard.

To establish if the system was truly homogeneous, a sample was taken from a reaction and monitored *in situ via* NMR, then compared to the bulk reaction solution being stirred and sampled periodically. The reaction using two equivalents of guanidine **11** was found to give a different conversion and rate between the NMR sample and the stirred reaction mixture, and the NMR sample showed a longer induction period, suggesting there is still a phase spilt

present, **Graph 4.3.7**. When using only one equivalent of guanidine **11**, the two sets of data overlap very well, showing this to be a one phase system, **Graph 4.3.8**. Using half an equivalent of guanidine **11** also showed to be a one phase system, but the fast rate and limited conversion make it an unsuitable system to study.

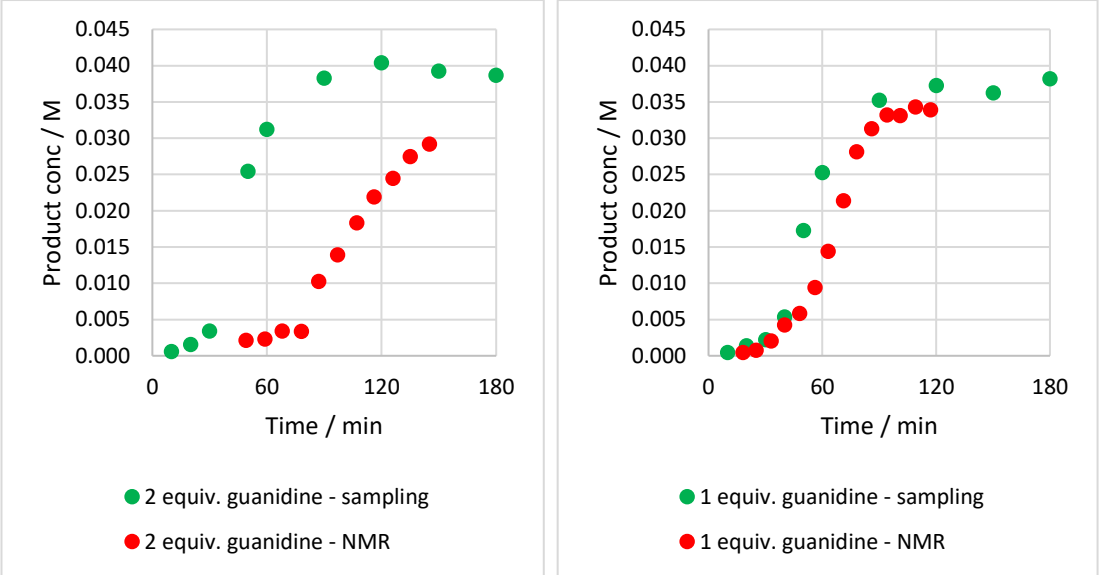

Graph 4.3.7 & 4.3.8 – Product **5** formation in the SM cross-coupling of boronic acid **3** (0.04 M) with 1,3-bis(trifluoromethyl)-5-bromobenzene **4** (0.04 M) monitored by ^{19}F NMR with 1-fluoronaphthalene as an internal standard. Using 2 or 1 equiv. guanidine **11**.

4.4. Cross-Coupling

4.4.1. Boronic acid vs boronic esters

Under the new homogenous conditions, independent reactions were carried out for the boronic acid **3**, pinacol ester **1** and neopentyl glycol ester **2** cross-coupling reactions, **Scheme 4.4.1**, **Graph 4.4.1**. There now appears to be differences in the rate of product **5** formation between the three reactions, but as the reaction is complete by approximately one hour, it is difficult to say how different the three reactions truly are. For this reason, the catalyst loading was lowered to slow the reaction down and study the initial rates in more detail.

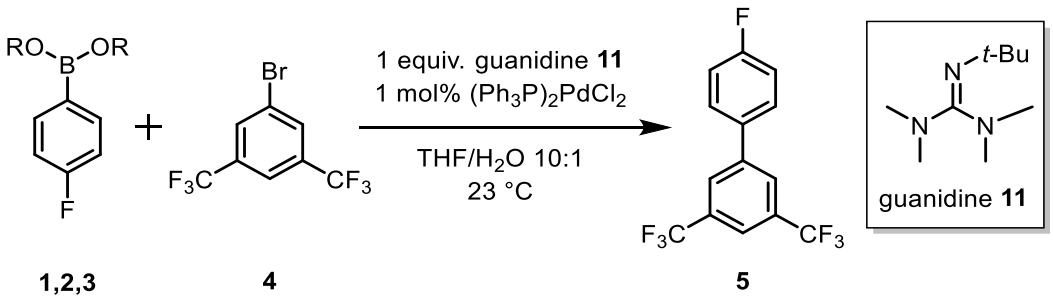

1,2,3 **4** **5**

Scheme 4.4.1 – SM cross-coupling of boronic acid **3**/ester **1**/**2** (1 equiv.) with 1,3-bis(trifluoromethyl)-5-bromobenzene **4** (1 equiv.) monitored by ^{19}F NMR with 1-fluoronaphthalene as an internal standard

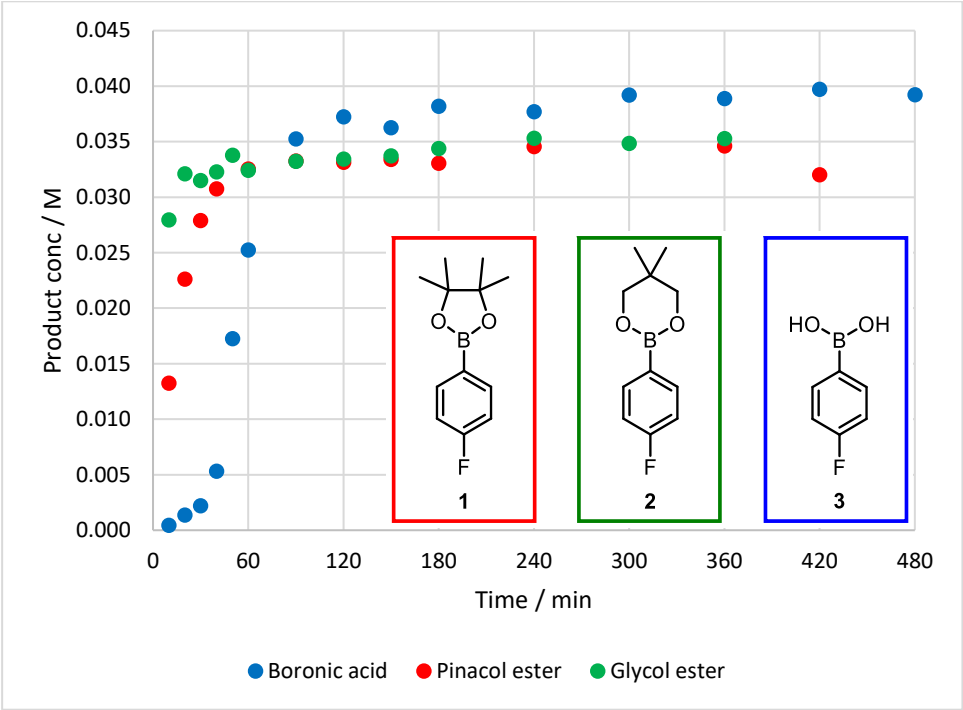

Graph 4.4.1 – SM cross-coupling of boronic acid **3**/ester **1**/**2** (0.04 M) with 1,3-bis(trifluoromethyl)-5-bromobenzene **4** (0.04 M) monitored by ^{19}F NMR with 1-fluoronaphthalene as an internal standard. (Procedure D)

Lower catalyst loading

Lowering the catalyst loading from 1 mol% to 0.5 mol% did not vastly change the rate of reaction but lowering it further to 0.25 mol% gave a much slower reaction that could be studied in depth, **Graph 4.4.2**. This change also gave a longer induction period, which is difficult to see at higher catalyst loadings, and makes an initial rate comparison difficult.

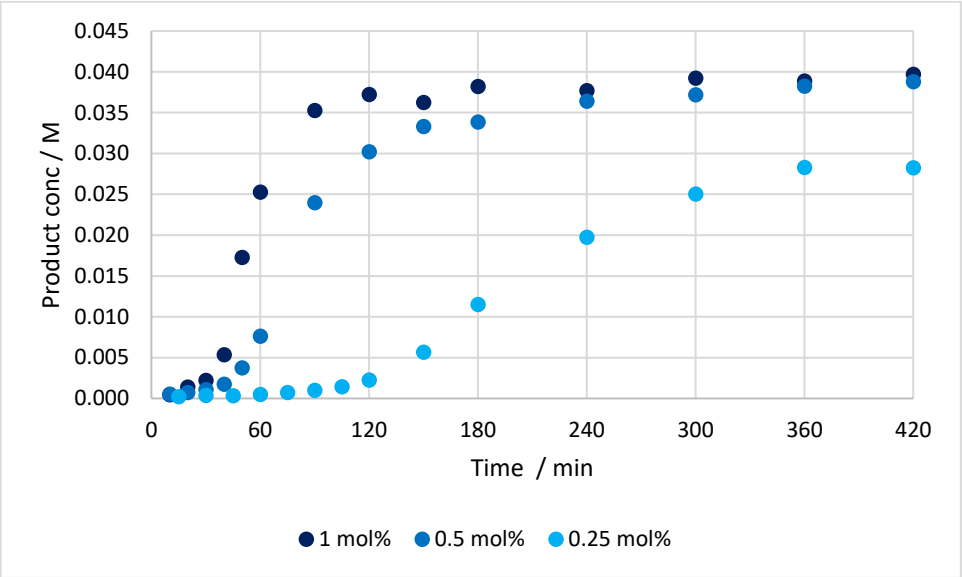

Graph 4.4.2 – Product **5** formation in the SM cross-coupling of boronic acid **3** (0.04 M) with 1,3-bis(trifluoromethyl)-5-bromobenzene **4** (0.04 M) monitored by ^{19}F NMR with 1-fluoronaphthalene as an internal standard. Varying catalyst loading. (Procedure E)

The profile of the boronic acid **3** coupling reaction under the new homogenous conditions, **Scheme 4.4.2**, is shown in **Graph 4.4.3**. This shows both starting materials, **3** & **4**, remain at the end of the reaction, suggesting the limiting reagent to be the base, rather than the boronic acid **3** or aryl halide **4**, or palladium decomposition.

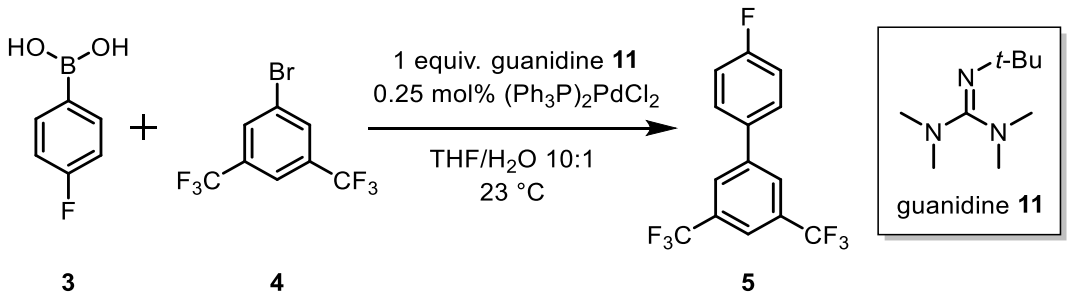

3 **4** **5**

Scheme 4.4.2 – SM cross-coupling of boronic acid **3** (1 equiv.) with 1,3-bis(trifluoromethyl)-5-bromobenzene **4** (1 equiv.) monitored by ^{19}F NMR with 1-fluoronaphthalene as an internal standard

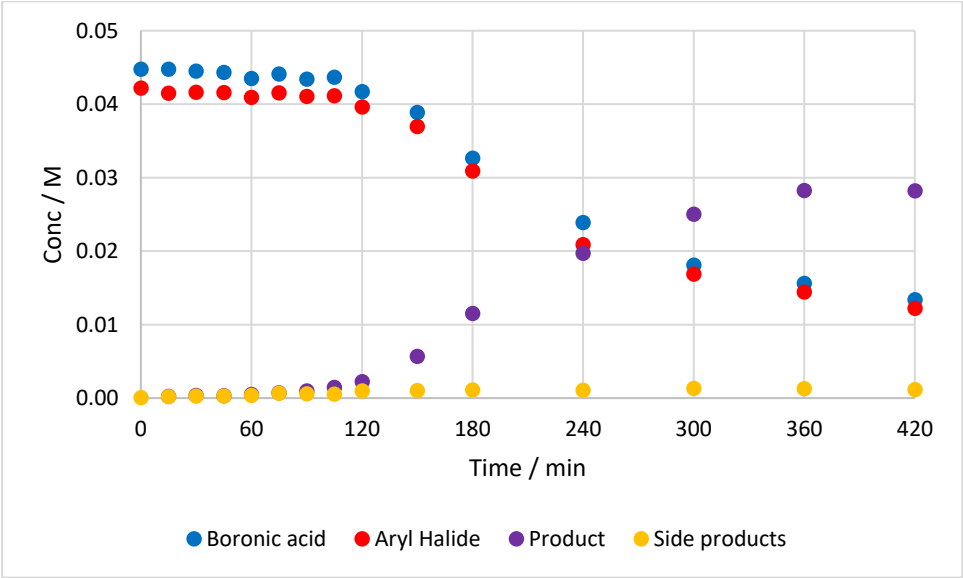

Graph 4.4.3 – SM cross-coupling of boronic acid **3** (0.045 M) with 1,3-bis(trifluoromethyl)-5-bromobenzene **4** (0.042 M) monitored by ^{19}F NMR with 1-fluoronaphthalene as an internal standard. (Procedure E)

Ester comparison

Using the lower catalyst conditions, the ester coupling reactions were re-investigated, **Scheme 4.4.3**, **Graph 4.4.4**, revealing the two esters, **1** & **2**, to have the same rate of coupling while the boronic acid **3** couples at a slower rate. The ester reactions also have a much shorter induction period (~50 min) in comparison to the corresponding boronic acid **3** (~120 min). Despite the differences in rate and induction period, the three reactions all form the same amount of side products at the same rate, **Graph 4.4.5**. After 7 hours, both esters, **1** & **2**, reached the maximum conversion of ~82%, whereas the boronic acid **3** had only reached 66%.

After 24 hours the boronic acid **3** reaches 75% conversion, while the ester reactions remain unchanged.

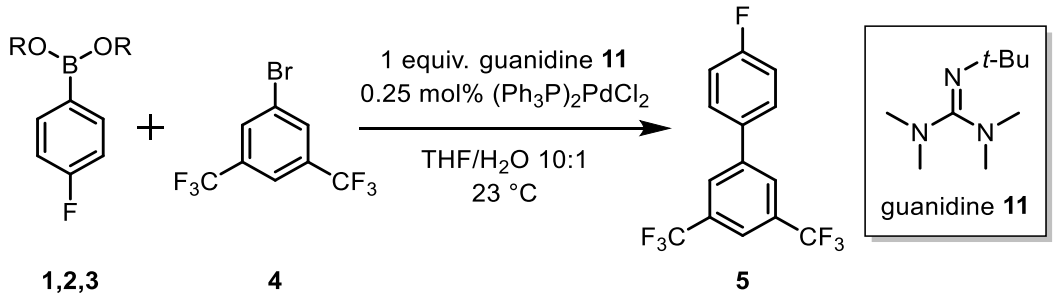

1,2,3 **4** **5**

Scheme 4.4.3 – SM cross-coupling of boronic acid **3**/ester **1**/**2** (1 equiv.) with 1,3-bis(trifluoromethyl)-5-bromobenzene **4** (1 equiv.) monitored by ^{19}F NMR with 1-fluoronaphthalene as an internal standard

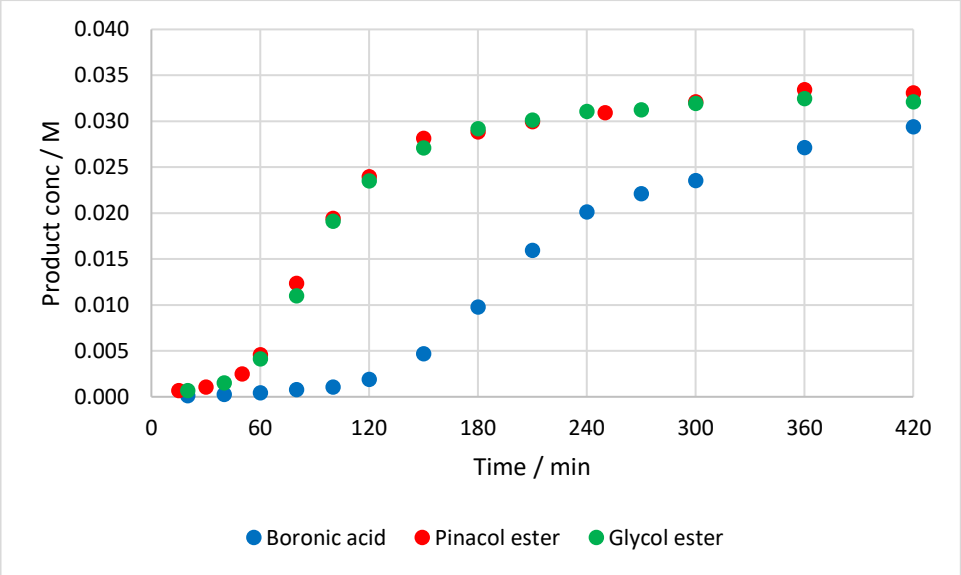

Graph 4.4.4 – Product **5** formation for SM cross-coupling of boronic acid **3**/ester **1**/**2** (0.04 M) with 1,3-bis(trifluoromethyl)-5-bromobenzene **4** (0.04 M) monitored by ^{19}F NMR with 1-fluoronaphthalene as an internal standard. (Procedure E)

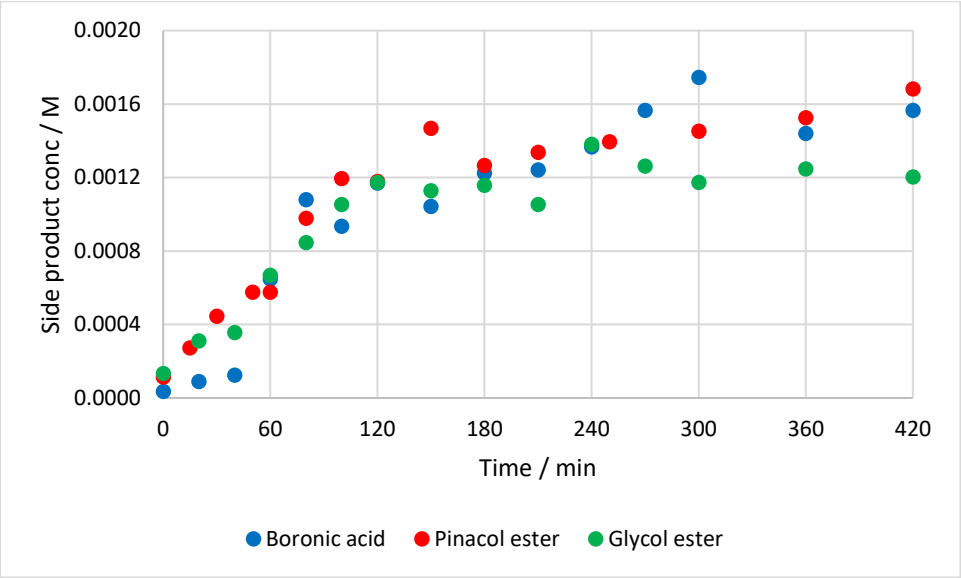

Graph 4.4.5 – Side product formation for SM cross-coupling of boronic acid **3**/ester **1/2** (0.04 M) with 1,3-bis(trifluoromethyl)-5-bromobenzene **4** (0.04 M) monitored by ^{19}F NMR with 1-fluoronaphthalene as an internal standard

4.4.2. Addition of alcohols

4.4.2.1. Neopentyl Glycol

To test if the faster rate and shorter induction period was a result of the use of the ester, or the presence of the diol, the reaction of the boronic acid **3** and one equivalent of glycol was carried out, **Scheme 4.4.4**. This reaction gave the same profile as the glycol ester **2** reaction, showing the isolated ester is not required for the improved reaction, **Graph 4.4.6**. The two reactions both reach roughly the same conversion, ~85% after 7 hours, **Appendix 8.4.2**, but the boronic acid **3** has a higher starting concentration as it is actually boroxine being added to the reaction, creating a higher concentration of boronic acid, **Chapter 3, Section 3.2.1**. The three reactions all form the same amount of side products (5%) at the same rate, **Appendix 8.4.2**. In addition, there is remaining starting material, both boronic acid **3** and aryl halide **4**, at the end of all three reactions, again suggesting the concentration of the guanidine **11** to be the limiting reagent.

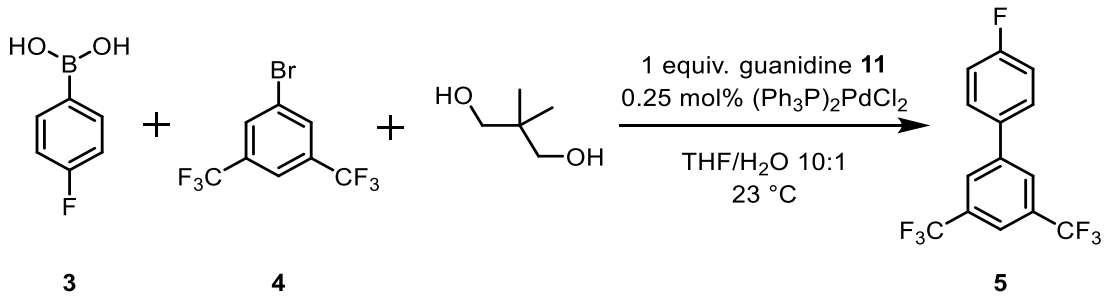

3 **4** **5**

Scheme 4.4.4 – SM cross-coupling of boronic acid **3**/ester **1**/**2** (1 equiv.) with 1,3-bis(trifluoromethyl)-5-bromobenzene **4** (1 equiv.) with addition of glycol, monitored by ^{19}F NMR with 1-fluoronaphthalene as an internal standard

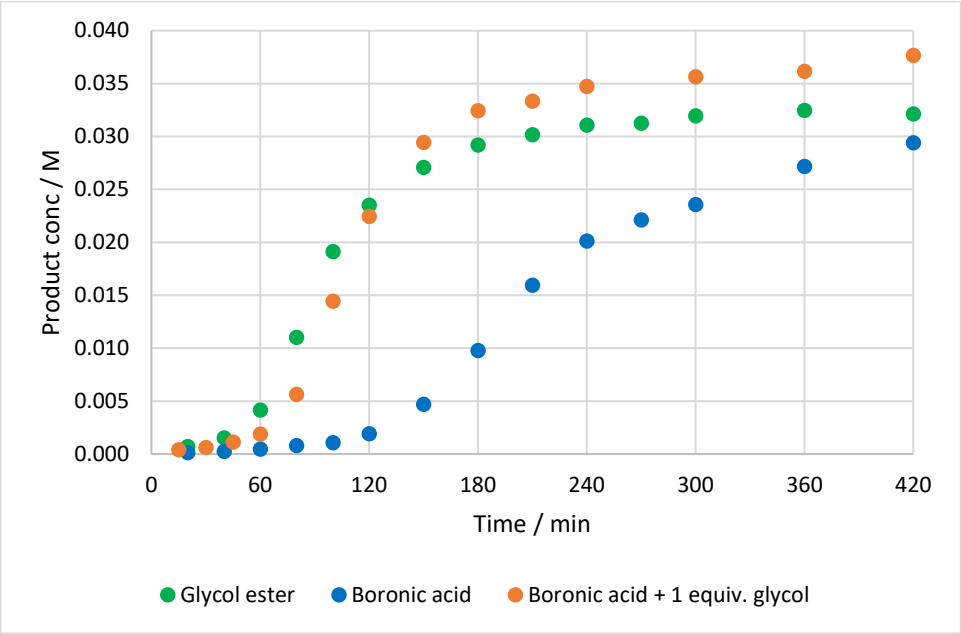

Graph 4.4.6 – Product **5** formation for the SM cross-coupling of boronic acid **3**/ester **1**/**2** (0.04 M) with 1,3-bis(trifluoromethyl)-5-bromobenzene **4** (0.04 M) with addition of glycol, monitored by ^{19}F NMR with 1-fluoronaphthalene as an internal standard. (Procedure E). (% product and side product graphs – Appendix 8.4.2).

To further study the effects of addition of diol to the reaction, the equivalents of glycol added to a standard boronic acid **3** coupling were varied, **Graph 4.4.7**. This shows that only half an equivalent of diol is needed to give the same reaction rate as the ester and reduction of induction period. At two equivalents, there is the reduction of induction period, but a slight decrease in the rate. By looking at percentage conversion, it is easier to see that the 0.25

equivalent and 2 equivalent reactions both give a lower conversion relative to the 1 equivalent or the ester reactions, **Graph 4.4.8**.

As 2 equivalents of diol was shown to be detrimental to the reaction, the glycol ester **2** reaction with an extra equivalent of diol was also tested, **Graph 4.4.9**, and found to give the same effect of shortening induction period but lowering rate.

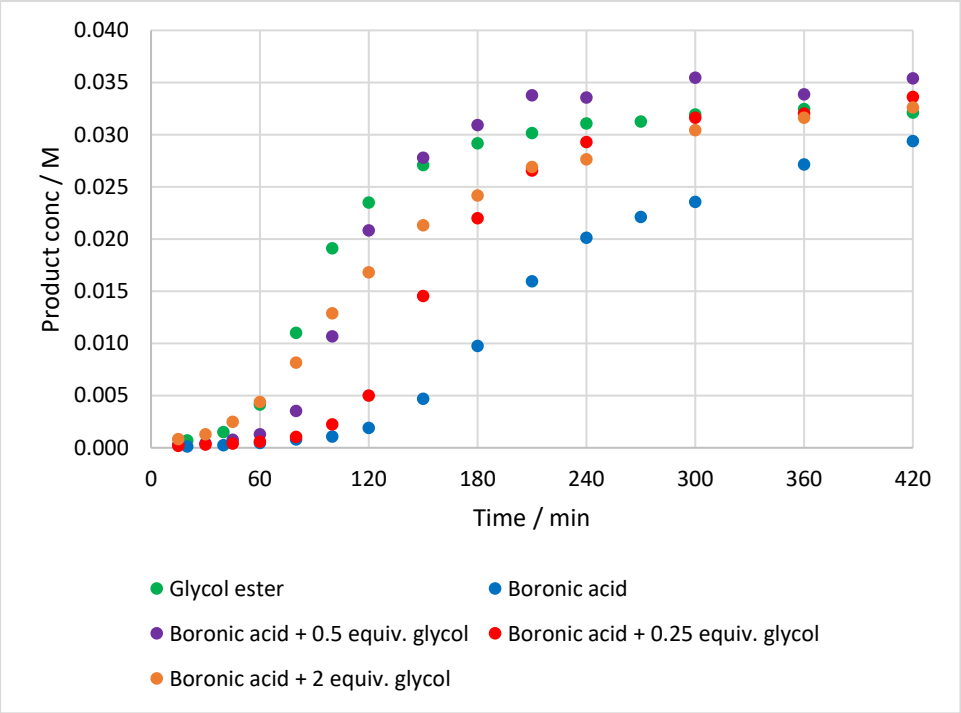

Graph 4.4.7 – Product **5** formation (concentration) for the SM cross-coupling of boronic acid **3**/ester **1**/**2** (0.04 M) with 1,3-bis(trifluoromethyl)-5-bromobenzene **4** (0.04 M) with addition of glycol, monitored by ^{19}F NMR with 1-fluoronaphthalene as an internal standard. (Procedure E)

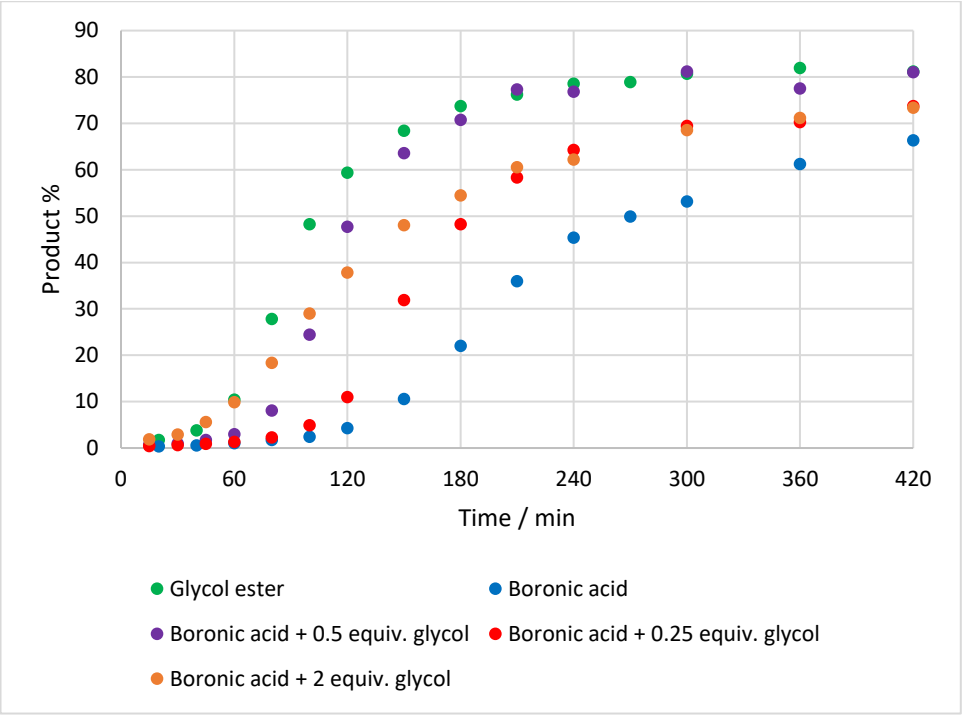

Graph 4.4.8 – Product **5** formation (percentage) for the SM cross-coupling of boronic acid **3**/ester **1/2** (0.04 M) with 1,3-bis(trifluoromethyl)-5-bromobenzene **4** (0.04 M) with addition of glycol, monitored by ^{19}F NMR with 1-fluoronaphthalene as an internal standard. (Procedure E)

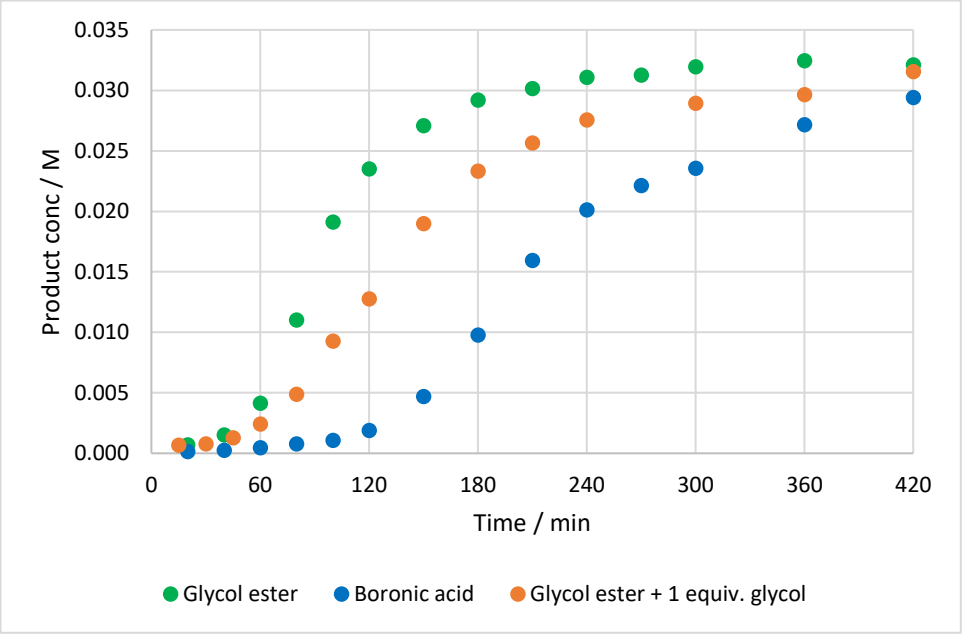

Graph 4.4.9 – Product **5** formation for the SM cross-coupling of boronic acid **3**/ester **1/2** (0.04 M) with 1,3-bis(trifluoromethyl)-5-bromobenzene **4** (0.04 M) with addition of glycol, monitored by ^{19}F NMR with 1-fluoronaphthalene as an internal standard. (Procedure E)

4.4.2.2. Pinacol

The same study of diol effects was carried out with the pinacol, **Scheme 4.4.5**. Adding one equivalent of pinacol to the boronic acid **3** coupling gave the same reaction profile as the pinacol ester **1** coupling, **Graph 4.4.10**. The detrimental effect of excess diol is also shown by adding an equivalent of pinacol to a pinacol ester **1** coupling, **Graph 4.4.11**.

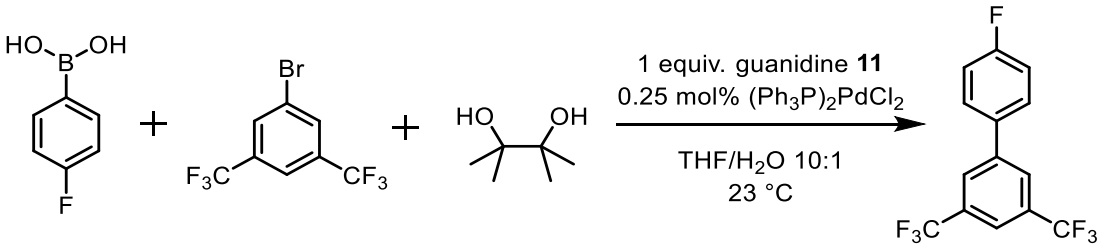

3 **4** **5**

Scheme 4.4.5 – SM cross-coupling of boronic acid **3**/ester **1/2** (1 equiv.) with 1,3-bis(trifluoromethyl)-5-bromobenzene **4** (1 equiv.) with addition of pinacol, monitored by ^{19}F NMR with 1-fluoronaphthalene as an internal standard

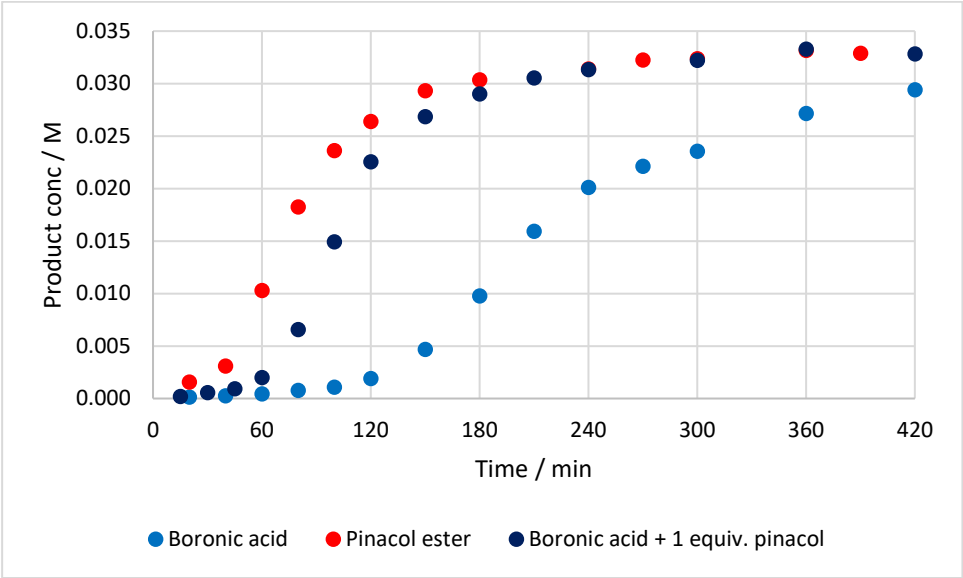

Graph 4.4.10 – Product **5** formation for the SM cross-coupling of boronic acid **3**/ester **1/2** (0.04 M) with 1,3-bis(trifluoromethyl)-5-bromobenzene **4** (0.04 M) with addition of pinacol, monitored by ^{19}F NMR with 1-fluoronaphthalene as an internal standard. (Procedure E)

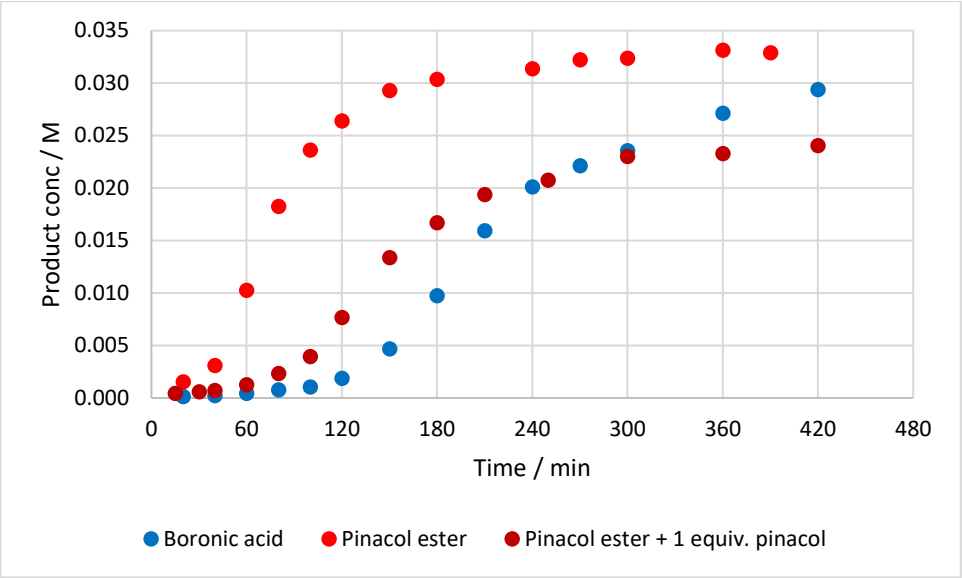

Graph 4.4.11 – Product **5** formation for the SM cross-coupling of boronic acid **3**/ester **1/2** (0.04 M) with 1,3-bis(trifluoromethyl)-5-bromobenzene **4** (0.04 M) with addition of pinacol, monitored by ^{19}F NMR with 1-fluoronaphthalene as an internal standard. (Procedure E)

4.4.2.3. Other alcohols

As the use of 1 equiv. diol has been shown to shorten the induction period and increase the rate, mono-alcohol, 2-propanol, was tested to see the effect on the reaction. One equivalent of 2-propanol was added to a standard boronic acid **3** cross-coupling, **Scheme 4.4.6**, **Graph 4.4.12**. Rather than shorten the induction period, 2-propanol increased it. By shifting the results to remove this increase (70 minutes), the reaction profile matches that of the standard boronic acid **3** coupling, showing there is no change to the rate of reaction, only the length of induction period, **Graph 4.4.12**. Despite the difference in induction period, the two reactions form the same amount of side products (3.5 %) at the same rate, **Graph 4.4.13**.

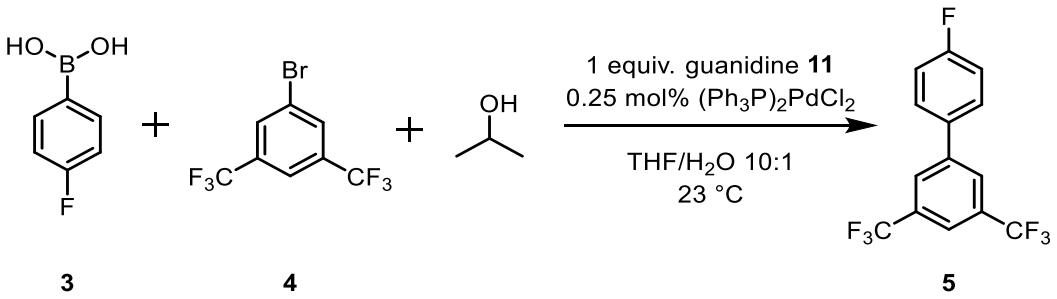

3 **4** **5**

Scheme 4.4.6 – SM cross-coupling of boronic acid **3** (1 equiv.) with 1,3-bis(trifluoromethyl)-5-bromobenzene **4** (1 equiv.) with addition of 2-propanol (1 equiv.), monitored by ^{19}F NMR with 1-fluoronaphthalene as an internal standard

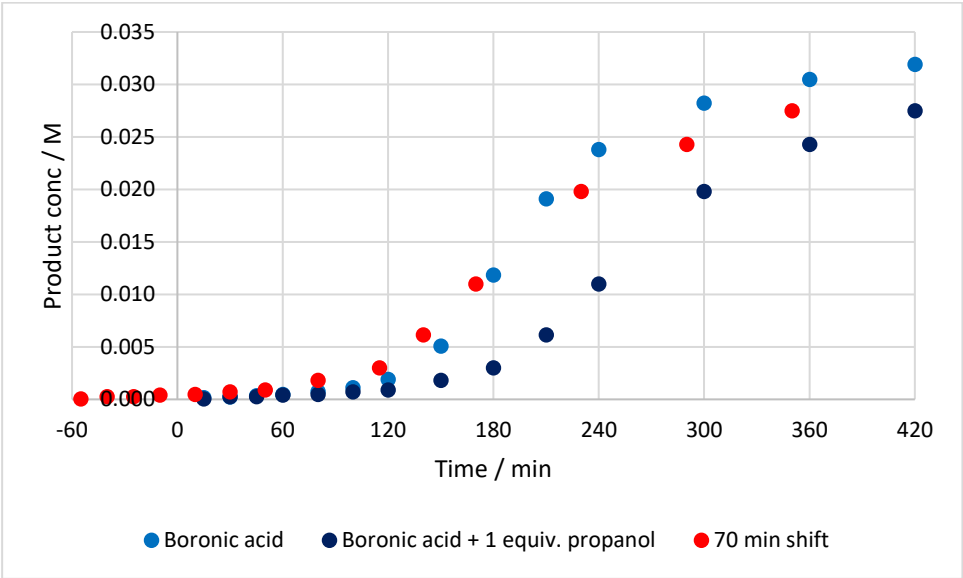

Graph 4.4.12 – Product **5** formation of SM cross-coupling of boronic acid **3** (0.04 M) with 1,3-bis(trifluoromethyl)-5-bromobenzene **4** (0.04 M) with addition of 2-propanol (0.04 M), monitored by ^{19}F NMR with 1-fluoronaphthalene as an internal standard. (Procedure L)

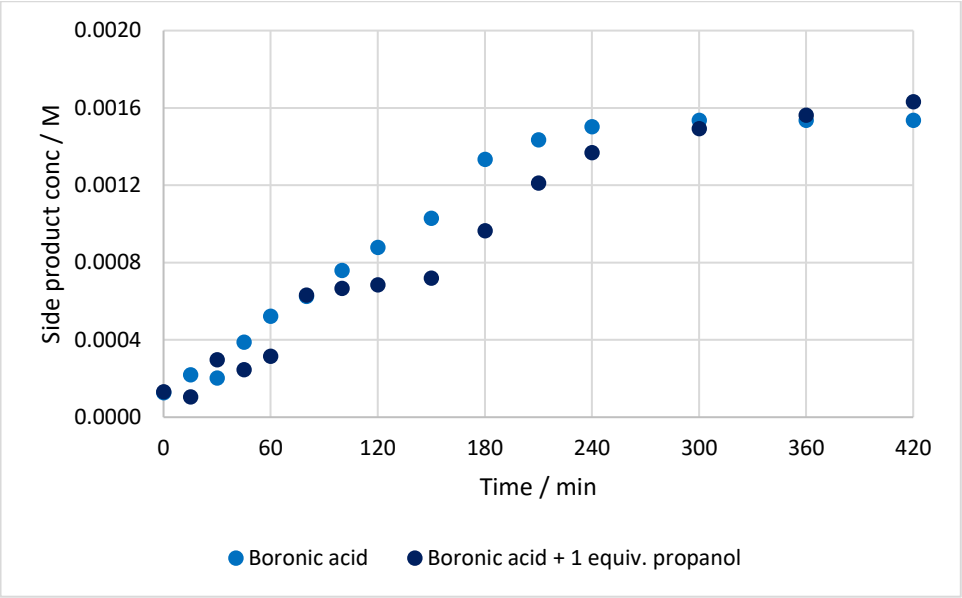

Graph 4.4.13 – Side product formation of SM cross-coupling of boronic acid **3** (0.04 M) with 1,3-bis(trifluoromethyl)-5-bromobenzene **4** (0.04 M) with addition of 2-propanol (0.04 M), monitored by ^{19}F NMR with 1-fluoronaphthalene as an internal standard

A triol, 1,1,1-tris(hydroxymethyl)ethane, was also investigated, and found to have an interesting effect on the reaction, **Scheme 4.4.7**. 1 equiv. was found to completely remove the induction period, **Graph 4.4.14**. Lower equivalents were found to give a slower rate, **Graph 4.4.14**. All three triol reactions reached a lower conversion (~50 %) compared to the standard boronic acid **3** coupling (73 %), after 7 hours. but all four reactions produced roughly the same amount of side products (~3 %) at the same rate, **Appendix 8.4.3**.

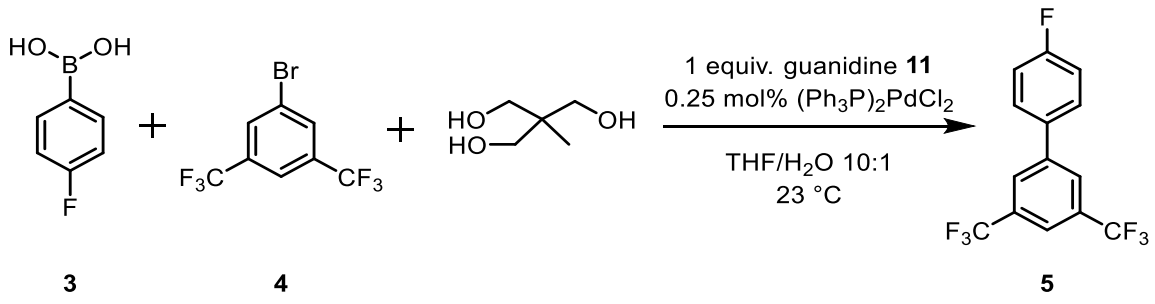

3 **4** **5**

Scheme 4.4.7 – SM cross-coupling of boronic acid **3** (1 equiv.) with 1,3-bis(trifluoromethyl)-5-bromobenzene **4** (1 equiv.) with addition of 1,1,1-tris(hydroxymethyl)ethane, monitored by ^{19}F NMR with 1-fluoronaphthalene as an internal standard

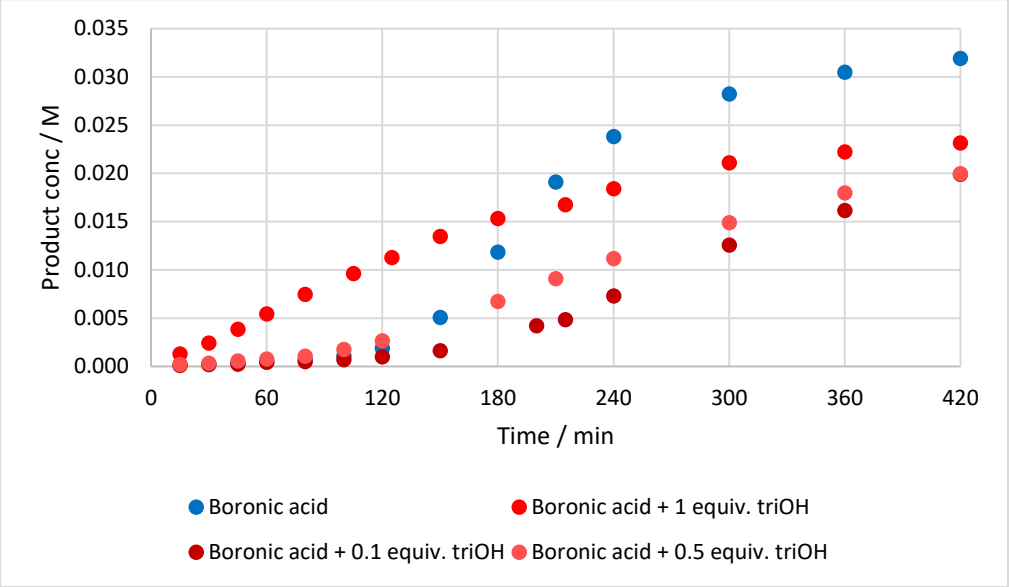

Graph 4.4.14 – Product **5** formation in the SM cross-coupling of boronic acid **3** (0.04 M) with 1,3-bis(trifluoromethyl)-5-bromobenzene **4** (0.04 M) with addition of 1,1,1-tris(hydroxymethyl)ethane, monitored by ^{19}F NMR with 1-fluoronaphthalene as an internal standard. (Procedure L)

4.5. Changing catalyst

4.5.1. $Pd(OAc)_2$

Issues with the reproducibly of the system were noticed after investigating different procedures and order of addition. Five reactions that should give identical results were found to differ greatly, **Graph 4.5.1**. The amount of catalyst needed was so small, less than 1 mg, it could not be accurately weighed, so stock solutions were used. But it was found that the catalyst had limited solubility in THF/water, so the use of stock solutions still gave irreproducible results. So, work began with an alternative catalyst, palladium acetate, $Pd(OAc)_2$, **Scheme 4.5.1**.

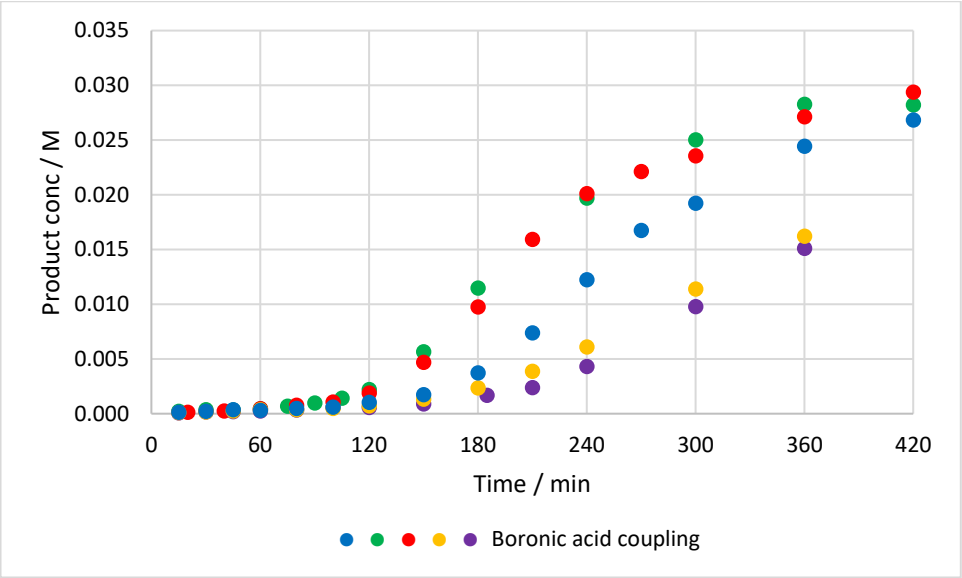

Graph 4.5.1 – Results from five separate, individual reactions – reproducibility issues using $Pd(PPh_3)_2Cl_2$. Product **5** formation in five individual SM cross-coupling reactions of boronic acid **3** (0.04 M) with 1,3-bis(trifluoromethyl)-5-bromobenzene **4** (0.04 M) monitored by ^{19}F NMR with 1-fluoronaphthalene as an internal standard. (Procedure E & G)

The same catalyst loading of $Pd(OAc)_2$ (0.25 mol%) was found to give a much slower reaction in comparison to $Pd(PPh_3)_2Cl_2$, **Graph 4.5.2**. A study of catalyst loading showed 0.75 mol% $Pd(OAc)_2$ to give a reaction profile similar to that of 0.25 mol% $Pd(PPh_3)_2Cl_2$. However, when this reaction was repeated, using stock solutions, it showed a different profile, without the induction period, and reached a higher conversion, **Graph 4.5.3**. The reaction was repeated using stock solutions, and the new profile was shown to be the true reaction profile, initial rate = 2.53×10^{-4} M min^{-1}, **Graph 4.5.4**. The amount of side products, boronic acid homocoupling **6** and oxidation **8**, produced also changed with the change of catalyst, **Graph 4.5.4**. $Pd(PPh_3)_2Cl_2$ reactions were found to form around 4% side products, whereas the use of $Pd(OAc)_2$ reduced this to around 1.5%.

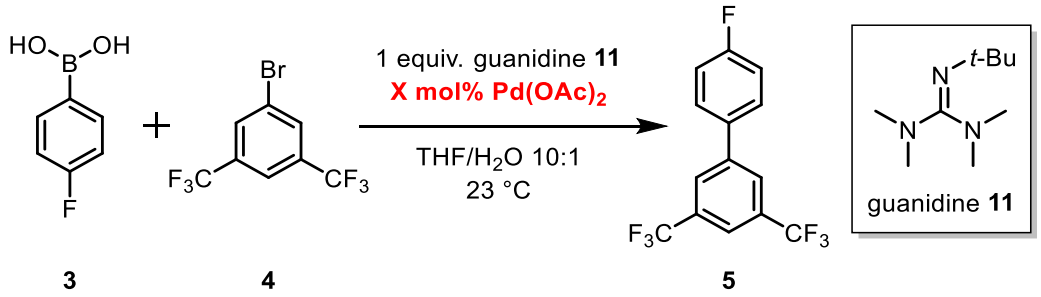

3 **4** **5**

Scheme 4.5.1 – SM cross-coupling of boronic acid **3** (1 equiv.) with 1,3-bis(trifluoromethyl)-5-bromobenzene **4** (1 equiv.) monitored by ^{19}F NMR with 1-fluoronaphthalene as an internal standard

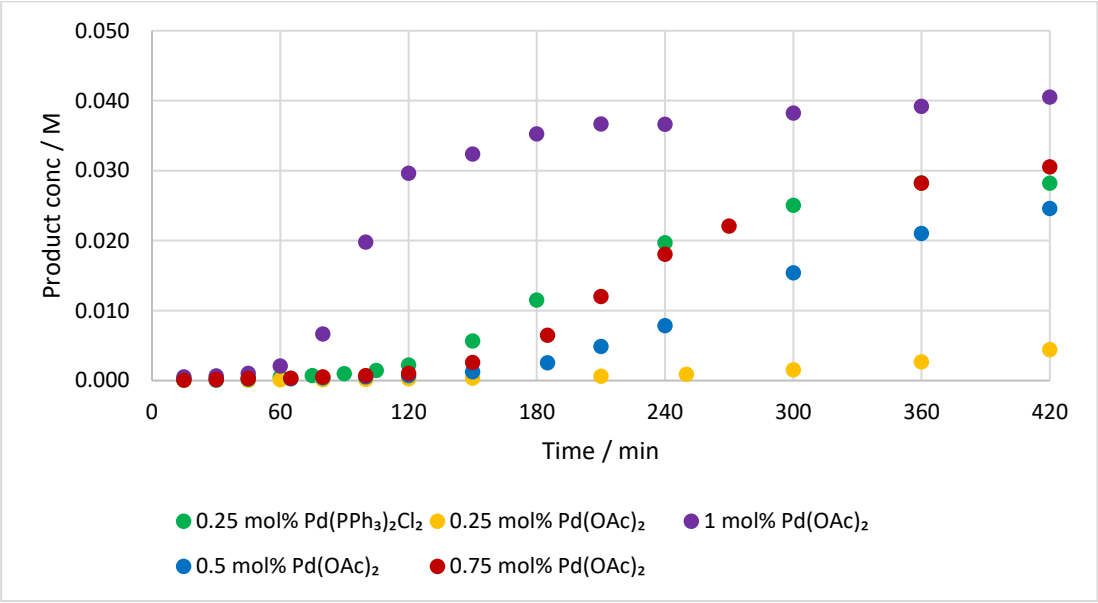

Graph 4.5.2 – Varying $Pd(OAc)_2$ loading. Product **5** formation in the SM cross-coupling of boronic acid **3** (0.04 M) with 1,3-bis(trifluoromethyl)-5-bromobenzene **4** (0.04 M) monitored by ^{19}F NMR with 1-fluoronaphthalene as an internal standard. (Procedure E & L)

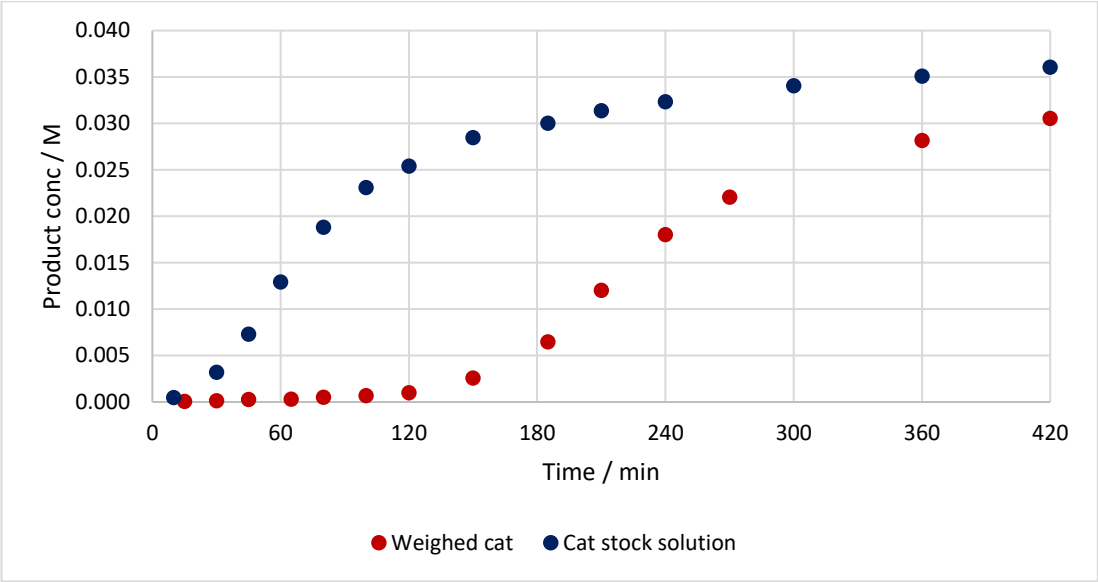

Graph 4.5.3 – Difference between weighing the catalyst directly and using a catalyst stock solution. Product **5** formation in the SM cross-coupling of boronic acid **3** (0.04 M) with 1,3-bis(trifluoromethyl)-5-bromobenzene **4** (0.04 M) monitored by ^{19}F NMR with 1-fluoronaphthalene as an internal standard. (Procedure E, weighed, vs procedure I, cat sol)

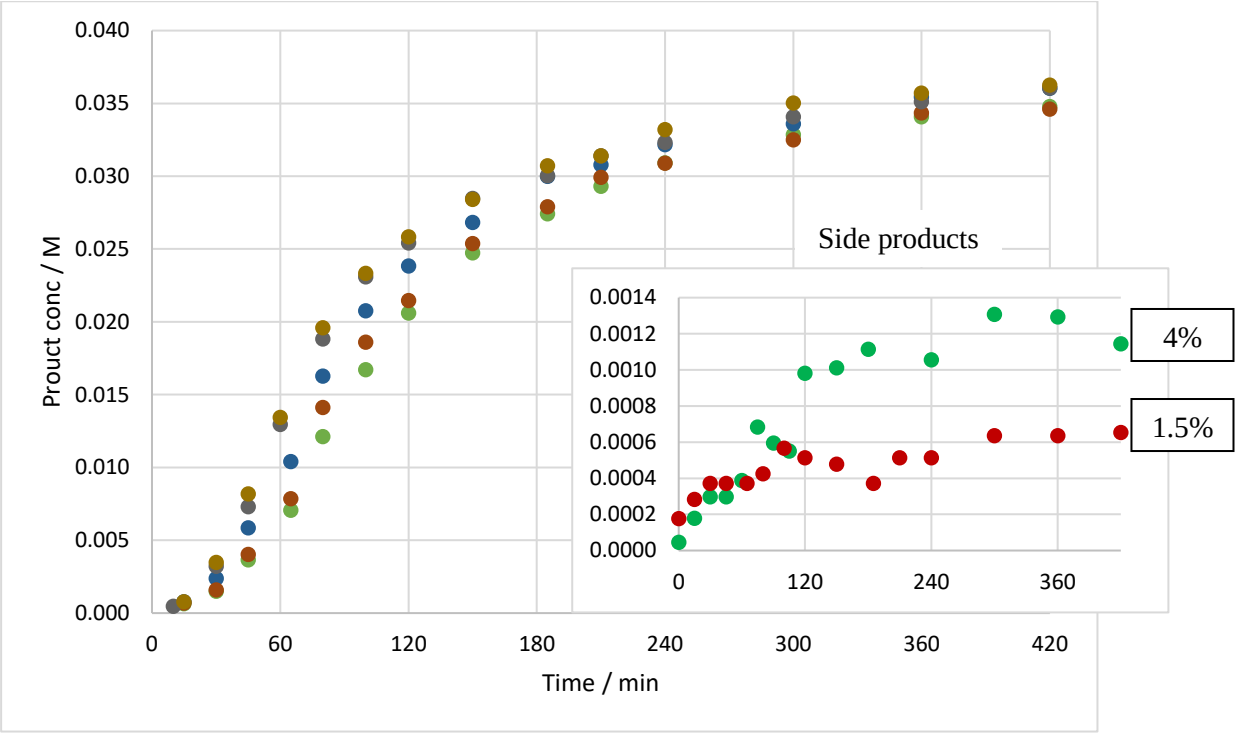

Graph 4.5.4 – Product formation in the SM cross-coupling of boronic acid (0.04 M) with 1,3-bis(trifluoromethyl)-5-bromobenzene (0.04 M) monitored by ^{19}F NMR with 1-fluoronaphthalene as an internal standard – showing the use of catalyst stock solution to be reproducible in five separate reactions. Insert graph shows change in side product formation with change in catalyst; • $Pd(PPh_3)_2Cl_2$ = 4%, • $Pd(OAc)_2$ = 1.5%.

This is where new issues of irreproducibility arose. For the reaction, a catalyst stock solution was prepared in THF/water 10:1. But it was found that leaving this solution for different periods of time before use gave varying results, **Graph 4.5.5**. This could be due to the palladium acetate reacting with water, as reported in the literature.[14] The different reactivity shown in **Graph 4.5.5** could be due to which species is present from the palladium acetate/water reaction and whether that species is reactive or not, **Scheme 4.5.2**.

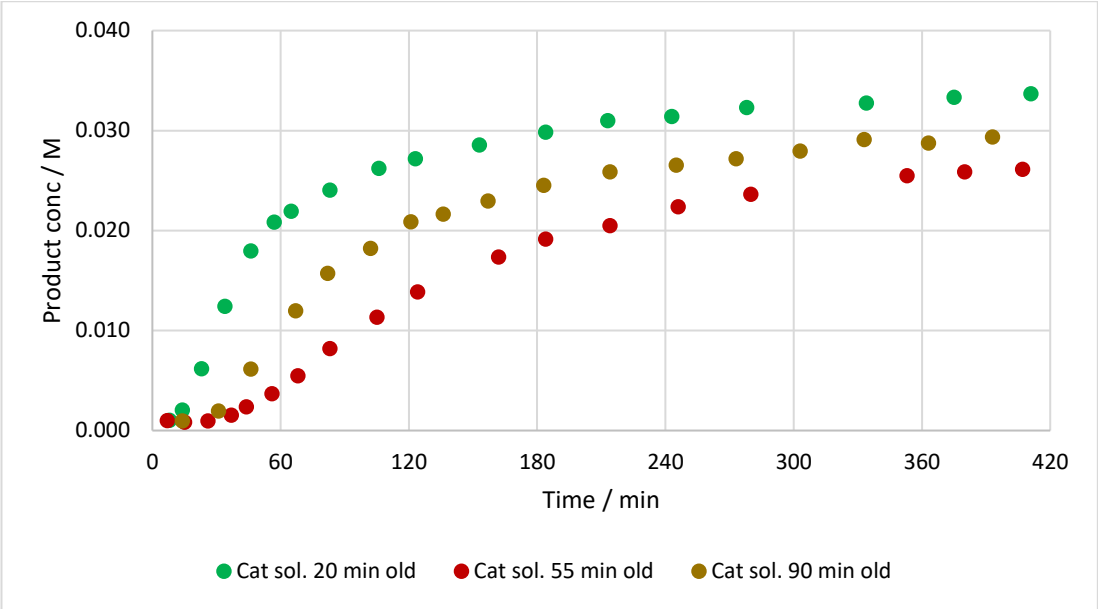

Graph 4.5.5 – Product **5** formation in the SM cross-coupling of boronic acid **3** (0.04 M) with 1,3-bis(trifluoromethyl)-5-bromobenzene **4** (0.04 M) monitored by ^{19}F NMR with 1-fluoronaphthalene as an internal standard – Varied results depending on age of catalyst solution. (Procedure G)

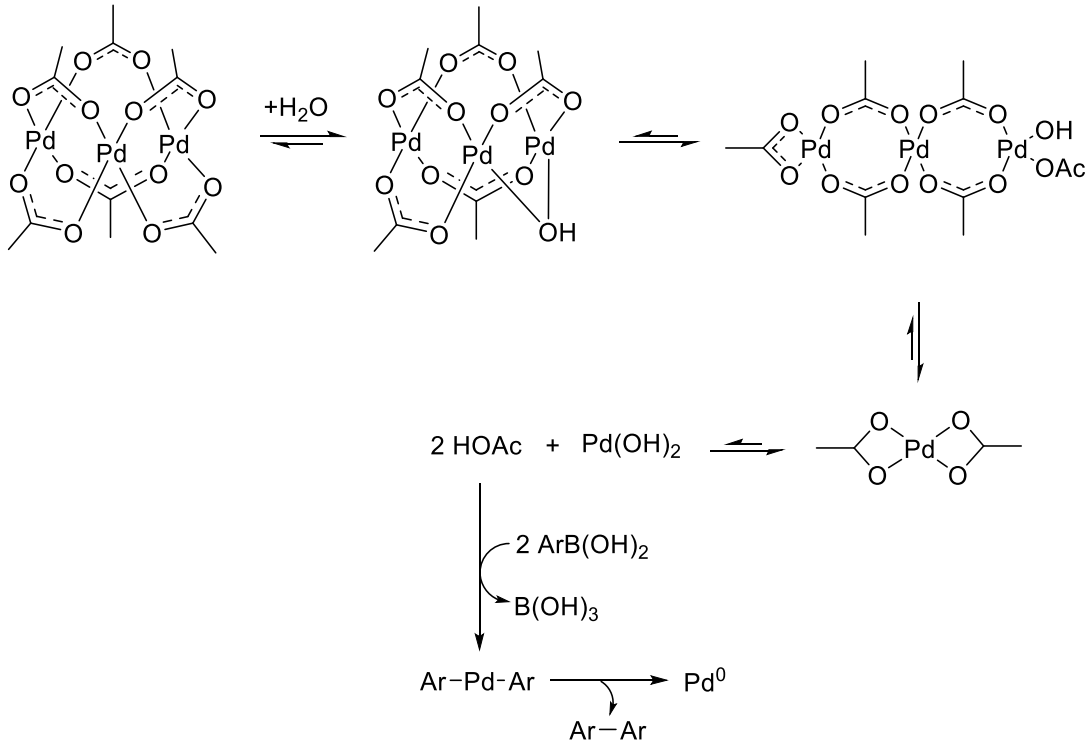

Scheme 4.5.2 – Palladium acetate reaction with water.[14]

From here, the catalyst stock solution was instead made in neat THF, but the rate of reaction was still found to be irreproducible, **Graph 4.5.6**. Despite the differences in the rate of reaction, the $Pd(OAc)_2$ reactions all consistently reached a conversion of ~70%.

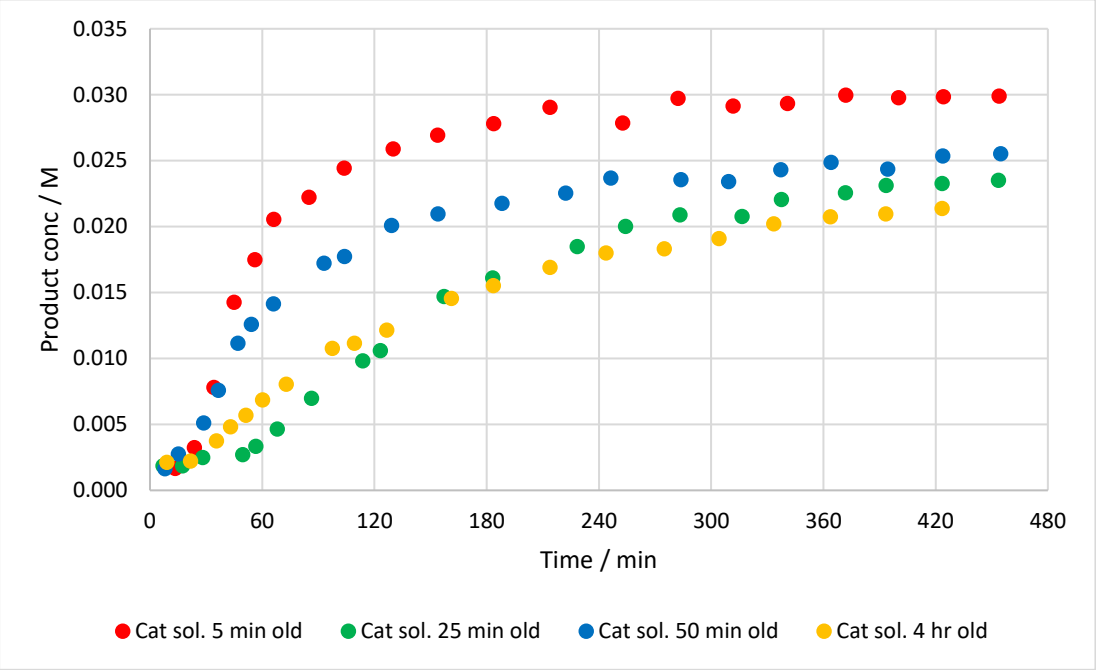

Graph 4.5.6 – Product **5** formation in the SM cross-coupling of boronic acid **3** (0.04 M) with 1,3-bis(trifluoromethyl)-5-bromobenzene **4** (0.04 M) monitored by ^{19}F NMR with 1-fluoronaphthalene as an internal standard – Irreproducible reaction. (Procedure Q)

4.5.2. $PdCl_2(PhCN)_2$

Bis(benzonitrile)palladium(II) chloride, $PdCl_2(PhCN)_2$, was found to give a similar conversion to palladium acetate, so was further investigated to study phosphine-free SM conditions, **Scheme 4.5.3**. A study of the catalyst loading revealed the reaction to be first order with respect to the catalyst, **Graph 4.5.7**. The fact that the initial rate graph does not have a zero intercept on the x-axis suggests there is a small amount of catalyst poison or inhibitor present in the system.

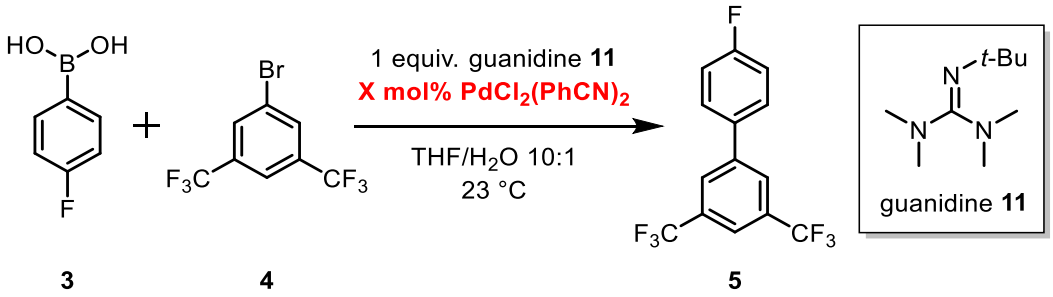

3 **4** **5**

Scheme 4.5.3 – SM cross-coupling of boronic acid **3** (1 equiv.) with 1,3-bis(trifluoromethyl)-5-bromobenzene **4** (1 equiv.) monitored by ^{19}F NMR with 1-fluoronaphthalene as an internal standard

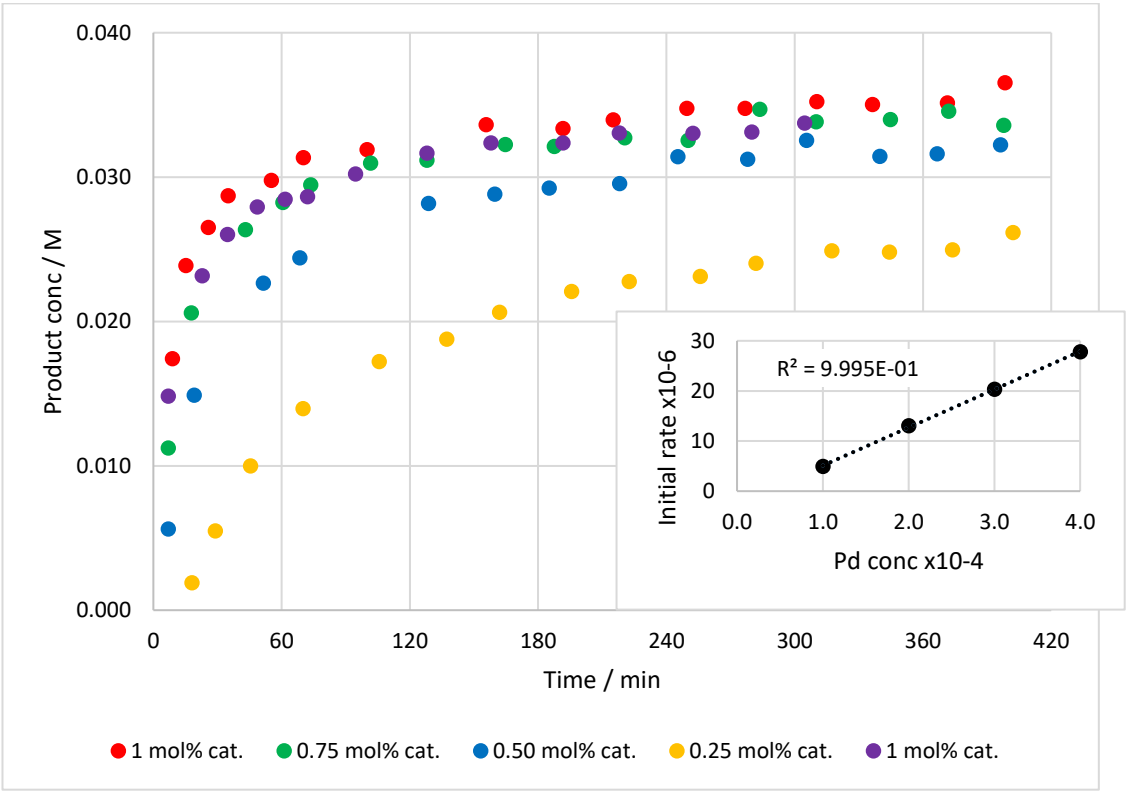

Graph 4.5.7 – Product **5** formation in the SM cross-coupling of boronic acid **3** (0.04 M) with 1,3-bis(trifluoromethyl)-5-bromobenzene **4** (0.04 M) monitored by ^{19}F NMR with 1-fluoronaphthalene as an internal standard – Varying catalyst loading. Insert graph shows initial rates vs palladium concentration. (Procedure S)

Mol % Pd	% conversion **5**	% side products	Initial rate / M min^{-1}
● 1.00	83%	4%	2.78 x 10^{-5}
● 0.75	80%	4%	2.03 x 10^{-5}
● 0.50	75%	3%	1.03 x 10^{-5}
● 0.25	60%	4%	4.89 x 10^{-6}

Fig 4.5.1 – SM cross-coupling of boronic acid (0.04 M) with 1,3-bis(trifluoromethyl)-5-bromobenzene (0.04 M) monitored by 19F NMR with 1-fluoronaphthalene as an internal standard – Varying catalyst loading. Conversion after 10 hours.

The effect of changing the equivalents of guanidine **11** was studied, **Graph 4.5.8**. As shown earlier, lowering the equivalents of guanidine **11** gives an increase in rate, whereas increasing the equivalents (1.25) gave a much slower reaction.

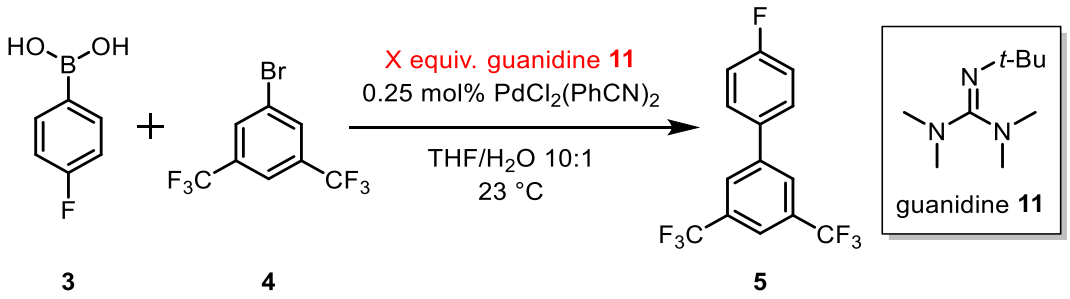

3 **4** **5**

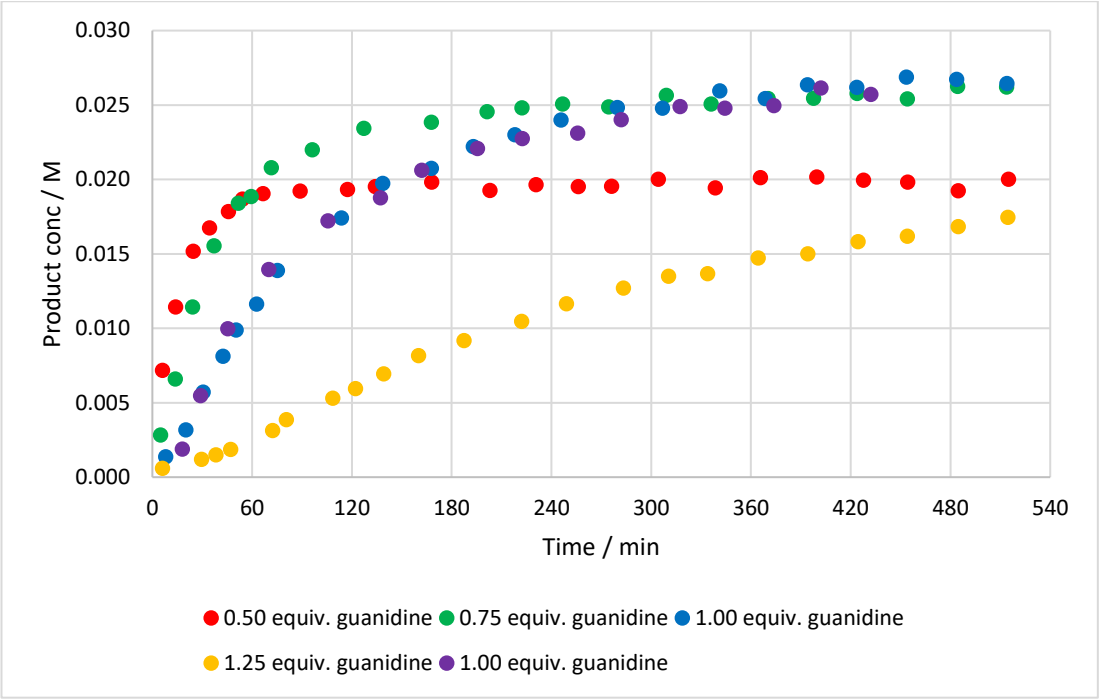

Graph 4.5.8 – Product **5** formation in the SM cross-coupling of boronic acid **3** (0.04 M) with 1,3-bis(trifluoromethyl)-5-bromobenzene **4** (0.04 M) monitored by ^{19}F NMR with 1-fluoronaphthalene as an internal standard – Varying concentration of guanidine (Procedure T)

Equiv. guanidine	% conversion **5**	% side products	Initial rate / M min^{-1}
1.25	40%	6%	4.70×10^{-5}
1.00	62%	4%	1.92×10^{-4}
0.75	61%	2%	4.00×10^{-4}
0.50	46%	2%	4.26×10^{-4}

Fig 4.5.2 – SM cross-coupling of boronic acid **3** (0.04 M) with 1,3-bis(trifluoromethyl)-5-bromobenzene **4** (0.04 M) monitored by ^{19}F NMR with 1-fluoronaphthalene as an internal standard – Varying concentration of guanidine **11**. Conversion after 9 hours

Esters

The reactions of the pinacol ester **1** and glycol ester **2** were reinvestigated using $PdCl_2(PhCN)_2$, **Scheme 4.5.4**, **Graph 4.5.9**. This showed the boronic acid **3** and glycol ester **2** to give very

similar profiles, 4.4 x 10^{-4}, but the pinacol ester **1** to give a much slower reaction, 7.7 x 10^{-5}. After 24 hours, the boronic acid **3** and glycol ester **2** reactions had a final conversion of 80%, compared to the pinacol ester **1** which only reached 40%.

What was interesting about this study was that the boronic acid **3** results shown here are very different to that of previous studies under the same conditions, **Graph 4.5.8**. This shows that there are still reproducibility issues with this system. Further studies showed the boronic acid **3** to give different profiles between runs, with no correlation as to what is causing the issue, **Graph 4.5.10**.

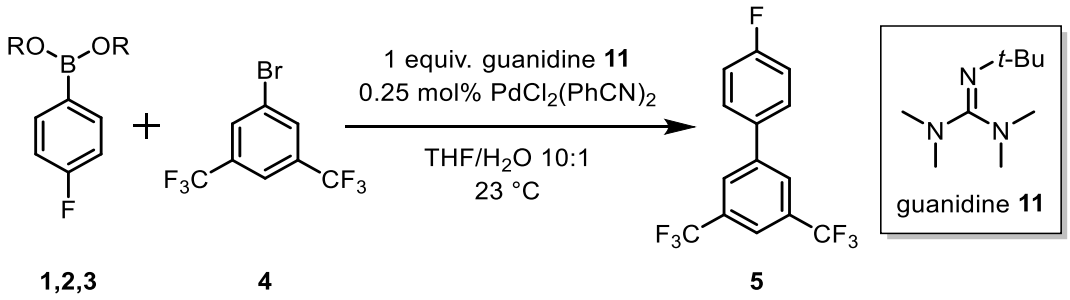

Scheme 4.5.4 – SM cross-coupling of boronic acid **3**/ester **1**/**2** (1 equiv.) with 1,3-bis(trifluoromethyl)-5-bromobenzene **4** (1 equiv.) monitored by ^{19}F NMR with 1-fluoronaphthalene as an internal standard

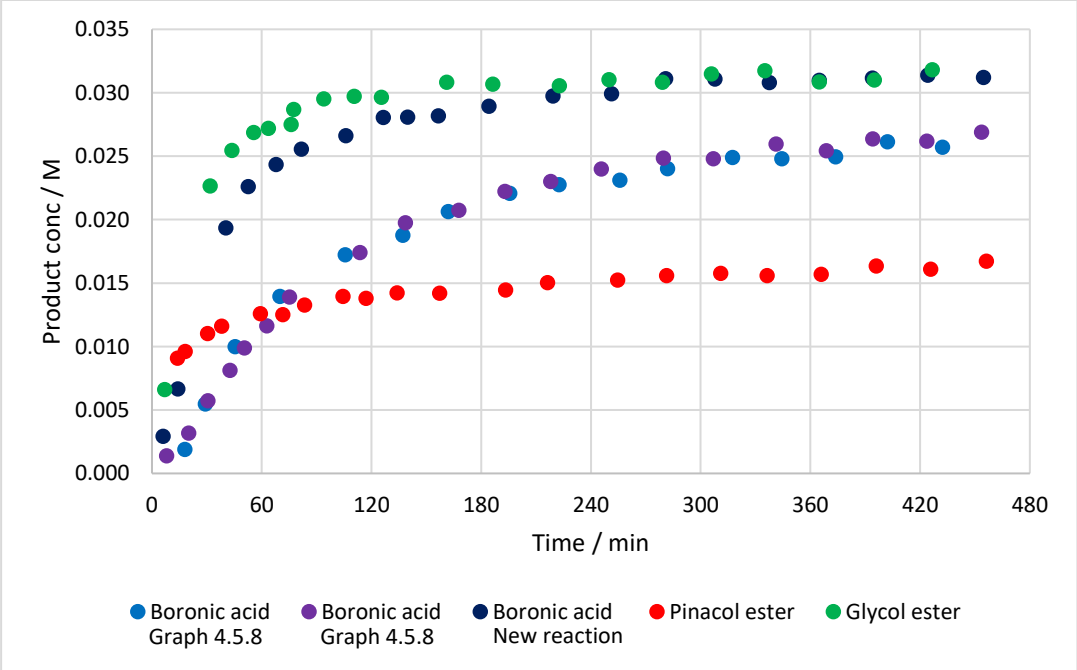

Graph 4.5.9 – Product **5** formation in the SM cross-coupling of boronic acid **3**/ester **1**/**2** (0.04 M) with 1,3-bis(trifluoromethyl)-5-bromobenzene **4** (0.04 M) monitored by ^{19}F NMR with 1-fluoronaphthalene as an internal standard. (Procedure O)

		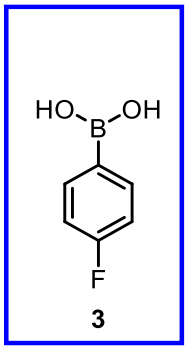 **3** Boronic acid	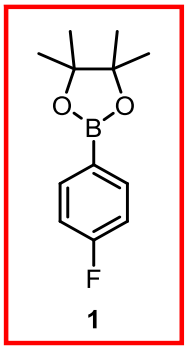 **1** Pinacol ester	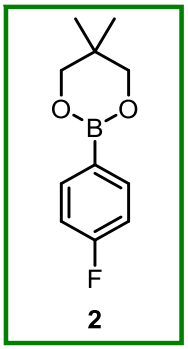 **2** Glycol ester
$Pd(OAc)_2$	Product	68%	76%	70%
	Side products	5%	3%	2%
$PdCl_2(PhCN)_2$	Product	75%	51%	84%
	Side products	4%	3%	4%
$PdCl_2(PhCN)_2$	Product	68%	54%	58%
	Side products	4%	2%	2%

Fig 4.5.3 – Comparison for final conversion of boronic acid **3**/ester **1**/**2** SM couplings, **Scheme 4.5.4**, after 24 hours using different catalysts. One acid to ester comparison using $Pd(OAc)_2$ and two separate comparisons using $PdCl_2(PhCN)_2$, showing the reproducibility issues when using $PdCl_2(PhCN)_2$

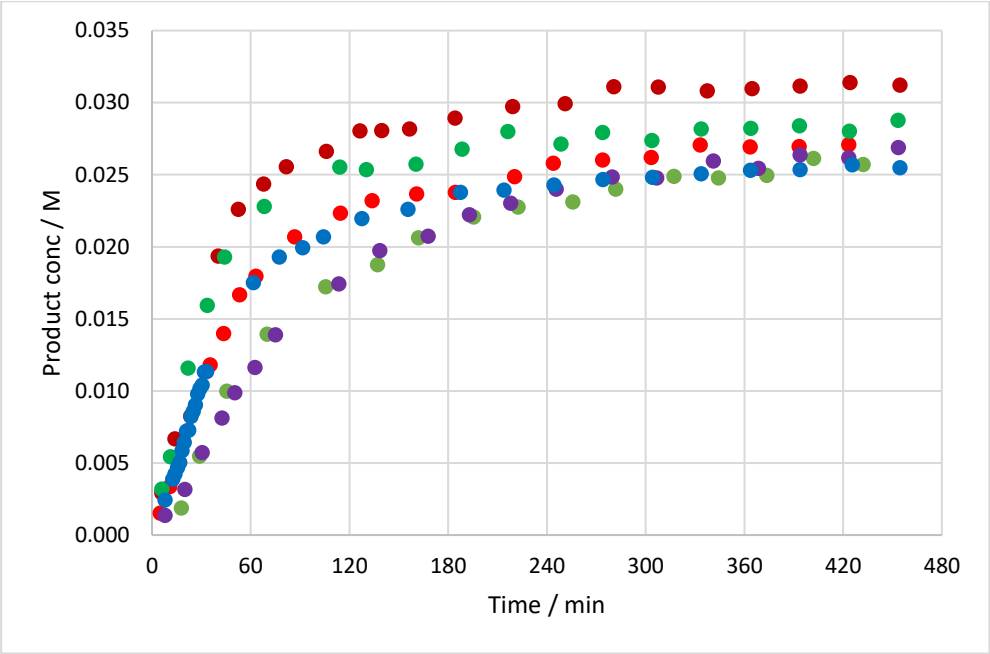

Graph 4.5.10 – Product **5** formation in the SM cross-coupling of boronic acid **3** (0.04 M) with 1,3-bis(trifluoromethyl)-5-bromobenzene **4** (0.04 M) monitored by ^{19}F NMR with 1-fluoronaphthalene as an internal standard – Irreproducible results using $PdCl_2(PhCN)_2$

4.5.3. [(cinnamyl)PdCl]$_2$

Previous work within our research group showed the palladium (π-cinnamyl) chloride dimer, [(cinnamyl)PdCl]$_2$, gave good SM cross-coupling with similar substrates, so was further investigated as a catalyst for phosphine-free SM cross-coupling, **Scheme 4.5.5**. Initial results using 0.25 mol % showed the reaction to be much faster than previous catalysts at this loading, initial rate = 4 x 10^{-4} M min^{-1}, **Graph 4.5.11**. The catalyst loading was lowered to 0.10 mol%, but multiple, identical runs showed the reaction to be irreproducible, **Graph 4.5.12**.

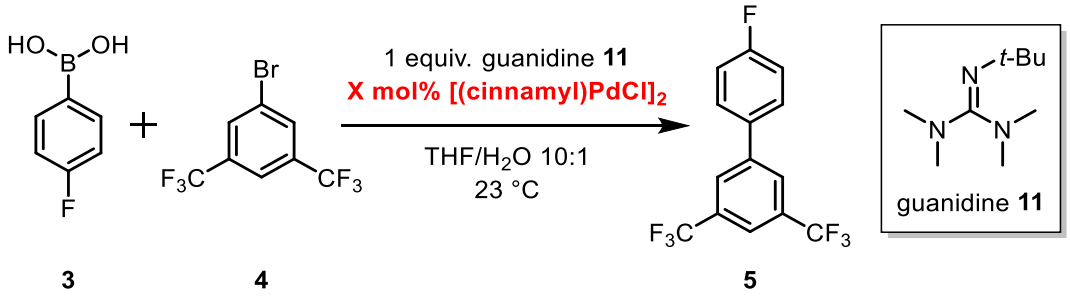

Scheme 4.5.5 – SM cross-coupling of boronic acid **3** (1 equiv.) with 1,3-bis(trifluoromethyl)-5-bromobenzene **4** (1 equiv.) monitored by ^{19}F NMR with 1-fluoronaphthalene as an internal standard

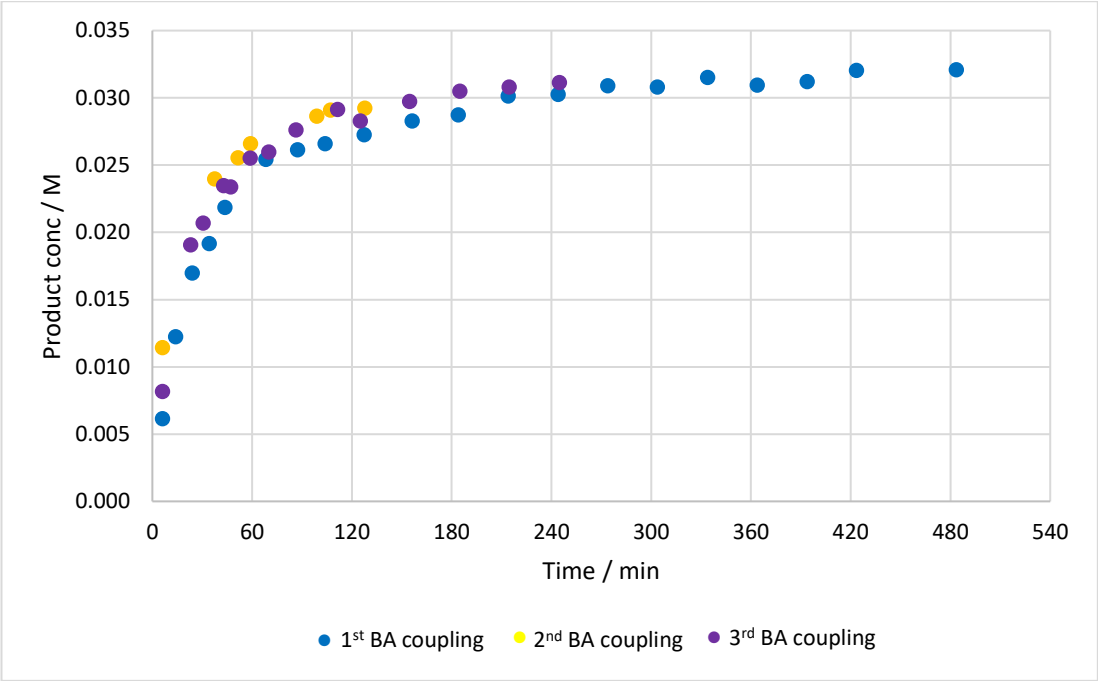

Graph 4.5.11 – Product **5** formation in the SM cross-coupling of boronic acid **3** (0.04 M) with 1,3-bis(trifluoromethyl)-5-bromobenzene **4** (0.04 M) monitored by ^{19}F NMR with 1-fluoronaphthalene as an internal standard using 0.25 mol% $[(cinnamyl)PdCl]_2$. (Procedure R)

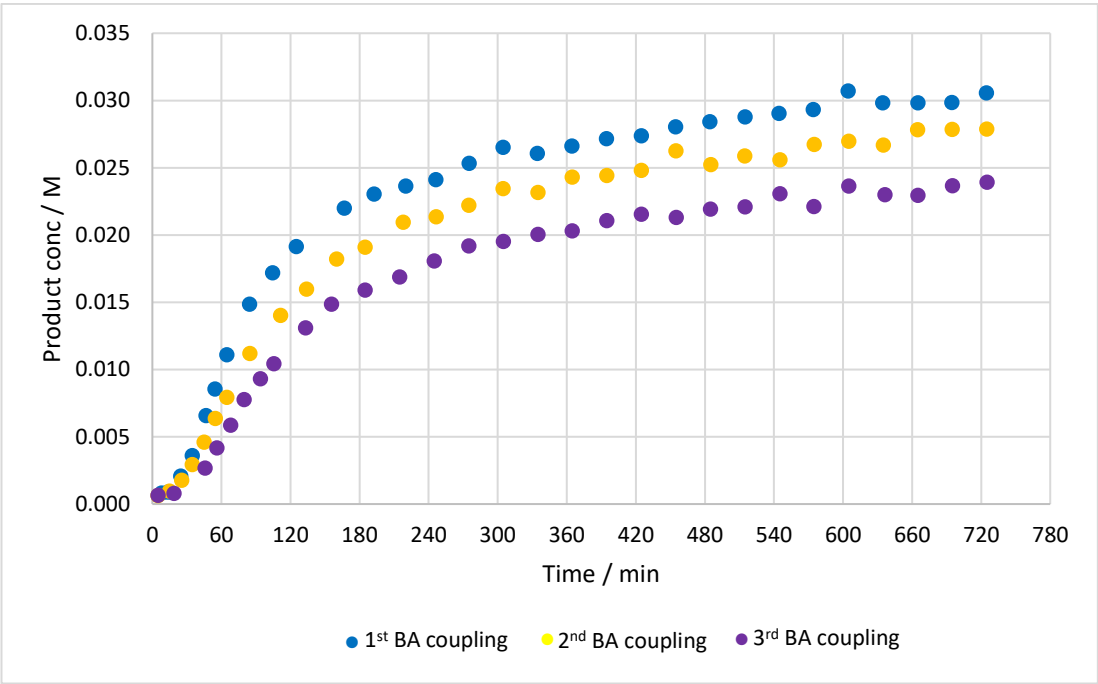

Graph 4.5.12 – Product **5** formation in the SM cross-coupling of boronic acid **3** (0.04 M) with 1,3-bis(trifluoromethyl)-5-bromobenzene **4** (0.04 M) monitored by ^{19}F NMR with 1-fluoronaphthalene as an internal standard using 0.10 mol% $[(cinnamyl)PdCl]_2$. (Procedure S)

Repeating the reaction at 10 mol% showed there to be a trend between reaction profile and age of catalyst stock solution. When the catalyst solution is made and used quickly, within 10 minutes, the reaction profile is either much faster or slower than it should be, **Graph 4.5.13**. If the catalyst solution is used after around 30 minutes, the results are comparable to each other, but still slightly faster, **Graph 4.5.14**. If the catalyst solution is used after 100 minutes, the results are now reproducible, 7.7 x 10^{-5} M min^{-1}, **Graph 4.5.15**.

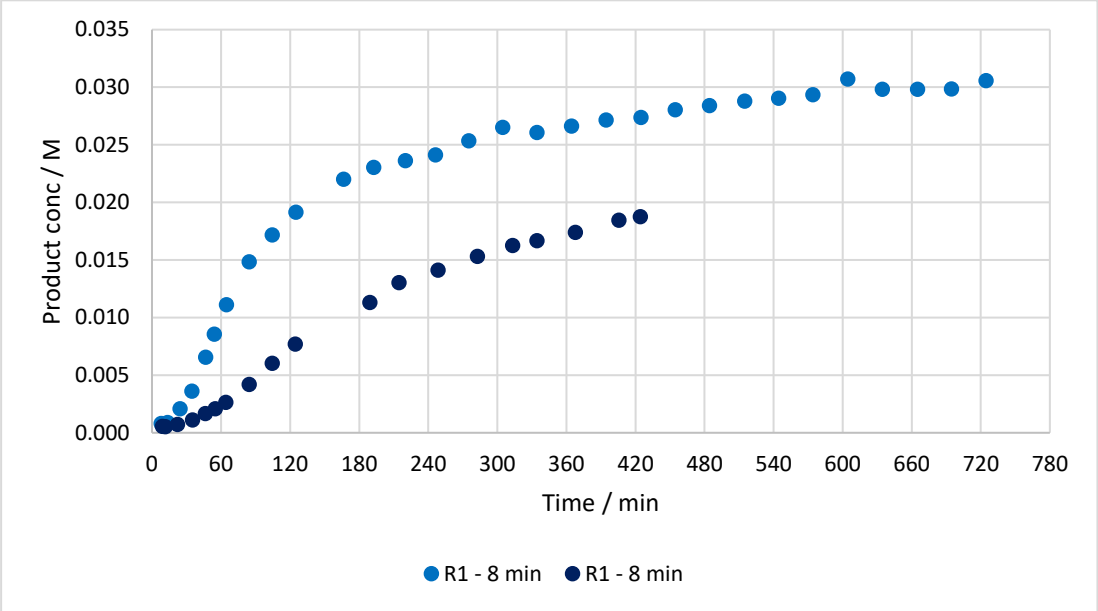

Graph 4.5.13 – Product **5** formation in the SM cross-coupling of boronic acid **3** (0.04 M) with 1,3-bis(trifluoromethyl)-5-bromobenzene **4** (0.04 M) monitored by ^{19}F NMR with 1-fluoronaphthalene as an internal standard – Both reactions carried out 8 minutes after catalyst solution was made

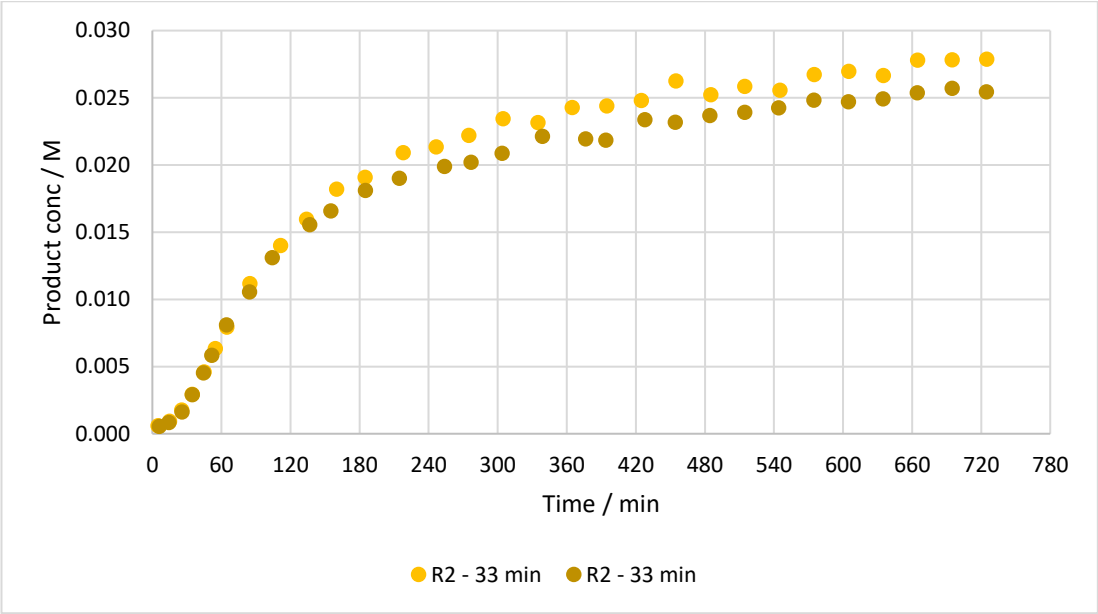

Graph 4.5.14 – Product formation in the SM cross-coupling of boronic acid **3** (0.04 M) with 1,3-bis(trifluoromethyl)-5-bromobenzene **4** (0.04 M) monitored by ^{19}F NMR with 1-fluoronaphthalene as an internal standard – Both reactions carried out 33 minutes after catalyst solution was made

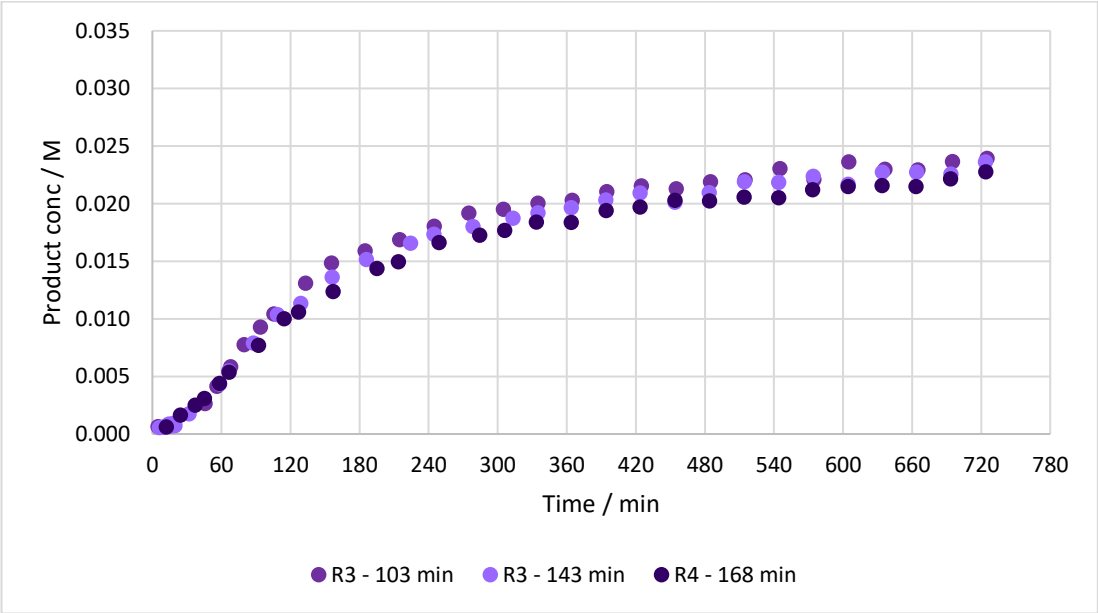

Graph 4.5.15 – Product **5** formation in the SM cross-coupling of boronic acid **3** (0.04 M) with 1,3-bis(trifluoromethyl)-5-bromobenzene **4** (0.04 M) monitored by ^{19}F NMR with 1-fluoronaphthalene as an internal standard – Three reactions carried out over 100 minutes after catalyst solution was made

This effect of age of catalyst stock solution was further confirmed by making a stock solution, waiting 100 minutes, then carrying out 3 reactions which all gave the same profile and rate, 2.49 x 10^{-4} M min^{-1} (± 0.05 x 10^{-4}), **Graph 4.5.16**. The link between age of catalyst stock solution and reproducibility could be due to a solubility issue of the $[(cinnamyl)PdCl]_2$ in THF, or due to slow dissociation of the cinnamyl ligand.

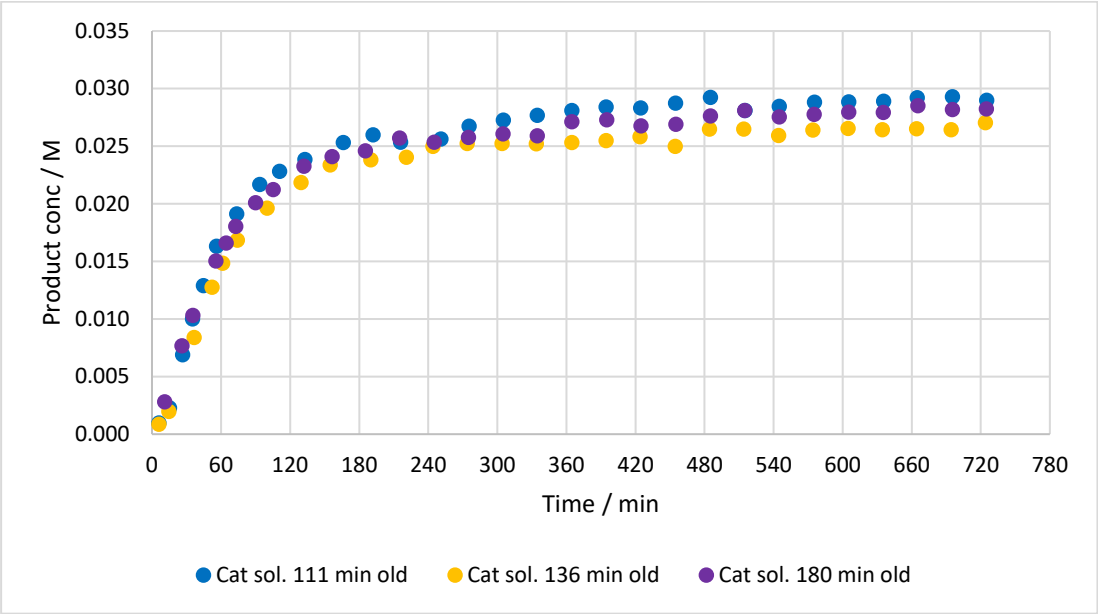

Graph 4.5.16 – Product **5** formation in the SM cross-coupling of boronic acid **3** (0.04 M) with 1,3-bis(trifluoromethyl)-5-bromobenzene **4** (0.04 M) monitored by ^{19}F NMR with 1-fluoronaphthalene as an internal standard – All reactions carried out over 100 minutes after catalyst solution was made. (Procedure S)

Esters

Now the system has been shown to be reproducible, the ester reactions were reinvestigated, **Scheme 4.5.6**, **Graph 4.5.17**. The boronic acid **3** reaction was carried out in duplicate to ensure reproducibility of the system and gave the same profile and rate. The neopentyl glycol ester **2** reaction proceeded with the same profile and rate as the boronic acid **3** (glycol ester rate = 3.04 x 10^{-4} M min^{-1}, boronic acid rate = 3.27 x 10^{-4} M min^{-1}), both reaching at least 80% conversion (boronic acid **3** = 82% after 12 hours, 85% over 24 hours; glycol ester **2** = 76% after 12 hours, 80% after 24 hours). Whereas the pinacol ester **1** reaction was much slower rate (7.90 x 10^{-5} M min^{-1}), reaching only 56% conversion (52% after 12 hours, 56% after 24 hours). Despite the differences, all three reactions formed ~3% side products – protodeboronation **9**, boronic acid homocoupling **6** and boronic acid oxidation **8**.

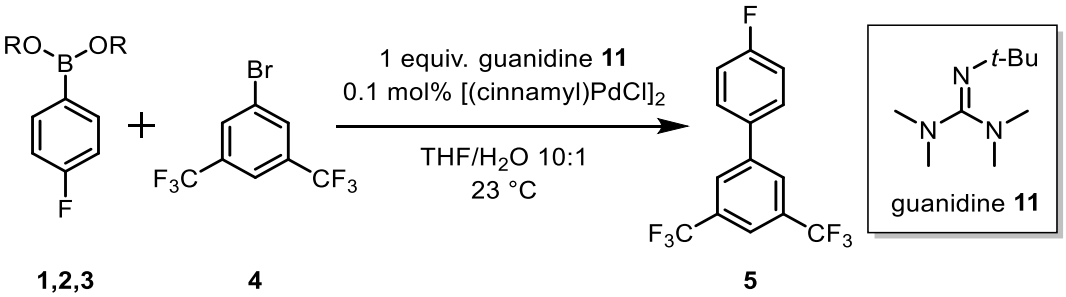

1,2,3 **4** **5**

Scheme 4.5.6 – SM cross-coupling of boronic acid **3**/ester **1**/**2** (1 equiv.) with 1,3-bis(trifluoromethyl)-5-bromobenzene **4** (1 equiv.) monitored by ^{19}F NMR with 1-fluoronaphthalene as an internal standard

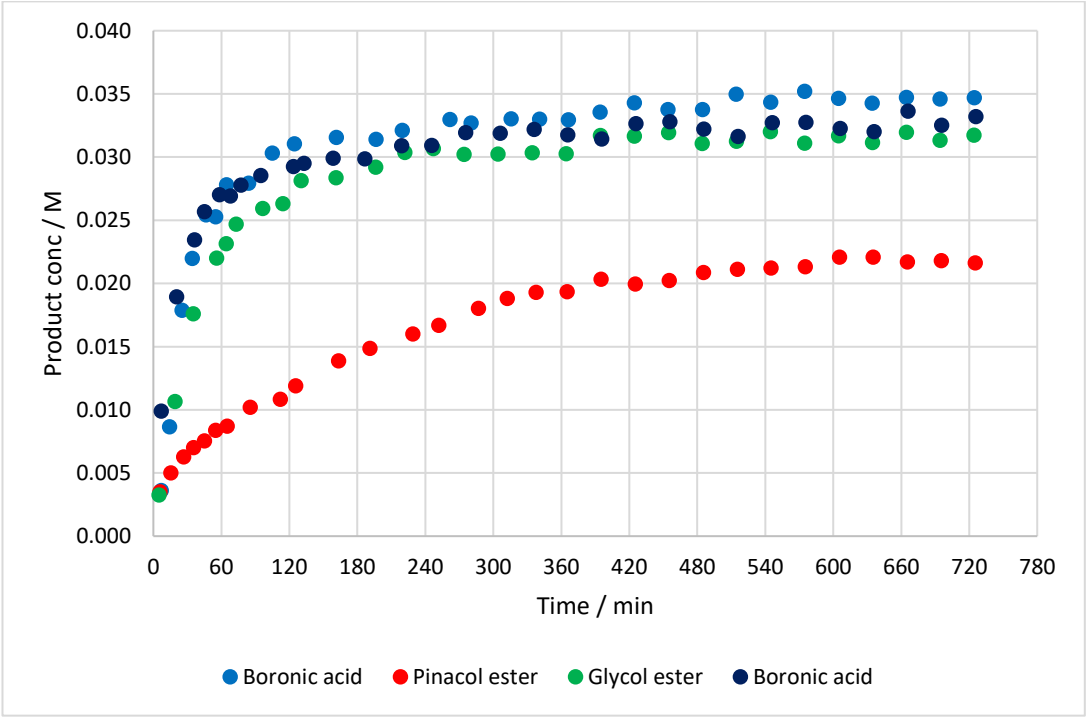

Graph 4.5.17 – Product **5** formation in the SM cross-coupling of boronic acid **3**/ester **1**/**2** (0.04 M) with 1,3-bis(trifluoromethyl)-5-bromobenzene **4** (0.04 M) monitored by ^{19}F NMR with 1-fluoronaphthalene as an internal standard. (Procedure S)

4.5.4. Catalyst summary

Throughout the course of this research, four different catalysts have been studied to find homogenous phosphine-free SM conditions. All four give high final conversion in the SM cross-coupling, **Scheme 4.5.7**, **Fig 4.5.4**, but only the $[(cinnamyl)PdCl]_2$ gives reproducible results, and only when the catalyst solution is used after 100 minutes.

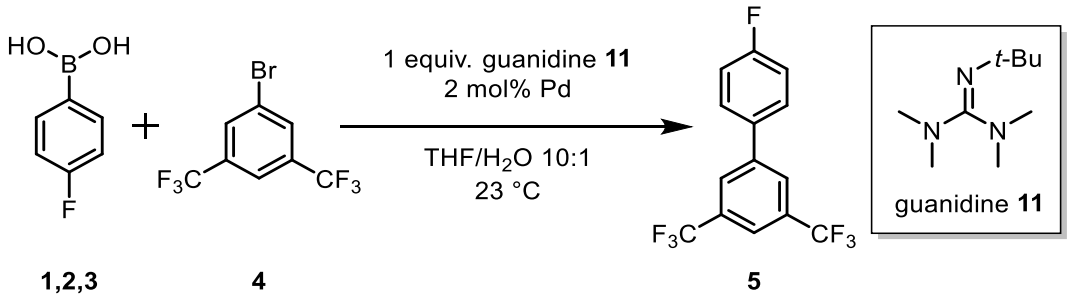

Scheme 4.5.7 – SM cross-coupling of boronic acid **3** (1 equiv.) with 1,3-bis(trifluoromethyl)-5-bromobenzene **4** (1 equiv.) monitored by ^{19}F NMR with 1-fluoronaphthalene as an internal standard

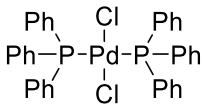	$Pd(OAc)_2$
85%	86%
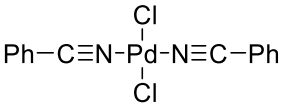	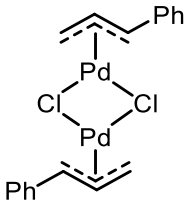
84%	85%

Fig 4.5.4 – Product **5** NMR conversion in the SM cross-coupling of boronic acid **3** (0.04 M) with 1,3-bis(trifluoromethyl)-5-bromobenzene **4** (0.04 M) by ^{19}F NMR with 1-fluoronaphthalene as an internal standard after 24 hours

4.6. Competition Reactions

One of the goals of this project was to be able to monitor the competition reaction between a boronic acid and boronic ester, **Fig 4.6.1**. However, in the presence of guanidine **11**, both the boronic acid and boronic ester signals are not observed by ^{19}F NMR as they are in an equilibrium which lies in favour of the boronate species, further discussed in **Chapter 5 – boronate formation**. To be able to follow the consumption of the starting material a quench is needed, to push the equilibrium back to boronic acid/ester. The quench used in the coupling reactions is acetic acid, but an independent study showed the addition of acetic acid to pinacol ester **1** greatly changed the ratio of ester to acid, **Fig 4.6.2**. This meant that if samples were taken and quenched, that sample would no longer give a true representation of the amount of boronic acid/ester in the system, **Scheme 4.6.1**.

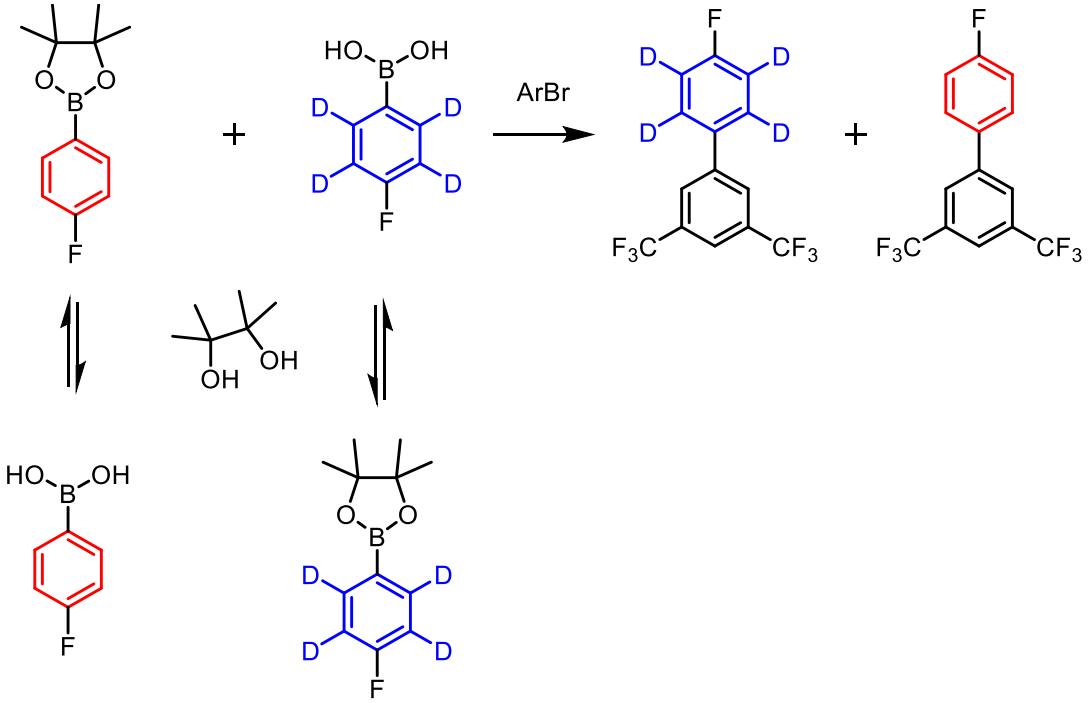

Fig 4.6.1 – Competition reaction

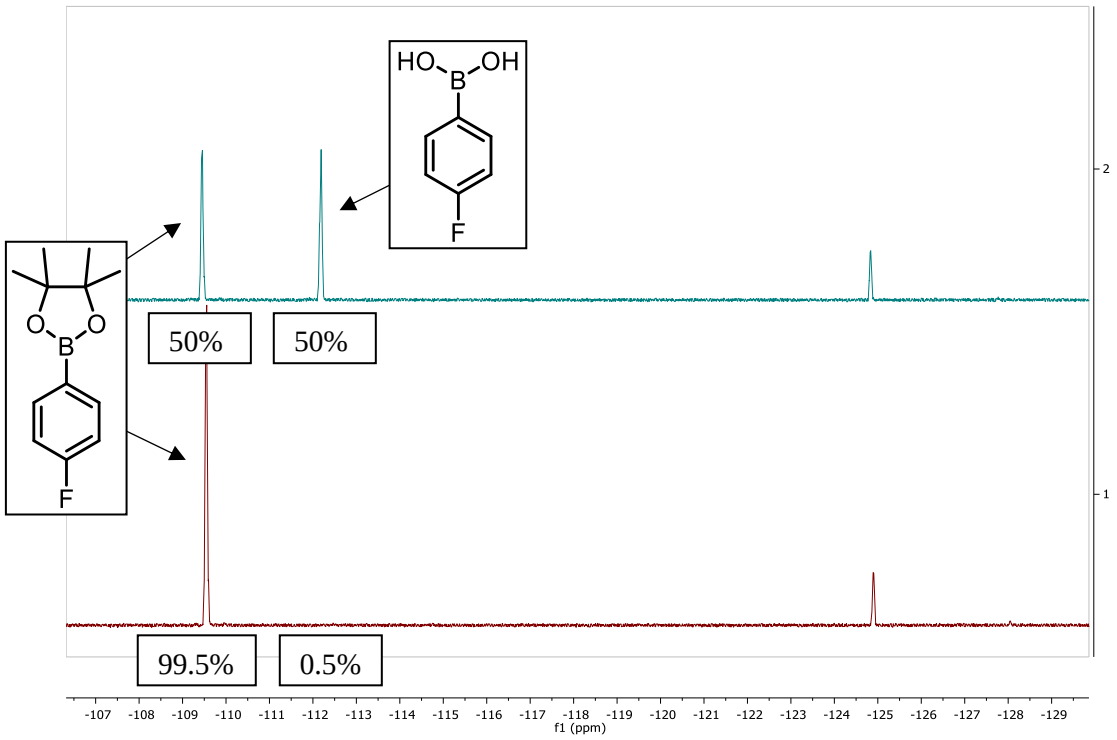

Fig 4.6.2 – Pinacol ester **1** (0.04 M) before quench (bottom spectrum) and after acetic acid quench (top spectrum) – 10:1 THF/water, 300K. ^{19}F NMR with 1-fluoronaphthalene as an internal standard

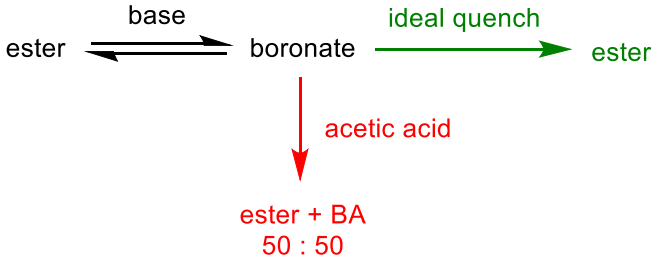

Scheme 4.6.1 – From the boronate, the ideal quench would remove the base and return the ester peak without changing the ratio of ester to boronic acid (green arrow). But the acetic acid quench instead forms 50:50 boronic acid to ester (red arrow) so the sample is no longer a true representation of the reaction mixture

An alternative quench investigated was boric acid. This would form a boronate with the guanidine **11**, pushing the boronic acid/ester equilibrium backwards. While the boric acid quench did return the boronic acid **3** signal, it also produced varying amounts of fluorobenzene **9**, −113.10 ppm, from boronic acid protodeboronation, **Fig 4.6.3**. When invertigating the pinacol ester **1**, the addition of boric acid was also found to change the ratio of boronic acid **3** to ester **1**, **Fig 4.6.4**.

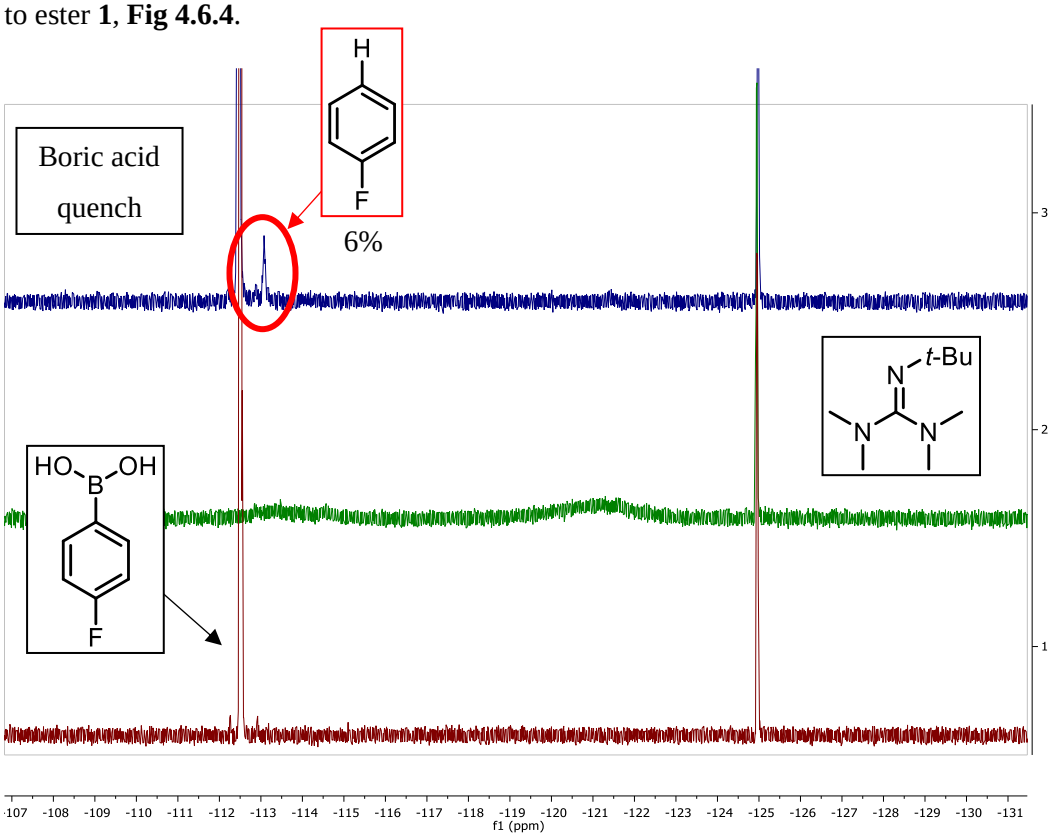

Fig 4.6.3 – 4-Fluorophenyl boronic acid **3** (0.04 M) without base (bottom spectrum). Addition of 1 equiv. guanidine **11** (middle spectrum). Addition of boric acid (excess) to boronic acid **3**/guanidine solution (top spectrum) – 10:1 THF/water, 300 K. ^{19}F NMR with 1-fluoronaphthalene as an internal standard

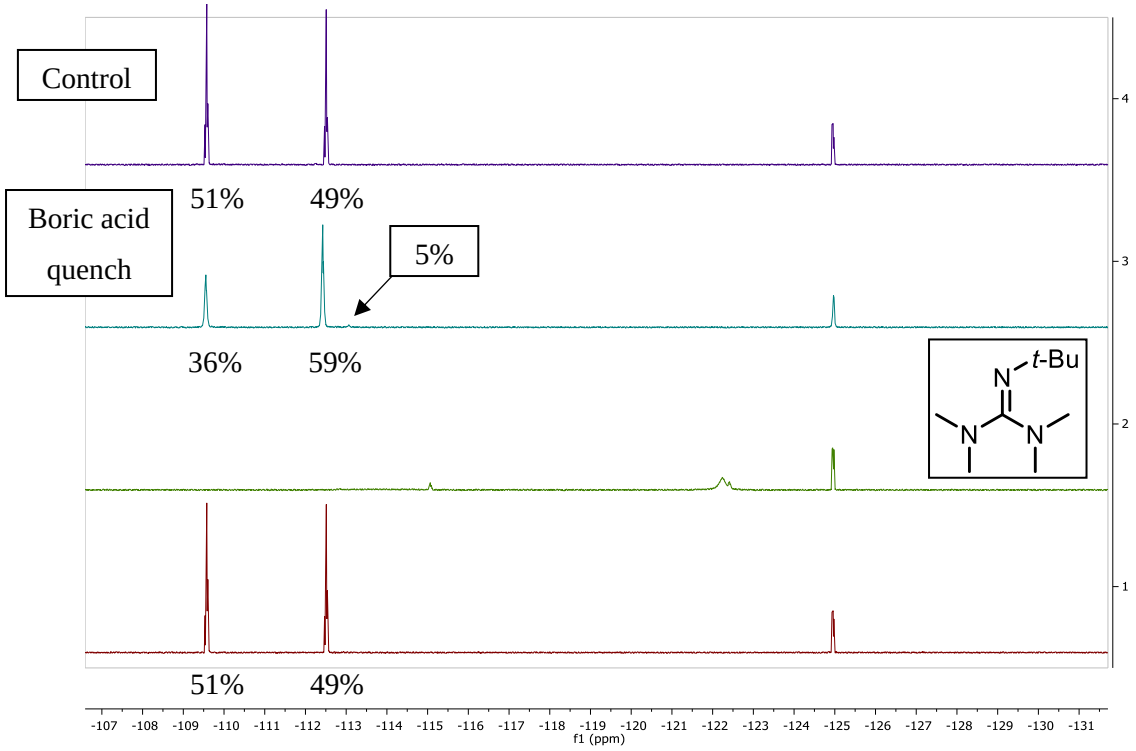

Fig 4.6.4 – Pinacol ester **1** (0.02 M) and 4-fluorophenyl boronic acid **3** (0.02M) in 10:1 THF/water (bottom spectrum), addition of 1 equiv. guanidine **11** (0.04 M) (spectrum 2), addition of boric acid (excess) to ester/acid/guanidine solution (spectrum 3), control sample of ester **1**/acid **3** 1:1 in 10:1 THF/water. 300K. ^{19}F NMR with 1-fluoronaphthalene as an internal standard

Despite the quench issues when using a boronic ester, a competition reaction of two boronic acids could be investigated using an acetic acid quench, **Scheme 4.6.2**, **Graph 4.6.1**. The data from the competition reaction could then be plotted as ratio of the two boron species (R) vs conversion (F), **Graph 4.6.2**. By fitting the data, a relative rate is obtained, which shows the para F boronic acid **3** to couple at a faster rate relative to the para CF_3 boronic acid **12**.

$$k_{rel} = \frac{F}{CF_3} = 1.76.$$

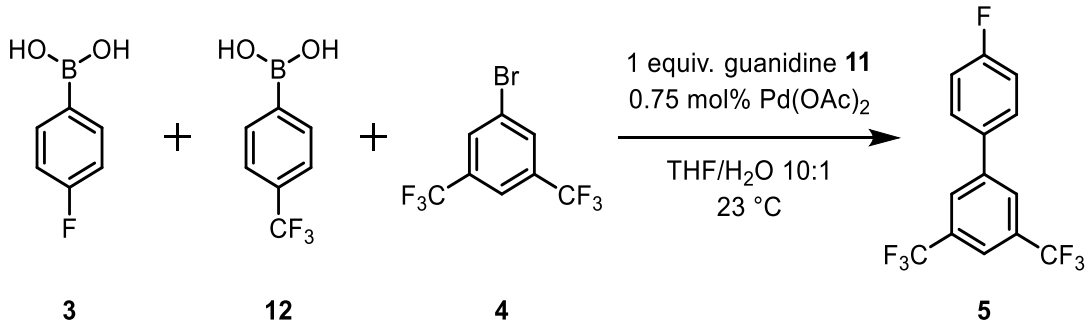

3 **12** **4** **5**

Scheme 4.6.2 – Competition SM cross-coupling of 4-fluorophenyl boronic acid **3** (0.5 equiv.) and 4-trifluoromethylphenyl boronic acid **12** (0.5 equiv.) with 1,3-bis(trifluoromethyl)-5-bromobenzene **4** (1 equiv.) monitored by ^{19}F NMR with 1-fluoronaphthalene as an internal standard

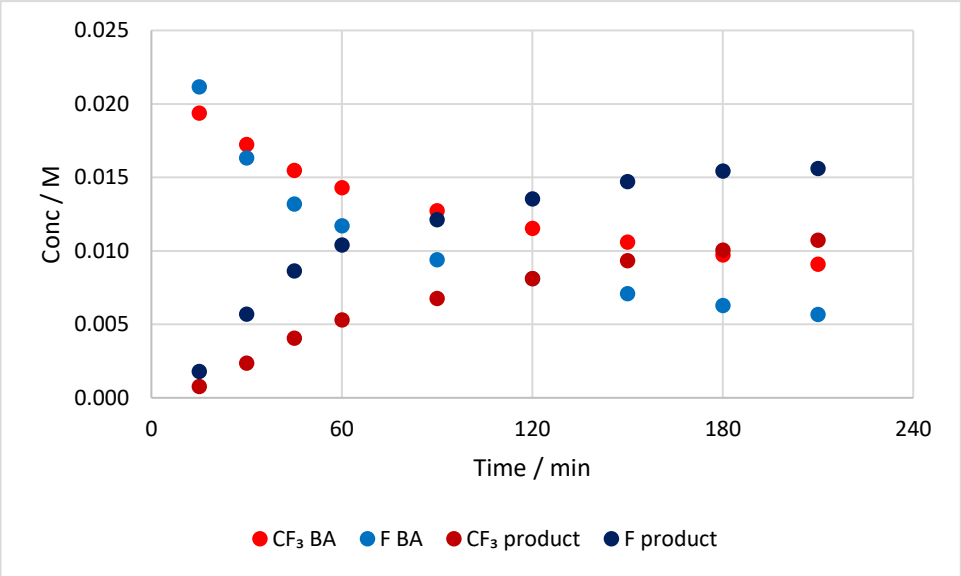

Graph 4.6.1 – Competition SM cross-coupling of 4-fluorophenyl boronic acid **3** (0.023 M) and 4-trifluoromethylphenyl boronic acid **12** (0.021 M) with 1,3-bis(trifluoromethyl)-5-bromobenzene **4** (0.04 M) monitored by ^{19}F NMR with 1-fluoronaphthalene as an internal standard. (Procedure M)

$$F = 1 - \frac{\left(\frac{R}{R_0}\right)^{\frac{1}{k_{rel}-1}}}{\frac{1+R_0}{1+R}} \qquad R = \frac{[CF_3]}{[F]} \qquad k_{rel} = \frac{CF_3}{F} = 0.568$$

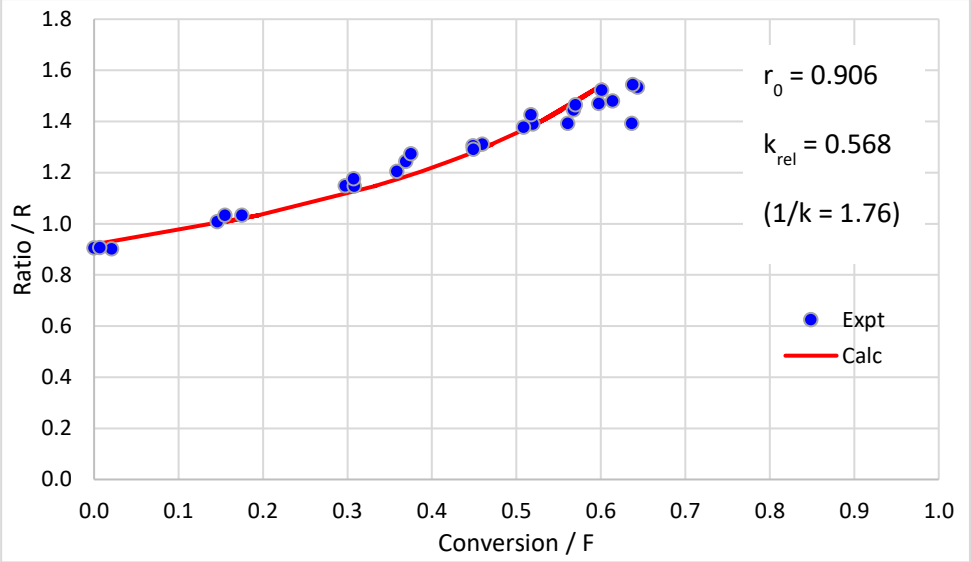

Graph 4.6.2 – Ratio (R) vs conversion (F) for the competition SM cross-coupling of 4-fluorophenyl boronic acid **3** (0.5 equiv.) and 4-trifluoromethylphenyl boronic acid **12** (0.5 equiv.) with 1,3-bis(trifluoromethyl)-5-bromobenzene **4** (1 equiv.) monitored by ^{19}F NMR with 1-fluoronaphthalene as an internal standard

4.7. Bases

To see how the guanidine **11** compared to other bases, especially those commonly used in SM reactions, a base screen was carried out using either $Pd(OAc)_2$ or $PdCl_2(PhCN)_2$, as these catalysts give consistent high yields despite the irreproducible rate of reaction. These reactions were monitored for final conversion only, calculated from ^{19}F NMR using 1-fluoronaphthalene as an internal standard.

4.7.1. Organic bases

Organic bases more commonly used in SM couplings, such as triethylamine and DABCO,[1–5] were tested under the newly developed conditions, **Scheme 4.7.1**, and found to give very poor results, **Fig 4.7.1**. A range of other organic bases were also tested, **Scheme 4.7.1**, all giving poor results, with the exception of phosphazene base P_2-Et, **Fig 4.7.1**. This base was tested as it is reported to work well by Dreher *et al.* in a study of Pd-catalysed cross-coupling reactions using four different organic superbases, which also included guanidine **11** – the base used in these studies.[12] P_2-Et is a strong base which gives high conversion, 76%. Whereas, the other bases tested are all weaker than the guanidine **11**, suggesting a strong base is needed for efficient coupling under these conditions. The phosphazene base is the only base tested in this study that forms a boronate species, shown by ^{19}F and ^{11}B NMR and further discussed in **Chapter 5 – Boronate formation**. DMAP was shown to give no product formation, in agreement with literature.[6]

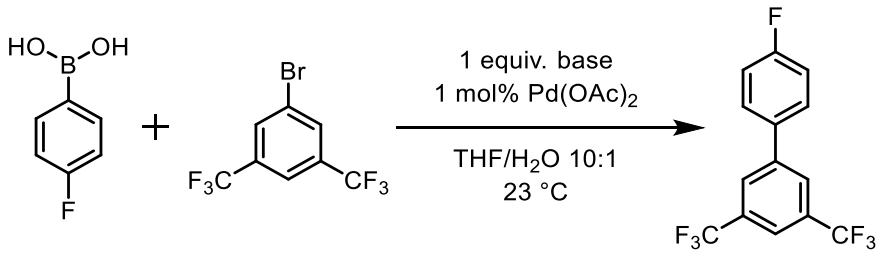

3 **4** **5**

Scheme 4.7.1 – SM cross-coupling of boronic acid **3** (1 equiv.) with 1,3-bis(trifluoromethyl)-5-bromobenzene **4** (1 equiv.) by ^{19}F NMR with 1-fluoronaphthalene as an internal standard

	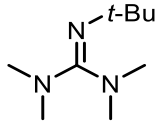	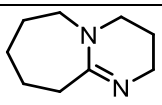	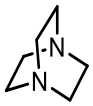	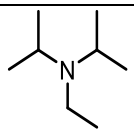
	Guanidine **11**	DBU	DABCO	Diisopropylethylamine
% conversion	**88%**	7%	13%	4%
	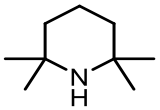	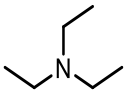	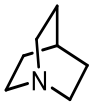	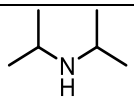
	2,2,6,6-tetramethylpiperidine	Triethylamine	Quinuclidine	Diisopropylamine
% conversion	21%	4%	23%	11%
	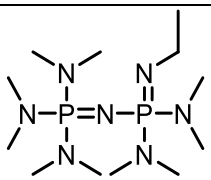	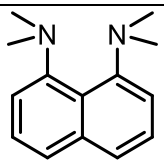	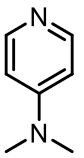	
	Phosphazene base P_2-Et	Proton sponge	DMAP	
% conversion	**76%**	3%	0%	

Fig 4.7.1 – SM cross-coupling of boronic acid **3** (0.04 M) with 1,3-bis(trifluoromethyl)-5-bromobenzene **4** (0.04 M) testing organic bases. Yields after 24 hours by ^{19}F NMR with 1-fluoronaphthalene as an internal standard. (Procedure U)

The addition of catalytic amounts of guanidine **11** in addition to 1 equivalent of organic base was also tested, **Scheme 4.7.2**. The reaction using 1 equiv. DABCO gave 5% product conversion. Under the same conditions, with 10 mol% guanidine **11** added, the reaction reached 19% conversion. This shows that guanidine **11** does give an improved yield, but catalytic amounts are not enough to give high yields.

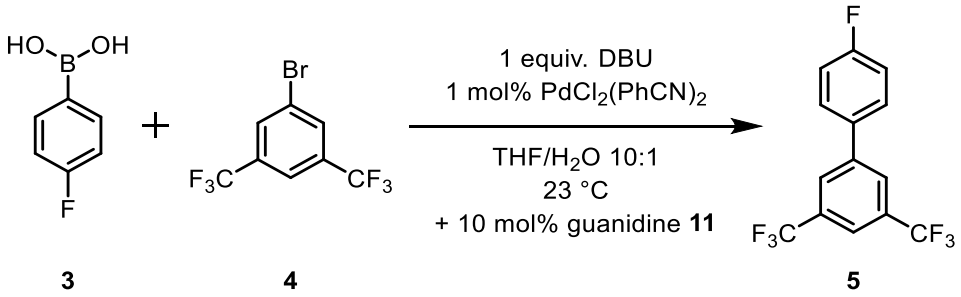

3 **4** **5**

Scheme 4.7.2 – SM cross-coupling of boronic acid **3** (1 equiv.) with 1,3-bis(trifluoromethyl)-5-bromobenzene **4** (1 equiv.) by ^{19}F NMR with 1-fluoronaphthalene as an internal standard

4.7.2. Guanidines

To examine the effect of steric bulk around the guanidine, the *t*-Bu group was replaced with hydrogen – 1,1,3,3-tetramethylguanidine (TMG) **13**, **Fig 4.7.3**, and tested for SM cross-coupling under the newly developed conditions, **Scheme 4.7.3**. This base, **13**, was found to give only 1% conversion to product, suggesting the need for a bulky substituent on the imine nitrogen. 2-Butyl-1,1,3,3-tetramethylguanidine **14** was synthesized using a literature procedure[15] and tested in SM cross-coupling, **Fig 4.7.3**. This base gave higher conversion than the NH guanidine **13**, 48%, but still not as high as the *tert*-butyl guanidine **11**, 88%. The difference in basicity between the three species should be relatively low, as demonstrated by the small difference between acetamidine, guanidine and TMG, **Fig 4.7.2**, so this effect is unlikely due to the strength of the base.[16,17] The reason for the difference between the three bases could instead be due to the interaction between the guanidine and palladium catalyst.

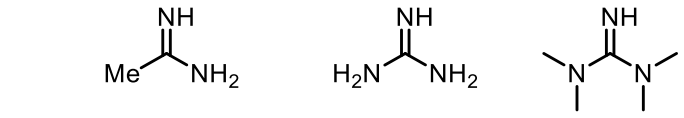

	acetamidine	guanidine	TMG **13**
pKa	12.4	13.6	13.6

Fig 4.7.2 – Structure of amidines and guanidine derivatives – pKa of the conjugate acid in H_2O.[16] TMG = 1,1,3,3-tetramethylguanidine **13**

In a study using guanidine as a ligand for $Pd(OAc)_2$ in SM coupling, Zhang *et al.* report steric bulk of the guanidine to be important for the activity of the ligand and catalyst.[13] The effects

seen here could be due to guanidine binding to the catalyst which kills the reactivity. The NH guanidine **13**, having no bulky substituent, would bind the strongest of the three, hence the minimal reactivity. The butyl guanidine **14**, being less bulking than the *tert*-butyl **11**, could bind to an extent but not as well as the NH **13**, hence the giving higher conversion that the NH guanidine **13** but not as high as *tert*-butyl guanidine **11**. The *tert*-butyl group is perhaps too bulky to bind, therefore leaving the catalyst unchanged and able to give high conversion to the desired product. This effect is investigated further in the next section; **4.7.3. Inhibitors**.

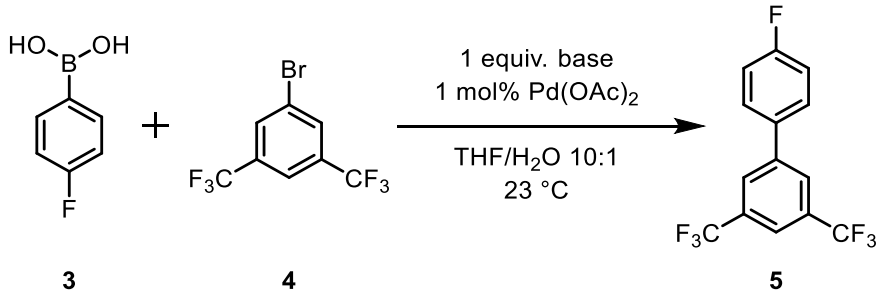

3 **4** **5**

Scheme 4.7.3 –SM cross-coupling of boronic acid **3** (1 equiv.) with 1,3-bis(trifluoromethyl)-5-bromobenzene **4** (1 equiv.) by ^{19}F NMR with 1-fluoronaphthalene as an internal standard.

	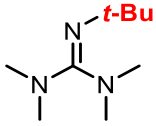 **11**	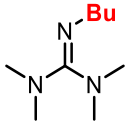 **14**	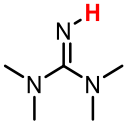 **13**
% conversion	88%	56%	1%

Fig 4.7.3 – SM cross-coupling of boronic acid **3** (0.04 M) with 1,3-bis(trifluoromethyl)-5-bromobenzene **4** (0.04 M) testing guanidines **11**/**13**/**14**. Yields after 24 hours by ^{19}F NMR with 1-fluoronaphthalene as an internal standard. (Procedure U)

4.7.3. Inhibitors

To assess if poor performing bases act as inhibitors in the reaction, they were added to the standard reaction and compared to a control reaction, **Scheme 4.7.4**. The addition of 1 equivalent of NH guanidine **13** was found to vastly reduce the amount of product formed, from 88% to 10%, **Fig 4.7.4**. This shows the NH guanidine **13** to be inhibiting the reactivity.

The organic base that gave the lowest conversion was DMAP, so 1 equivalent of DMAP was added to a *t*-Bu guanidine **11** coupling and found to give only 3% conversion, showing DMAP to be an inhibitor in the reaction, **Fig 4.7.4**.

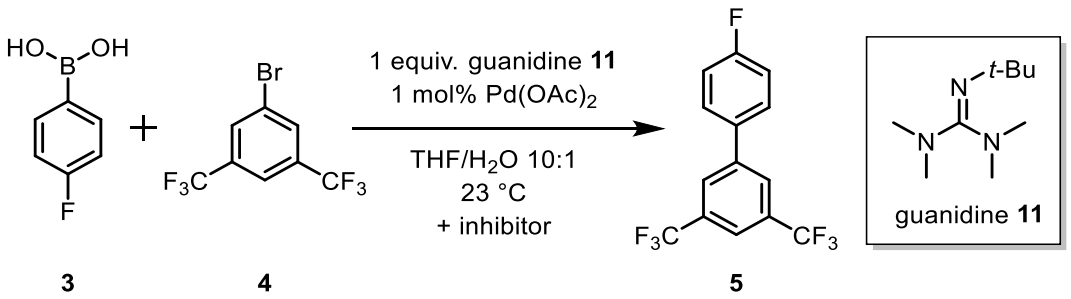

3 **4** **5**

Scheme 4.7.4 – SM cross-coupling of boronic acid (1 equiv.) with 1,3-bis(trifluoromethyl)-5-bromobenzene (1 equiv.) by ^{19}F NMR with 1-fluoronaphthalene as an internal standard

Base + inhibitor	Product
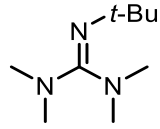 **11**	88%
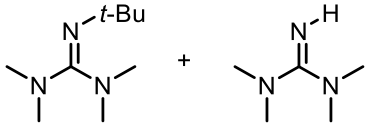 **11** + **13** 1 equiv. each	10%
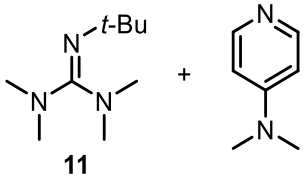 **11** + 1 equiv. each	3%

Fig 4.7.4 – SM cross-coupling of boronic acid **3** (0.04 M) with 1,3-bis(trifluoromethyl)-5-bromobenzene **4** (0.04 M) testing potential inhibitors. Yields after 24 hours by ^{19}F NMR with 1-fluoronaphthalene as an internal standard

Adding half an equivalent NH guanidine **13** to a standard *t*-Bu guanidine **11** coupling, **Scheme 4.7.5**, is enough to kill the reactivity. The standard coupling under these conditions reaches a conversion of 82%, but the addition of half an equivalent NH guanidine **13** resulted in < 5% conversion by ^{19}F NMR. The effect of NH guanidine **13** on a working reaction was also investigated, under conditions shown in **Scheme 4.7.5**. The standard *t*-Bu guanidine **11** coupling was carried out and run to 30 min, at this point half an equivalent of NH guanidine **13** was added. The control reaction reached a final conversion of 75%, whereas the NH guanidine **13** spiked reaction only reached 40%. The conversion of the control reaction at 30 minutes was 36%, showing that once the spike had been added there was very little further product formation, confirming the hypothesis of the NH guanidine **13** acting as an inhibitor.

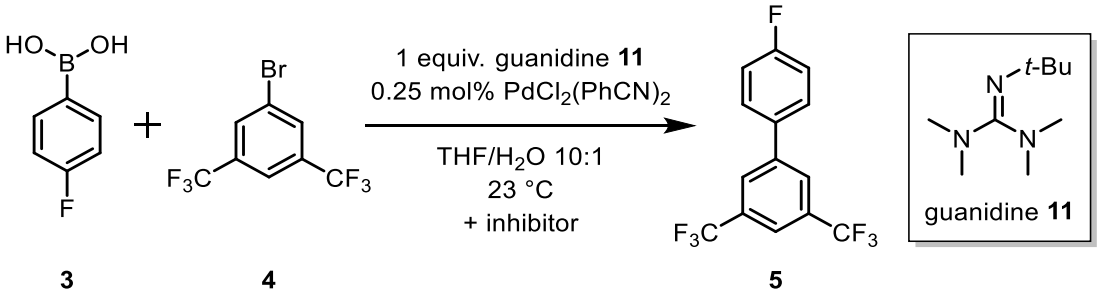

Scheme 4.7.5 – SM cross-coupling of boronic acid (1 equiv.) with 1,3-bis(trifluoromethyl)-5-bromobenzene (1 equiv.) by ^{19}F NMR with 1-fluoronaphthalene as an internal standard

The effect of adding a phosphorus ligand to the reaction was also studied, **Scheme 4.7.6**. Without the addition of this ligand, the reaction reaches a conversion of 68%. Addition of 2 mol% triphenylphosphine greatly reduced this cross-coupling to only 13% conversion, **Fig 4.7.5**. The addition of this ligand also greatly increased the amount of fluorophenol **8**, from boronic acid oxidation, produced. One hypothesis for the reduced conversion is that the addition of a phosphorus ligand now allows the formation of an oxo-palladium species. But as the use of guanidine **11** forms a boronate species, there is no boronic acid present to undergo oxo-palladium transmetalation. The guanidine **11** has also been shown to act as a ligand for $Pd(OAc)_2$,[13] so could now be in competition with the phosphine ligand between an active and inactive catalytic species. Further ligand effect studies are needed to identify the cause of the lowered reactivity and the active catalyst.

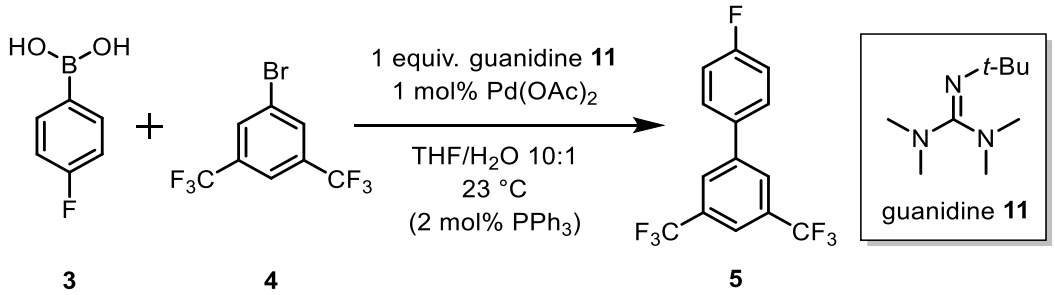

3 **4** **5**

Scheme 4.7.6 – SM cross-coupling of boronic acid **3** (1 equiv.) with 1,3-bis(trifluoromethyl)-5-bromobenzene **4** (1 equiv.) by ^{19}F NMR with 1-fluoronaphthalene as an internal standard

	% Product **5**	% Total side products	% Protodeboronation **9**	% BA homocoupling **6**	% Fluorophenol **8**
Standard conditions	68%	4%	2%	1%	1%
Standard conditions + **2 mol% PPh_3**	13%	17%	0%	0%	17%

Fig 4.7.5 – Comparison of reaction with and without addition of triphenylphosphine. SM cross-coupling of boronic acid **3** (0.04 M) with 1,3-bis(trifluoromethyl)-5-bromobenzene **4** (0.04 M) by ^{19}F NMR with 1-fluoronaphthalene as an internal standard

4.7.4. Inorganic bases

SM cross-coupling typically employs an inorganic base.[18] So a comparison was carried out to evaluate how the guanidine **11** compares to different inorganic bases, **Scheme 4.7.7**, **Fig 4.7.6**. The base originally used at the beginning of this study, potassium carbonate, was found to give very poor results, only 15% product, in comparison to 88% when using guanidine **11**. Three other weak inorganic bases were tested and also found to give low yields. The one inorganic base studied that gave good conversion was potassium hydroxide, KOH. This is a much stronger base, so provides further evidence for the requirement of a strong base for efficient coupling under these conditions. KOH is the only base examined, other than the phosphazene and the guanidine range, which forms a boronate species, shown by ^{19}F and ^{11}B NMR and

further discussed in **Chapter 5 – Boronate formation**. This highlights the potential importance of the boronate species for efficient coupling.

Increasing the amount of KOH from 1 equiv. to 3 equiv. resulted in an increase in product formation, 50% to 82%, but also increased side product formation from 4% to 14%. There was a slight increase in both boronic acid homocoupling **6** (1.5% to 3.5%) and oxidation **8** (1.5% to 2%), but also gave a large rise to protodeboronation **9**, 1% with 1 equiv. compared to 8.5% with 3 equiv. KOH. The high amount of inorganic base present also creates phase separation, which prohibits *in situ* reaction monitoring by standard NMR, and instead requires sampling to monitor the reaction conversion.

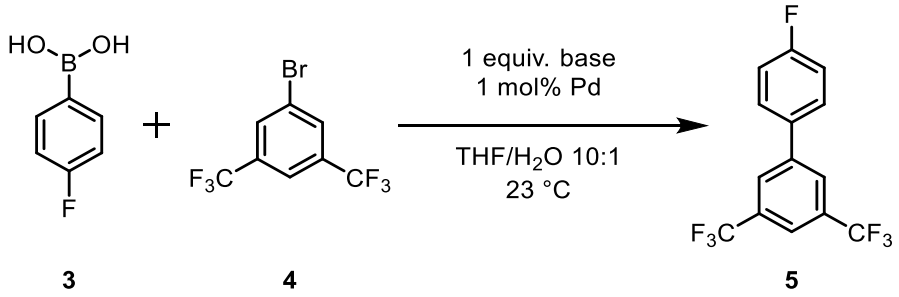

3 **4** **5**

Scheme 4.7.7 – SM cross-coupling of boronic acid **3** (1 equiv.) with 1,3-bis(trifluoromethyl)-5-bromobenzene **4** (1 equiv.) by ^{19}F NMR with 1-fluoronaphthalene as an internal standard. Pd = $Pd(OAc)_2$ or $PdCl_2PhCN_2$

	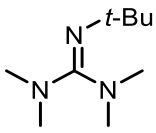 **11**	K_2CO_3	K_3PO_4	Cs_2CO_3	$NaHCO_3$	KOH
Product	**88%**	15%	14%	11%	8%	**50%**

Fig 4.7.6 – SM cross-coupling of boronic acid **3** (0.04 M) with 1,3-bis(trifluoromethyl)-5-bromobenzene **4** (0.04 M) testing commonly used inorganic bases (1 equiv.). Yields after 24 hours by ^{19}F NMR with 1-fluoronaphthalene as an internal standard. (Procedure U)

The addition of a catalytic amount of *t*-Bu guanidine **11** to a reaction with stoichiometric inorganic base was investigated, **Scheme 4.7.8**. The reaction using one equiv. potassium carbonate reached a conversion of 15%. When this reaction was repeated with 10 mol% *t*-Bu guanidine **11** added it reached a higher conversion of 31%. While this is an improvement in

yield, it shows that catalytic amounts of guanidine are not enough to give high conversion, despite the reported use of guanidine as a ligand in SM cross-coupling using potassium carbonate.[13]

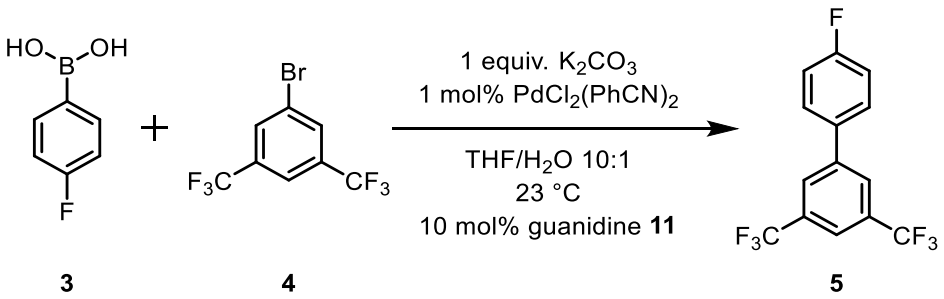

3 **4** **5**

Scheme 4.7.8 – SM cross-coupling of boronic acid **3** (1 equiv.) with 1,3-bis(trifluoromethyl)-5-bromobenzene **4** (1 equiv.) by ^{19}F NMR with 1-fluoronaphthalene as an internal standard.

4.8. Boronic acid scope

A range of boronic acids were tested under the new homogenous conditions to assess the scope of the reaction, **Scheme 4.8.1**, **Fig 4.8.1**. Aliquots of the reaction were taken after 24 hours and NMR conversion were determined by ^{19}F NMR against 1-fluoronaphthalene as an internal standard. The reaction was found to be tolerant of both electron donating and withdrawing substituents, giving the desired biaryl products in excellent conversion (71 – 90%), and all giving less than 1 % total side products.

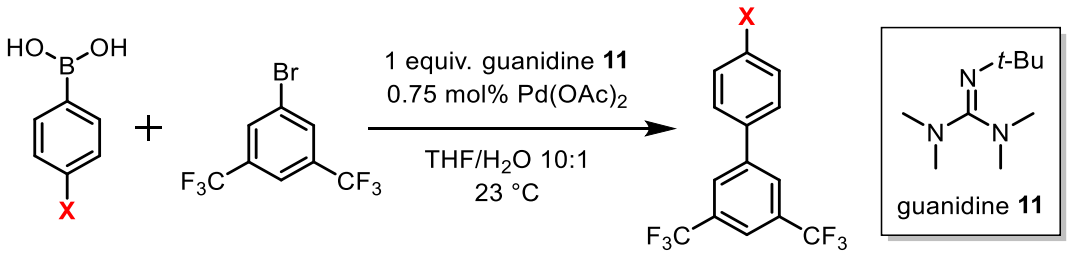

4

Scheme 4.8.1 – SM cross-coupling of boronic acid (1 equiv.) with 1,3-bis(trifluoromethyl)-5-bromobenzene **4** (1 equiv.) by ^{19}F NMR with 1-fluoronaphthalene as an internal standard

	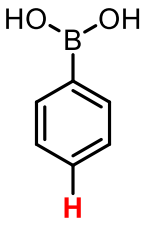	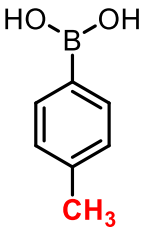	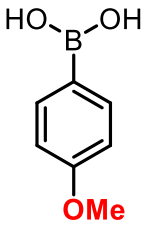	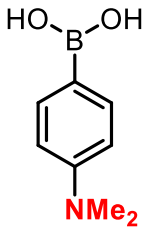
NMR conversion	84%	86%	85%	83%
	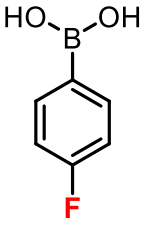	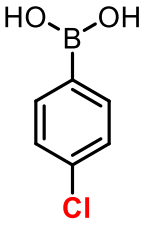	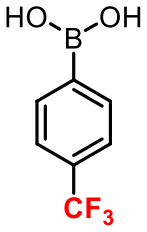	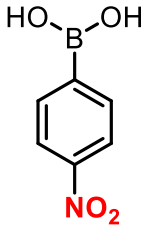
NMR conversion	90%	77%	79%	71%

Fig 4.8.1 – SM cross-coupling of boronic acid (0.04 M) with 1,3-bis(trifluoromethyl)-5-bromobenzene **4** (0.04 M). Yields after 24 hours by ^{19}F NMR with 1-fluoronaphthalene as an internal standard. (Procedure O)

4.9. Aryl halide range

A range of aryl halides were also examined to assess if more electron rich aryl halides are competent coupling partners under the developed reaction conditions, **Scheme 4.9.1**, **Fig 4.9.1**. Chlorides were found to give very poor conversion, less than 10%. Both bromide and iodide reagents were found to work well, with switching the bis 3,5-trifluoromethyl substituent **4** to a 4-fluoro substituent still giving 71% product conversion.

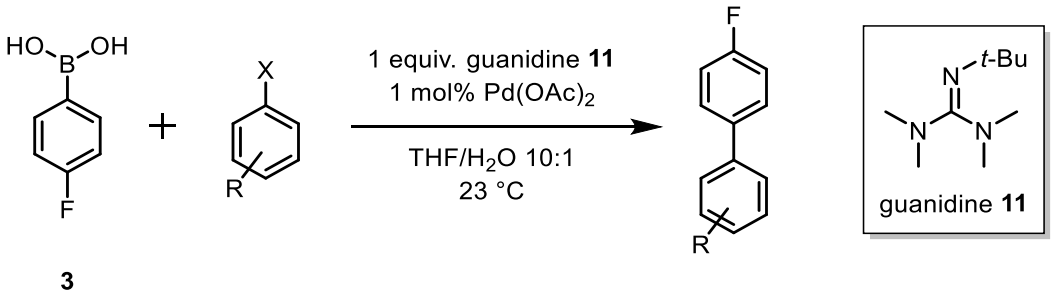

3

Scheme 4.9.1 – SM cross-coupling of boronic acid **3** (1 equiv.) with aryl halide (1 equiv.) by ^{19}F NMR with 1-fluoronaphthalene as an internal standard

	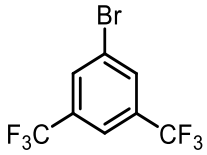	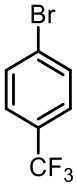	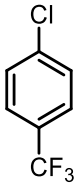
Yield	90%	85%	2%
Side products	3%	6%	14%
	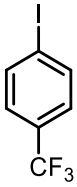	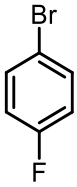	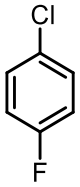
Yield	84%	71%	7%
Side products	1%	9%	6%

Fig 4.9.1 – SM cross-coupling of boronic acid **3** (0.04 M) with aryl halide (0.04 M). Yields after 24 hours by ^{19}F NMR with 1-fluoronaphthalene as an internal standard. (Procedure O – swap boronic acid for aryl halide)

4.10. Conclusion

New conditions for a homogenous, phosphine-free SM cross-coupling using guanidine **11** as a base have been developed. Despite issues with reproducibility and catalyst degradation, a system has been found which allowed for the study and comparison of the reactivity of boronic acid **3** and boronic esters **1**/**2**, **Scheme 4.10.1**, **Graph 4.10.1**. This study showed the pinacol ester **1** to have a much slower rate of reaction, (7.90×10^{-5} M min^{-1}), in comparison to the boronic acid **3** and glycol ester **2**, (glycol ester rate = 3.04×10^{-4} M min^{-1}, boronic acid rate = 3.27×10^{-4} M min^{-1}), but this has been found to be highly dependent on reaction conditions.

The use of an inorganic base showed the boronic acid **3**, pinacol ester **1** and neopentyl glycol ester **2** to couple at the same rate, **Chapter 3**, whereas the use of guanidine **11** with $Pd(PPh_3)_2Cl_2$, **Scheme 4.10.2**, showed the two esters **1**/**2** to couple at the same rate to each other and at a faster rate relative to the boronic acid **3**, as well as reducing the induction period, **Graph 4.10.2**.

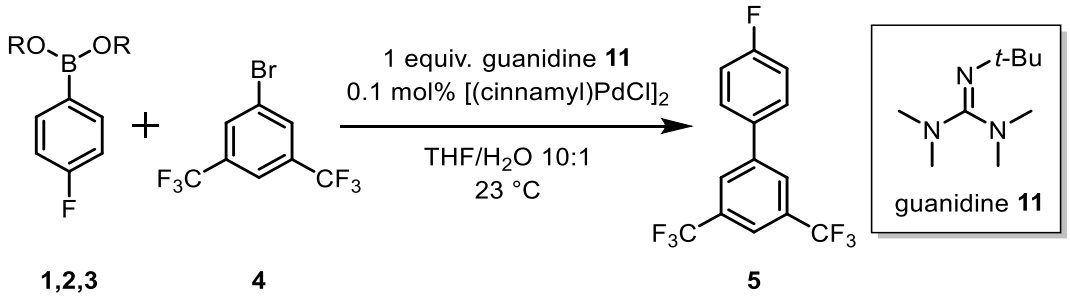

1,2,3 **4** **5**

Scheme 4.10.1 – SM cross-coupling of boronic acid **3**/ester **1**/**2** (1 equiv.) with 1,3-bis(trifluoromethyl)-5-bromobenzene **4** (1 equiv.) monitored by ^{19}F NMR with 1-fluoronaphthalene as an internal standard

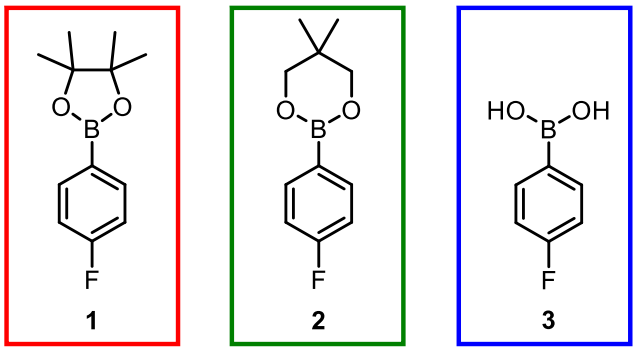

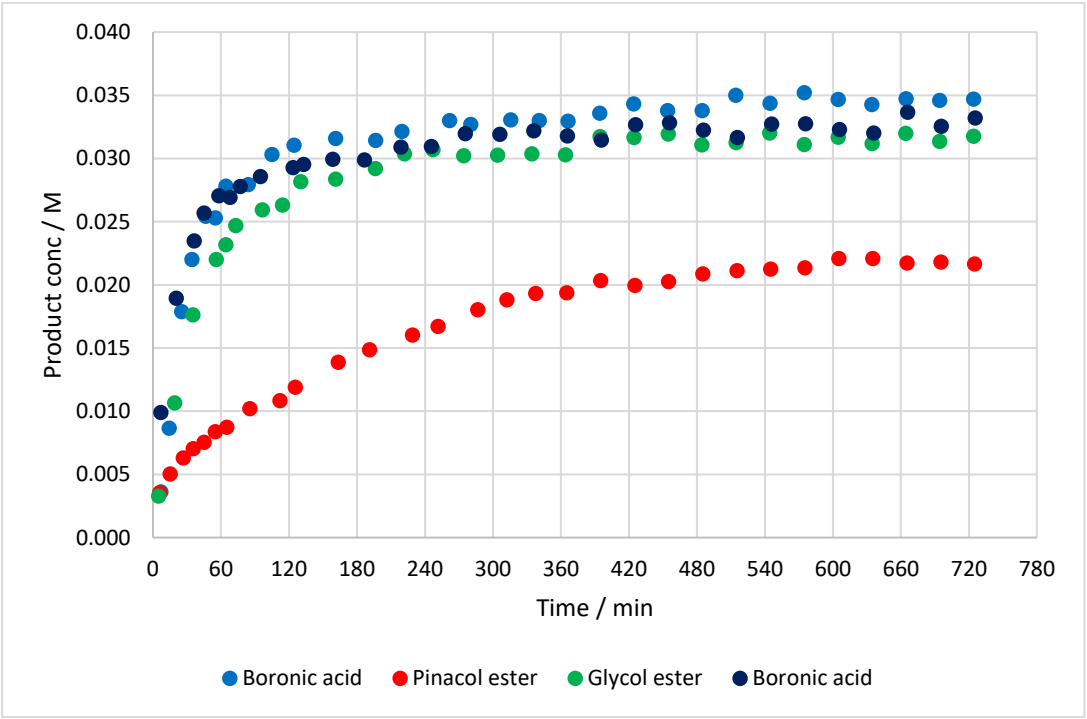

Graph 4.10.1 – Product **5** formation in the SM cross-coupling of boronic acid **3**/ester **1**/**2** (0.04 M) with 1,3-bis(trifluoromethyl)-5-bromobenzene **4** (0.04 M) monitored by ^{19}F NMR with 1-fluoronaphthalene as an internal standard

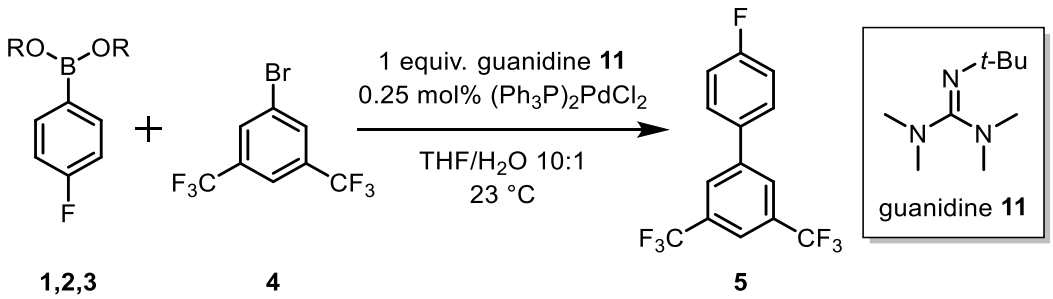

1,2,3 **4** **5**

Scheme 4.10.2 – SM cross-coupling of boronic acid **3**/ester **1**/**2** (1 equiv.) with 1,3-bis(trifluoromethyl)-5-bromobenzene **4** (1 equiv.) monitored by ^{19}F NMR with 1-fluoronaphthalene as an internal standard

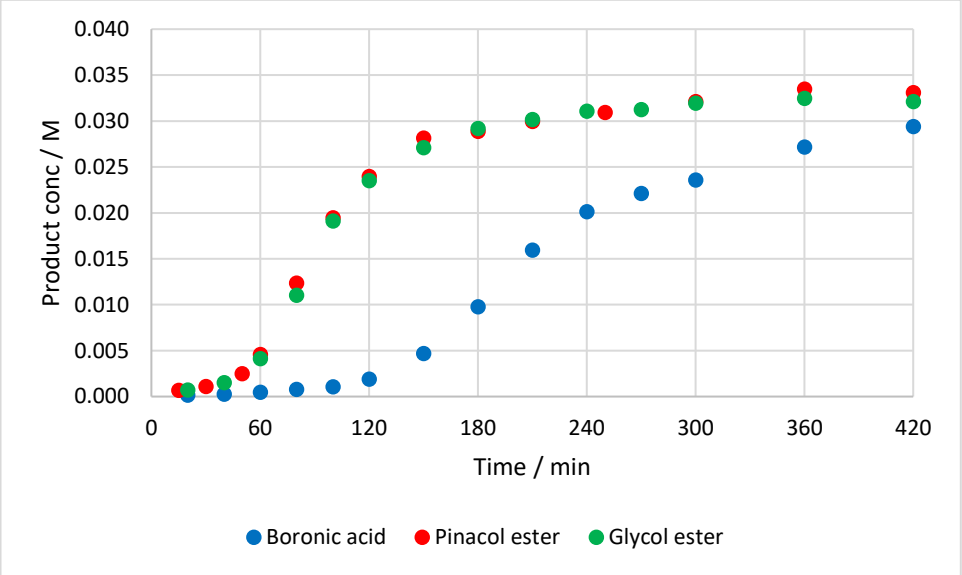

Graph 4.10.2 – Product **5** formation for SM cross-coupling of boronic acid **3**/ester **1**/**2** (0.04 M) with 1,3-bis(trifluoromethyl)-5-bromobenzene **4** (0.04 M) monitored by ^{19}F NMR with 1-fluoronaphthalene as an internal standard

The new developed conditions allowed a base screen to be carried out, revealing the need for a strong base to give efficient coupling, **Scheme 4.10.3**, **Fig 4.10.1 & 4.10.2**. The evidence gathered suggests that this is due to the ability of these strong bases to form a boronate species. This is important due to the two different transmetalation pathways, **Fig 4.10.3**. There is literature evidence for both pathways, see **Chapter 1, Section 1.2.2.3**. Under these conditions, using a phosphine-free catalyst system, it appears the transmetalation step requires a boronate species – the boronate pathway. The lack of reactivity from weak bases is likely due to the absence of boronate species, and the phosphine-free catalyst being unable to undergo efficient

ligand exchange to allow the oxo-palladium pathway. This shows the potential ability to control the pathway of transmetalation depending on the strength of the base used, **Fig 4.10.4**.

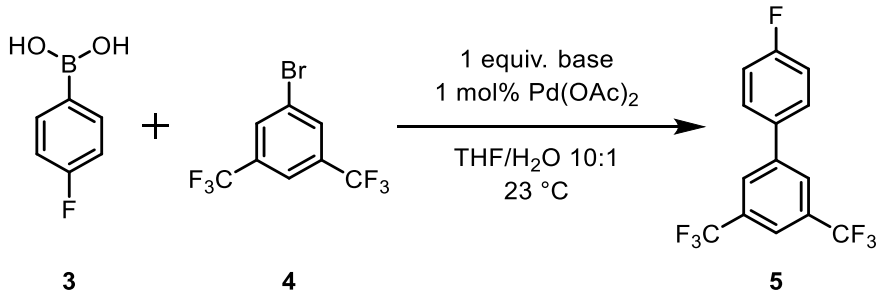

3 **4** **5**

Scheme 4.10.3 – SM cross-coupling of boronic acid **3** (1 equiv.) with 1,3-bis(trifluoromethyl)-5-bromobenzene **4** (1 equiv.) by ^{19}F NMR with 1-fluoronaphthalene as an internal standard. Pd = $Pd(OAc)_2$ or $PdCl_2PhCN_2$

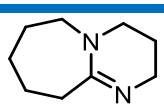		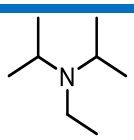	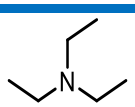
K_3PO_4	Cs_2CO_3	$NaHCO_3$	K_2CO_3
<15 % yield			

Fig 4.10.1 – Weak bases studied. SM cross-coupling of boronic acid **3** (0.04 M) with 1,3-bis(trifluoromethyl)-5-bromobenzene **4** (0.04 M). Yields after 24 hours by ^{19}F NMR with 1-fluoronaphthalene as an internal standard

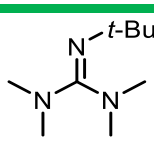	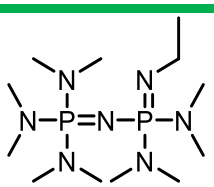	KOH
88%	76%	50%

Fig 4.10.2 – Strong bases studied. SM cross-coupling of boronic acid **3** (0.04 M) with 1,3-bis(trifluoromethyl)-5-bromobenzene **4** (0.04 M). Yields after 24 hours by ^{19}F NMR with 1-fluoronaphthalene as an internal standard

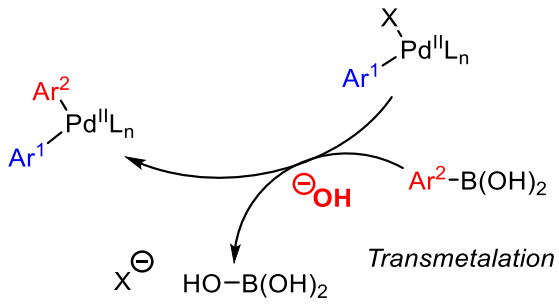

Fig 4.10.3 – Transmetalation step of the SM mechanism

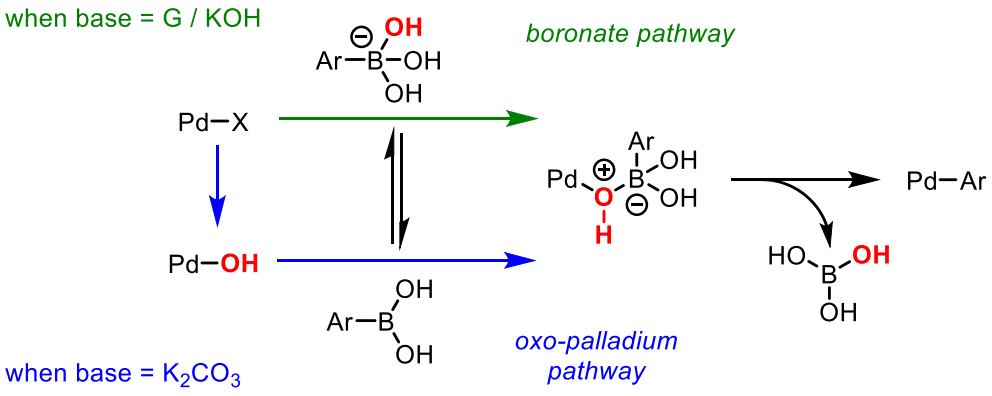

Fig 4.10.4 – Transmetalation pathway controlled by strength of base. G = guanidine **11**

4.11. References

(1) Uozumi, Y.; Nakai, Y. *Org. Lett.* **2002**, *4* (17), 2997–3000.

(2) Littke, A. F.; Fu, G. C. *Angew. Chemie Int. Ed.* **1998**, *37* (24), 3387–3388.

(3) Felpin, F.-X. *J. Org. Chem.* **2005**, *70* (21), 8575–8578.

(4) Cwik, A.; Hell, Z.; Figueras, F. *Org. Biomol. Chem.* **2005**, *3* (24), 4307–4309.

(5) Papp, A.; Tóth, D.; Molnár, Á. *React. Kinet. Catal. Lett.* **2006**, *87* (2), 335–342.

(6) Yin, L.; Zhang, Z.; Wang, Y. *Tetrahedron* **2006**, *62* (40), 9359–9364.

(7) Maegawa, T.; Kitamura, Y.; Sako, S.; Udzu, T.; Sakurai, A.; Tanaka, A.; Kobayashi, Y.; Endo, K.; Bora, U.; Kurita, T.; Kozaki, A.; Monguchi, Y.; Sajiki, H. *Chem. - A Eur. J.* **2007**, *13* (20), 5937–5943.

(8) Peng, Y.-Y.; Liu, J.; Lei, X.; Yin, Z. *Green Chem.* **2010**, *12* (6), 1072–1075.

(9) Li, J.-H.; Wang, D.-P. *European J. Org. Chem.* **2006**, *2006* (9), 2063–2066.

(10) Li, J.-H.; Li, J.; Wang, D.; Pi, S.; Xie, Y.; Zhang, M.; Hu, X.-C. *J. Org. Chem.* **2007**, *72* (6), 2053–2057.

(11) Schlosser, M. *Pure Appl. Chem.* **1988**, *60* (11).

(12) Buitrago Santanilla, A.; Christensen, M.; Campeau, L.-C.; Davies, I. W.; Dreher, S. D. *Org. Lett.* **2015**, *17* (13), 3370–3373.

(13) Li, S.; Lin, Y.; Cao, J.; Zhang, S. *J. Org. Chem.* **2007**, *72* (11), 4067–4072.

(14) Carole, W. A.; Colacot, T. J. *Chem. - A Eur. J.* **2016**, *22* (23), 7686–7695.

(15) Gao, J.; He, L.-N.; Miao, C.-X.; Chanfreau, S. *Tetrahedron* **2010**, *66* (23), 4063–4067.

(16) Schlosser, M. *Pure Appl. Chem.* **1988**, *60* (11).

(17) Dardonville, C.; Caine, B. A.; Navarro de la Fuente, M.; Martín Herranz, G.; Corrales Mariblanca, B.; Popelier, P. L. A. *New J. Chem.* **2017**, *41* (19), 11016–11028.

(18) Lennox, A. J. J.; Lloyd-Jones, G. C. *Angew. Chemie Int. Ed.* **2013**, *52* (29), 7362–7370.

Chapter 5

Boronate formation

5.1. Introduction

Boric acid has been studied for its conversion to a tetrahedral oxoanion $B(OH)_4^-$ and interchange reaction in basic solution, **Scheme 5.1.1** .[1] The two site exchange was originally suggested to proceed via two separate reactions, **Scheme 5.1.2**, but ^{11}B NMR studies shown this not to be the case, as it would give two distinct signals by ^{11}B NMR. Instead a coalesced signal is observed, leading the conclusion to be the interchange is a bimolecular reaction via a dimer species, **Scheme 5.1.3**.

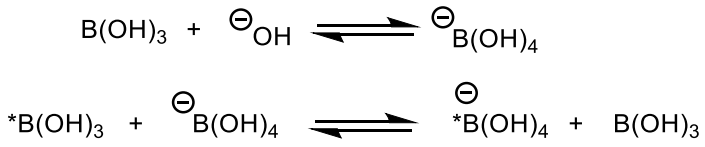

Scheme 5.1.1 – Boric acid reaction in basic solution and two-site interchange of boric acid, studied under conditions: 0.007-0.017 M boric acid solutions of pH 8-10 at 5-52 °C and 0.1-250 MPa.[1]

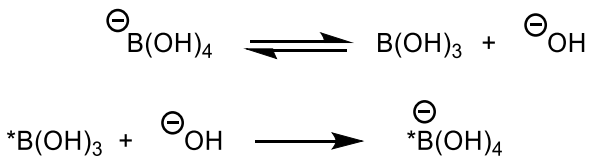

Scheme 5.1.2 – Proposed pathway for boric acid interchange

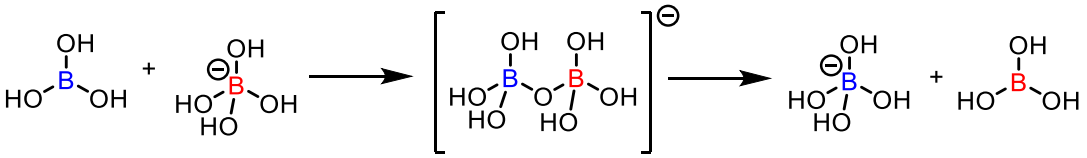

Scheme 5.1.3 – Dimer pathway for boric acid interchange

The boronate formation of methylboronic acid has been studied by ^{11}B NMR, and the pH of the solution found to affect the position of the boronic acid/boronate equilibrium, **Scheme 5.2.4**.[2] At pH 1.0, a signal peak is seen at 35 ppm for the boronic acid, but in solutions of pH 9.4 – 11.4, there is a broad peak which chemical shift between that of the boronic acid and boronate – pH 10.38, chemical shift ~22 ppm, indicating the two species are in rapid equilibrium. At high pH (13.0), only a singal peak can be seen for the boronate species at 5 ppm. Throughout the study, only a signal peak is ever observed by ^{11}B NMR.

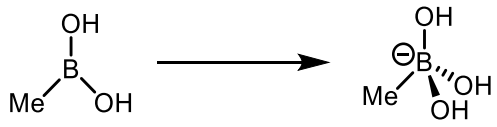

Scheme 5.2.4 – Methylboronic acid–methylboronate study by ^{11}B NMR. pH 1.0 – 13.0. 45.38 °C.

A study by Hartwig *et al.* found that mixing 4-fluorophenylboronic acid **3** with potassium carbonate in 1:1 acetone/water formed a mixture of boronic acid and trihydroxyborate, confirmed by ^{19}F and ^{11}B NMR, **Scheme 5.1.5**.[3] A single signal at the chemical shift (^{19}F = −116.2; ^{11}B = 13.8), between the boronic acid (^{19}F = −110.9; ^{11}B = 28.7) and the trihydroxyboronate (^{19}F = −119.7; ^{11}B = 3.5) indicated that the equilibrium between the two species occurred on the NMR time scale. Increasing base concentration was found to increase the ratio of trihydroxyboronate to boronic acid; 1:1 at 0.03 M base to 1:3 at 0.15 M base.

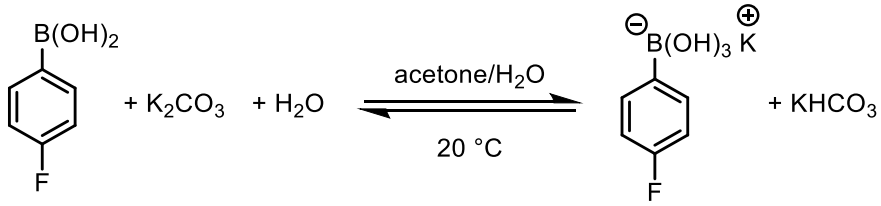

Scheme 5.1.5 – Ratio of 4-fluorophenyl boronic acid **3** (0.060 M) to trihydroxyborate, with addition of potassium carbonate. 1:1 acetone/water.

5.2. Guanidine effects

From studying the effect of guanidine **11** as a base for the SM cross-coupling (**Chapter 4**), an interesting effect on the boronic acid **3** was observed. In the cross-coupling reactions, there is a loss of signal observed by ^{19}F NMR attributed to the loss of the boronic acid **3** signal, **Fig 5.2.1**. This change in spectra was not observed in the preliminary studies using potassium carbonate. In order to find the extent of the effect that guanidine **11** has on the boronic acid **3** signal, a titration of guanidine **11** against boronic acid **3** was carried out, **Scheme 5.2.1**, **Fig 5.2.2**.

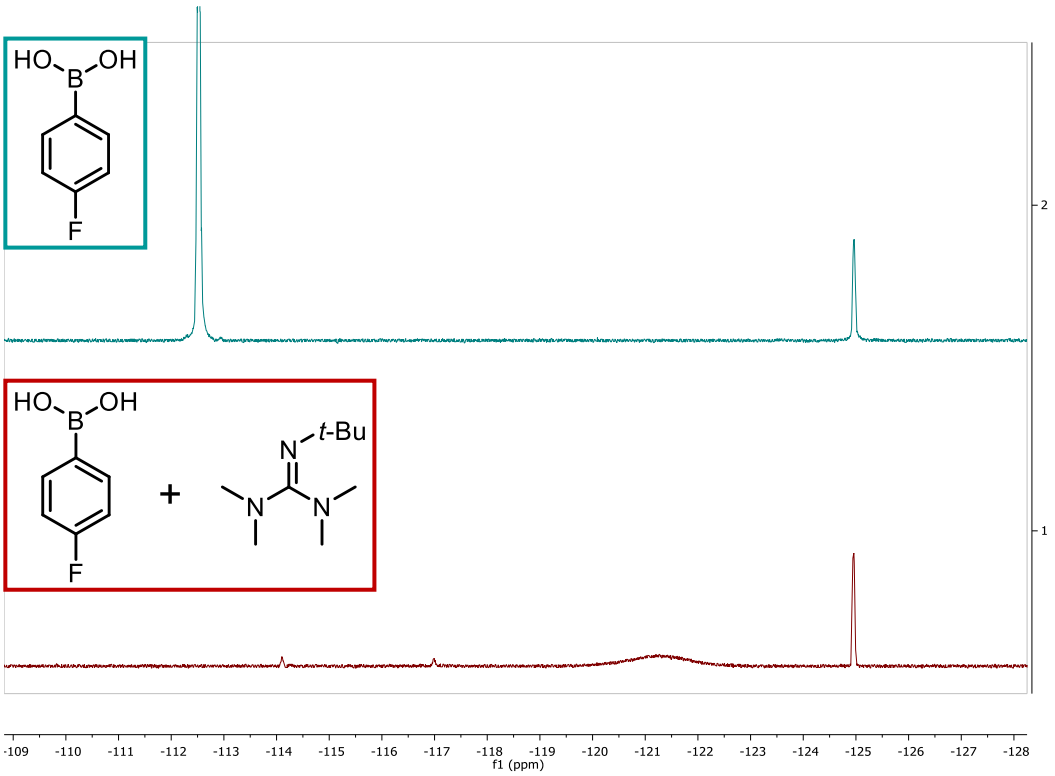

Fig 5.2.1 – Boronic acid **3** before addition of base (top spectrum), boronic acid **3** after addition of 1 equiv. guanidine **11** (bottom spectrum). ^{19}F NMR, 300 K, 10:1 THF/water, with 1-fluoronaphthalene as an internal standard (−125 ppm)

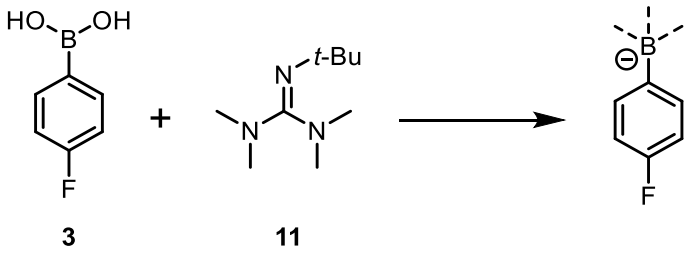

Scheme 5.2.1 – Boronic acid **3**/guanidine **11** adduct formation

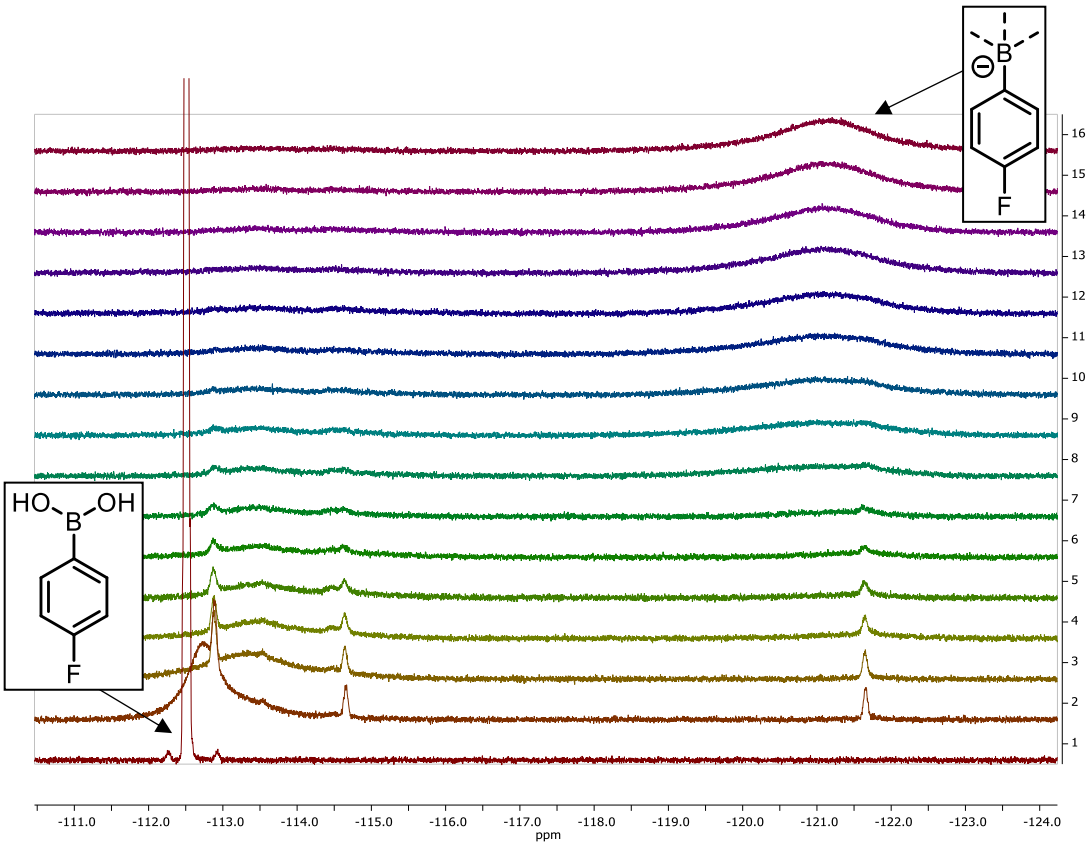

Fig 5.2.2 – Boronic acid **3** + guanidine **11** – to 3 equiv. guanidine **11** (top spectrum) in steps of 0.2. ^{19}F NMR, 300 K, 10:1 THF/water. (Appendix 8.5.1 – stacked spectra up to 1 equiv. guanidine **11**)

As the concentration of guanidine **11** is increased, the concentration of boronic acid **3** observed by ^{19}F NMR decreases, relative to a sample of boronic acid **3** without base, using 1-fluoronaphthalene as an internal standard, **Fig 5.2.2**. This reaches a maximum at 1.2 equiv. guanidine **11**, where the total fluorine concentration is only 25%, **Graph 5.2.1**. Further increasing the concentration of guanidine **11** forms a new fluorine signal at −121.18 ppm, which increases with increasing amounts of guanidine **11**, **Fig 5.2.2**. After the addition of 3 equiv. of guanidine **11**, the total concentration is 65% – 60% for this new signal at −121.18 ppm and 5% from the remaining very small and broad boronic acid **3** signal. The change in species from boronic acid **3** to the new signal is also shown by ^{11}B NMR, **Fig 5.2.3**.

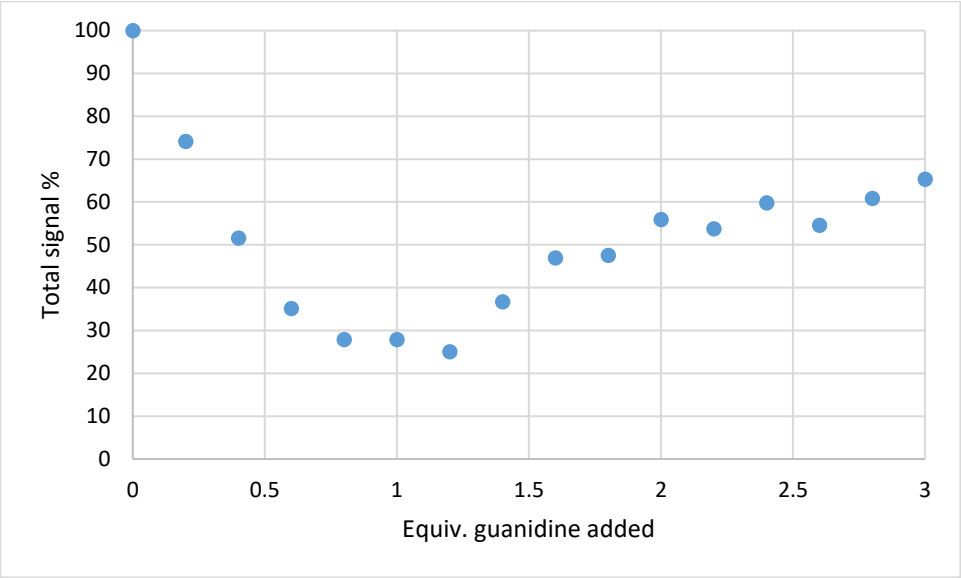

Graph 5.2.1 –Total signal vs equiv. guanidine **11** – boronic acid **3** (0.04 M) + guanidine **11** in 10:1 THF/water calculated using ^{19}F NMR, 300 K, with 1-fluoronaphthalene as an internal standard (−125 ppm)

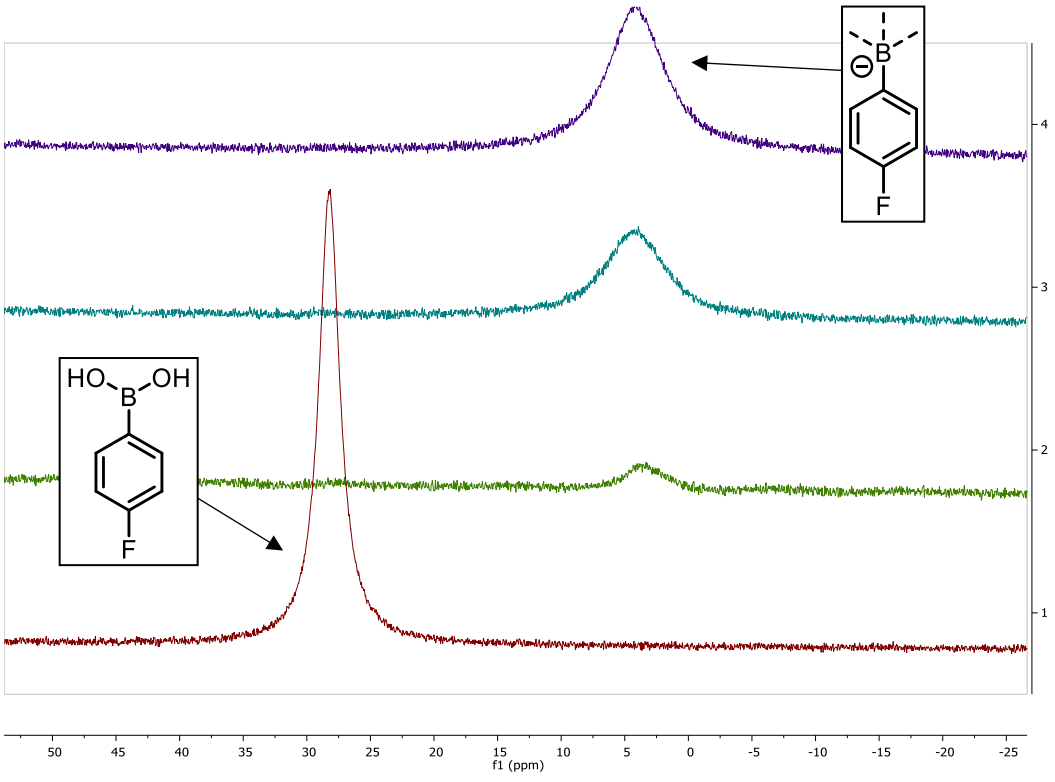

Fig 5.2.3 – Boronic acid **3** + guanidine **11** – 0 (bottom), 1, 2, 3 (top) equiv. guanidine **11**. ^{11}B NMR, 300 K, 10:1 THF/water.

There are three possible species which could be formed from the boronic acid **3**/guanidine **11** interaction, **Fig 5.2.4**. The guanidine **11** could formally bind to the boronic acid **3**, through B-N coordination, forming a Lewis type adduct, **15**. Alternatively, the boronic acid **3** could be deprotonated by the guanidine **11** to form a Brønsted acid salt adduct, **16**. However, the most likely result is the formation of a boronate complex **17,**[4–6] which can happen in two ways. Either, through reaction of the boronic acid **3** first with water, leading to a tricoordinate boronate species with a highly acidic proton, which can then be deprotonated by the guanidine **11** to give a Lewis acid salt adduct, **17**. Or, the use of base **11** can deprotonate water, forming hydroxide which can then react with the boronic acid **3** to form boronate complex **17**.

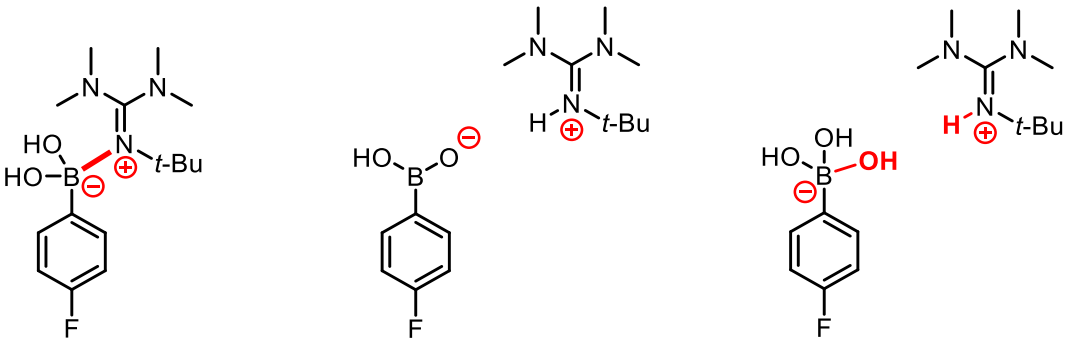

Fig 5.2.4 – Possible species formed from reaction of boronic acid **3** and guanidine **11**

To investigate the complex being formed, attempts at crystal growth were undertaken, using slow evaporation techniques. This, however, proved unsuccessful and instead gave crystals of a hydrolysed guanidine complex **18**, **Fig 5.2.5**.

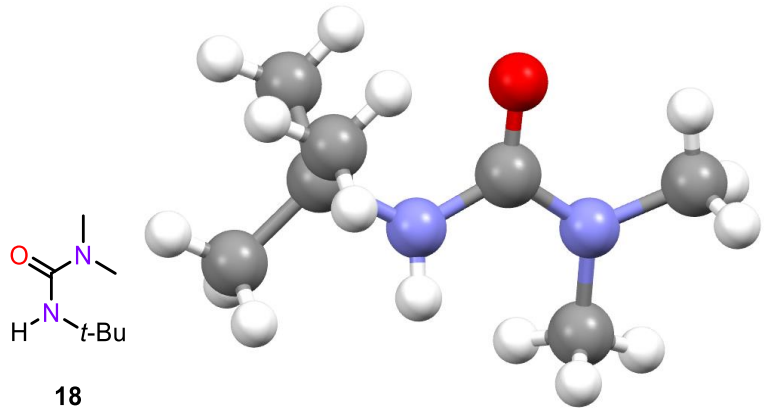

18

Fig 5.2.5 – Hydrolysed guanidine **18** crystals from a slow evaporation of boronic acid **3**/guanidine **11** (1:1) in 10:1 THF/water. Crystal structure solved by x-ray diffraction methods (Experimental 7.3.1).

A simpler model system was tested, by using boric acid and guanidine **11**, as oppose to boronic acid **3** with addition bulk and electronic properties, **Scheme 5.2.2**. Slow evaporation gave crystals which show hydrogen bonding between protonated guanidine, tricoordinate boron species, and carbonate from the air, **Fig 5.2.6**.

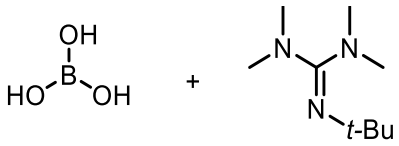

Scheme 5.2.2 – Boric acid/guanidine crystals from a slow evaporation of boric acid/guanidine **11** (1:1) in 10:1 THF/water

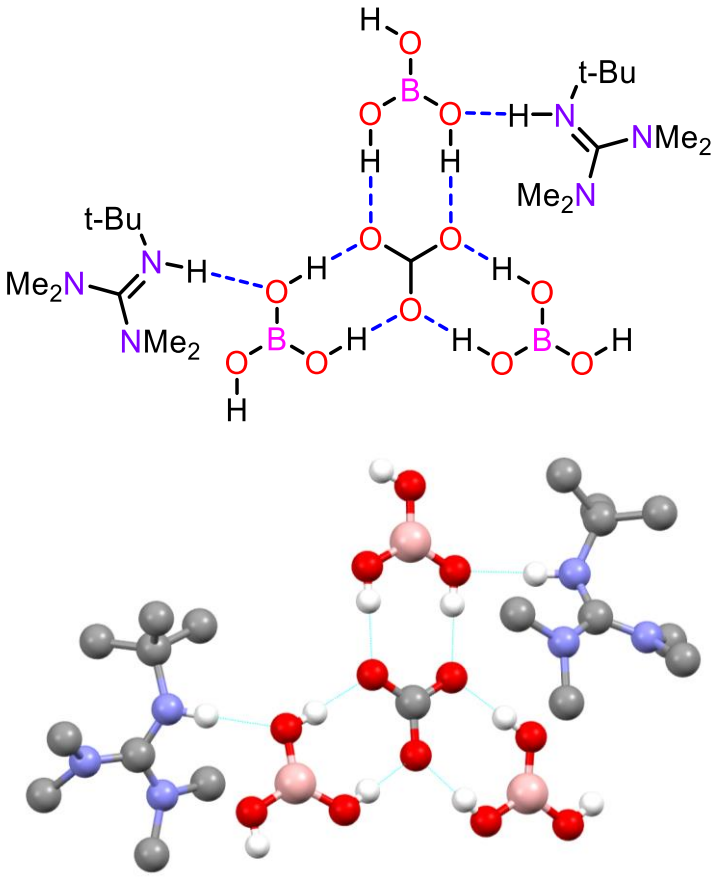

Figure 5.2.6 – Boric acid/guanidine crystals from a slow evaporation of boric acid/guanidine **11** (1:1) in 10:1 THF/water. Crystal structure solved by x-ray diffraction methods (Experimental 7.3.2).

5.2.1. Intermediates

On further investigation using ^{19}F NMR, it was found that at low amounts of guanidine **11** relative to the boronic acid **3** (−112.51 ppm), some type of intermediate(s) are formed, giving three new low intensity signals at −112.87 ppm, −114.66 ppm and −121.65 ppm, which integrate 2:1:1 respectively, **Fig 5.2.7**. There are two suggestions for what species would give rise to these signals, **Fig 5.2.8**.

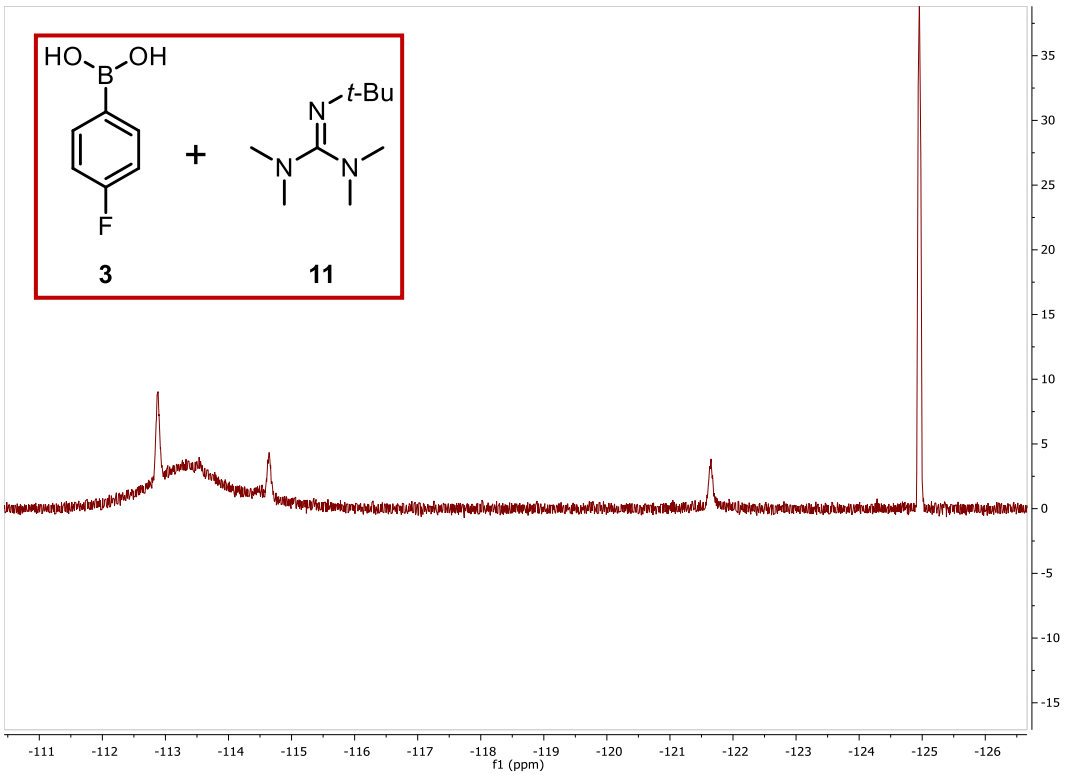

Fig 5.2.7 – Intermediate signals observed by ^{19}F NMR with 1-fluoronaphthalene as an internal standard (−125 ppm) – boronic acid **3** (0.04 M) + 0.4 equiv. guanidine **11** – 300 K, 10:1 THF/water.

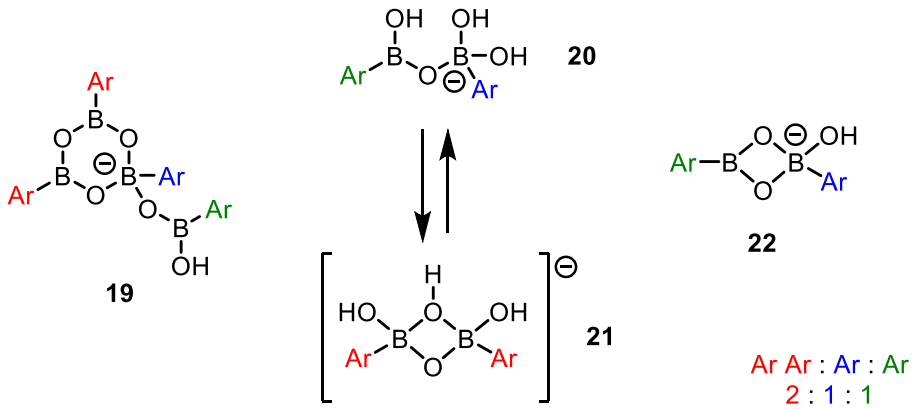

Fig 5.2.8 – Possible species formed from boronic acid **3** + guanidine **11** reaction

We postulate the first to be boroxine type species **19**, where one boron is now tricoordinate and bonded to another boronic acid moiety through a shared oxygen atom, **Fig 5.2.8**. This species would have three signals, integrating 2:1:1 for the three different fluorine atoms in this

structure. At high base concentration, this species would be broken and pushed towards formation of the boronate complex **17**.

A second possibility is that the three signals are from two different substances. The signals integrating 1:1 (−114.66 ppm and −121.65 ppm) could be from a dimer type complex **20** of boronic acid bound to a boronate species through a shared oxygen atom, **Fig 5.2.8**. This complex would have two distinct signals by ^{19}F NMR, with one shift being very close to the free boronic acid signal (−112.51 ppm) and one shift close to the free boronate signal (−121.18 ppm), **Scheme 5.2.3**. This complex is only seen at low concentration amounts of base, as at high amounts of base the equilibrium is pushed to fully form the boronate **17**. The third signal at −112.87 ppm could be from complex **21**, which would integrate for 2 relative to the dimer species, **Fig 5.2.8**. The problem with complex **21** is the chemical shift of the signal should be between that of a boronic acid −112.51 ppm and a boronate −121.18 ppm. But the actual chemical shift (−112.87 ppm) it has is very close that that of a boronic acid.

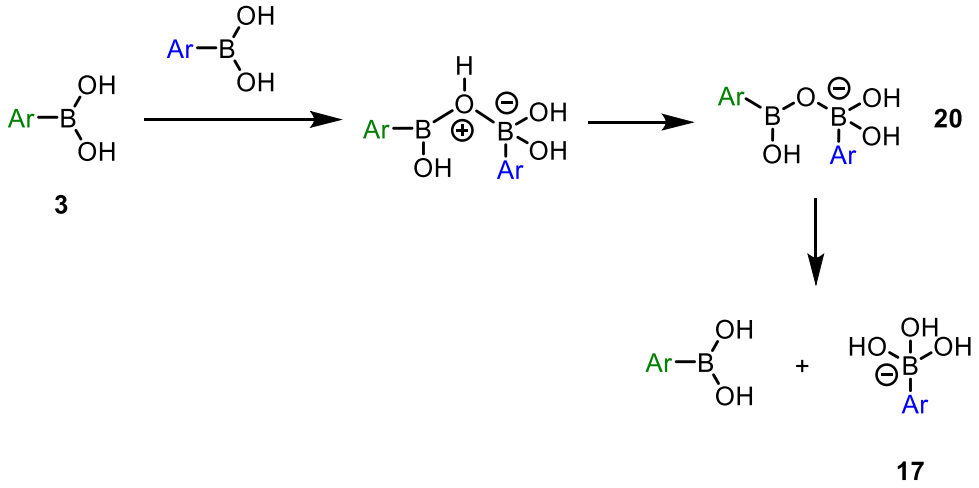

Scheme 5.2.3 – Possible route for the formation of complex **20**

An alternative to dimer complex **20** is complex **22**, which would also give two signals integrating 1:1, one boronic acid like (−112.51 ppm) and one boronate like (−121.18 ppm). Similar species have been found in a study using ESI-MS to investigate the intermediates in the SM reaction, **Fig 5.2.9**.[7]

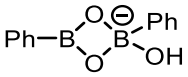

Fig 5.2.9 – Species found by ESI-MS in the reaction of organoboron (0.30 mmol) with (*E*)-bromostilbene (0.25 mmol), KOH (0.5 mmol), $Pd(OAc)_2$ (1.25 µmol), PPh_3 (2.5 µmol), MeOH (1.5 mL), THF (1.5 mL), 25 °C – dilution with water/acetonitrile mixture

Similar structures to the intermediates proposed have also been shown to form from boric acid studies, investigating boric acid interchange and reaction with 1,2-dihydric alcohols and related organic compounds, **Scheme 5.2.4 & 5.2.5**.[1]

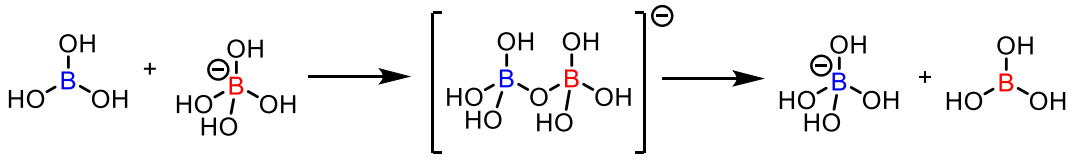

Scheme 5.2.4 – Dimer pathway for boric acid interchange

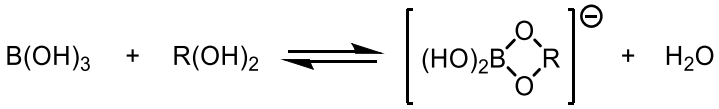

Scheme 5.2.5 – Formation of rings and dimers from boric acid and 1,2-dihydric alcohols

In order to study these signals, the NMR parameters were changed. The standard ^{19}F NMR experiment is carried out with 8 scans, 6 second relaxation delay between scans and no background suppression. We found increasing the scans to 128 and the delay to 20 seconds gave much improved signal to noise for these intermediates, so we could study the system in more detail. A large change as a result of background suppression was also found. Running the experiment without background suppression allows all species present to be seen, as the boronic acid **3** signal becomes very broad with the addition of base. This broadening meant it was difficult to find the true integration of the signal at −112.87 ppm. By running background suppression samples, the true integration and decay of this species with addition of base can be monitored, **Fig 5.2.10**.

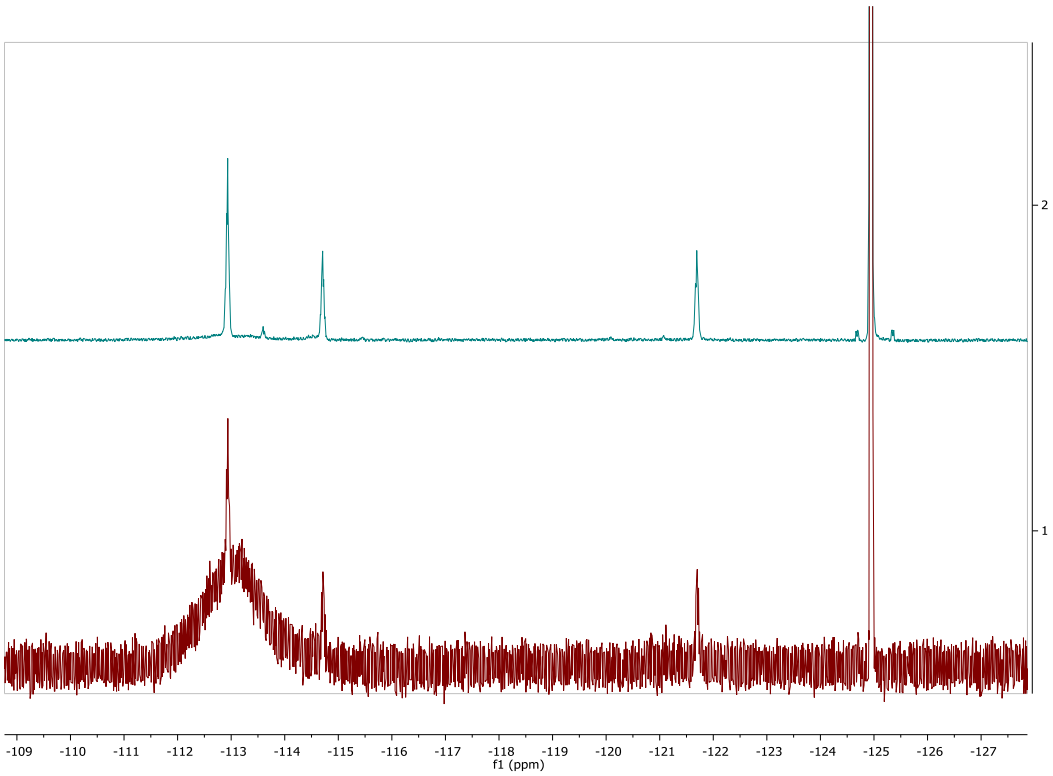

Fig 5.2.10 – Original parameter (8 scans, 6 sec delay, and no background suppression) bottom spectrum vs new parameters (128 scans, 20 sec delay, background suppression) top spectrum. Boronic acid **3** + 0.4 equiv. guanidine **11** – ^{19}F NMR with 1-fluoronaphthalene as an internal standard (−125 ppm), 300 K, 10:1 THF/water.

5.3. KOH effects

The formation of the boronate complex **17** was unseen in early work using a weak inorganic base – potassium carbonate. To see if an organic base was needed, potassium hydroxide was tested as a strong inorganic base, **Scheme 5.3.1**. This was found to give the same result as with the use of guanidine **11**, going through the same intermediate signals, and forming a broad signal around −121 ppm for a boronate complex, **Fig 5.3.1**. This meant further studies could be carried out using either the guanidine **11** or potassium hydroxide, as they gave the same boronate formation. (Appendix 8.5.2 – ^{11}B NMR.)

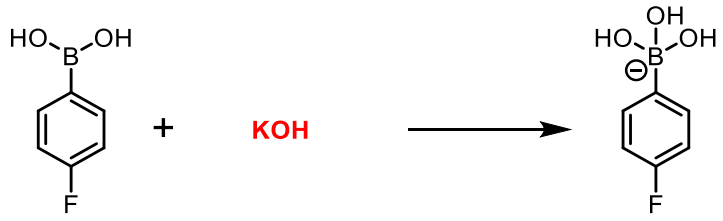

3 **17**

Scheme 5.3.1 – Boronate **17** formation using KOH

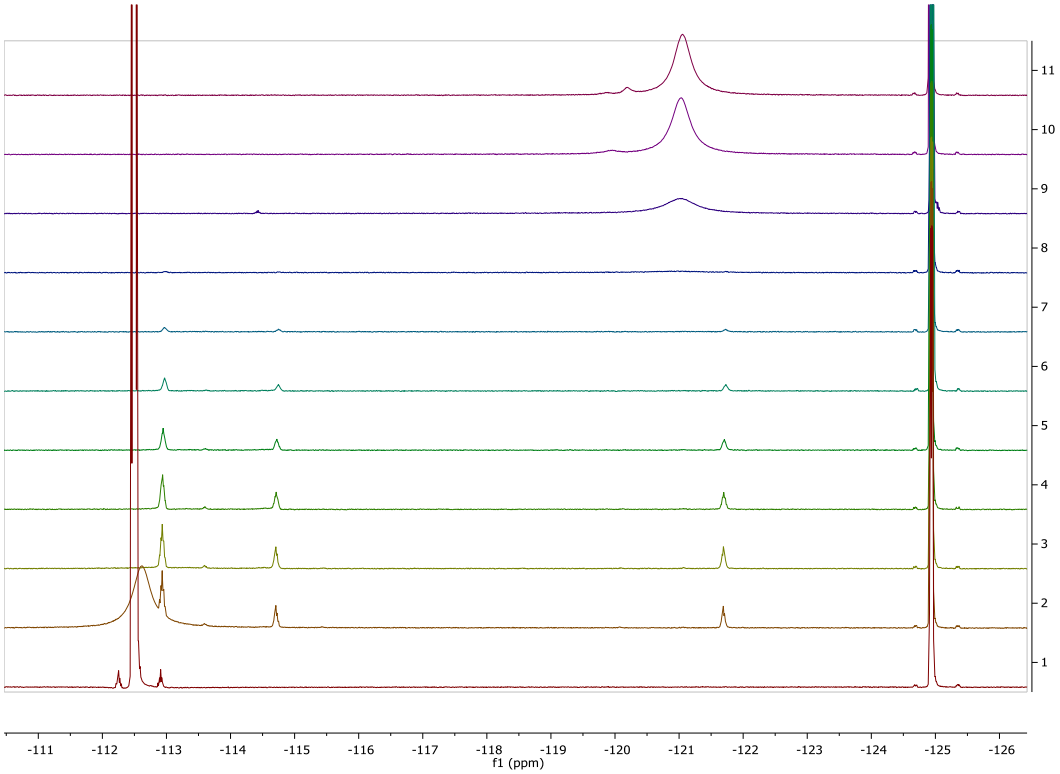

Fig 5.3.1 – Boronic acid **3** + KOH – to 2 equiv. KOH (top spectrum) in steps of 0.2. ^{19}F NMR – 128 scans & 20 sec delay, with 1-fluoronaphthalene as an internal standard (−125 ppm). 300 K, 10:1 THF/water.

5.4. Esters and diols

When studying the cross-coupling of the boronic esters **1**/**2** using guanidine **11**, it was found that the boronate signal formed was sharper in comparison to that of the boronic acid **3**, **Fig 5.4.1**. The same effect was seen in coupling of the boronic acid **3** and a given diol, showing a preformed ester species was not required for this signal change. Two structures were suggested

for where the diol in the system could be bound, **Fig 5.4.2**. It could be a boronic ester boronate complex **23**, or the ester could hydrolyse *in situ*, releasing the diol which could then be hydrogen bound to the guanidine **24**, or there could be a combination of both effects.

To investigate this signal change and potential change in species, control studies were carried out looking at the reaction of the esters **1**/**2** with guanidine **11**, **Scheme 5.4.1**, and how pre-mixing the boronic acid **3** and guanidine **11** and adding varying amounts of different diols and alcohols effects the system.

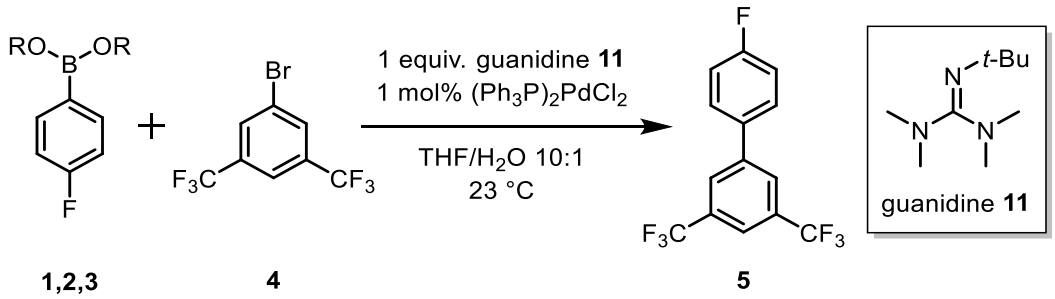

1,2,3 **4** **5**

Scheme 5.4.1 – SM cross-coupling of boronic acid **3**/ester **1**/**2** (1 equiv.) with 1,3-bis(trifluoromethyl)-5-bromobenzene **4** (1 equiv.) monitored by ^{19}F NMR with 1-fluoronaphthalene as an internal standard

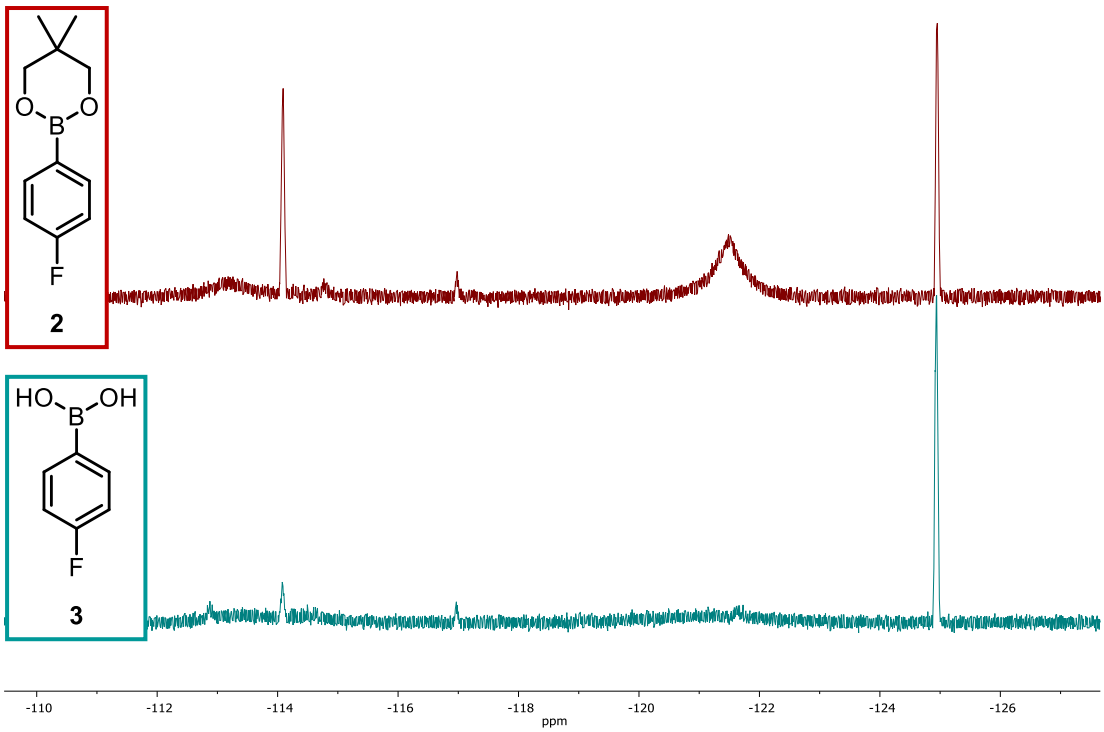

Fig 5.4.1 – Comparison of boronic acid **3** coupling (bottom spectrum) and glycol ester **2** coupling (top spectrum). ^{19}F NMR with 1-fluoronaphthalene as an internal standard (−125 ppm).

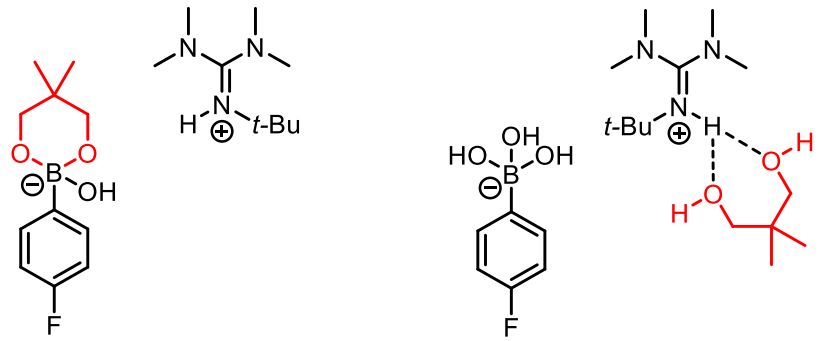

Fig 5.4.2 – Possible diol coordination in boronic acid **3**/guanidine **11** solution

5.4.1. Neopentyl glycol

Ester

The neopentyl glycol ester **2** was tested for its boronate formation, **Scheme 5.4.2**. The glycol ester **2** in 10:1 THF/water gives two signals by ^{19}F NMR – glycol ester **2** –111.13 ppm and boronic acid **3** –112.50 ppm, as previously seen and discussed in **Chapter 2**. Addition of 0.2 equiv. guanidine **11** to this solution removed the ester signal entirely, reduced and shifted the boronic acid **3** signal (–112.78 ppm), and created two new intermediate signals at −114.83 ppm and −121.58 ppm, **Fig 5.4.3**. With increasing amounts of guanidine **11**, the boronic acid **3** signal decreases and a signal at −121.31 ppm for the boronate species increase. After the addition of 1 equiv. guanidine **11**, this boronate signal is sharp, in comparison to the signal seen for boronic acid **3** with 1 equiv. guanidine **11**, with further increases to the equivalents of guanidine **11** resulting in a larger boronate signal, **Fig 5.4.4**. After the addition of 3 equiv. guanidine **11**, the total fluorine signal is 97% (compared to 65% for the boronic acid **3**), **Graph 5.4.1**. The same effect is seen when using KOH instead of guanidine **11**, **Appendix 8.5.3**.

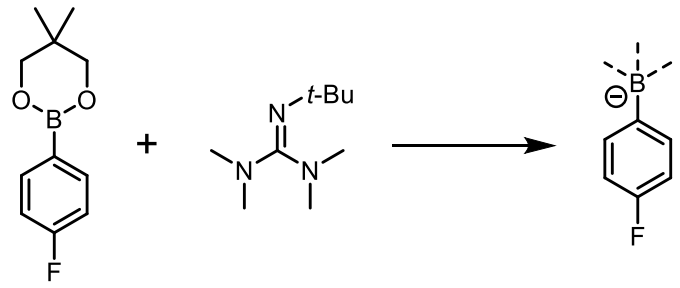

2 **11**

Scheme 5.4.2 – Glycol ester **2** + guanidine **11**. 300 K, 10:1 THF/water

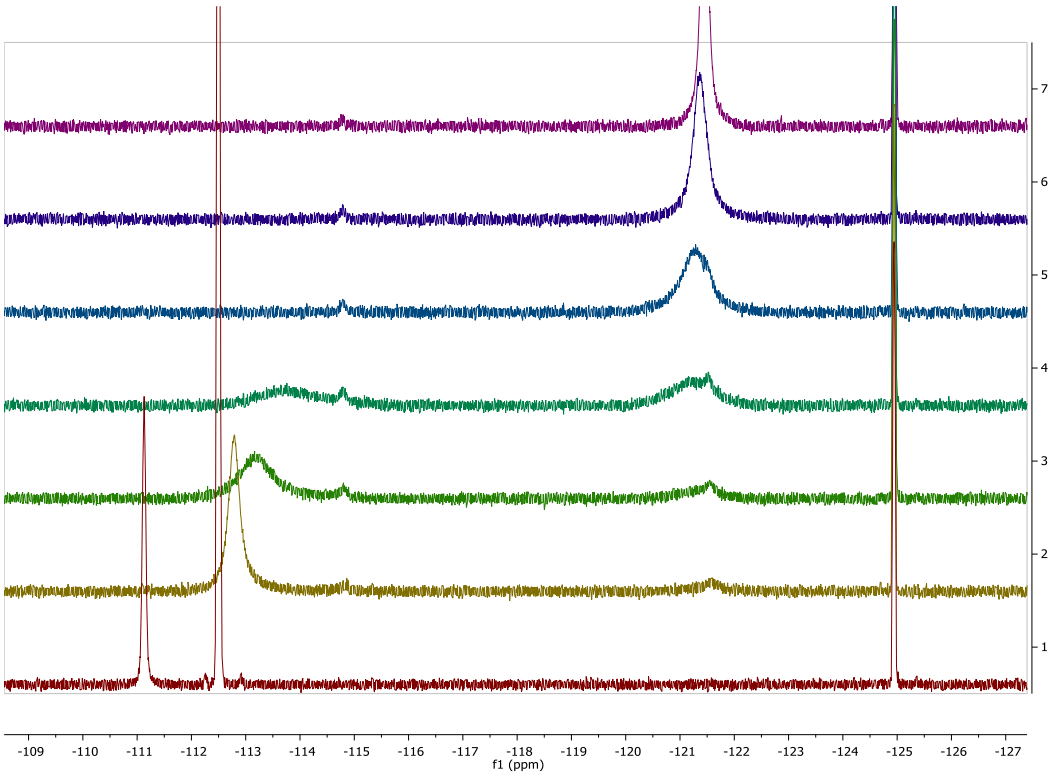

Fig 5.4.3 – Glycol ester **2** + guanidine **11** – glycol ester **2**, no base (bottom spectrum), then to 1.2 equiv. guanidine **11** (top spectrum) in steps of 0.2. ^{19}F NMR, 300 K, 10:1 THF/water, with 1-fluoronaphthalene as an internal standard (−125 ppm)

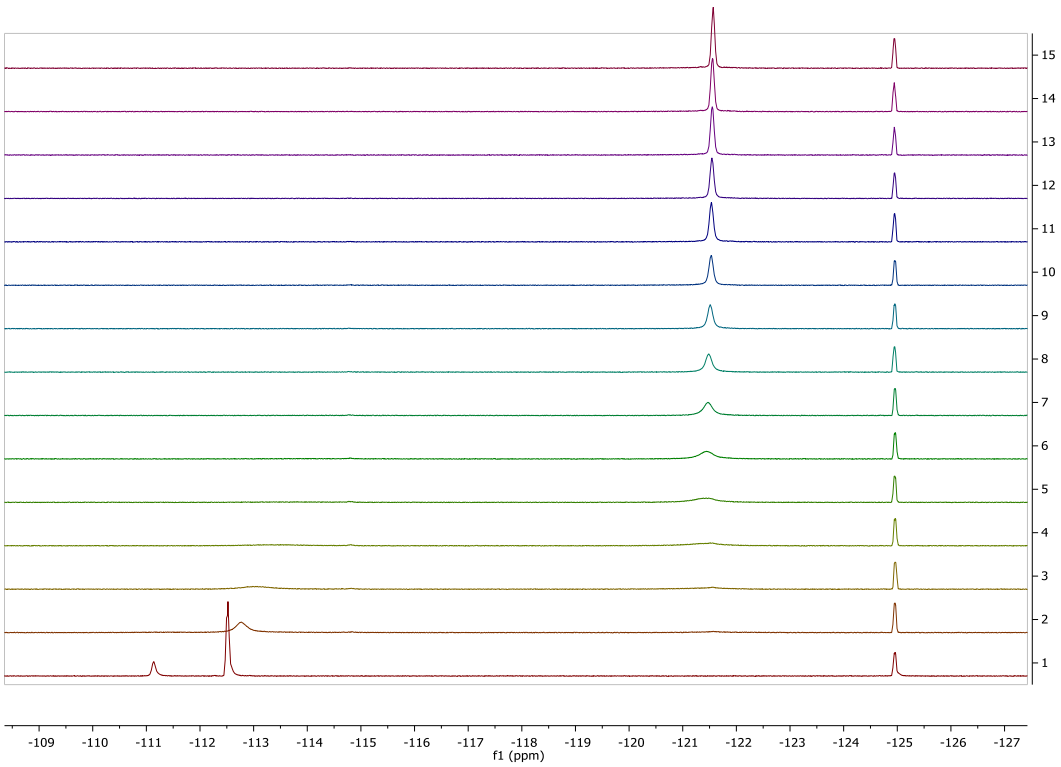

Fig 5.4.4 – Glycol ester **2** + guanidine **11** – glycol ester **2**, no base (bottom spectrum) then to 2.8 equiv. guanidine **11** (top spectrum) in steps of 0.2. ^{19}F NMR, 300 K, 10:1 THF/water, with 1-fluoronaphthalene as an internal standard (−125 ppm)

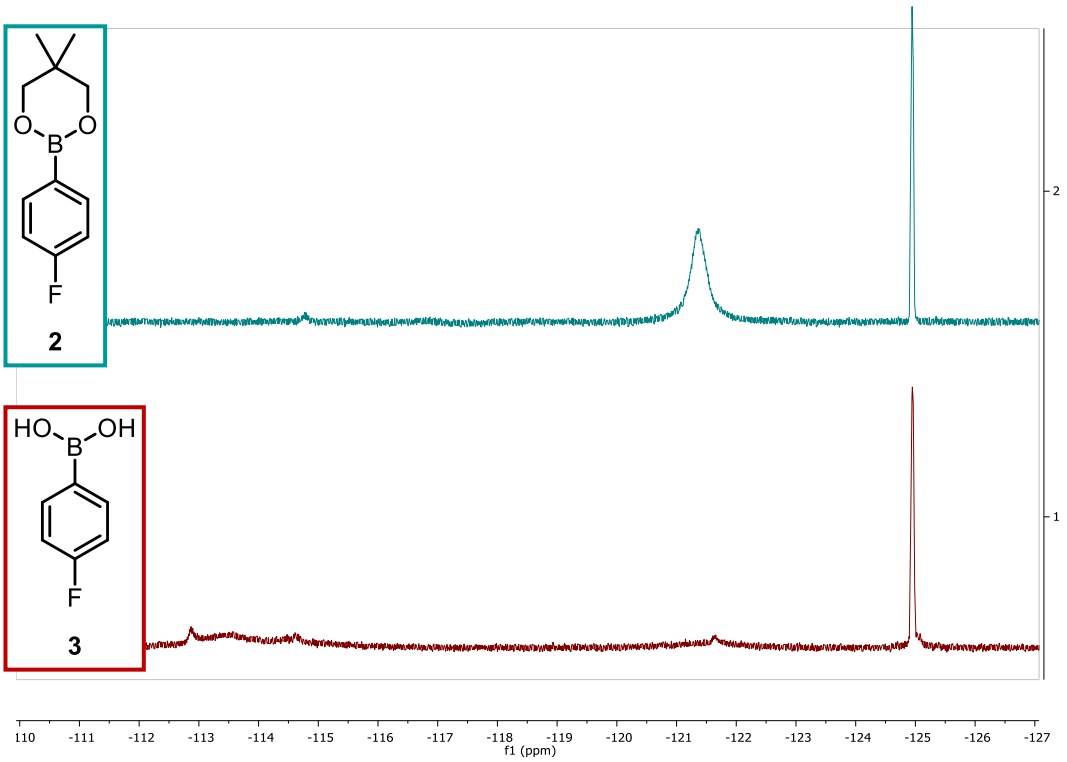

Fig 5.4.5 – Comparison of glycol ester **2** + 1 equiv. guanidine **11** (top spectrum) and boronic acid **3** + 1 equiv. guanidine **11** (bottom spectrum). ^{19}F NMR, 300 K, 10:1 THF/water, with 1-fluoronaphthalene as an internal standard (−125 ppm)

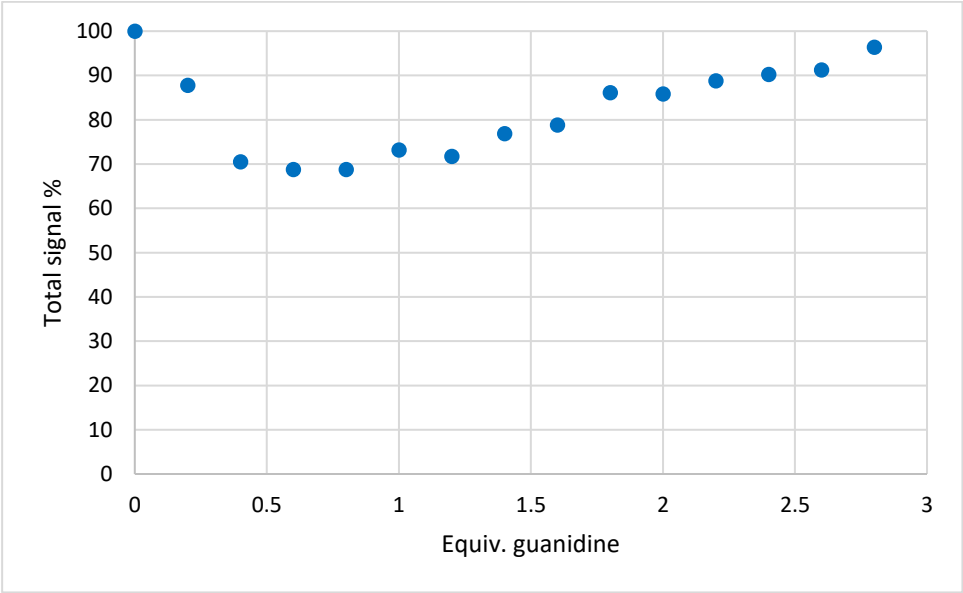

Graph 5.4.1 – Total signal vs equiv. guanidine **11** – glycol ester **2** + guanidine **11** in 10:1 THF/water at 300 K, calculated using ^{19}F NMR with 1-fluoronaphthalene as an internal standard (−125 ppm)

Diol

Treatment of a solution of boronic acid **3** in THF/water with 3 equiv. guanidine **11** resulted in a very broad signal, as shown earlier. Glycol was then added in 0.1 equiv. aliquots, **Scheme 5.4.3**, **Fig 5.4.6**. As little as 0.1 equiv. of glycol caused the boronate signal to sharpen, and then increasing the equivalents of diol increases this boronate signal. The same effect is seen when using KOH instead of guanidine **11**, **Appendix 8.5.3**.

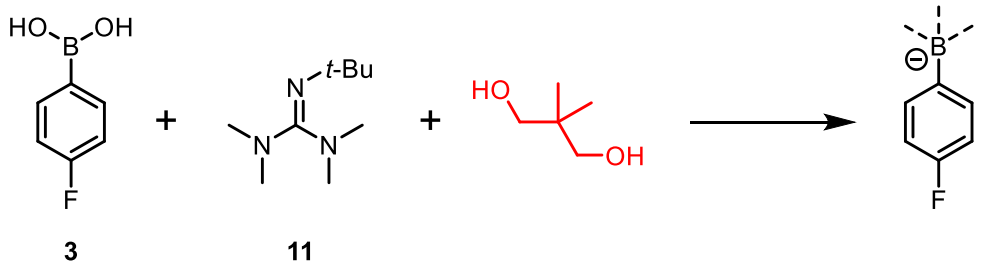

3 **11**

Scheme 5.4.3 – Boronic acid **3** + guanidine **11** – adding glycol

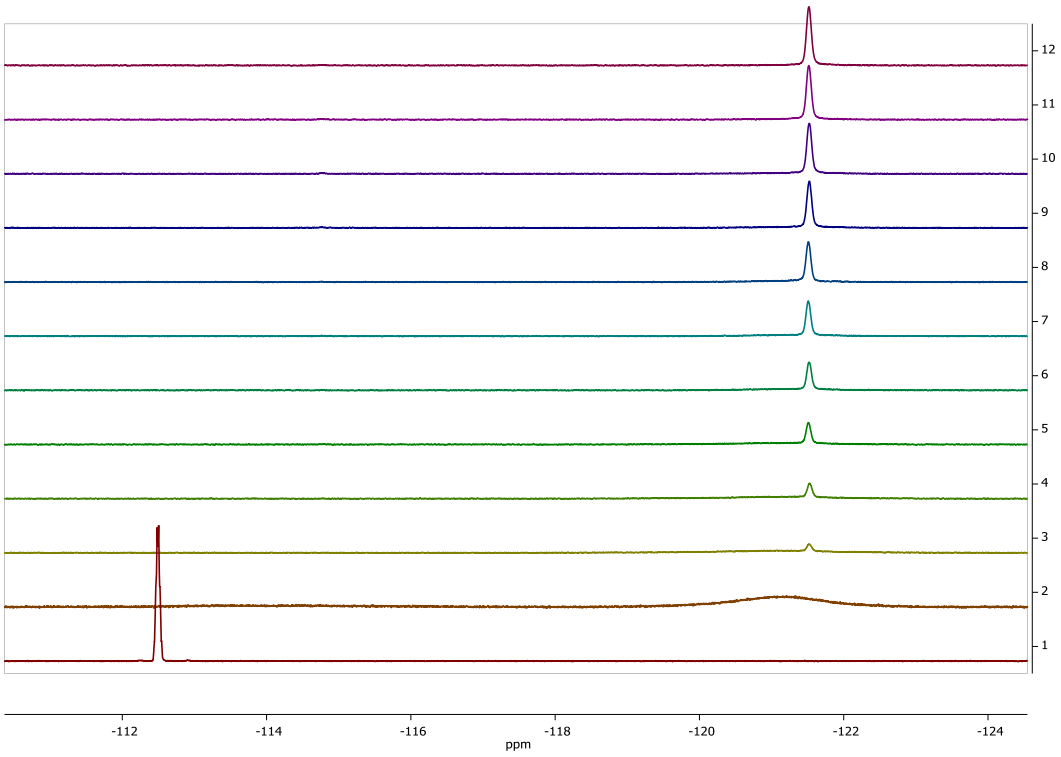

Fig 5.4.6 – Boronic acid **3** + 3 equiv. guanidine **11** + glycol – boronic acid **3**, no base (bottom spectrum), addition of 3 equiv. guanidine **11** (spectrum 2), then varying equiv. glycol to 1 equiv. (top spectrum) in steps of 0.1. ^{19}F NMR, 300 K, 10:1 THF/water, with 1-fluoronaphthalene as an internal standard (−125 ppm)

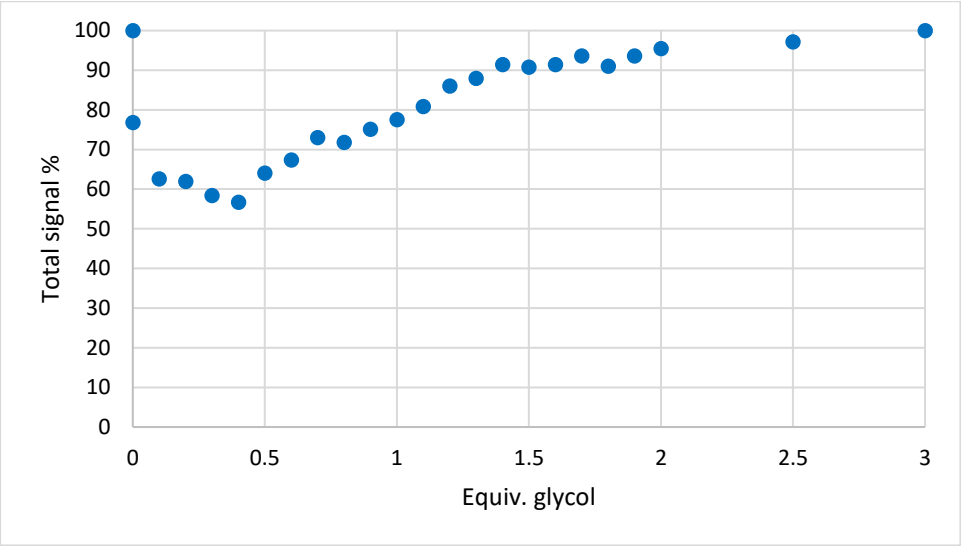

Graph 5.4.2 – Total signal vs glycol equiv. – boronic acid **3** + 3 equiv. guanidine **11** + glycol in 10:1 THF/water at 300 K, calculated using ^{19}F NMR with 1-fluoronaphthalene as an internal standard (−125 ppm)

5.4.2. Pinacol

Ester

The pinacol ester **1** was tested for its boronate formation, **Scheme 5.4.4**. As the hydrolysis of the pinacol ester **1** is slow (**Chapter 2**), the initial NMR spectrum shows the pinacol ester **1** −109.59 ppm as the main signal, with only a very small boronic acid **3** signal −112.52 ppm. The addition of 0.2 equiv. guanidine **11** reduced the pinacol ester **1** signal, increased the boronic acid **3** signal −112.81 ppm and formed two new small signals for the intermediate, −115.09 ppm and −122.43 ppm, **Fig 5.4.7**. The fact that these two signals are present, and not the third signal at −112.87 ppm as seen with the boronic acid **3**, supports these two signals being from a boronic acid/boronate dimer **20**/**22**, rather than a boroxine type intermediate **19**, **Fig 5.4.8**. A broad signal can also be seen under the −122.43 ppm intermediate signal – the boronate, **Fig 5.4.7**.

Further increasing the amount of guanidine **11** reduces the boronic acid **3** and ester **1** signals and increases the boronate signal, −122.27 ppm. After the addition of 1 equiv. guanidine **11** both the ester **1** and acid **3** signals are consumed, and the boronate is the major signal, but both small intermediate signals can still be seen. The same effect is seen when using KOH instead of guanidine **11**, **Appendix 8.5.4**.

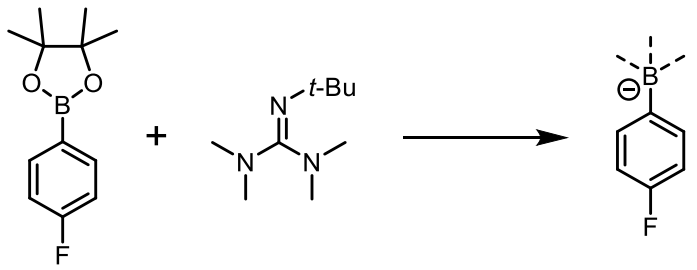

1 **11**

Scheme 5.4.4 – Pinacol ester **1** + guanidine **11**

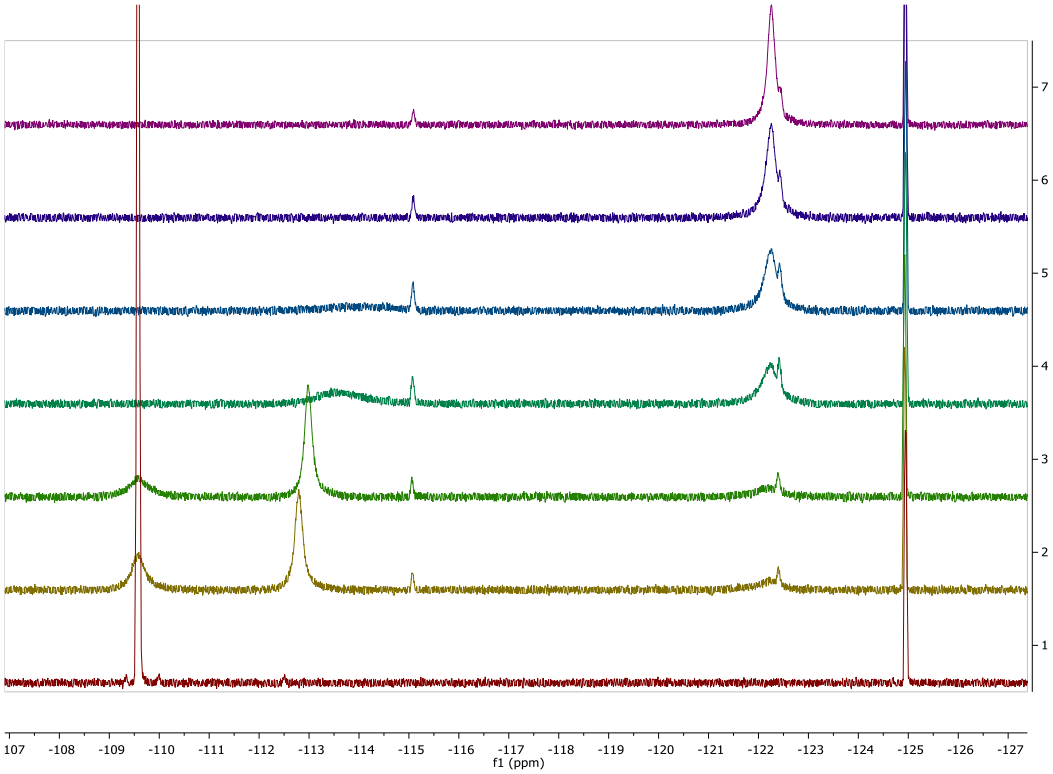

Fig 5.4.7 – Pinacol ester **1** + guanidine **11** – pinacol ester **1**, no base (bottom spectrum), then to 1.2 equiv. guanidine **11** (top spectrum) in steps of 0.2. ^{19}F NMR, 300 K, 10:1 THF/water, with 1-fluoronaphthalene as an internal standard (−125 ppm)

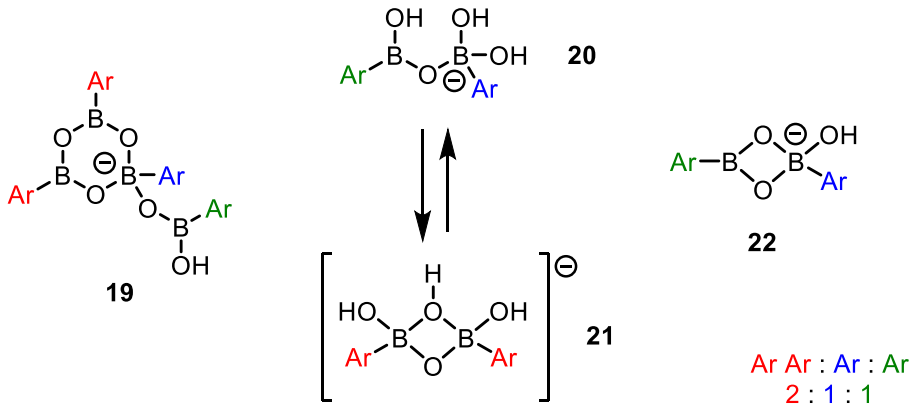

Fig 5.4.8 – Possible species formed from boronic acid **3** + guanidine **11** reaction

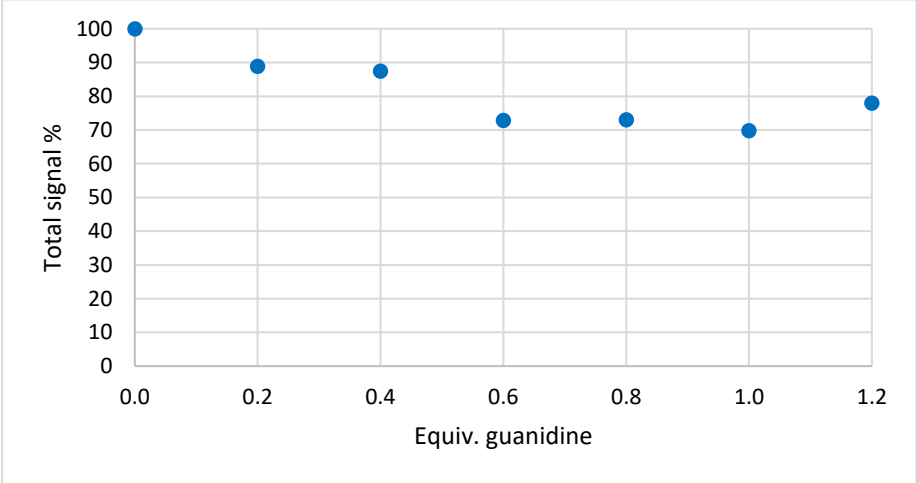

Graph 5.4.3 – Total signal vs equiv. guanidine **11** – pinacol ester **1** + guanidine **11** in 10:1 THF/water at 300 K, calculated using ^{19}F NMR with 1-fluoronaphthalene as an internal standard (−125 ppm)

Diol

Starting with neat boronic acid **3** in 10:1 THF/water, 2 equiv. of KOH were added. Pinacol was then added in steps of 0.2 equiv., **Scheme 5.4.5**, **Fig 5.4.9**. With the first addition of 0.2 equiv. pinacol, a different effect was seen in comparison to the glycol. The boronate signal (−121.08 ppm) did not sharpen, instead a new signal at −121.86 ppm appeared. With increasing amounts of pinacol, this new signal grew and the boronate signal decreased. This new signal is also much sharper in comparison to the boronate signal. The ^{11}B NMR also shows this effect of a new signal with the addition of pinacol, **Fig 5.4.10**. This suggests that the addition of pinacol is forming a pinacol ester boronate **25**, which has a different chemical

shift to the boronic acid boronate **17**, **Scheme 5.4.5**. This difference is not seen in the pinacol ester **1** investigation as the boronic acid boronate **17** is not formed. The ester system already has a preformed ester, so would form an ester boronate **25**, as there is no boronic acid **3** present.

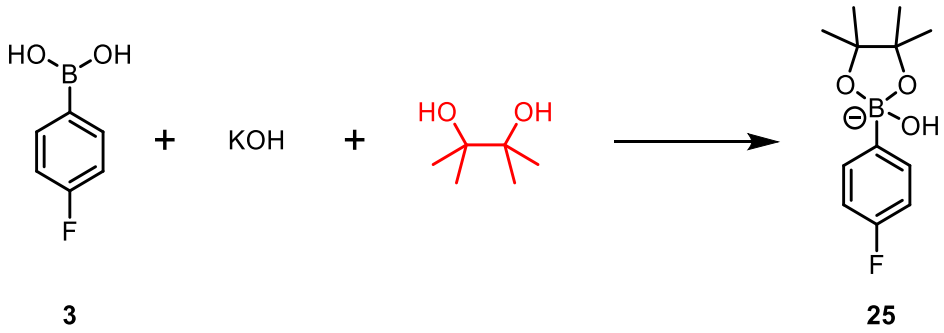

3 **25**

Scheme 5.4.5 – Formation of a pinacol ester boronate **25**

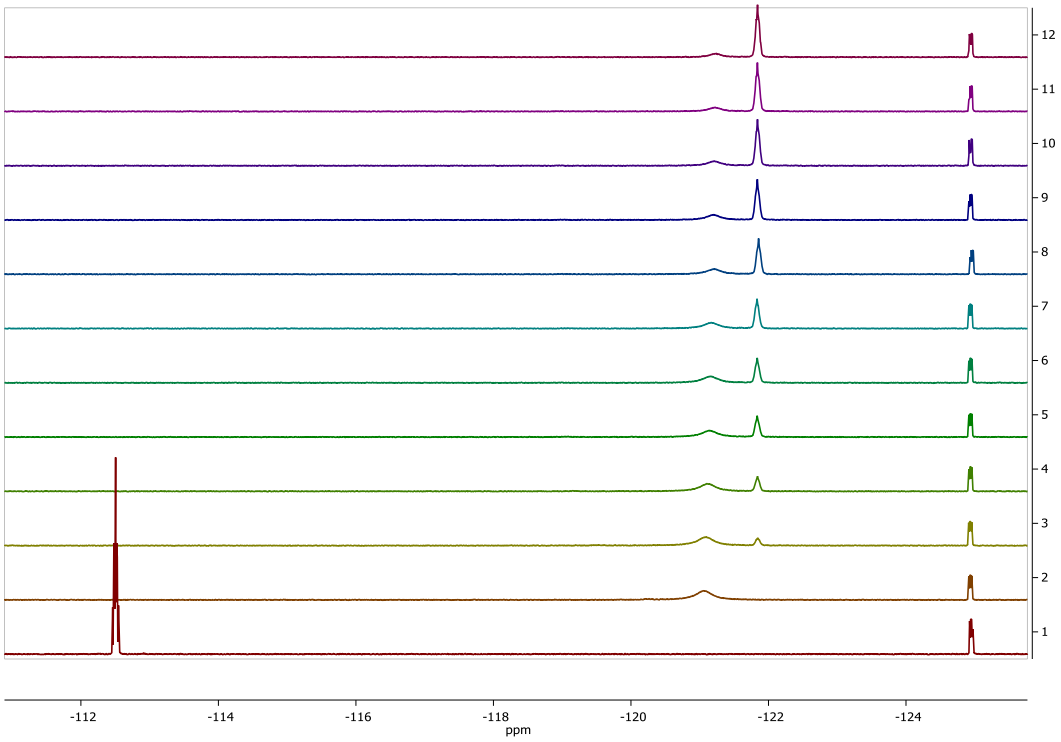

Fig 5.4.9 – Boronic acid **3** + 2 equiv. KOH + pinacol – boronic acid **3**, no base (bottom spectrum), addition of KOH (spectrum 2), then varying equiv. pinacol to 2 equiv. (top spectrum) in steps of 0.2. ^{19}F NMR, 300 K, 10:1 THF/water, with 1-fluoronaphthalene as an internal standard (−125 ppm)

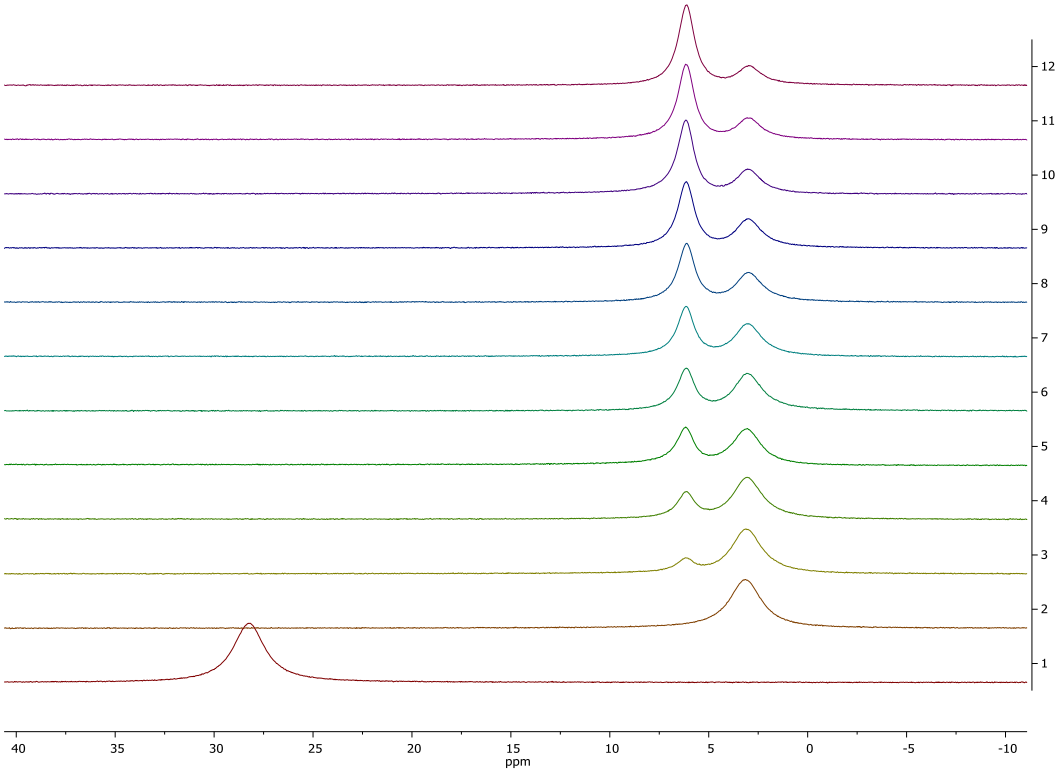

Fig 5.4.10 – Boronic acid **3** + 2 equiv. KOH + pinacol – boronic acid **3**, no base (bottom spectrum), addition of KOH (spectrum 2), then varying equiv. pinacol to 2 equiv. (top spectrum) in steps of 0.2. ^{11}B NMR, 300 K, 10:1 THF/water

5.4.3. Comparison

Both esters **1**/**2** are shown to sharpen and increase the intensity of the boronate signal, however, further inspection of the ^{19}F NMR shows the two esters form different boronate species to the boronic acid **3**, **Fig 5.4.11**. This suggests the species being formed is a boronic ester boronate complex **23**, **Fig 5.4.12**. The intermediates formed are also different for the pinacol ester **1**, as shown by chemical shift, suggesting the diol also affects the possible boronic acid/boronate dimer **20**, **Fig 5.4.14** & **5.4.15**. The glycol ester boronate **23** and boronic acid boronate **17** have very similar chemical shifts (difference of 0.11 ppm) so their intermediates could also be different species, but with a chemical shift too close to tell the difference.

	No base	Intermediate signal 1	Intermediate signal 2	Boronate
Pinacol ester **1**	−109.57 ppm	−115.06 ppm	−122.36 ppm	−121.89 ppm (**25**)
Glycol ester **2**	−111.12 ppm	−114.71 ppm	−121.70 ppm	−121.17 ppm (**23**)
Boronic acid **3**	−112.51 ppm	−114.71 ppm	−121.70 ppm	−121.06 ppm (**17**)

Fig 5.4.11 – Comparison of signals of different species present with the addition of KOH by ^{19}F NMR, relative to 1-fluoronaphthalene as an internal standard, 10:1 THF/water, 300 K

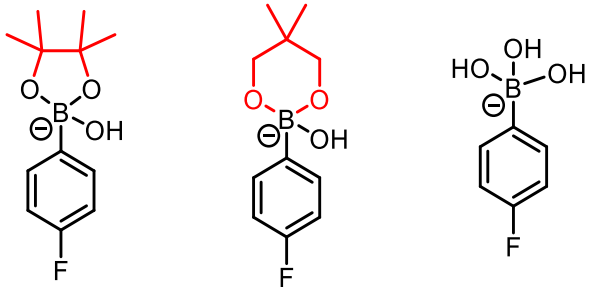

25 **23** **17**

Fig 5.4.12 – Different boronate complexes formed

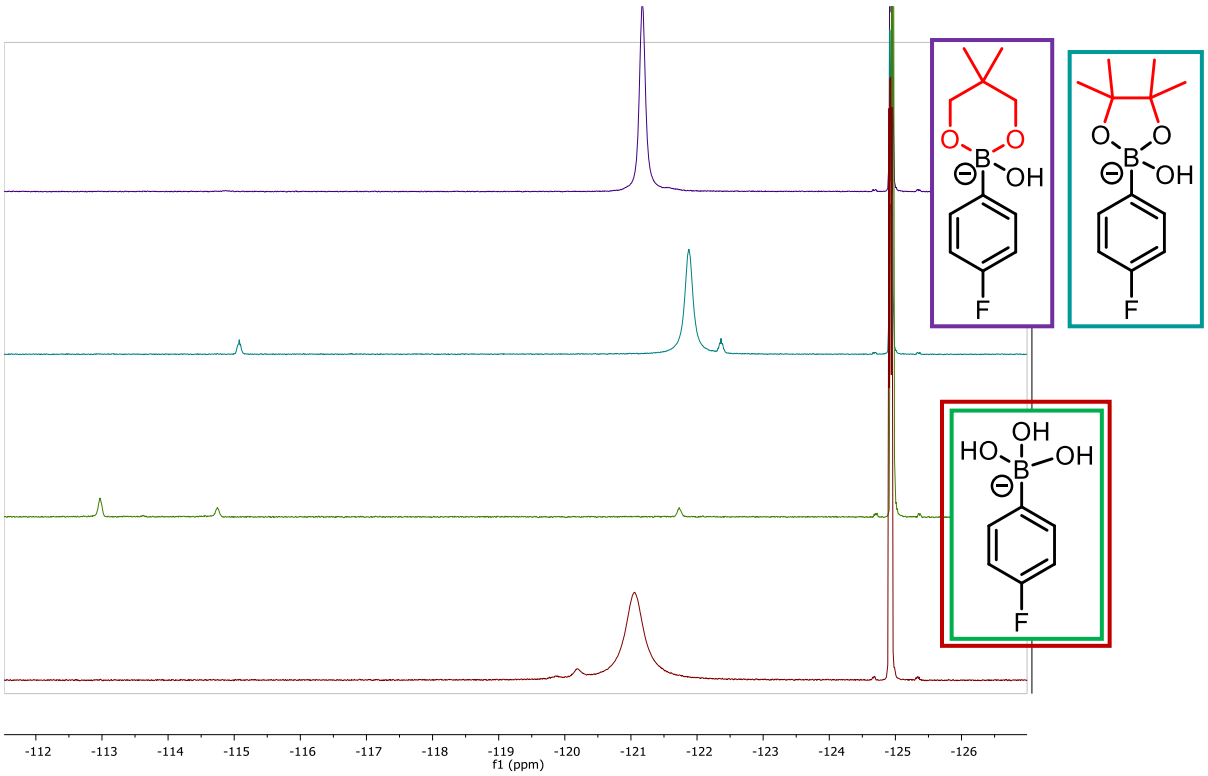

Fig 5.4.13 – Boronate comparison – Glycol ester **2** + 1 equiv. KOH (top spectrum), pinacol ester **1** + 1 equiv. KOH (next), boronic acid **3** + 1 equiv. KOH (next), boronic acid **3** + 3 equiv. KOH (bottom spectrum). ^{19}F NMR, 300 K, 10:1 THF/water, with 1-fluoronaphthalene as an internal standard (−125 ppm)

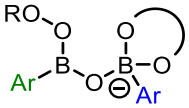

Fig 5.4.14 – Possible diol coordination in potential dimer **20**

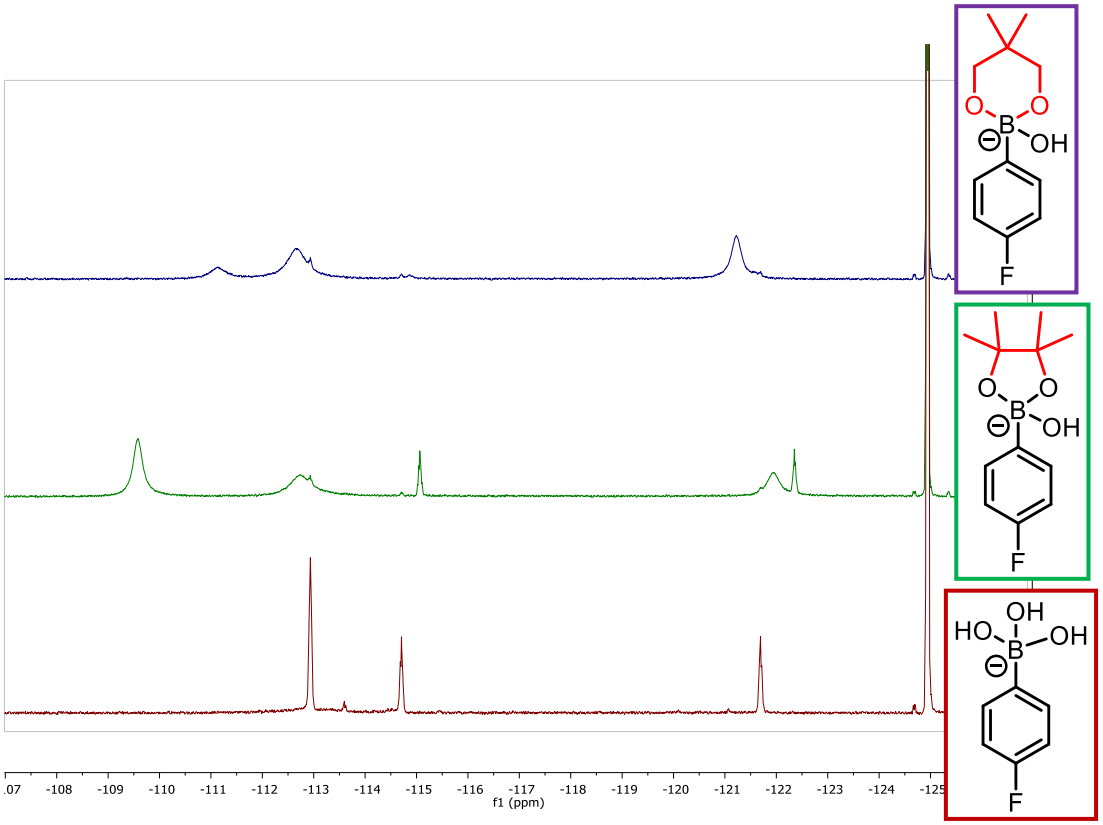

Fig 5.4.15 – Intermediate signals comparison – Glycol ester **2** + 0.4 equiv. KOH (top spectrum), pinacol ester **1** + 0.4 equiv. KOH (next), boronic acid **3** + 0.4 equiv. KOH (bottom spectrum). ^{19}F NMR, 300 K, 10:1 THF/water, with 1-fluoronaphthalene as an internal standard (−125 ppm)

There is literature precedent for the formation of boronic ester boronates. A study by Smith *et al.* investigating the ability of boronic acids to transport saccharides in and out of liposomes found the boronic acid to reversibly bind with the diol of the monosaccharide to form tetrahedral boronate species, **Scheme 5.4.6**.[8] They also studied the diol complexation with a borinic acid, and found only the chelated tetrahedral borinate anion to be produced, **Scheme 5.4.7**.

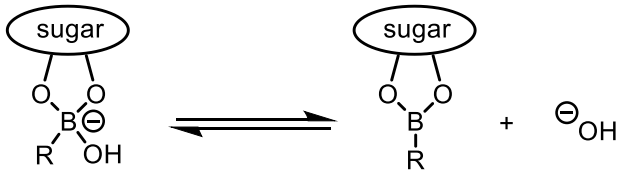

Scheme 5.4.6 – The boronate is the major structure in bulk, aqueous solution

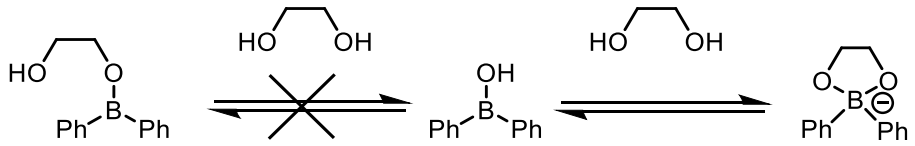

Scheme 5.4.7 – Complexation between borinic alcohol and diol in aqueous solution

5.4.4. Other alcohols

Other alcohols were tested to see their effect on the boronate formation, **Scheme 5.4.8**, **Fig 5.4.16**. The first spectrum (top, purple) shows the boronic acid **3** with no base, −112.50 ppm. The next spectrum shows the boronic acid **3** + 2 equiv. guanidine **11**, forming the broad signals at the boronic acid **3** and boronate **17** regions. The effect of 1 equiv. 1,1,1-tri(hydroxymethyl)ethane is shown next (green spectrum), and found to sharpen and shift the boronic acid signal (−113.06 ppm) and sharpen the boronate signal (−119.74 ppm). The chemical shift of this boronate signal suggests this is a different boronate species than the boronic acid boronate 17 (−121.06 ppm), **Scheme 5.4.9**. The next two spectra (yellow and red) show the effect of the addition of 1 equiv. 2-propanol and 1 equiv. 2,2-dimethyl-1-propanol. Neither of these alcohols gave any change by ^{19}F or ^{11}B NMR, suggesting a diol is needed to influence the species in the system.

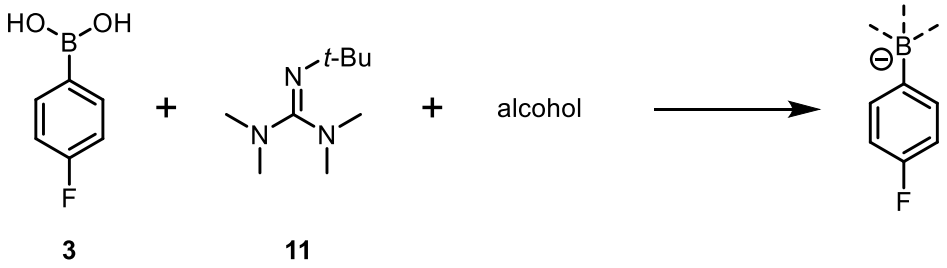

Scheme 5.4.8 – Boronic acid **3** + guanidine **11** – adding alcohol

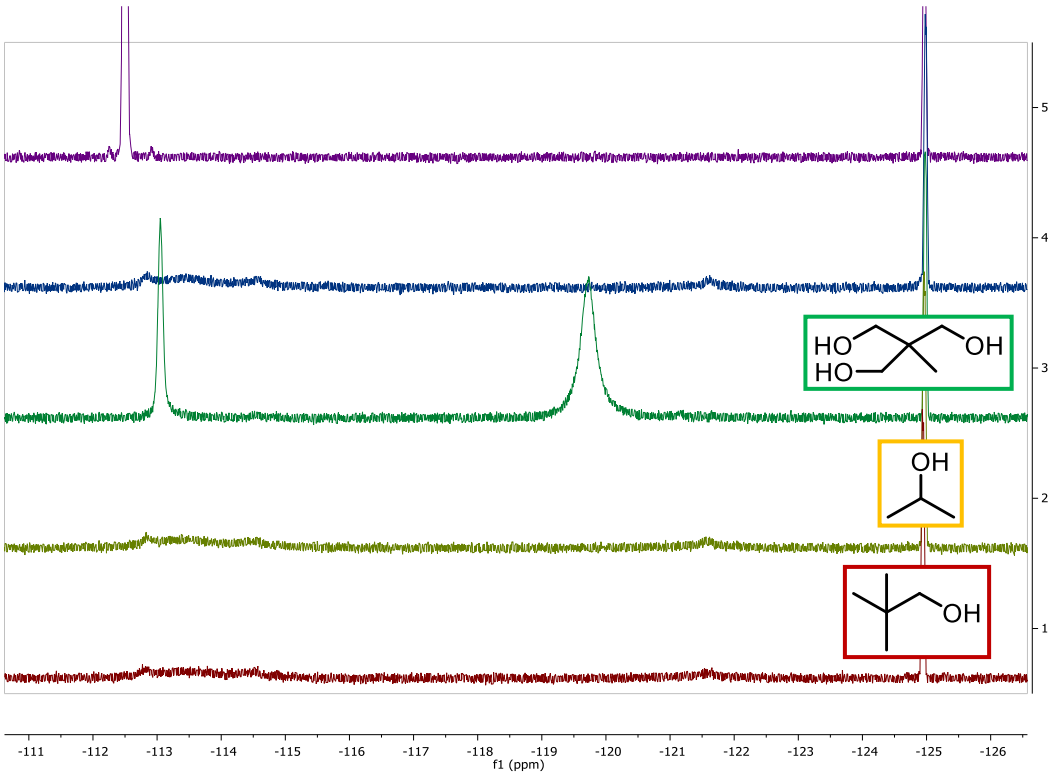

Fig 5.4.16 – Boronic acid **3** + 2 equiv. guanidine **11** – effects of different alcohols on the boronate signal. ^{19}F NMR, 300 K, 10:1 THF/water, with 1-fluoronaphthalene as an internal standard (−125 ppm). Boronic acid **3**, no base (top spectrum), boronic acid **3** + 2 equiv. guanine **11** (blue spectrum), + 1 equiv. 1,1,1-tri(hydroxymethyl)ethane, + 1 equiv. 2-propanol, + 1 equiv. 2,2-dimethyl-1-propanol (bottom spectrum)

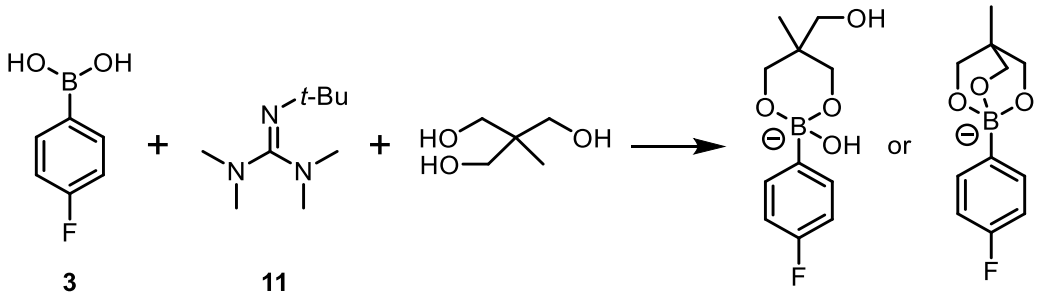

Scheme 5.4.9 – Possible boronate formation using 1,1,1-tri(hydroxymethyl)ethane

Further evidence that a diol is needed is shown by the addition of increasing equivalents of mono-alcohol which still resulted in no change to the spectra. 1, 2 and 3 equiv. of 1-propanol were added to a boronic acid **3**/guanidine **11** solution but gave no change, **Fig 5.4.17** – spectrum 4, 5, 6.

Addition of 1 equiv. trifluoroethanol also gave no change to the spectrum (spectrum 3), but 1 equiv. glycerol sharpened both the boronic acid **3** (−112.76 ppm), and boronate (−121.19 ppm), signals, **Scheme 5.4.10** – spectrum 2. 1 equiv. ethylene glycol only sharpened the boronate signal, −121.50 ppm, leaving the broad boronic acid **3** signal unchanged, **Scheme 5.4.11** – spectrum 1.

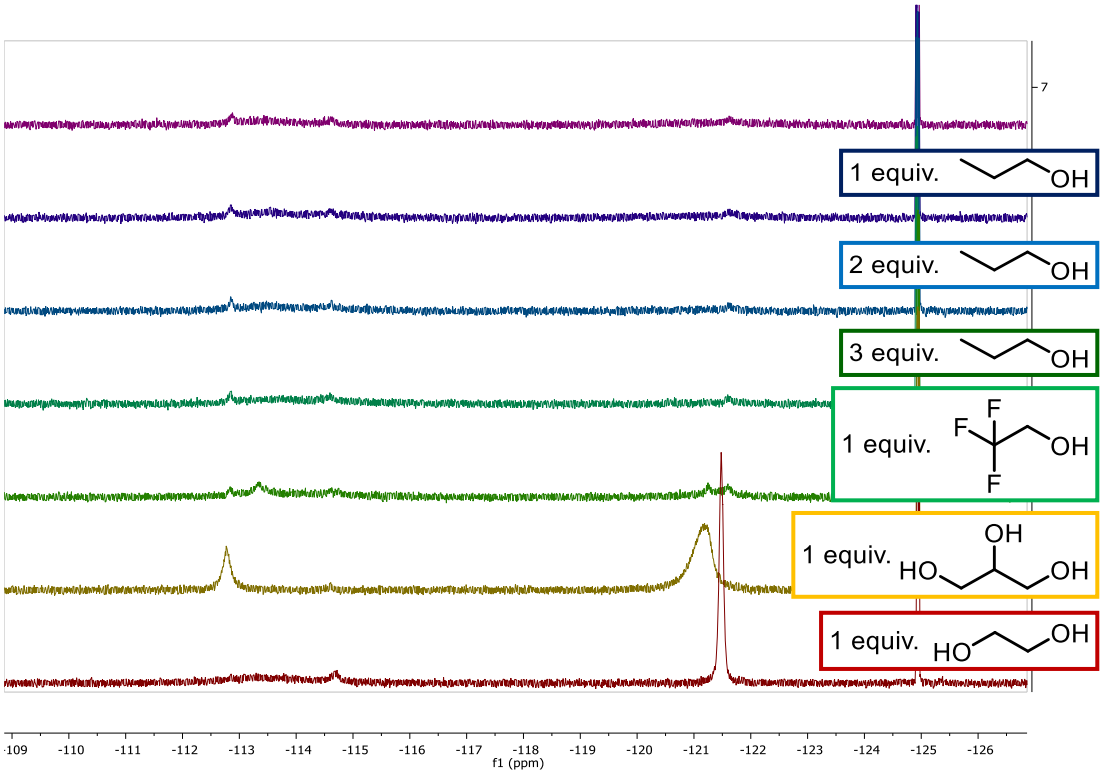

Fig 5.4.17 – Boronic acid **3** + 1 equiv. guanine **11** – effects of different alcohols on the boronate signal. ^{19}F NMR, 300 K, 10:1 THF/water, with 1-fluoronaphthalene as an internal standard (−125 ppm). Boronic acid **3** + 1 equiv. guanidine **11** (top spectrum), + 1 equiv. 1-propanol, + 2 equiv. 1-propanol, + 3 equiv. 1-propanol, + 1 equiv. trifluoroethanol, + 1 equiv. glycerol, + 1 equiv. ethylene glycol (bottom spectrum)

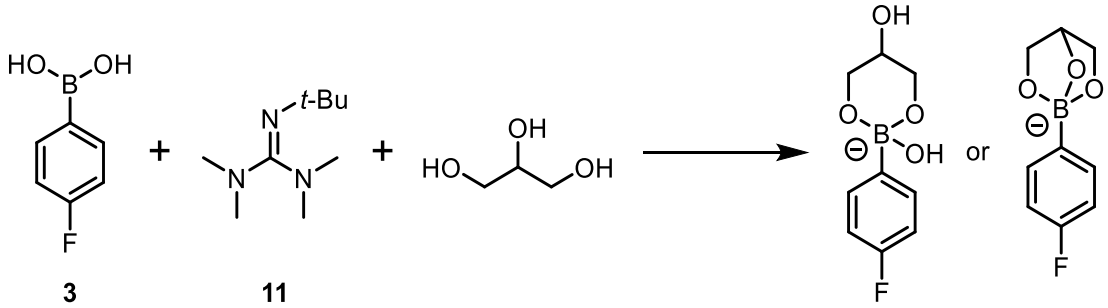

Scheme 5.4.10 – Possible boronate formation using glycerol

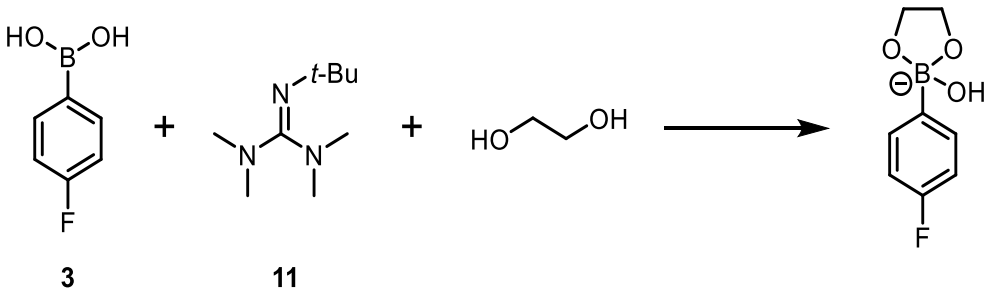

Scheme 5.4.11 – Possible boronate formation using ethylene glycol

5.4.5. Catechol

Catechol was investigated to be able to fluorine label the alcohol and track that by ^{19}F NMR as well as the boronic acid **3**. Preliminary studies of unlabelled catechol showed a similar effect as the other diols studied, **Scheme 5.4.12**, **Fig 5.4.18**. Intermediate signals, integrating 1:1 were seen at −114.46 ppm and −120.75 ppm. But unlike the other diols, both the boronic acid **3** (−112.50 ppm) and boronate signal (−120.54 ppm) could be seen in the system. When studying 3-fluorocatechol, **Scheme 5.4.13**, the same signals were observed by at slightly different chemical shifts, indicating the formation of different species, **Fig 5.4.19**. Looking at the fluorine label on the alcohol also showed an interesting change, of the 3-fluorocatechol signal (−138.16 ppm) decreasing with addition of base, and the formation of a new peak at −144.80 ppm, **Fig 5.4.20**.

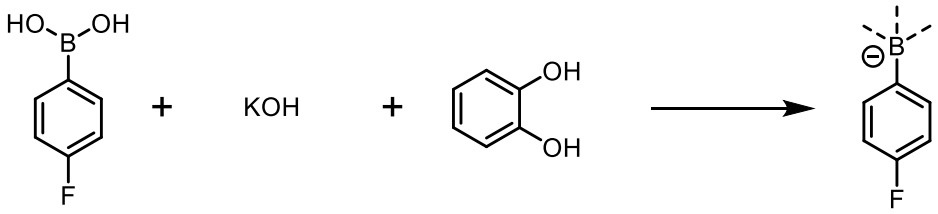

Scheme 5.4.12 – Boronic acid **3** + KOH – adding catechol

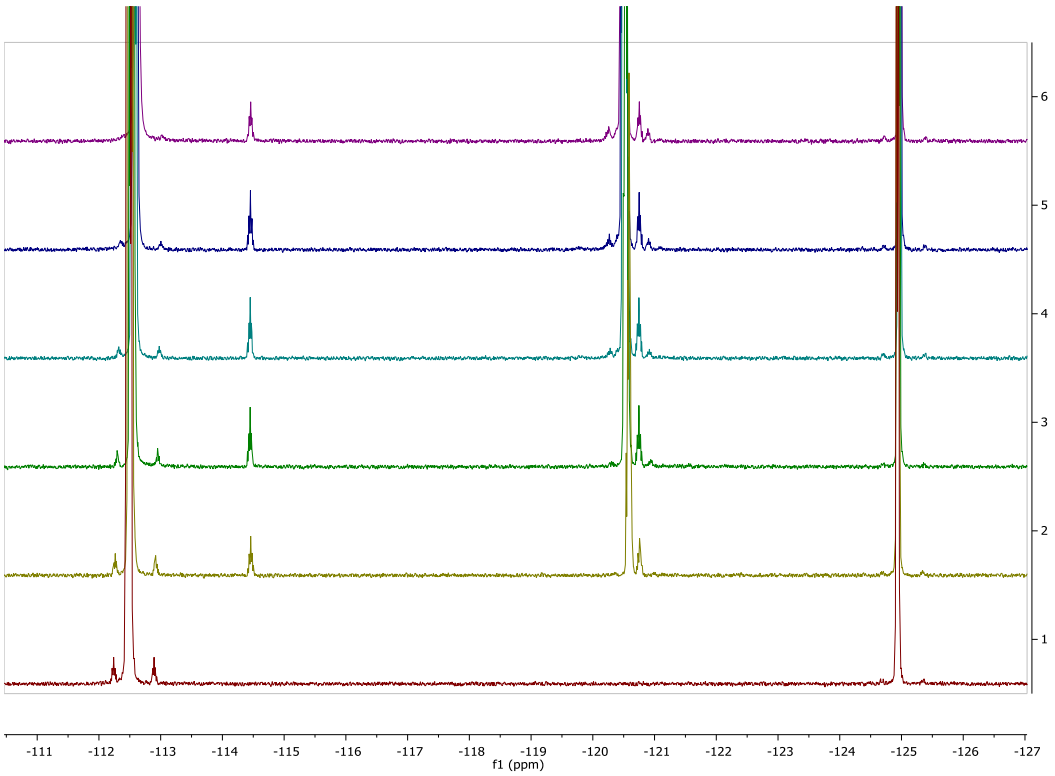

Fig 5.4.18 – Boronic acid **3** + 1 equiv. catechol + KOH – varying KOH to 1 equiv. (top spectrum) in steps of 0.2. ^{19}F NMR, 300 K, 10:1 THF/water, with 1-fluoronaphthalene as an internal standard (−125 ppm)

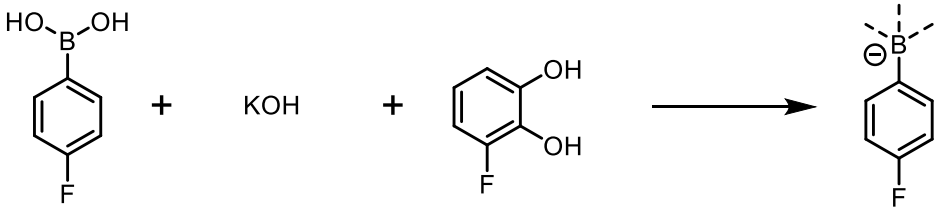

Scheme 5.4.13 – Boronic acid **3** + KOH – adding 3-fluorocatechol

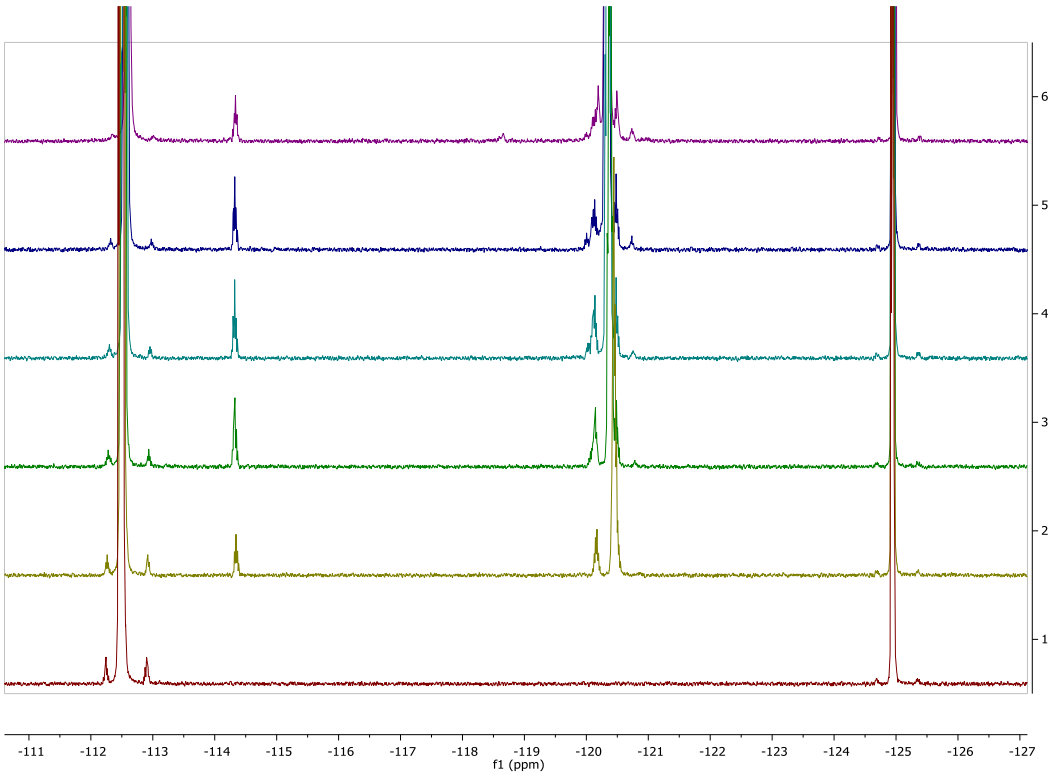

Fig 5.4.19 – Boronic acid **3** + 1 equiv. 3-fluorocatechol + KOH – varying KOH to 1 equiv. (top spectrum) in steps of 0.2. Boronic acid region. ^{19}F NMR, 300 K, 10:1 THF/water, with 1-fluoronaphthalene as an internal standard (−125 ppm)

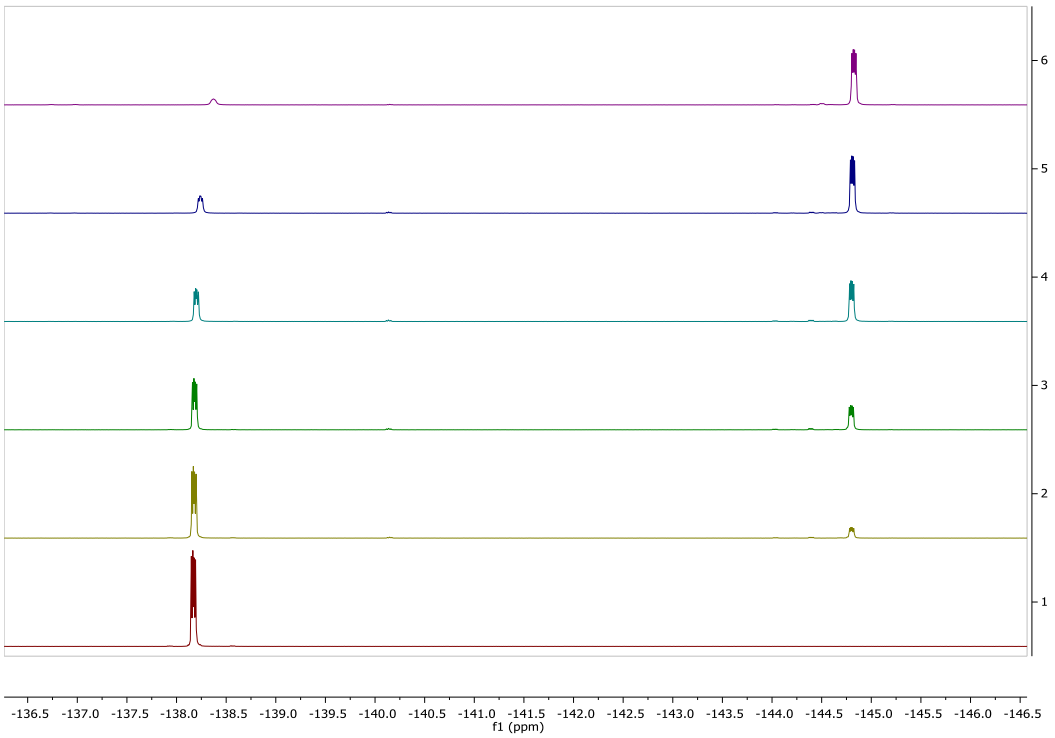

Fig 5.4.20 – Boronic acid **3** + 1 equiv. 3-fluorocatechol + KOH – varying KOH to 1 equiv. (top spectrum) in steps of 0.2. 3-fluorocatechol region. ^{19}F NMR, 300 K, 10:1 THF/water, with 1-fluoronaphthalene as an internal standard (−125 ppm)

5.5. Base screen

A range of bases were tested using the newly developed SM cross-coupling conditions, **Chapter 5**. To see if there is a correlation between boronate formation and efficient coupling, the bases were tested individually for their boronate formation, **Scheme 5.5.1**, **Fig 5.5.1**.

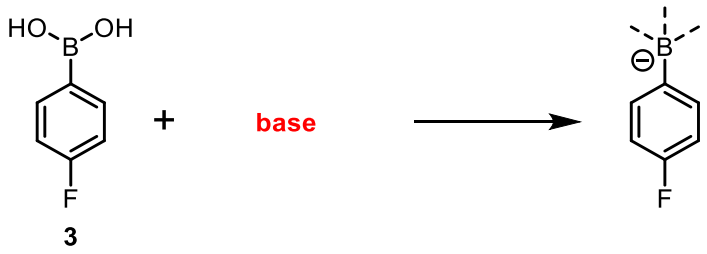

Scheme 5.5.1 – Potential boronate formation using different bases

	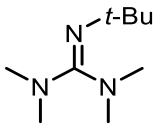	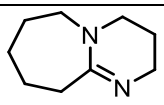	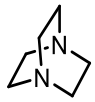	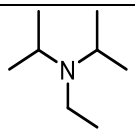
	Guanidine **11**	DBU	DABCO	Diisopropylethylamine
% conversion	**88%**	7%	13%	4%
	Yes	No	No	No
	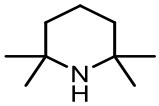	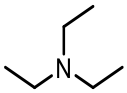	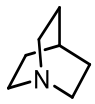	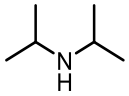
	2,2,6,6-tetramethylpiperidine	Triethylamine	Quinuclidine	Diisopropylamine
% conversion	21%	4%	23%	11%
	No	No	No	No
	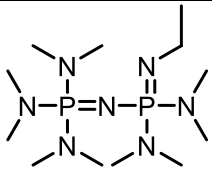	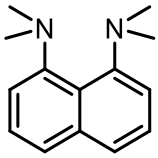	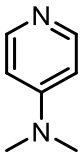	
	Phosphazene base P_2-Et **26**	Proton sponge	DMAP	
% conversion	**76%**	3%	0%	
	Yes	No	No	

Fig 5.5.1 – Organic base screening and their boronate formation. SM cross-coupling of boronic acid **3** (0.04 M) with 1,3-bis(trifluoromethyl)-5-bromobenzene **4** (0.04 M). Yields (of desired product **5**) after 24 hours by ^{19}F NMR with 1-fluoronaphthalene as an internal standard

The only two organic bases shown to give boronate formation are the guanidine **11** (−121.06 ppm) and phosphazene base **26** (−122.00 ppm), **Fig 5.5.2** & **5.5.3**. These are also the only two bases tested which give efficient SM cross-coupling (88% – guanidine **11**, 76% – phosphazene **26**). The other bases tested do not reach conversions higher than 23%. This shows that a correlation between boronate formation and SM cross-coupling conversion, under the newly developed phosphine-free conditions. Bases that are unable to form a boronate undergo very poor coupling under these conditions, in comparison to bases which do form a boronate species.

Adding different equivalents of the phosphazene **26** was tested to see if the same trend was observed when compared to the guanidine **11**, **Scheme 5.5.2**. At low amounts of phosphazene **26**, the three intermediate signals can be seen at –112.86 ppm, −114.65 ppm and −121.64 ppm, and at high equivalents the major signal is the boronate, −122.00 ppm, **Fig 5.5.3**.

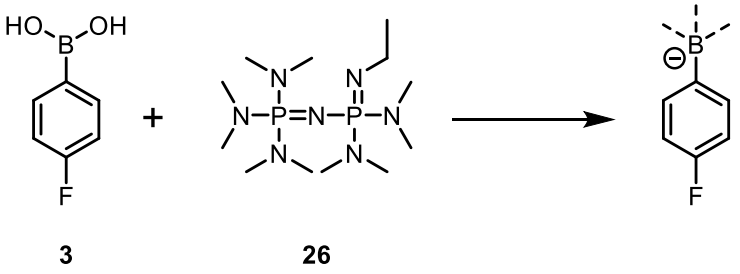

3 **26**

Scheme 5.5.2 – Boronate formation using phosphazene base **26**

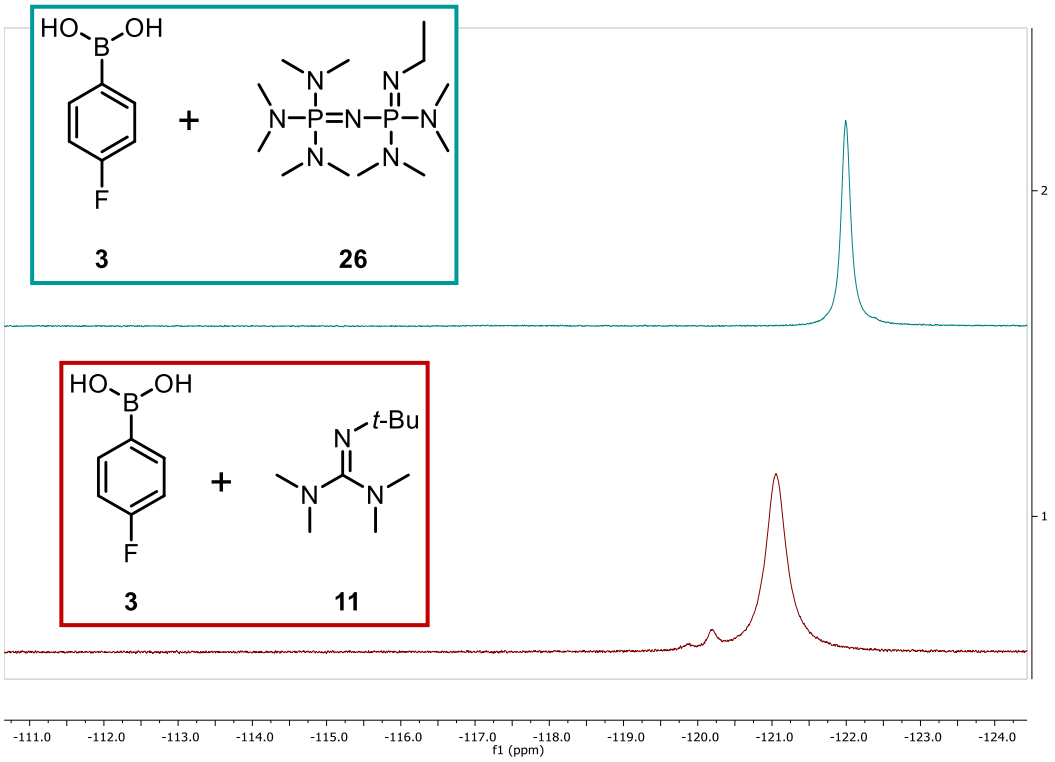

Fig 5.5.2 – Boronate formation starting from boronic acid **3** using guanidine **11** (bottom spectrum) or phosphazene **26** (top spectrum). ^{19}F NMR, 300 K, 10:1 THF/water

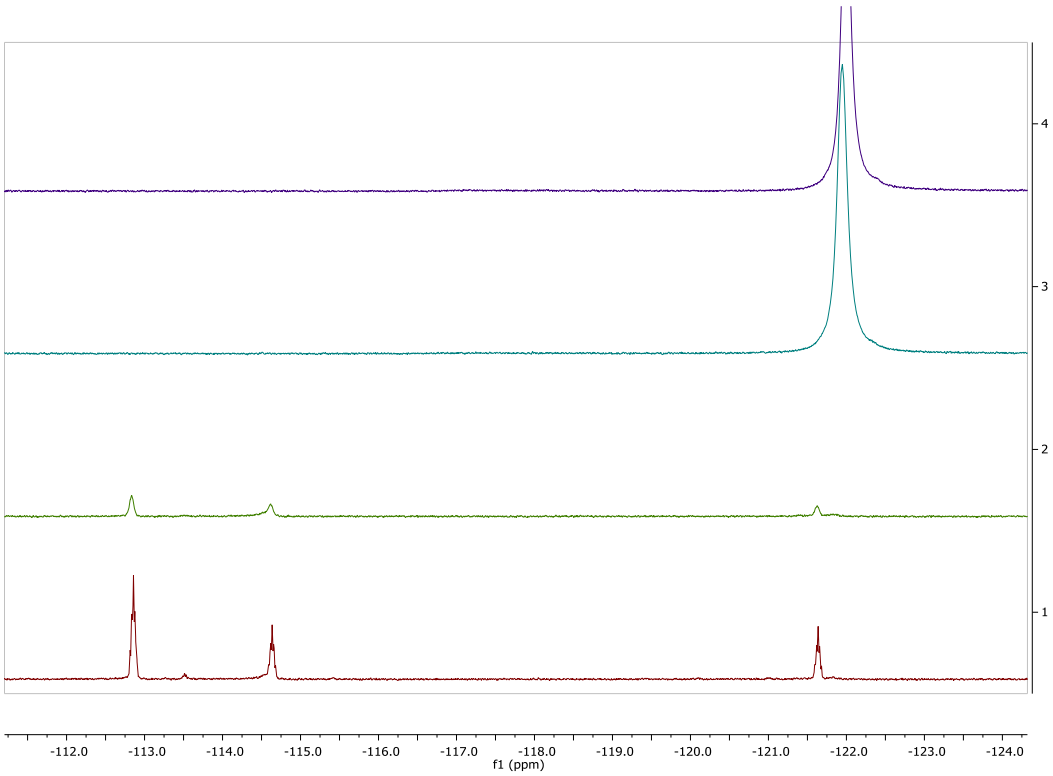

Fig 5.5.3 – Boronic acid **3** + phosphazene base **26** – 0.4 (bottom), 1, 2, 3 (top) equiv. base. ^{19}F NMR, 300 K, 10:1 THF/water

The initial coupling conditions used potassium carbonate and did not show any boronate formation by ^{19}F or ^{11}B NMR. The newly developed conditions reinvestigated the use of potassium carbonate and found it to give poor conversion, 15%, so it was studied independently for potential boronate formation, **Scheme 5.5.3**. The three intermediate signals (−113.00 ppm, −114.77 ppm and −121.73 ppm) can be seen, and increase with increasing amounts of base, but the major species throughout is the boronic acid **3**, **Fig 5.5.4**. There is no boronate signal. This is also shown clearly by the ^{11}B NMR, **Fig 5.5.5**.

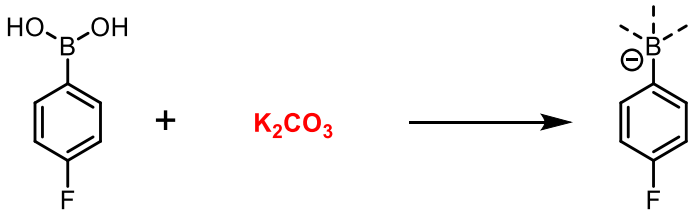

3

Scheme 5.5.3 – Potential boronate formation using potassium carbonate

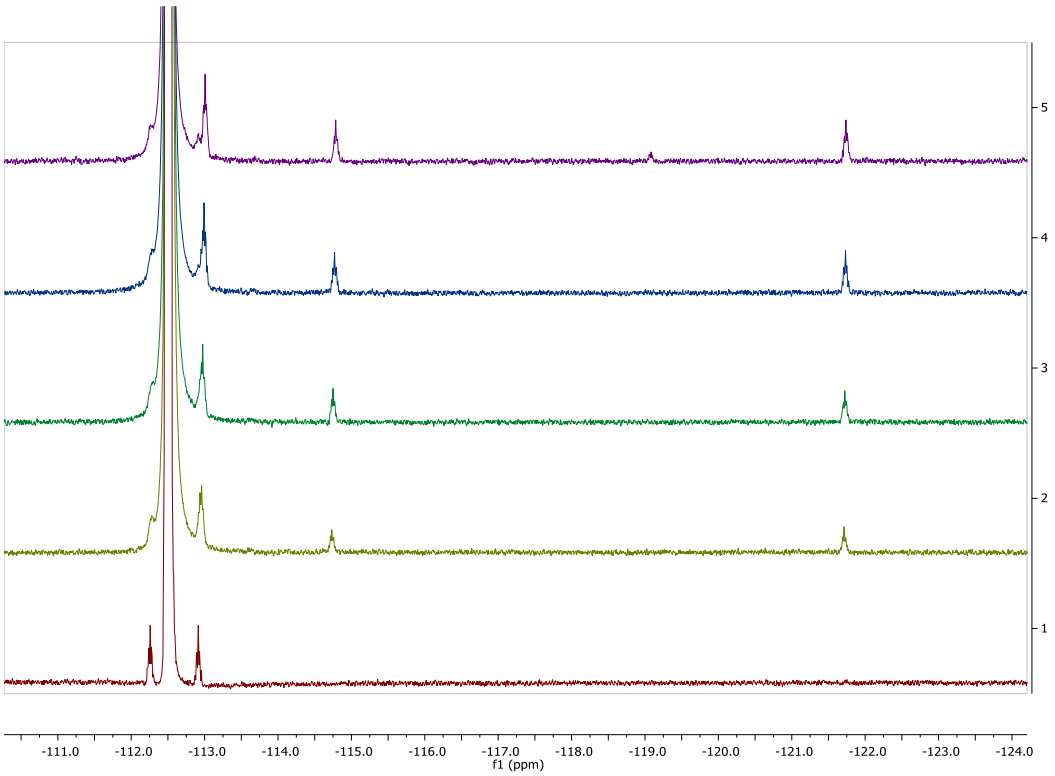

Fig 5.5.4 – Boronic acid **3** + K_2CO_3 – 0 (bottom), 0.4, 1, 2, 3 (top) equiv. K_2CO_3. ^{19}F NMR, 300 K, 10:1 THF/water

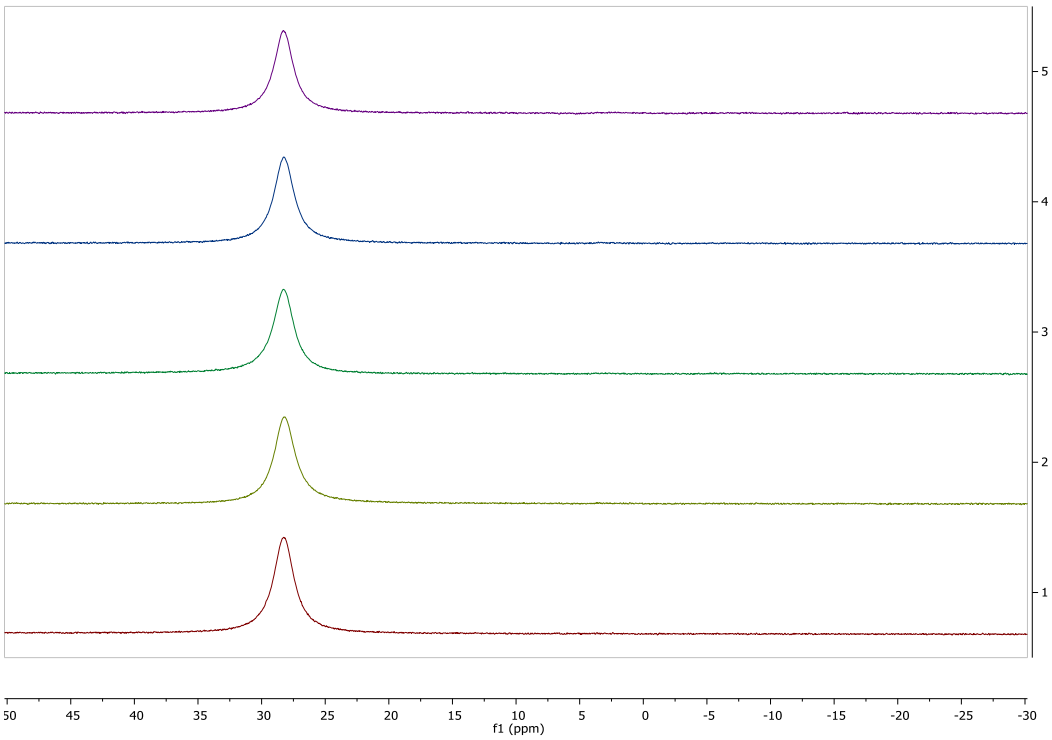

Fig 5.5.5 – Boronic acid **3** + K_2CO_3 – 0 (bottom), 0.4, 1, 2, 3 (top) equiv. K_2CO_3. ^{11}B NMR, 300 K, 10:1 THF/water

5.6. Guanidine screen

Results from studies in **Chapter 4** suggested that the reason the other guanidines (**13** & **14**) tested gave poor conversion in SM cross-coupling could be due to catalyst binding inhibiting the reaction, as opposed to the poor coupling seen by other bases due to inability to form a boronate. To test this theory each of the guanidines (**13** & **14)** were tested independently for the ability to form a boronate species with the boronic acid **3**, **Scheme 5.6.1**, **Fig 5.6.1**.

Looking at the addition of 1 equiv. base, the *t*-Bu **11** and *n*-Bu **14** guanidines give very similar results by ^{19}F NMR – both result in a large loss of signal by ^{19}F NMR, compared to the boronic acid **3** with no base, using 1-fluoronaphthalene as an internal standard, and give small intermediate signals at −112.86 ppm, −114.61 ppm and −121.63 ppm, and a very broad trace boronic acid **3** signal −113.45 ppm, **Fig 5.6.2**. However, the ^{11}B NMR shows only the *t*-Bu guanidine **11** fully removes the boronic acid signal, and has a new boronate signal at 3.72 ppm, whereas the *n*-Bu guanidine **14** does have the boronate signal 3.72 ppm, but still has a clear boronic acid **3** signal at 26.94 ppm, **Fig 5.6.3**. The use of NH guanidine **13** greatly reduces the total ^{19}F NMR signal, but the major signal is still from the boronic acid **3**, **Fig 5.6.2**, also shown

in the ^{11}B NMR, **Fig 5.6.3**. Varying the equivalents of each guanidine was also investigated, **Appendix 8.5.6**.

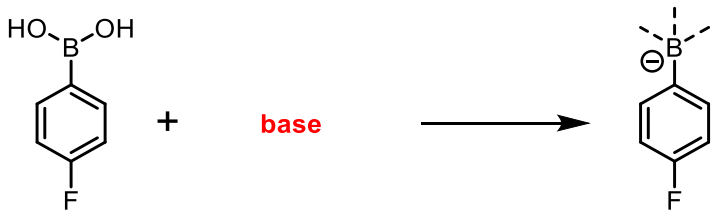

Scheme 5.6.1 – Boronate formation from boronic acid **3** + guanidine **11**/**13**/**14**

	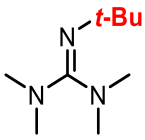 **11**	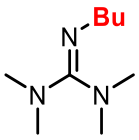 **14**	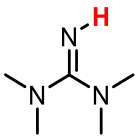 **13**
SM coupling conversion	88%	56%	1%
Boronate	Yes	Yes	Minor
Intermediates	Yes	Yes	Yes

Fig 5.6.1 – Guanidine screening

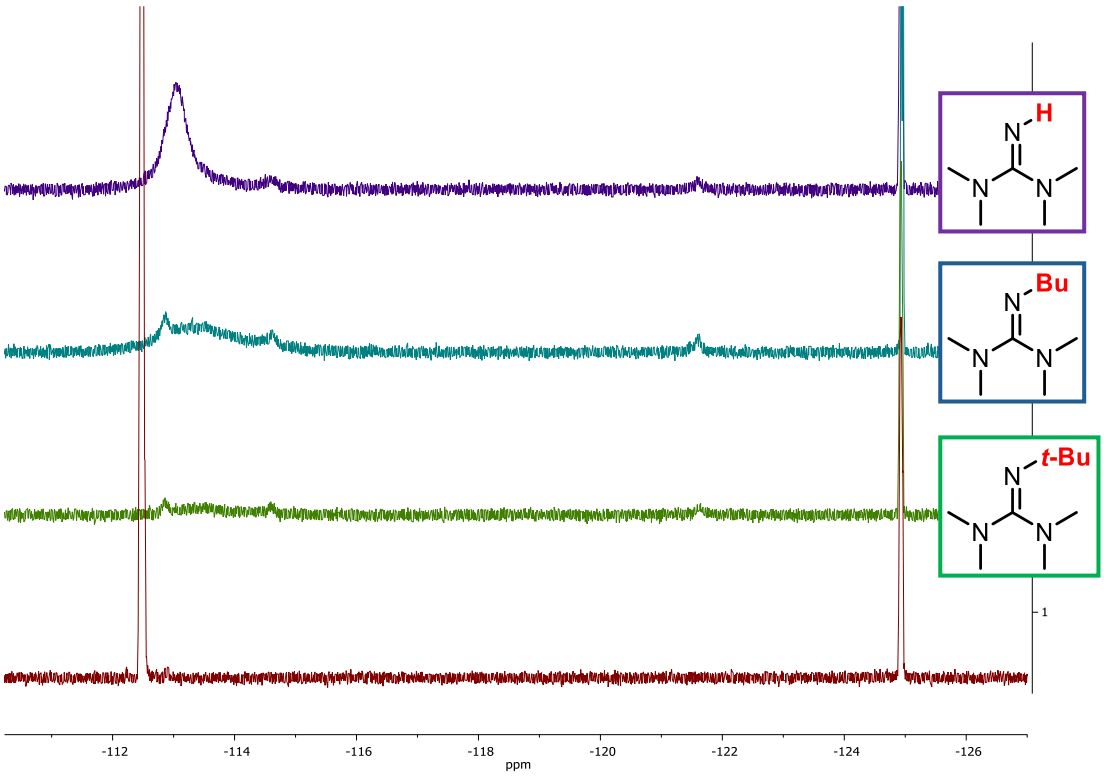

Fig 5.6.2 – Comparison – boronic acid **3** + 1 equiv. guanidine – NH guanidine **13** (top spectrum), *n*-Bu guanidine **14**, *t*-Bu guanidine **11**, no base (bottom spectrum). ^{19}F NMR, 300 K, 10:1 THF/water, with 1-fluoronaphthalene as an internal standard (−125 ppm)

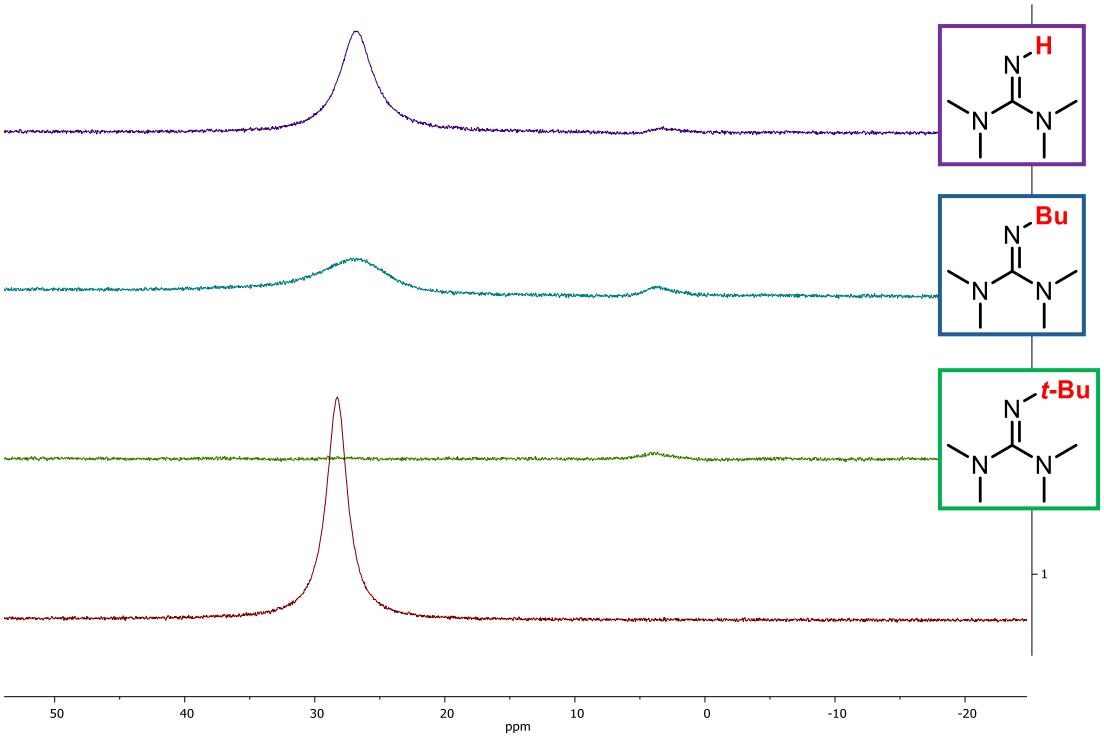

Fig 5.6.3 – Comparison – boronic acid **3** + 1 equiv. guanidine – NH guanidine **13** (top spectrum), *n*-Bu guanidine **14**, *t*-Bu guanidine **11**, no base (bottom spectrum). ^{11}B NMR, 300 K, 10:1 THF/water

5.7. Boronic Acid Studies

5.7.1. 4-Fluoroboronic acid

To further test the effects of base on the 4-fluorophenyl boronic acid **3**, higher concentrations were investigated to see if the relative signal integrations were affected by concentration, **Scheme 5.7.1**. A range of concentrations from 0.10 M to 0.01 M were tested, **Fig 5.7.1**. 0.02 M and 0.01 M were too dilute to give signal by ^{19}F NMR. But the other tests, from 0.04 M to 0.10 M all gave intermediate signals that integrated 2:1:1, showing that whatever species is being formed is unaffected by total boron concentration, **Fig 5.7.2**.

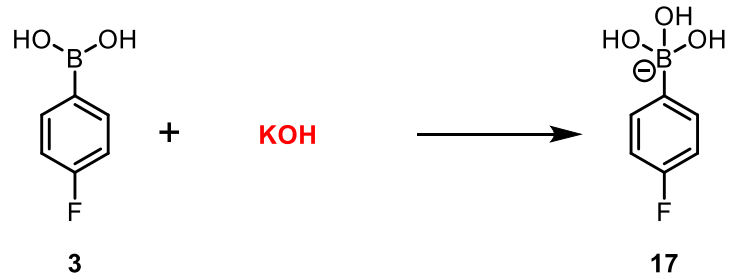

3 17

Scheme 5.7.1 – 4-Fluorophenyl boronic acid boronate **17** formation using KOH

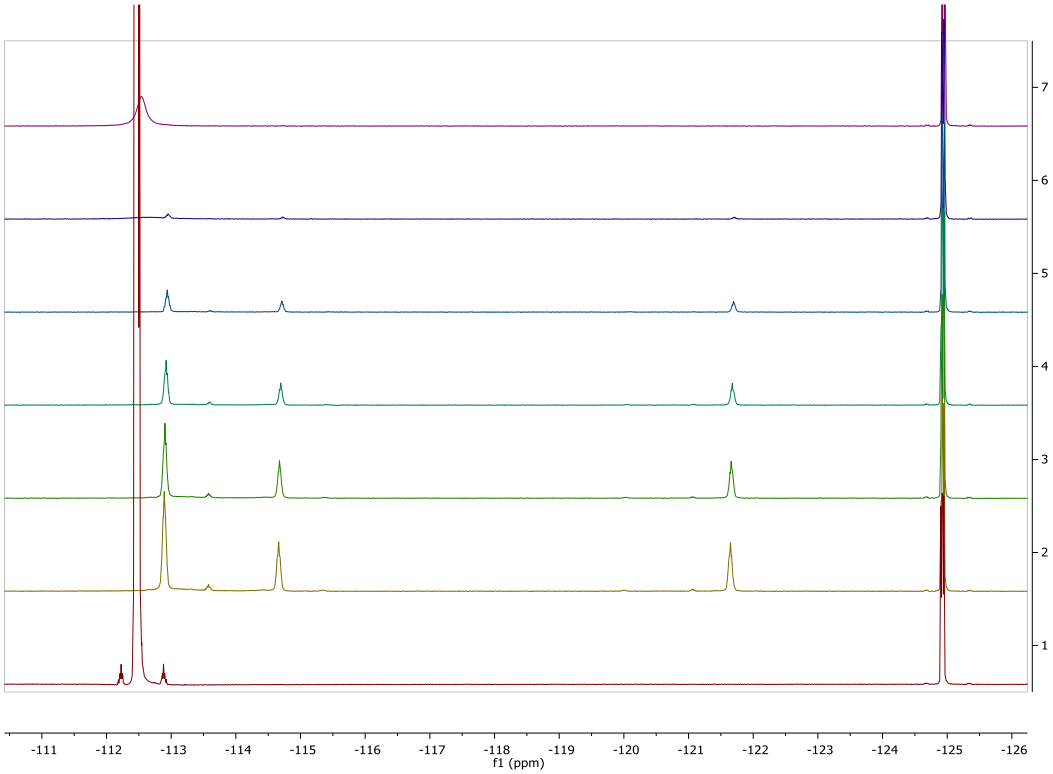

Fig 5.7.1 – Different concentrations of boronic acid **3** + 1 equiv. KOH – Boronic acid **3** with no base (bottom), 0.1M, 0.08M, 0.06M, 0.04M, 0.02M, 0.01M (top). ^{19}F NMR – 128 scans & 20 sec delay, 300 K, 10:1 THF/water, with 1-fluoronaphthalene as an internal standard (−125 ppm)

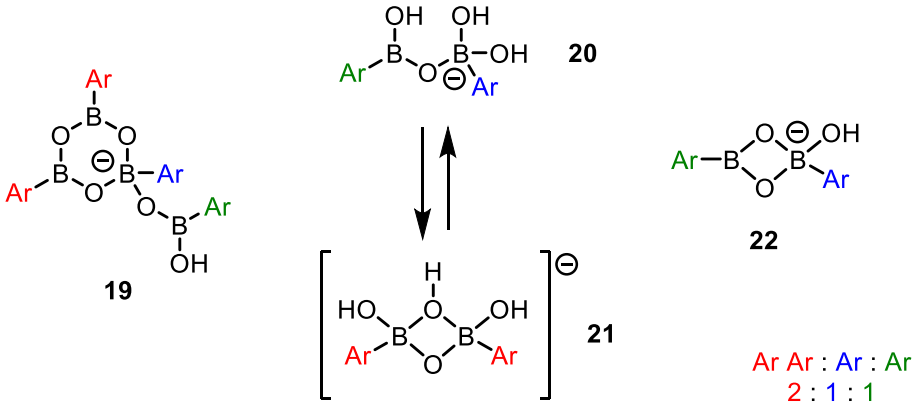

Fig 5.7.2 – Possible species formed from boronic acid **3** + guanidine **11** reaction

5.7.2. 2-Fluoroboronic acid

The boronate formation of other boronic acids was investigated, **Scheme 5.7.2**. By ^{19}F NMR, the 2-fluorophenyl boronic acid **27** was found to remain as a single signal that shifts from −106.42 ppm (boronic acid **27**) to −109.40 ppm (boronate **28**), **Fig 5.7.3**. Rather than one signal decreasing and a new signal increasing, as seen for the 4-fluorophenyl boronic acid **3**. 2-Fluorophenyl boronic acid **27** also does not appear to go through an intermediate species, as the 4-fluorophenyl boronic acid **3** does. The addition of base does result in a much broader signal – line width without base = 30 Hz, line width at 0.2 equiv. KOH = ~200 Hz. This broadening is likely due to the boronic acid **27** being in rapid exchange with the boronate species **28**. (Appendix 8.5.7 – ^{11}B NMR).

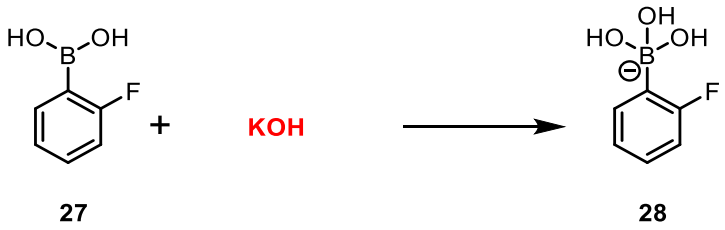

Scheme 5.7.2 – 2-Fluorophenyl boronic acid boronate **28** formation using KOH

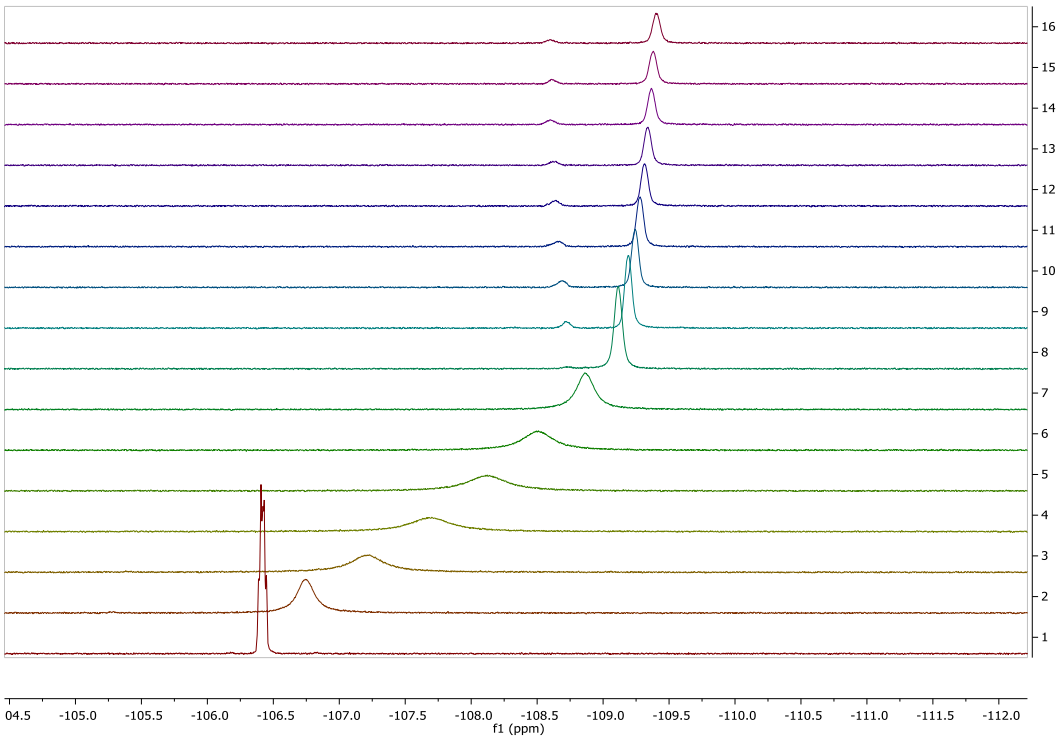

Fig 5.7.3 – 2-Fluorophenyl boronic acid **27** + KOH – to 3 equiv. KOH (top spectrum) in steps of 0.2. ^{19}F NMR, 300 K, 10:1 THF/water, with 1-fluoronaphthalene as an internal standard (−125 ppm). New signal at −108.5 ppm is seen at high base concentrations, but further studies are needed to identify this signal

5.7.3. 3-Fluoroboronic acid

As the 2-fluorophenyl boronic acid **27** gave a very different result compared to the 4-fluorophenyl boronic acid **3**, the 3-fluorophenyl boronic acid **29** was also investigated, **Scheme 5.7.3**. With the addition of 0.2 equiv. KOH, the boronic acid **29** signal is shifted and reduced by ^{19}F NMR, **Fig 5.7.4**. With increasing amounts of base, the boronic acid **29** signal shifts from −116.17 ppm to −117.13 ppm, suggesting that as with the 2-fluorophenyl boronic acid **27**, this is the boronic acid **29** becoming the boronate **30**. The addition of base results in a much broader signal, again due to the boronic acid/boronate equilibrium. At high base the signal sharpens, showing there is no longer a rapid equilibrium and the boronate **30** to be the major species. (Appendix 8.5.8 – ^{11}B NMR).

After the addition of 0.2 equiv. KOH, there are three new signals visible, at −116.61 ppm, −117.38 ppm and −118.21 ppm, which integrate approximately 2:1:1, although this is difficult

to accurately determine due to the broad shifting signals underneath these new signals. This could be the same intermediate(s) as seen for the 4-fluorophenyl boronic acid **3**, **Fig 5.7.5**.

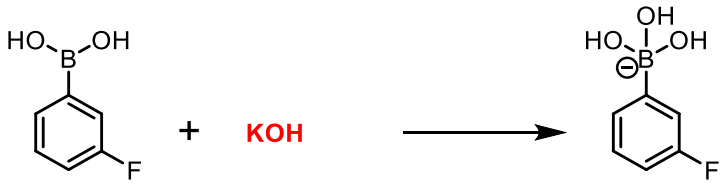

29 **30**

Scheme 5.7.3 – 3-Fluorophenyl boronic acid boronate **30** formation using KOH

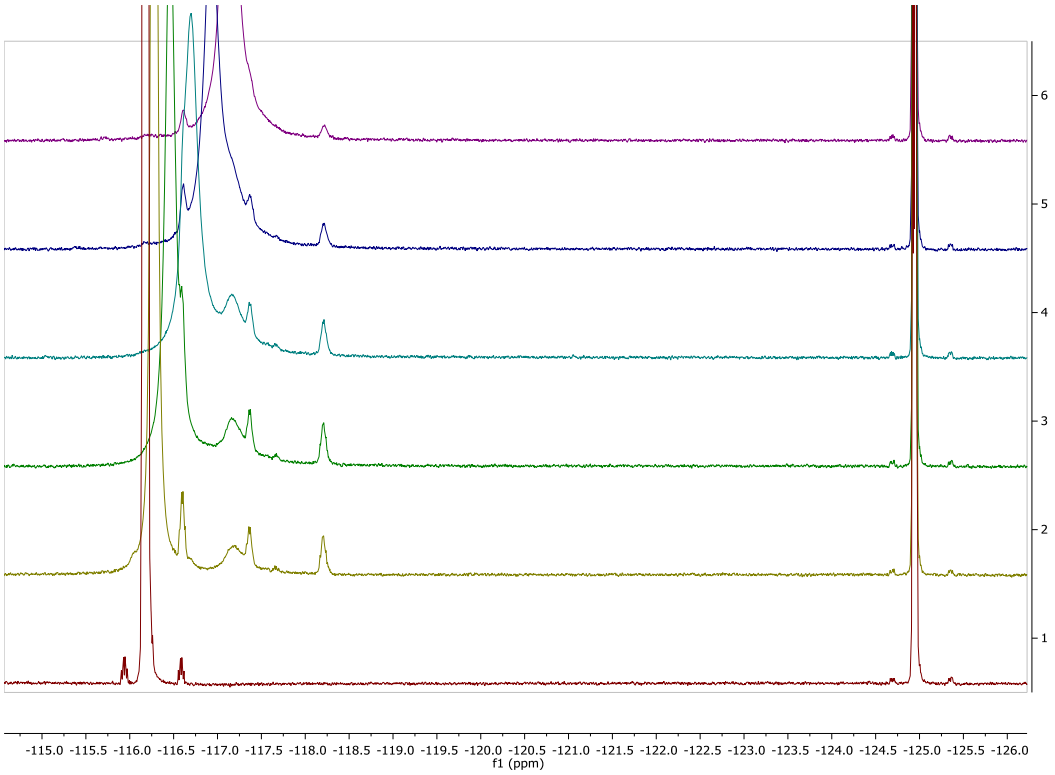

Fig 5.7.4 – 3-Fluorophenyl boronic acid **29** + KOH – to 1 equiv. KOH (top spectrum) in steps of 0.2. ^{19}F NMR, 300 K, 10:1 THF/water, with 1-fluoronaphthalene as an internal standard (−125 ppm)

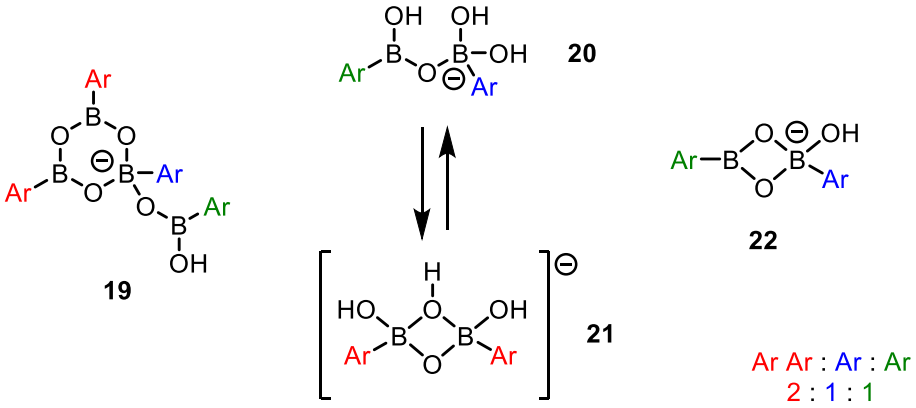

Fig 5.7.5 – Possible species formed from boronic acid **3** + guanidine **11** reaction

5.7.4. Mixed boronic acid tests

Mixed tests were carried out to investigate how the presence of a different boronic acid affected the signals, especially for the intermediate species seen at low amounts of base. If the boronic acid/boronate dimer is being formed, then mixing different boronic acids could allow for the potential formation of mixed intermediate species, **Fig 5.6.7**. As the 3-fluoro **29** and 4-fluoro **3** boronic acids gave similar results, in terms of intermediate signal formation, these two boronic acids were the best choice for testing the presence of a mixed intermediate species.

	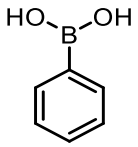 **31**	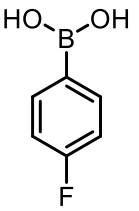 **3**	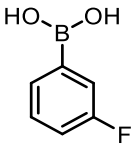 **29**	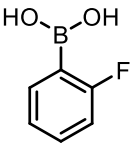 **27**
pKa 1:1 H_2O/dioxane 70 °C	11.25	10.97	10.46	10.14

Fig 5.7.6 – The different boronic acid tested and pKa values, determined by ^{11}B NMR pH titration at 70 °C.[9]

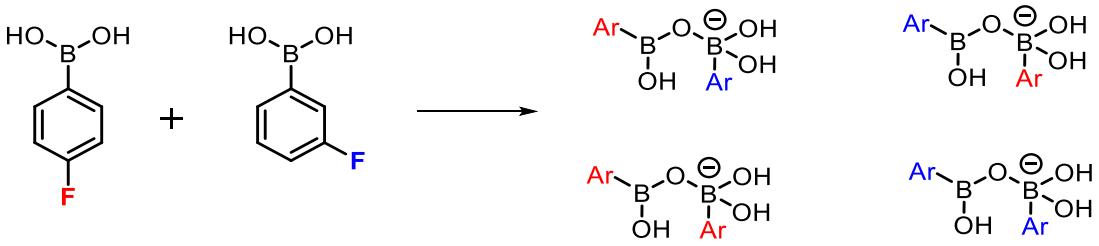

Fig 5.7.7 – Mixed boronic acid studies

3F BA + 4F BA

Mixing the 3-fluoro **29** and 4-fluoro **3** boronic acids 1:1 and adding low amounts of base (<1 equiv.) showed a range of intermediate signals, **Scheme 5.7.4** & **Fig 5.7.8**. The 4-fluoro **3** gave three signals at −112.87 ppm, −114.67 ppm and −121.66 ppm, and the 3-fluoro **29** gave two signals at −117.36 ppm and −118.25 ppm. No new signals for mixed intermediates were seen, suggesting the fluorine groups are too far apart, in the respective intermediates being formed, to affect each other. However, what is interesting is the change in integration seen as a result of mixing the boronic acids. The 3-fluoro **29** intermediate signals are difficult to integrate due to the broad boronic acid **29**/boronate **30** signal in a very small region. But the 4-fluoro **3** intermediate signals at −114.67 ppm and −121.66 ppm, for the possible boronic acid/boronate dimer **20**, now integrate 1:0.3, compared to the usual 1:1. This suggests that there are mixed intermediate species present, and that the 4-fluoro **3** is the boronic acid part of the species, and the 3-fluoro **29** is the boronate part, hence the lower integration for the 4-fluoro boronate intermediate signal. This agrees with the 3-fluoro **29** being the more Lewis acid boronic acid, hence forming a boronate species more easily. (Appendix 8.5.9 – ^{11}B NMR).

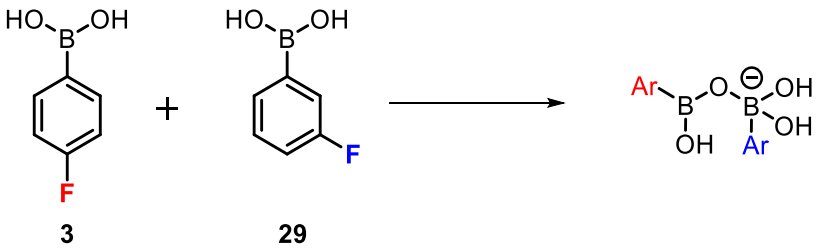

Scheme 5.7.4 – Possible 4-fluoro/3-fluoro mixed intermediate species

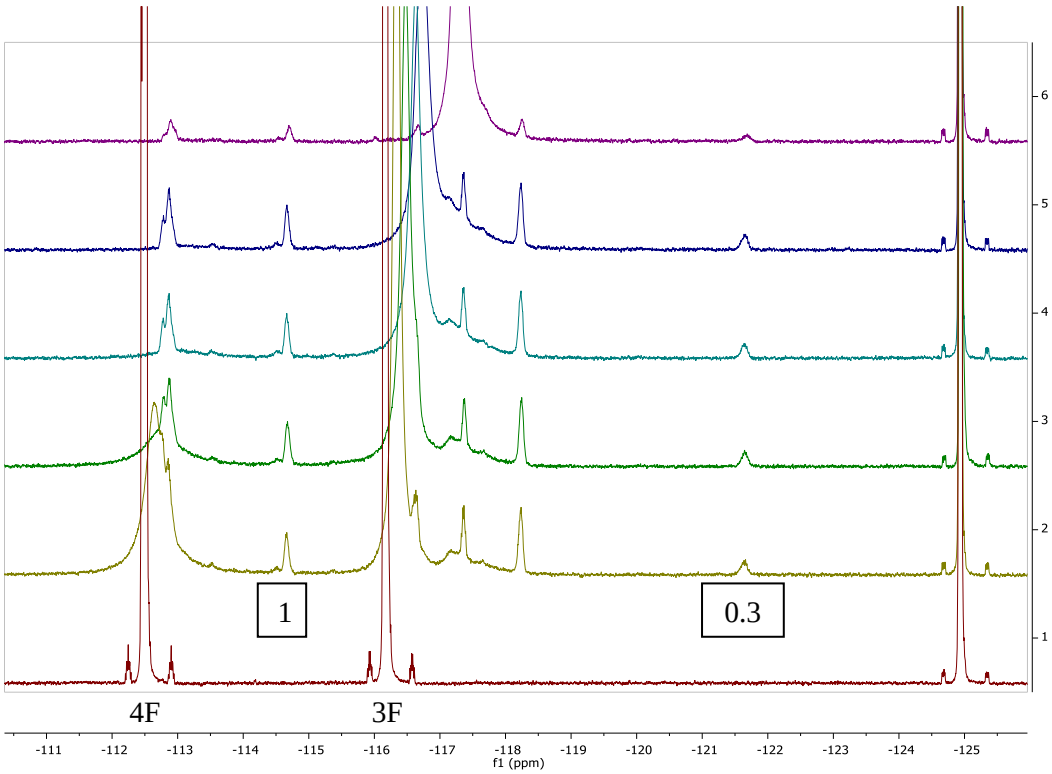

Fig 5.7.8 – 3-Fluorophenyl boronic acid **29** (0.02M) + 4-fluorophenyl boronic acid **3** (0.02M) + KOH – KOH equiv. = 0, 0.2, 0.3, 0.4, 0.5, 1 (top spectrum). ^{19}F NMR – 128 scans & 20 sec delay, 300 K, 10:1 THF/water, with 1-fluoronaphthalene as an internal standard (−125 ppm)

Phenyl BA + 4F BA

4-Fluorophenyl boronic acid **3** was mixed with unlabelled phenyl boronic acid **31** to see if this gave a change to intermediate signals, **Fig 5.7.9**. Upon addition of base (KOH), three signals are formed at −113.10 ppm, −114.80 ppm and −121.79 ppm, integrating 1.5:1:1. Despite the presence of another boronic acid, the potential dimer signals (−114.80 ppm and −121.79 ppm) are unaffected, but the integration of the third signal at −113.10 ppm is, **Fig 5.7.10**. Further studies are needed to find the reason for this change. (Appendix 8.5.9 – ^{11}B NMR).

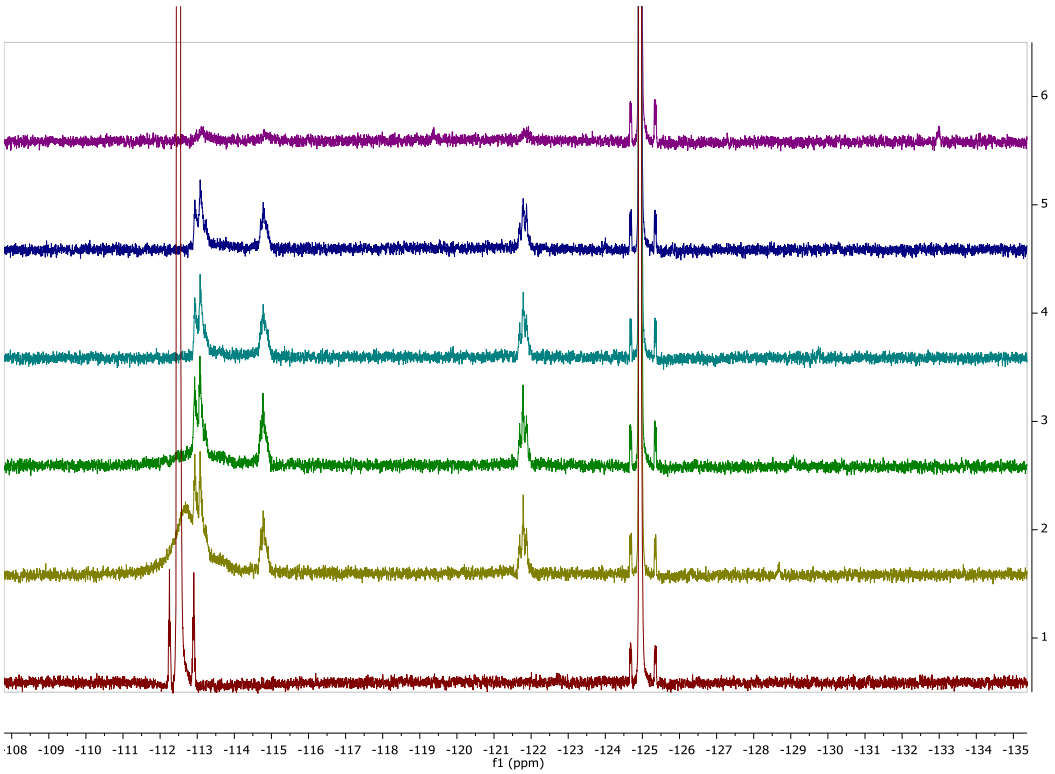

Fig 5.7.9 – Phenyl boronic acid **31** (0.02M) + 4-fluorophenyl boronic acid **3** (0.02M) + KOH – KOH equiv. = 0, 0.2, 0.3, 0.4, 0.5, 1 (top spectrum). ^{19}F NMR – 128 scans & 20 sec delay, 300 K, 10:1 THF/water, with 1-fluoronaphthalene as an internal standard (−125 ppm)

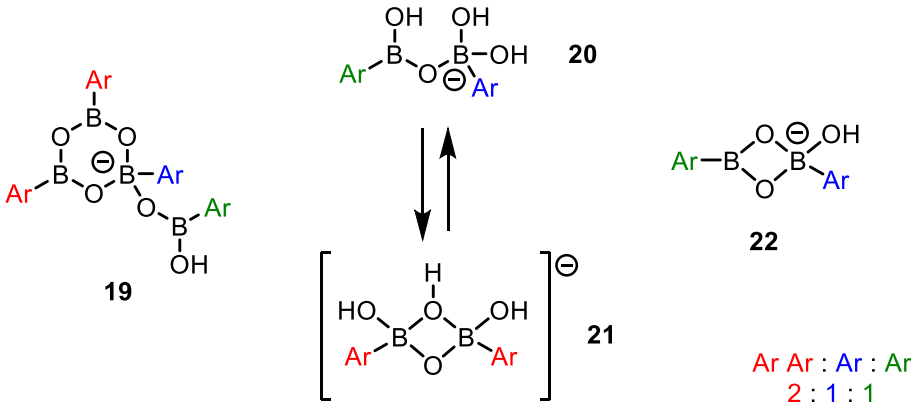

Fig 5.7.10 – Possible species formed from boronic acid **3** + guanidine **11** reaction

5.8. Conclusion

The formation of a boronate species using guanidine **11** and KOH has been studied using ^{19}F and ^{11}B NMR. This boronate species is found to differ when diols are present, suggesting the formation of a boronic ester boronate, such as the pinacol ester boronate **25**, **Scheme 5.8.1**, **Fig 5.8.1**. Mono-alcohols have been shown not to give this change in spectra, only diols or triols.

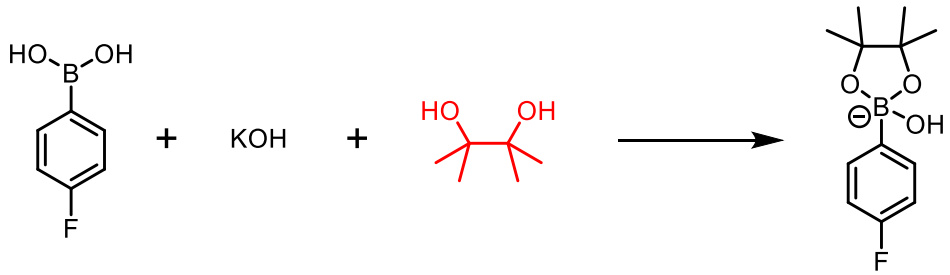

3 **25**

Scheme 5.8.1 – Formation of a pinacol ester boronate **25**

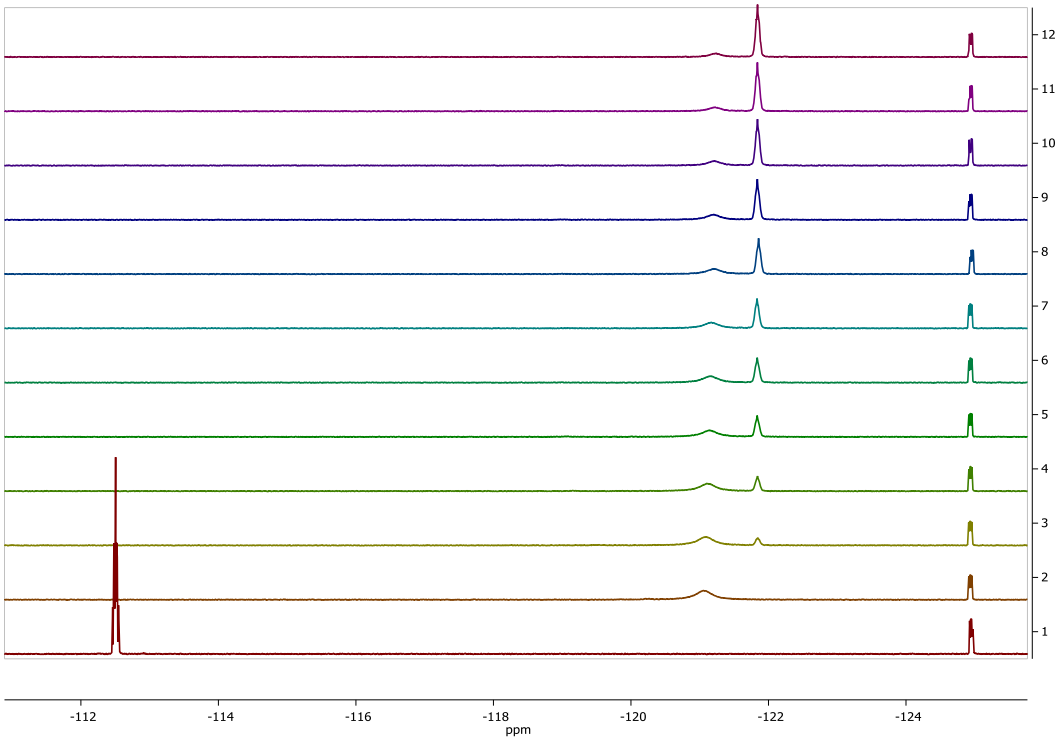

Fig 5.8.1 – Boronic acid **3** + 2 equiv. KOH + pinacol – boronic acid **3**, no base (bottom spectrum), addition of KOH (spectrum 2), then varying equiv. pinacol to 2 equiv. (top spectrum) in steps of 0.2. ^{19}F NMR, 300 K, 10:1 THF/water, with 1-fluoronaphthalene as an internal standard (−125 ppm)

A correlation has been found between ability of a base to form a boronate and efficient SM cross-coupling under the newly developed phosphine-free conditions, **Scheme 5.8.2**. Only guanidine **11**, KOH and phosphazene **26**, from the bases tested, form the boronate species and give efficient coupling. All other bases give poor cross-coupling results and do not form the boronate species. In addition to the formation of the boronate species, intermediate signals were found and possible structures suggested, **Fig 5.8.2**. Further studies are needed to identify the true structure of these intermediate signals.

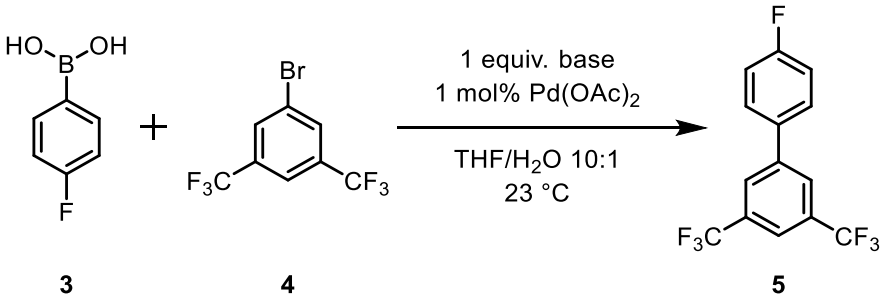

Scheme 5.8.2 – SM cross-coupling of boronic acid **3** (1 equiv.) with 1,3-bis(trifluoromethyl)-5-bromobenzene **4** (1 equiv.) by ^{19}F NMR with 1-fluoronaphthalene as an internal standard

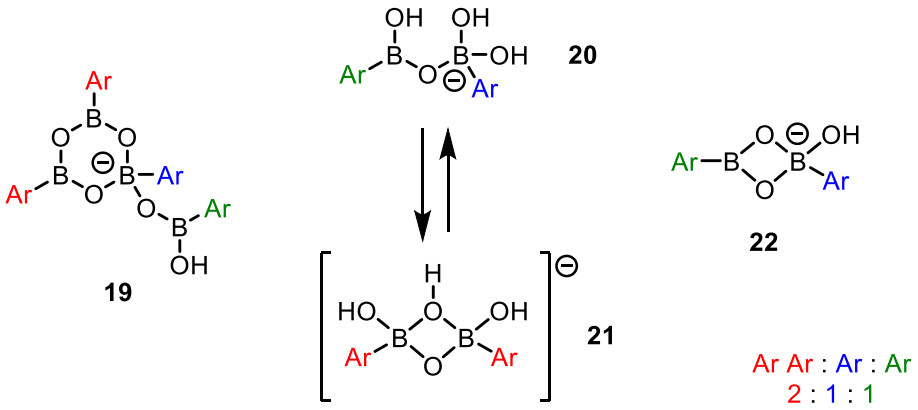

Fig 5.8.2 – Possible species formed from boronic acid **3** + guanidine **11** reaction

5.9. References

(1) Ishihara, K.; Nagasawa, A.; Umemoto, K.; Ito, H.; Saito, K. *Inorg. Chem.* **1994**, *33* (17), 3811–3816.

(2) Kono, Y.; Ishihara, K.; Nagasawa, A.; Umemoto, K.; Saito, K. *Inorganica Chim. Acta* **1997**, *262* (1), 91–96.

(3) Carrow, B. P.; Hartwig, J. F. *J. Am. Chem. Soc.* **2011**, *133* (7), 2116–2119.

(4) Lorand, J. P.; Edwards, J. O. *J. Org. Chem.* **1959**, *24* (6), 769–774.

(5) Hall, D. G. In *Boronic Acids*; Wiley-VCH Verlag GmbH & Co. KGaA: Weinheim, Germany, 2011; pp 1–133.

(6) Lennox, A. J. J.; Lloyd-Jones, G. C. *Chem. Soc. Rev.* **2014**, *43* (1), 412–443.

(7) Nunes, C. M.; Monteiro, A. L. *J. Braz. Chem. Soc.* **2007**, *18* (7), 1443–1447.

(8) Westmark, P. R.; Gardiner, S. J.; Smith, B. D. *J. Am. Chem. Soc.* **1996**, *118* (45), 11093–11100.

(9) Cox, P. Protodeboronation, 2016. Thesis - University of Edinburgh

Chapter 6

Conclusions & future work

6.1 Conclusions

Under the phosphine-free SM conditions investigated, **Scheme 6.1.1**, it appears that the strength of the base has an effect on the pathway of transmetalation and correlates to the efficiency of SM cross-coupling. Using strong bases, such as guanidine **11** or KOH, forms a boronate species and undergoes efficient coupling, presumably *via* the boronate pathway. Whereas the use of weak bases, which are unable to form a boronate species do not promote this cross-coupling effectively, suggesting the presence of a boronate to be crucial to allow efficient coupling to occur *via* the boronate pathway, **Fig 6.1.1**.

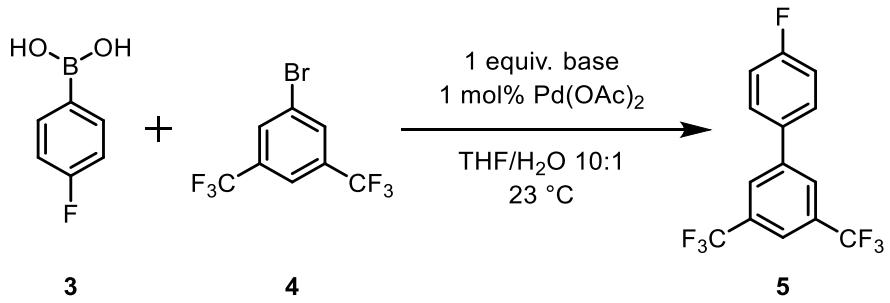

Scheme 6.1.1 – SM cross-coupling of boronic acid **3** (1 equiv.) with 1,3-bis(trifluoromethyl)-5-bromobenzene **4** (1 equiv.)

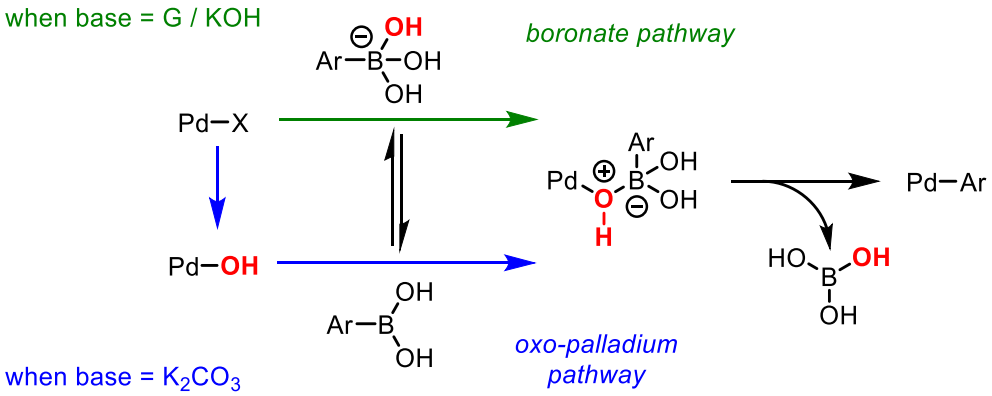

Fig 6.1.1 – Transmetalation pathway controlled by strength of base. G = guanidine **11**

Studies into the effect of the addition of diols to a boronic acid **3** solution with guanidine **11**/KOH, revealed the boronate species, and intermediate(s), formed differ when different diols are present. This suggests the formation of a boronic acid boronate **17** and boronic ester boronates species **23**/**25** depends on the presence of diol in the system, **Fig 6.1.2 & 6.1.3**. However, this does not rule out the possibility of diol coordination to the guanidine.

The formation of the boronate species has also been shown to form intermediate(s), by the presence of three new peaks by ^{19}F NMR. These peaks also differ in chemical shifts between the pinacol ester **1** and boronic acid **3**. Different species have been suggested, **Fig 6.1.4**, but the true structure of the intermediate(s) is still unknown.

	No base	Intermediate signal 1	Intermediate signal 2	Boronate
Pinacol ester **1**	−109.57 ppm	−115.06 ppm	−122.36 ppm	−121.89 ppm (**25**)
Glycol ester **2**	−111.12 ppm	−114.71 ppm	−121.70 ppm	−121.17 ppm (**23**)
Boronic acid **3**	−112.51 ppm	−114.71 ppm	−121.70 ppm	−121.06 ppm (**17**)

Fig 6.1.2 – Comparison of signals of different species present with the addition of KOH by ^{19}F NMR, relative to 1-fluoronaphthalene as an internal standard, 10:1 THF/water, 300 K

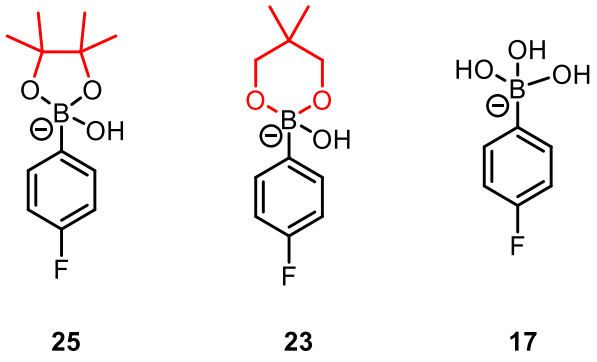

Fig 6.1.3 – Different boronate complexes formed

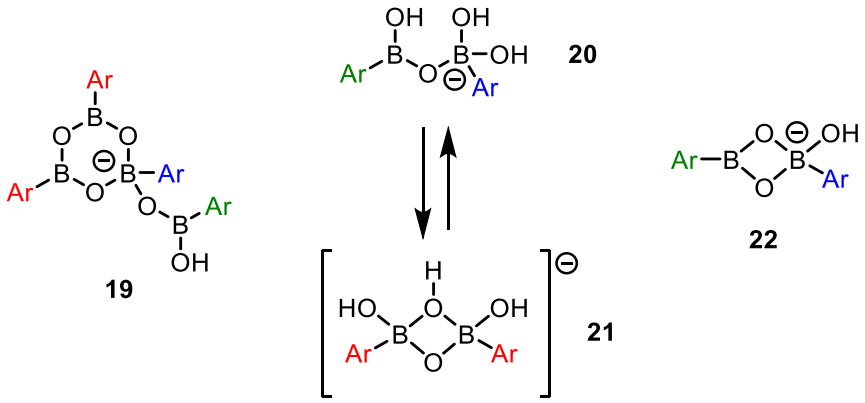

Fig 6.1.4 – Possible species formed from boronic acid **3** + guanidine **11**/KOH reaction

6.2. Future work

The newly developed conditions, **Scheme 6.2.1**, have been shown to work for a small range of *para*-substituted boronic acids. Further studies investigating *ortho*- and *meta*-substituted boronic acids using the newly developed conditions would allow expansion of the substrate scope and test the boundaries of guanidine **11** promoted SM cross-couplings. These boronic acids, particularly *ortho*-substituted moieties, are also known to be more challenging coupling partners,[1–3] so it would be interesting to see if the use of guanidine **11** can offer superior conditions with more efficient coupling. It would also be interesting to investigate boronic acids which are prone to fast protodeboronation. The use of these conditions, which form a boronate species, could potentially offer a solution for the use of unstable boronic acids, if formation of the boronate acts to protect the boronic acid thereby limiting degradation pathways and favouring the desired cross-coupling. Previous research carried out in the group conducted a study of the protodeboronation of a range of boronic acids, lending itself for the corresponding cross-coupling reactions to be investigated, **Fig 6.2.1**.[4]

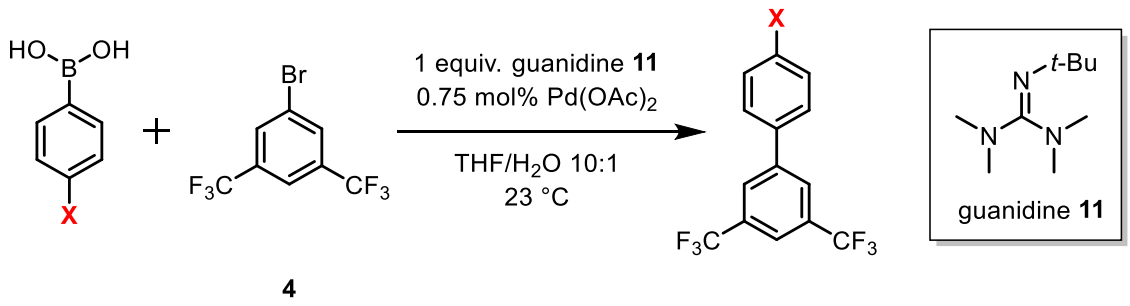

Scheme 6.2.1 – SM cross-coupling of boronic acid (1 equiv.) with 1,3-bis(trifluoromethyl)-5-bromobenzene **4** (1 equiv.)

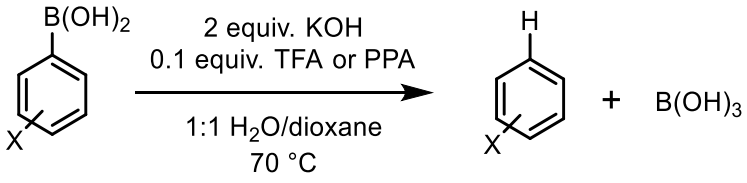

Boronic acid	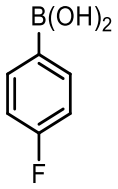	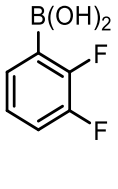	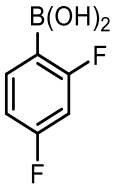		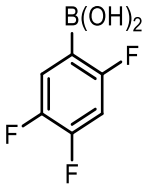
$t_{1/2}$	134 days	95 min	8 hr	3 hr	66 min
Boronic acid	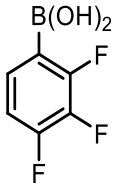	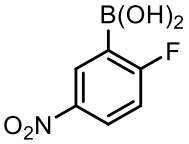	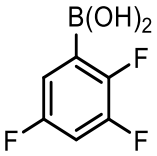	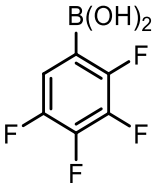	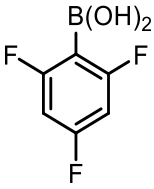
$t_{1/2}$	39 min	15 min	10 min	3 min	1 sec

Fig 6.2.1 – Measured rate constants for the protodeboronation of fluorinated boronic acids

Further studies are needed to find what the active catalytic species is in this newly developed system. Different catalysts have been shown to work well for the coupling, **Scheme 6.2.2**, **Fig 6.2.2**, but a number of issues were found with the reproducibility of the system. This could be due to catalyst activation. Studies using a Pd(0) species would help to determine if catalyst activation is the cause of the issues.

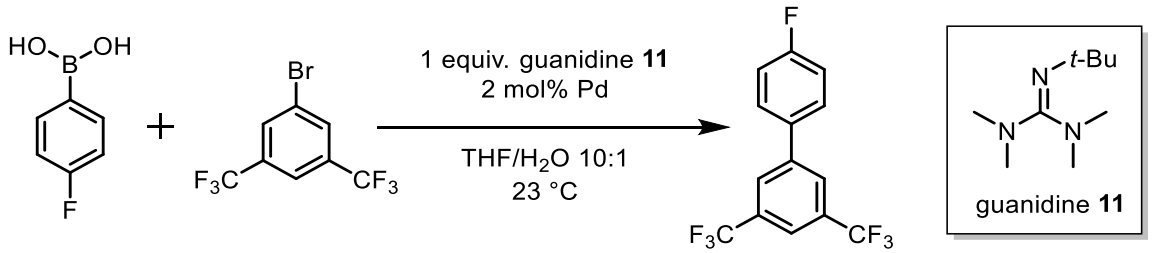

3 **4** **5**

Scheme 6.2.2 – SM cross-coupling of boronic acid **3** (1 equiv.) with 1,3-bis(trifluoromethyl)-5-bromobenzene **4** (1 equiv.) monitored by ^{19}F NMR with 1-fluoronaphthalene as an internal standard

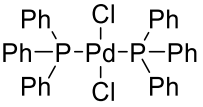	$Pd(OAc)_2$
85%	86%
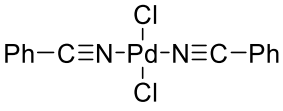	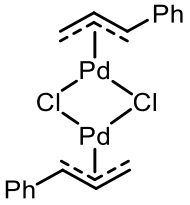
84%	85%

Fig 6.2.2 – Product **5** NMR conversion in the SM cross-coupling of boronic acid **3** (0.04 M) with 1,3-bis(trifluoromethyl)-5-bromobenzene **4** (0.04 M) by ^{19}F NMR with 1-fluoronaphthalene as an internal standard after 24 hours

Furthermore, studies adding a phosphine ligand, triphenylphosphine, to a phosphine-free guanidine reaction were found to result in poor conversion, **Scheme 6.2.3**, **Fig 6.2.3**. Further studies to probe the effect of adding ligands and determination of the catalyst intermediates are needed to explain this result. Finally, as there is literature evidence that guanidine can act as a ligand,[5] future investigations would examine if this is occurring and if it is beneficial.

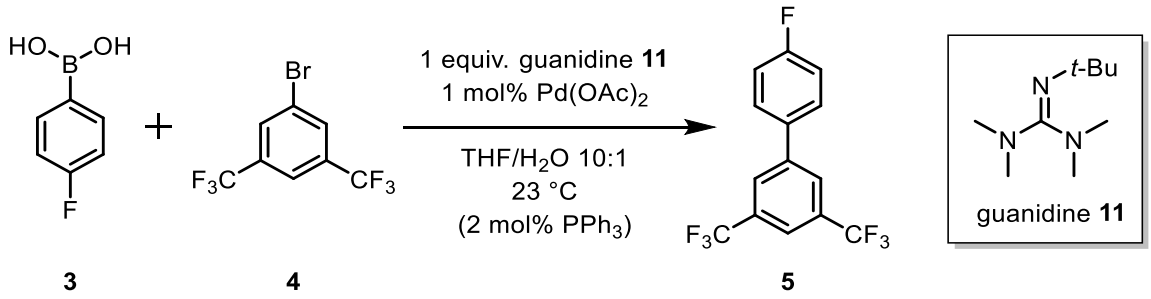

3 **4** **5**

Scheme 6.2.3 – SM cross-coupling of boronic acid **3** (1 equiv.) with 1,3-bis(trifluoromethyl)-5-bromobenzene **4** (1 equiv.) by ^{19}F NMR with 1-fluoronaphthalene as an internal standard

	% Product **5**	% Total side products	% Protodeboronation **9**	% BA homocoupling **6**	% Fluorophenol **8**
Standard conditions	68%	4%	2%	1%	1%
Standard conditions + **2 mol% PPh_3**	13%	17%	0%	0%	17%

Fig 6.2.3 – Comparison of reaction with and without addition of triphenylphosphine. SM cross-coupling of boronic acid **3** (0.04 M) with 1,3-bis(trifluoromethyl)-5-bromobenzene **4** (0.04 M) by ^{19}F NMR with 1-fluoronaphthalene as an internal standard

6.3. References

(1) Barder, T. E.; Walker, S. D.; Martinelli, J. R.; Buchwald, S. L. *J. Am. Chem. Soc.* **2005**, *127* (13), 4685–4696.

(2) Wolfe, J. P.; Singer, R. A.; Yang, B. H.; Buchwald, S. L. *J. Am. Chem. Soc.* **1999**, *121* (41), 9550–9561.

(3) Anderson, J. C.; Namli, H.; Roberts, C. A. *Tetrahedron* **1997**, *53* (44), 15123–15134.

(4) Cox, P. Protodeboronation, 2016. Thesis - University of Edinburgh

(5) Li, S.; Lin, Y.; Cao, J.; Zhang, S. *J. Org. Chem.* **2007**, *72* (11), 4067–4072.

Chapter 7

Experimental

7.1. General experimental details

7.1.1. Techniques

Unless otherwise stated, all reactions were performed under an inert nitrogen atmosphere, using standard Schlenk-line techniques on a vacuum line attached to a double manifold equipped with an oil pump (0.4 torr). Needles and other glassware were purged with an inert atmosphere of nitrogen prior to use. All glassware and NMR tubes used were prewashed sequentially with aqua regia, deionised water, saturated KOH in iPrOH, deionised water, dilute HCl, deionised water (3 times) and acetone (3 times) to remove any contaminants. The removal of solvents *in vacuo* was achieved using a rotary evaporator (with a water bath at temperatures up to 40 °C), or at 0.4 torr on a vacuum line at room temperature.

7.1.2. Reagents and solvents

All commercial reagents were obtained from Sigma-Aldrich, Fluorochem, Fisher Scientific, Acros Organics or Alfa Aesar. All boronic acids were obtained from Sigma-Aldrich, Fisher Scientific or Alfa Aesar and were used without further purification.

Anhydrous organic solvents were obtained from a solvent purification system (MBraun SPS 800) situated in the School of Chemistry, University of Edinburgh. Strauss flasks fitted with J. Young valves were used to collect and freeze-pump-thaw degas anhydrous solvent. Solvents that required degassing were subjected to four cycles of freeze-pump-thawing. Commercial grade solvents were used for extractions, TLC analysis and flash column chromatography. Deionised water was obtained through a membrane filtration system, which was then degassed by sparging with nitrogen.

Deuterated solvents for NMR analysis were purchased from Sigma-Aldrich, Cambridge Isotopes Limited, and Goss Scientific Limited.

7.1.3. Analysis

7.1.3.1. NMR spectroscopy

NMR spectra were recorded at 27 °C unless otherwise stated. ^{1}H, ^{11}B, $^{13}C\{^{1}H\}$ and ^{19}F NMR spectra were recorded on Bruker Ascend 400 MHz Cryoprobe spectrometers. Spectral processing and analysis were carried out using MestreNova versions 9 and 10. ^{1}H and $^{13}C\{^{1}H\}$ spectra were referenced to residual solvent signals. ^{10}B, ^{11}B and ^{19}F spectra were externally

referenced to ($BF_3.OEt_2$). ^{19}F spectra were internally referenced to 1-fluoronaphthalene (−128 ppm). Coupling constants (*J*) were calculated to the nearest 0.1 Hz using MestreNova (versions 9 and 10). The following abbreviations (and their combinations) are used to describe multiplicities: s (singlet), d (doublet), t (triplet), q (quartet), sept (septet), m (multiplet), app (apparent) and br (broad). NMR spectra were recorded using Norrell® 502, Norrell® S400 and Young's tap NMR tubes.

^{11}B spectra contained large background signals. These were removed by applying a backward linear prediction function (MestreNova – Toeplitz method, 0 to 16, 32k basis points and 24 coefficients). ^{11}B baselines were corrected carefully to ensure integrations were not affected (Whittaker smoother function, typically 40-80 Hz filter).

For ^{19}F spectra, phasing, baseline correction and integration of signals was carried out manually to minimise error. The boronic acid, boronic esters, aryl halide and 1-fluoronaphthalene internal standard were studied individually to find the required t_1 relaxation delay and optimal number of scans. For studying the cross-coupling reactions, standard NMR parameters used were 8 scans, 6 second relaxation delay between scans and no background suppression. To study boronate formation, parameters were changed to 128 scans and 20 second relaxation delay, with and without background suppression, as discussed in **Chapter 5**.

7.1.3.2. IR spectroscopy

Infrared (IR) spectra of compounds were recorded over the range 4000-400 cm^{-1} using a Bruker APLHA™ ATR-FTIR spectrometer, peaks are reported in cm^{-1}.

7.1.3.3. Mass spectrometry

High-resolution mass spectrometry was performed by the Mass Spectrometry department within the University of Edinburgh using a Finnigan MAT 900 XLP high resolution mass spectrometer.

7.1.3.4. Elemental analysis

Elemental analysis was performed by Elemental Analysis Service at the London Metropolitan University using a Carlo Erba FLASH 2000 Elemental Analyser.

7.1.3.5. Melting point analysis

Melting points were measured using a SMP10 melting point apparatus in open capillaries and are uncorrected.

7.1.3.6. Crystallography

Single-crystal X-ray diffraction data were measured on a Rigaku Oxford Diffraction SuperNova diffractometer using Mo Kalpha with the crystal temperature maintained at 120 K, within the University of Edinburgh. Structural models were refined by full-matrix least-squares using SHELXL.

7.2. Synthetic procedures

7.2.1. SM cross-coupling procedure[1]

Cross coupling procedures are outlined in **Section 6.3** Reaction Monitoring. The method outlined here was used for reactions carried out to determine isolated yields.

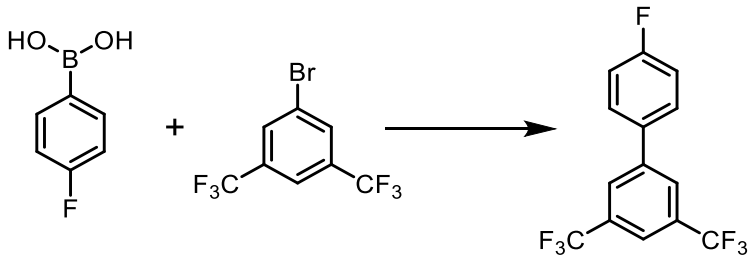

3 **4** **5**

To a 2-neck 100 ml RBF, 4-fluorophenyl boronic acid (154 mg, 1.10 mmol) and palladium acetate (2.5 mg, 1 mol%) were added. The flask was evacuated and backfilled with nitrogen three times. THF (25 mL) was added, followed by 1,3-bis(trifluoromethyl)-5-bromobenzene (190 µL, 1.10 mmol), 2-*tert*-butyl-1,1,3,3-tetramethylguanidine (220 µL, 1.10 mmol) and degassed water (2.5 mL). The reaction was stirred at room temperature overnight under static nitrogen. Deionised water (15 mL) was added, followed by hexane (15 mL). The solution was extracted using hexane, dried over anhydrous $MgSO_4$ and concentrated *in vacuo*. The crude product was filtered through silica (100% hexane) to give the product as a white solid (314 mg, 91%).

^{1}H NMR (400 MHz, $CDCl_3$) δ 7.97 (s, 2H), 7.86 (s, 1H), 7.63 – 7.54 (m, 2H), 7.25 – 7.16 (m, 2H). $^{13}C\{^{1}H\}$ NMR (101 MHz, $CDCl_3$) δ 163.3 (d, J = 249.4 Hz), 142.3, 134.4, 132.2 (q, J = 33.3 Hz), 129.0 (d, J = 8.4 Hz), 127.1 (d, J = 3.8 Hz), 123.3 (d, J = 272.8 Hz), 121.3 – 120.6 (m), 116.3 (d, J = 21.8 Hz). ^{19}F NMR (377 MHz, $CDCl_3$) δ −62.89 (6F), −112.81 (1F). Melting point = 50 – 52 °C. Lit. melting point = 51 – 52 °C.[1] IR (cm^{-1}) = 1276 (C-F), 1516 (C=C), 3100 (C-H aromatic). Data are in accordance with that previously reported.[1]

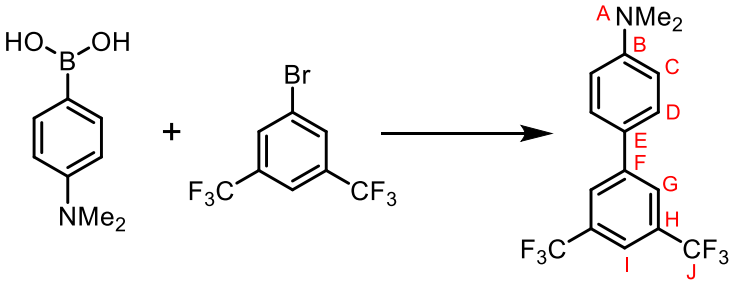

To a 2-neck 100 mL RBF, 4-(dimethylamino)phenylboronic acid (182 mg, 1.10 mmol) and palladium acetate (2.5 mg, 1 mol%) were added. The flask was evacuated and backfilled with nitrogen three times. THF (25 mL) was added, followed by 1,3-bis(trifluoromethyl)-5-bromobenzene (190 µL, 1.10 mmol), 2-*tert*-butyl-1,1,3,3-tetramethylguanidine (220 µL, 1.10 mmol) and degassed water (2.5 mL). The reaction was stirred at room temperature overnight under static nitrogen. Deionised (15 mL) water was added, followed by hexane (15 mL). The solution was extracted using hexane, dried over anhydrous $MgSO_4$ and concentrated *in vacuo*. Crude product was filtered through silica (100% hexane) to give the product as a white solid (282 mg, 82%).

^{1}H NMR (400 MHz, $CDCl_3$) δ 8.00 – 7.87 (G, m, 2H), 7.76 – 7.69 (I, m, 1H), 7.52 (D, d, *J* = 8.9 Hz, 2H), 6.81 (C, d, *J* = 8.9 Hz, 2H), 3.03 (A, s, 6H). ^{13}C{^{1}H} NMR (101 MHz, $CDCl_3$) δ 150.9 (B), 143.2 (F), 132.9 – 129.8 (m, H), 127.8 (E), 125.9 (D), 125.6 (G), 123.6 (d, *J* = 272.6 Hz, J), 119.5 – 118.8 (m, I), 112.6 (C), 40.3 (A). ^{19}F NMR (377 MHz, $CDCl_3$) δ −62.87. Melting point = 55 – 56 °C. IR (cm^{-1}) = 1116 (C-N), 1270 (C-F), 1529 (C=C), 2902 (C-H aromatic)

HRMS (EI^+) $C_{16}H_{13}F_6N^+$ $[M]^+$ found 333.09430, requires 333.09467 (+0.37 ppm)

7.2.2. Synthesis of boronic esters

7.2.2.1. Preparation of 4-fluorophenylboronic acid pinacol ester[2]

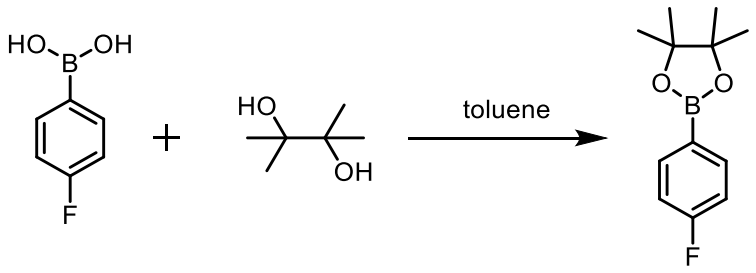

3 **1**

To a 250 mL RBF, 4-fluorophenyl-boronic acid (1.00 g, 7.15 mmol) and pinacol (0.97 g, 8.21 mol) were added simultaneously. Water (100 µL) and then toluene (25 mL) were added. The mixture was refluxed with a Dean-Stark trap for 1 hr. The solution was passed through a silica plug and washed with 50 mL of hexane/ethyl acetate (3:1). The filtrate was evaporated to give a pale tan liquid as the product (1.53 g, 96%).

^{1}H NMR (400 MHz, $CDCl_3$) δ 7.82 (dd, *J* = 8.5, 6.3 Hz, 2H), 7.14 – 6.93 (m, 2H), 1.35 (s, 12H). $^{13}C\{^{1}H\}$ NMR (101 MHz, CDCl3) δ 165.1 (d, J = 250.3 Hz), 137.0 (d, J = 8.3 Hz), 114.8 (d, J = 20.2 Hz), 83.9, 24.9. ^{19}F NMR (377 MHz, $CDCl_3$) δ −108.40. ^{11}B NMR (128 MHz, $CDCl_3$) δ 30.53. IR (cm^{-1}) = 1146 (C-F), 1356 (C-O), 1602 (C=C), 2979 (C-H aromatic). Data are in accordance with that previously reported.[2]

7.2.2.2. Preparation of 4-fluorophenylboronic acid glycol ester[3]

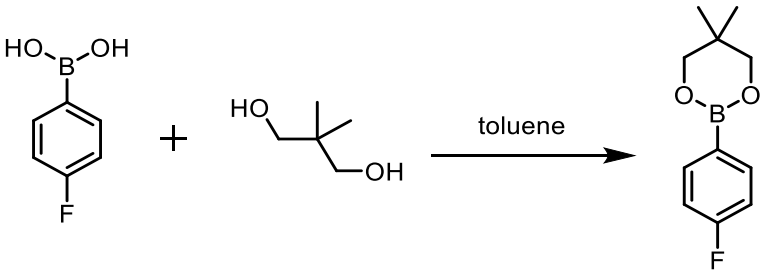

3 **2**

To a 25 mL RBF, 4-fluorophenyl-boronic acid (183 mg, 1.30 mmol) and neopentyl glycol (156 mg, 1.50 mmol) were added simultaneously. Water (20 µL) and then toluene (5 mL) were added. The mixture was refluxed with a Dean-Stark trap for 1 hr. Evaporation of the solvent to dryness affording a colourless solid (250 mg, 92%).

^{1}H NMR (400 MHz, $CDCl_3$) δ 7.78 (dd, *J* = 8.7, 6.4 Hz, 2H), 7.03 (dd, *J* = 9.3, 8.7 Hz, 2H), 3.76 (s, 4H), 1.02 (s, 6H). ^{13}C{^{1}H} NMR (101 MHz, $CDCl_3$) δ 164.8 (d, J = 249.3 Hz), 136.0 (d, J = 8.1 Hz), 114.6 (d, J = 20.2 Hz), 72.3, 31.9, 30.9, 21.9. ^{19}F NMR (377 MHz, $CDCl_3$) δ −109.87. ^{11}B NMR (128 MHz, $CDCl_3$) δ 26.79. Melting point = 67 – 69 °C. Lit. melting point = 64 – 67 °C.[3] IR (cm^{-1}) = 1136 (C-F), 1307 (C-O), 1596 (C=C), 2966 (C-H aromatic). Data are in accordance with that previously reported.[3]

7.2.3. Synthesis of 2-butyl-1,1,3,3-tetramethylguanidine[4]

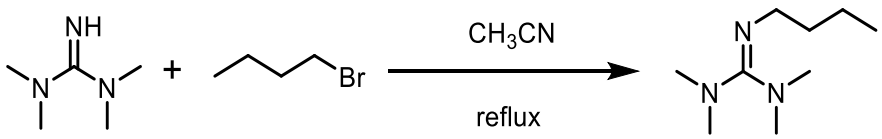

13 **14**

To a two-neck flask, 1,1,3,3-tetramethylguanidine (TMG, 2.32 g, 20.1 mmol), *n*-BuBr (3.29 g, 24.0 mmol) and CH_3CN (40 mL) were added under nitrogen. The mixture was heated to reflux for 17 hr with vigorous stirring. Solvent and the superfluous *n*-BuBr were removed under reduced pressure and a yellow oil was obtained. Aqueous NaOH (6 mL) was then added. The organic layer was extracted with CH_2Cl_2 and dried with anhydrous Na_2SO_4. Solvent was removed by evaporation under reduced pressure, followed by purification by distillation under reduced pressure (5.6 Torr, 65 °C) to give the product as a colourless oil (1.84 g, 53%).

^{1}H NMR (400 MHz, $CDCl_3$) δ 2.96 (t, *J* = 6.9 Hz, 2H), 2.60 (s, 6H), 2.50 (s, 6H), 1.42 – 1.30 (m, 2H), 1.28 – 1.11 (m, 2H), 0.75 (t, *J* = 7.3 Hz, 3H). ^{13}C{^{1}H} NMR (101 MHz, $CDCl_3$) δ 159.8, 49.1, 39.1, 34.9, 20.4, 13.9 IR (cm^{-1}) = 1360 (C-N), 1618 (C=N), 2868 (C-H alkane). Data are in accordance with that previously reported.[4]

7.2.4. Synthesis of [(cinnamyl)PdCl]$_2$[5]

H_2O (193 mL) was added to a three-neck RBF and degassed by nitrogen sparging for 30 minutes. $PdCl_2$ (1.37 g, 7.73 mmol) and KCl (1.15 g, 15.4 mmol) were added and the solution was stirred at room temperature for 1 hr. Cinnamyl chloride (3.30 mL, 23.7 mmol) was then added and the resulting reaction mixture stirred at room temperature overnight. The reaction was extracted with chloroform, and the aqueous layer washed with chloroform three times. The organic layers were combined, dried over $MgSO_4$, filtered and concentred *in vacuo*. The

crude product was recrystallised from chloroform and methyl *tert*-butyl ether, and the resulting solid was isolated by filtration and dried *in vacuo*, to give a yellow solid (1.11 mg, 56%).

Recrystallisation by slow diffusion (dissolved in chloroform, outer solvent methyl *tert*-butyl ether) was carried out to obtain pure product for use in catalysis.

^{1}H NMR (400 MHz, $CDCl_3$) δ 7.50 (d, *J* = 7.0 Hz, 4H), 7.38 – 7.31 (m, 2H), 7.29-7.25 (m, 4H), 5.80 (ddd, *J* = 11.9, 11.3, 6.8 Hz, 2H), 4.62 (d, *J* = 11.3 Hz, 2H), 3.97 (d, *J* = 6.8, 2H), 3.04 (d, *J* = 11.9 Hz, 2H). ^{13}C{^{1}H} NMR (101 MHz, $CDCl_3$) δ 137.0, 129.1, 128.5, 128.0, 105.9, 81.8, 59.4. Melting point = 204 – 205 °C. Lit. melting point = 218 – 220 °C. IR (cm^{-1}) = 1426 (C=C), 3055 (C-H aromatic). Data are in accordance with that previously reported.[6,7]

7.3. Crystals

7.3.1. Hydrolysed guanidine

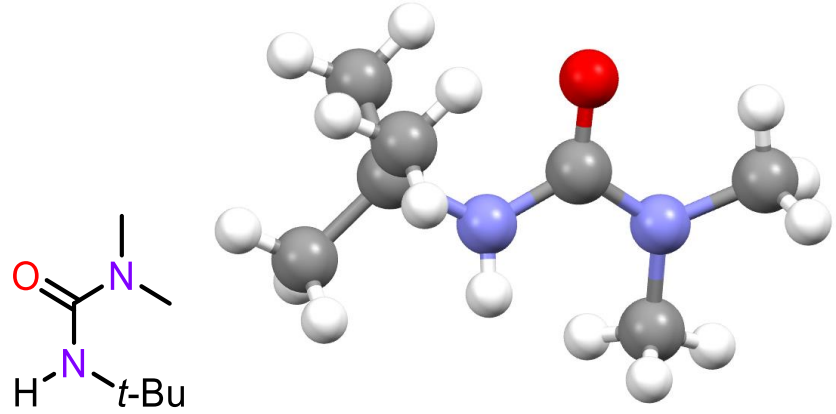

Colour	Atom
Red	O
Purple	N
Grey	C
White	H

Experimental. Single colourless block-shaped crystals of (**GL15003**) were recrystallised from a mixture of THF and water by slow evaporation. A suitable crystal (0.35×0.32×0.18) was selected and mounted on a MITIGEN holder in Paratone oil on a Rigaku Oxford Diffraction SuperNova diffractometer. The crystal was kept at *T* = 120.0 K during data collection. Using **Olex2** (Dolomanov et al., 2009), the structure was solved with the **ShelXT** (Sheldrick, 2015) structure solution program, using the Direct Methods solution method. The model was refined with version of **ShelXL** (Sheldrick, 2008) using Least Squares minimisation.

Crystal Data. $C_7H_{16}N_2O$, M_r = 144.22, orthorhombic, Pbca (No. 61), a = 9.9811(3) Å, b = 11.6989(3) Å, c = 15.1769(5) Å, $\alpha = \beta = \gamma = 90^{\circ}$, *V* = 1772.18(9) Å^3, *T* = 120.0 K, *Z* = 8, *Z'* =

1, μ(MoK$_\alpha$) = 0.073, 24121 reflections measured, 1614 unique (R_{int} = 0.0497) which were used in all calculations. The final wR_2 was 0.1141 (all data) and R_1 was 0.0451 (I > 2(I))

7.3.2. Boric acid/guanidine

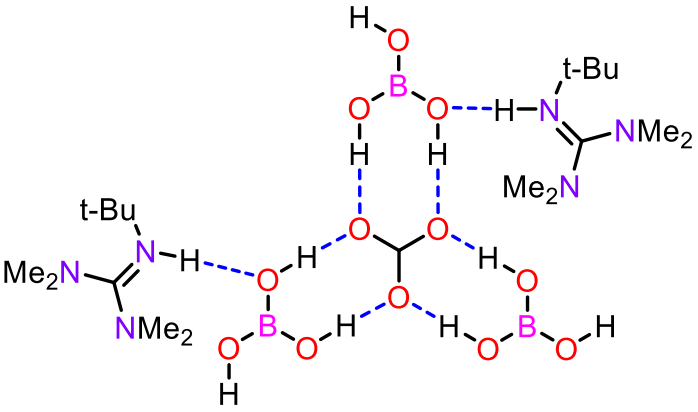

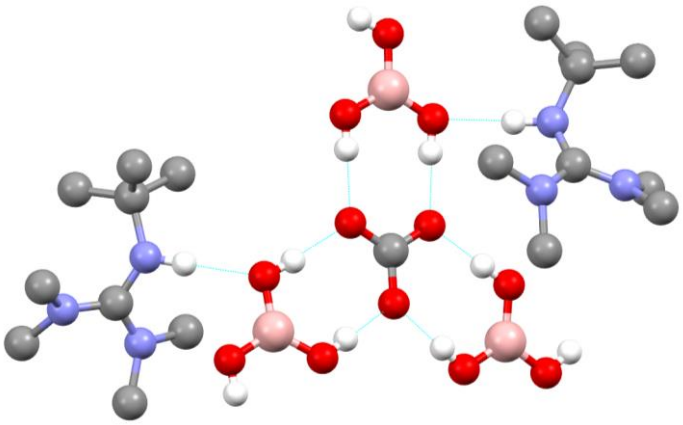

Colour	Atom
Red	O
Purple	N
Grey	C
White	H
Pink	B

Experimental. Single colourless block-shaped crystals of (**GL16002**) were recrystallised from a mixture of THF and water by slow evaporation. A suitable crystal (0.56×0.39×0.20) mm^3 was selected and mounted on a MITIGEN holder in Paratone oil on a Rigaku Oxford Diffraction SuperNova diffractometer. The crystal was kept at T = 120.0 K during data collection. Using **Olex2** (Dolomanov et al., 2009), the structure was solved with the **ShelXT** (Sheldrick, 2015) structure solution program, using the Direct Methods solution method. The model was refined with version 2014/7 of **ShelXL** (Sheldrick, 2015) using Least Squares minimisation.

Crystal Data. $C_{19}H_{55.515}B_3N_6O_{13.2575}$, M_r = 612.76, triclinic, P-1 (No. 2), a = 13.9255(4) Å, b = 16.4539(4) Å, c = 17.2543(5) Å, α = 63.314(3)°, β = 78.768(2)°, γ = 74.542(2)°, V = 3391.60(18) Å^3, T = 120.0 K, Z = 4, Z' = 2, μ(MoK$_\alpha$) = 0.097, 68679 reflections measured,

15850 unique (R_{int} = 0.0404) which were used in all calculations. The final wR_2 was 0.1926 (all data) and R_1 was 0.0674 (I > 2(I)).

7.4. Cross-Coupling Reaction monitoring

To fully investigate the Suzuki-Miyaura reaction, different general procedures were followed, to study and optimise parameters of the reaction.

Reactions were monitored by either taking NMR aliquots from a reaction in a Schleck flask being stirred at various intervals, or by being run without dilution, with a D_2O capillary in an NMR tube, and monitored *in situ*, or left until completion. If left until completion, reaction mixed was diluted with water, extracted with diethyl ether, dried with anhydrous $MgSO_4$, filtered and concentrated *in vacuo*. The crude material was then purified by column chromatography in 100% hexane.

7.4.1. General procedure A

Small Schlenk flask was charged with boronic acid or boronic ester, palladium catalyst, and potassium carbonate, then evacuated and backfilled with nitrogen three times. Aryl halide was then added, following by THF then water in a 10:1 ratio. Reactions were carried out in an oil bath at 55 °C, stirred at 750 rpm.

7.4.2. General procedure B

To allow for a t_0 sample to be taken, to find the true concentration of starting materials in the reaction, the boronic acid or ester and aryl halide were pre-dissolved in THF. For the reaction, a small Schlenk flask was charged with palladium catalyst and potassium carbonate, then evacuated and backfilled with nitrogen three times. The THF solution containing the boronic acid and aryl halide was then added simultaneously with water in a 10:1 ratio. Reactions were stirred (750 rpm unless otherwise stated) and monitored by taking NMR aliquots at various intervals and run without further dilution with a D_2O capillary.

7.4.3. General procedure C

Same as procedure B, except the boronic acid, aryl halide stock solution was made in 10:1 THF:water, removing the need to add water separately into the reaction.

7.4.4. General procedure D

Same as procedure C, except using 2-*tert*-butyl-1,1,3,3-tetramethylguanidine instead of potassium carbonate. Small Schlenk flask charged with palladium catalyst, then evacuated and backfilled with nitrogen three times. Guanidine was added followed by the boronic acid/aryl halide stock solution. The use of the guanidine required the temperature of the reaction to be lowered to room temperature, ~22 °C. Guanidine reactions also required the use of an acetic acid quench (50 µl) to samples to be able to monitor the progression of the reaction. The use of the quench is discussed in **Chapter 4**.

7.4.5. General procedure E

Same as procedure D, except order of addition. Small Schlenk flask charged with palladium catalyst, evacuated and backfilled with nitrogen three times. Boronic acid/aryl halide stock solution added, stirred for approximately 5 minutes then guanidine added neat last.

7.4.6. General procedure F

To eliminate errors in weighing small amounts of catalyst, a catalyst stock solution was made in 10:1 THF:water. A stock solution of boronic acid or ester and aryl halide was also made in 10:1 THF:water. A small Schlenk flask was evacuated and backfilled with nitrogen three times. If the base was solid (potassium carbonate) it was added prior to purging with nitrogen. If the base was liquid (guanidine) it was added after purging. Base addition was followed by addition of the boronic acid/aryl halide stock solution, stirred for approximately 5 minutes then catalyst stock solution was added last.

7.4.7. General procedure G

Same as procedure F, except different order of addition. Boronic acid/aryl halide solution added first, followed by catalyst stock solution, stirred for approximately 5 minutes then guanidine added neat last.

7.4.8. General procedure H

Same as procedure F, except order of addition. Catalyst solution added first, followed by guanidine, stirred for approximately 5 minutes then boronic acid/aryl halide solution added last.

7.4.9. General procedure I

Same as procedure F, except order of addition. Catalyst solution added first, followed by boronic acid/aryl halide solution, stirred for approximately 5 minutes then guanidine added last.

7.4.10. General procedure J

Guanidine was added to the boronic acid/aryl halide stock solution made in 10:1 THF:water. Catalyst stock solution also made in 10:1 THF:water. For the reaction, small Schlenk flask was evacuated and backfilled with nitrogen three times. Catalyst solution was added followed by stock solution containing boronic acid, aryl halide and guanidine.

7.4.11. General procedure K

Same as procedure J except order of addition. Stock solution containing boronic acid, aryl halide and guanidine added first, followed by catalyst solution.

7.4.12. General procedure L

Same as procedure J but without catalyst stock solution. Small Schlenk flask charged with palladium, evacuated and backfilled with nitrogen three times. Small volume of 10:1 THF/water added and mixed, followed by stock solution containing boronic acid, aryl halide and guanidine.

7.4.13. General procedure M

Same as procedure L but without adding 10:1 THF/water to catalyst prior to stock solution.

7.4.14. General procedure N

Catalyst stock solution made in 10:1 THF/water. Small Schlenk flask charged with boronic acid or ester, then evacuated and backfilled with nitrogen three times. 10:1 THF/water added, then ArBr neat, then catalyst solution. Guanidine added neat last.

7.4.15. General procedure O

Catalyst stock solution made in THF. Stock solution of aryl halide and guanidine made in neat THF. Small Schleck flask charged with boronic acid or ester, then evacuated and backfilled with nitrogen three times. Aryl halide/guanidine stock solution added, followed by water to create a 10:1 THF/water ratio overall. Catalyst solution added last.

7.4.16. General procedure P

Guanidine was added to the catalyst stock solution made in 10:1 THF/water. Boronic acid/aryl halide stock solution also made in 10:1 THF/water. For the reaction, small Schlenk flask was evacuated and backfilled with nitrogen three times. Boronic acid/aryl halide stock solution was added followed by catalyst guanidine stock solution.

7.4.17. General procedure Q

Same as procedure K except stock solution made in THF – no water. THF solution containing boronic acid, aryl halide and guanidine added, followed by THF solution of catalyst. Water added last to create a 10:1 ratio THF to water.

7.4.18. General procedure R

Same as procedure Q except order of addition. THF solution containing boronic acid, aryl halide and guanidine added, followed by water added to create a 10:1 ratio THF to water overall. THF catalyst solution added last.

7.4.19. General procedure S

Same as procedure R except adding THF prior to catalyst solution, to create different concentrations of catalyst in the reaction.

7.4.20. General procedure T

Stock solution of boronic acid and aryl halide made in THF. Guanidine added neat. Catalyst stock solution made in THF. Boronic acid/aryl halide stock solution added first, following by water, then guanidine, then catalyst stock solution last.

7.4.21. General procedure U

Stock solution of boronic acid and aryl halide made in THF. A catalyst stock solution was also made in THF. A small vial was evacuated and backfilled with nitrogen three times. If the base was solid it was added prior to purging with nitrogen. If the base was liquid, boronic acid/aryl halide stock solution was added after purging, followed by base. Water was then added, then catalyst solution was added last.

7.5. Internal standard studies

To be able to monitor the SM cross-coupling reaction in terms of concentration, an internal standard was required. D_2O capillaries were used to be able to lock the NMR without diluting

and changing the concentration of the reaction aliquot taken. The capillaries were then made to include an internal standard, sodium tetrafluoroborate, chosen as it gives a ^{19}F NMR peak at −150 ppm, distinct from all reaction peaks. However, sodium tetrafluoroborate was found to degrade over time, giving two new peaks by ^{19}F NMR at −131 ppm and −144 ppm. This made its integration difficult and the true concentration unreliable.

When monitoring the coupling reaction, the total concentration throughout the reaction should remain constant. But when using the sodium tetrafluoroborate capillaries it was found that the total concentration varied throughout the reaction, suggesting the concentration of the capillaries had changed by an unknown amount, **Graph 9**. Previous studies within the group had shown 1-fluoronaphthalene to be a suitable alternative internal standard, as it gave a single peak by ^{19}F NMR distinct for all others in the reaction mixture. By using a pre-mixed THF solution of 1-fluoronaphthalene (0.01 M) as the solvent for couplings, the total concentration throughout the reaction remained constant, **Graph 9**.

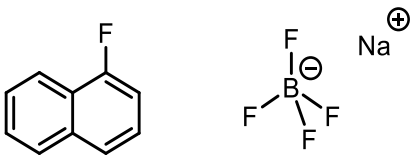

Fig X – 1-fluoronaphthalene and sodium tetrafluoroborate

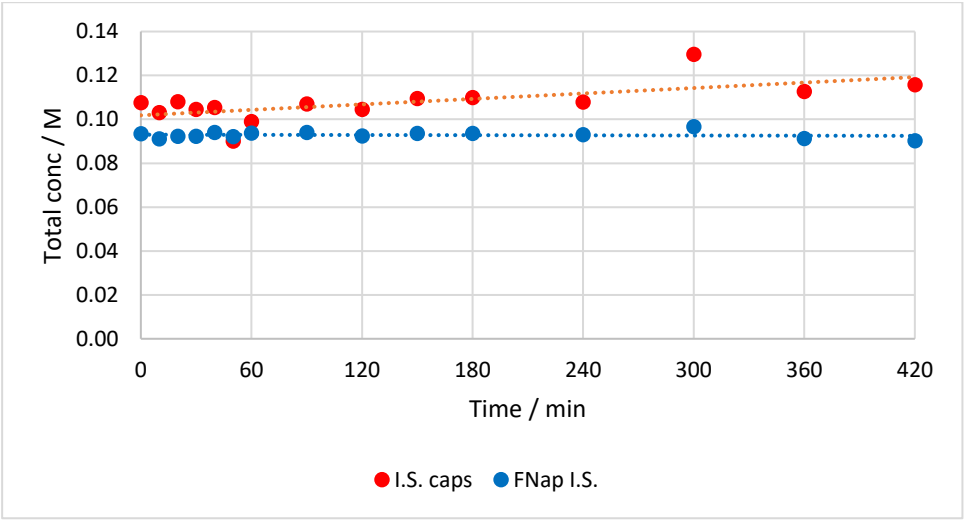

Graph 9 – SM cross-coupling of boronic acid (1 equiv.) with 1,3-bis(trifluoromethyl)-5-bromobenzene (1 equiv.) monitored by ^{19}F NMR. Internal standard studies: sodium tetrafluoroborate solution in capillaries vs 1-fluoronaphthalene in reaction solution

7.6. References

(1) Butters, M.; Harvey, J. N.; Jover, J.; Lennox, A. J. J.; Lloyd-Jones, G. C.; Murray, P. M. Aryl Trifluoroborates in Suzuki-Miyaura Coupling: The Roles of Endogenous Aryl Boronic Acid and Fluoride. *Angew. Chem Int. Ed. Int. Ed.* **2010**, *49* (30), 5156–5160.

(2) Lennox, A. J. J.; Lloyd-Jones, G. C. Preparation of Organotrifluoroborate Salts: Precipitation-Driven Equilibrium under Non-Etching Conditions. *Angew. Chem Int. Ed.* **2012**, *51* (37), 9385–9388.

(3) Wilson, D. A.; Wilson, C. J.; Moldoveanu, C.; Resmerita, A.-M.; Corcoran, P.; Hoang, L. M.; Rosen, B. M.; Percec, V. Neopentylglycolborylation of Aryl Mesylates and Tosylates Catalyzed by Ni-Based Mixed-Ligand Systems Activated with Zn. *J. Am. Chem. Soc.* **2010**, *132* (6), 1800–1801.

(4) Gao, J.; He, L.-N.; Miao, C.-X.; Chanfreau, S. Chemical Fixation of CO2: Efficient Synthesis of Quinazoline-2,4(1H, 3H)-Diones Catalyzed by Guanidines under Solvent-Free Conditions. *Tetrahedron* **2010**, *66* (23), 4063–4067.

(5) Colacot, T. J.; Johansson Seechurn, C. C. C.; Parisel, S. L. WO 2011/16145 A1, 2011.

(6) Zhang, H.; Hu, R.-B.; Liu, N.; Li, S.-X.; Yang, S.-D. Dearomatization of Indoles via Palladium-Catalyzed Allylic C–H Activation. *Org. Lett.* **2016**, *18* (1), 28–31.

(7) Evstigneeva, E. M.; Flid, V. R. Correlations between 13C NMR Chemical Shifts of [(1-R-η3-C3H4)PdCl]2 and Na[(1-R-η3-C3H4)PdCl2] and Substituent Constants. *Russ. Chem. Bull.* **2008**, *57* (6), 1194–1197.

Chapter 8

Appendix

8.3.1. Impact of changing stirring rate/vessel size in terms of side product formation

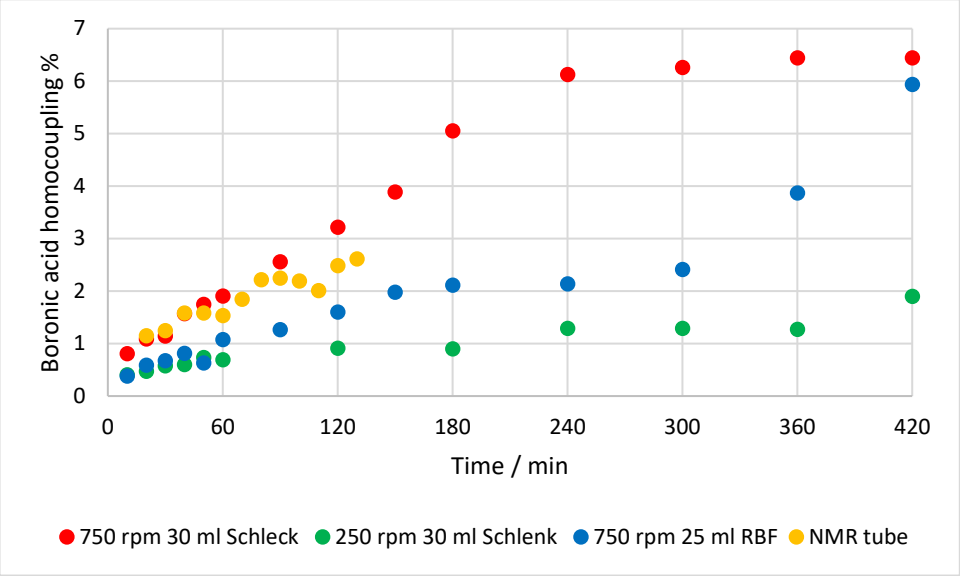

Graph 8.3.1.1 – Impact of changing stirring rate/vessel size in terms of boronic acid homocoupling from the SM reaction of 4-fluorophenylboronic acid (0.04 M) with 1,3-bis(trifluoromethyl)-5-bromobenzene (0.04 M) sampled over 7 hours and analysed by ^{19}F NMR with 1-fluoronaphthalene as an internal standard.

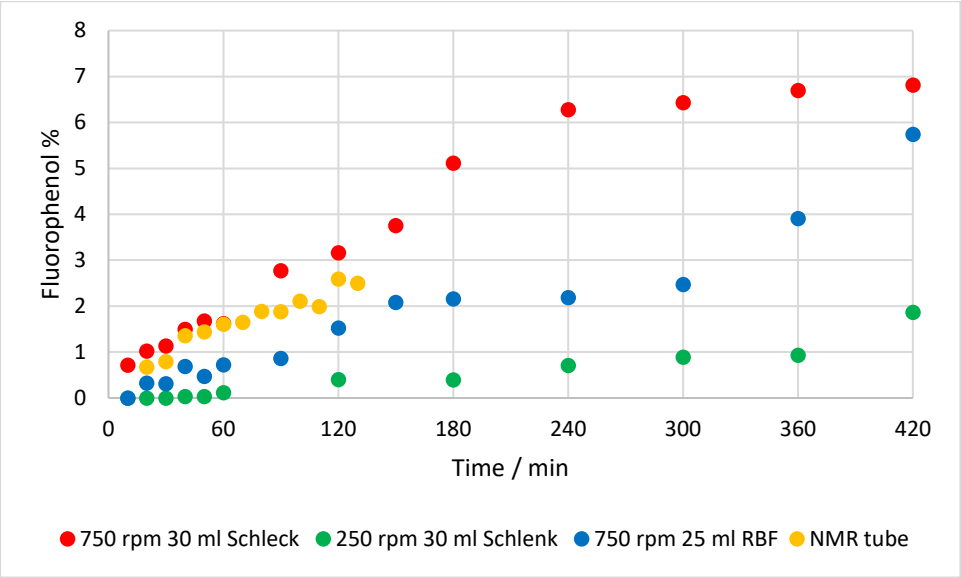

Graph 8.3.1.2 – Impact of changing stirring rate/vessel size in terms of fluorophenol formation from the SM reaction of 4-fluorophenylboronic acid (0.04 M) with 1,3-bis(trifluoromethyl)-5-bromobenzene (0.04 M) sampled over 7 hours and analysed by ^{19}F NMR with 1-fluoronaphthalene as an internal standard

8.3.2. Boronic acid/ester side product formation using an inorganic base

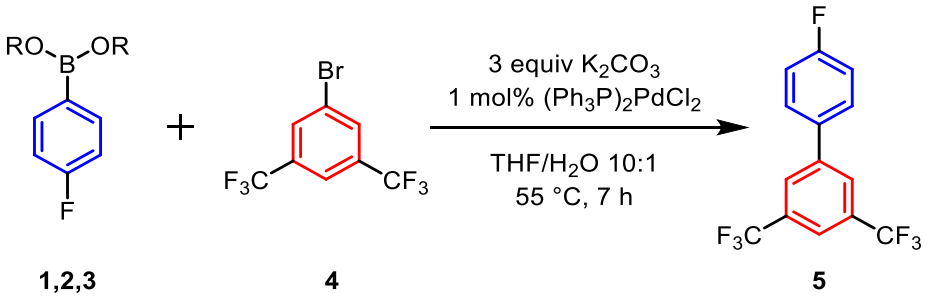

1,2,3 **4** **5**

Scheme 8.3.2.1 – SM reaction of boronic acid **3**/ester **1/2** (1 equiv.) with 1,3-bis(trifluoromethyl)-5-bromobenzene **4** (1 equiv.) monitored over 7 hours by ^{19}F NMR with 1-fluoronaphthalene as an internal standard.

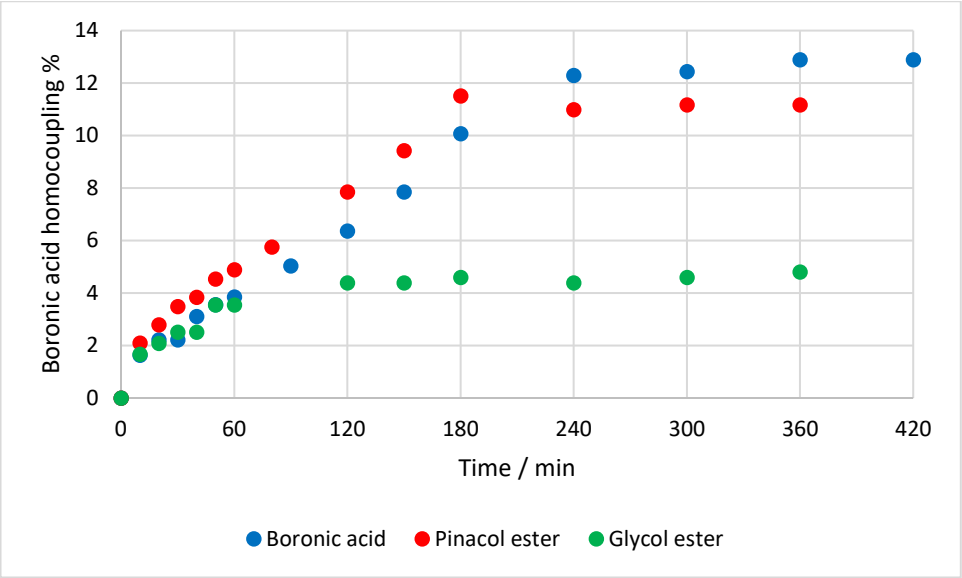

Graph 8.3.2.1 – Boronic acid homocoupling **6** formation SM reaction of boronic acid **3**/ester **1/2** (1 equiv.) with 1,3-bis(trifluoromethyl)-5-bromobenzene **4** (1 equiv.) monitored over 7 hours by ^{19}F NMR with 1-fluoronaphthalene as an internal standard.

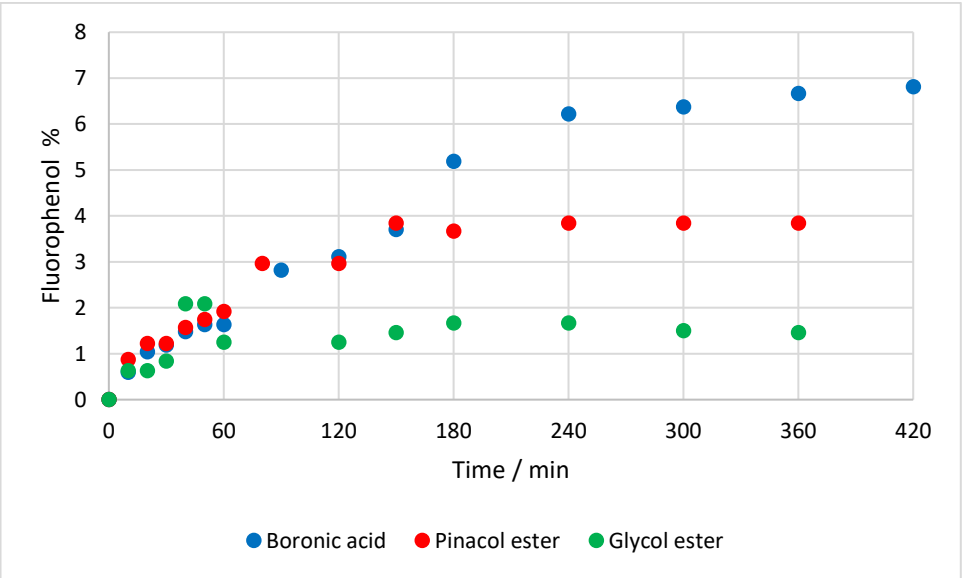

Graph 8.3.2.2 – Fluorophenol **8** formation SM reaction of boronic acid **3**/ester **1/2** (1 equiv.) with 1,3-bis(trifluoromethyl)-5-bromobenzene **4** (1 equiv.) monitored over 7 hours by ^{19}F NMR with 1-fluoronaphthalene as an internal standard.

8.4.1. Testing for a homogeneous system using 0.5 equiv. guanidine

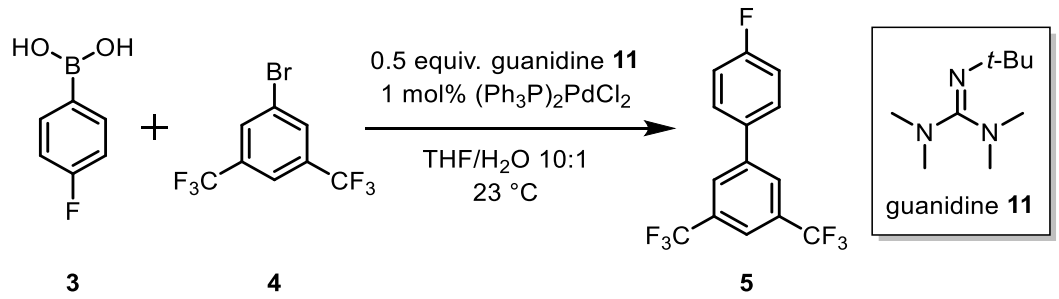

3 **4** **5**

Scheme 4.3.5 – SM cross-coupling of boronic acid **3** (1 equiv.) with 1,3-bis(trifluoromethyl)-5-bromobenzene **4** (1 equiv.) monitored by ^{19}F NMR with 1-fluoronaphthalene as an internal standard.

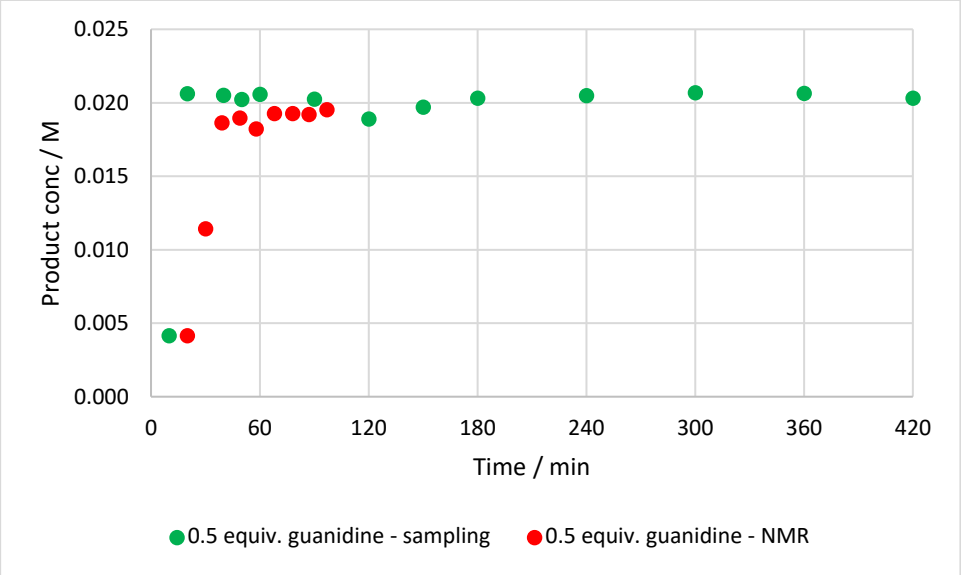

Graph 8.4.1.1 – Product **5** formation in the SM cross-coupling of boronic acid **3** (0.04 M) with 1,3-bis(trifluoromethyl)-5-bromobenzene **4** (0.04 M) monitored by ^{19}F NMR with 1-fluoronaphthalene as an internal standard. Using 0.5 equiv. guanidine **11**.

8.4.2. Varying equiv. glycol

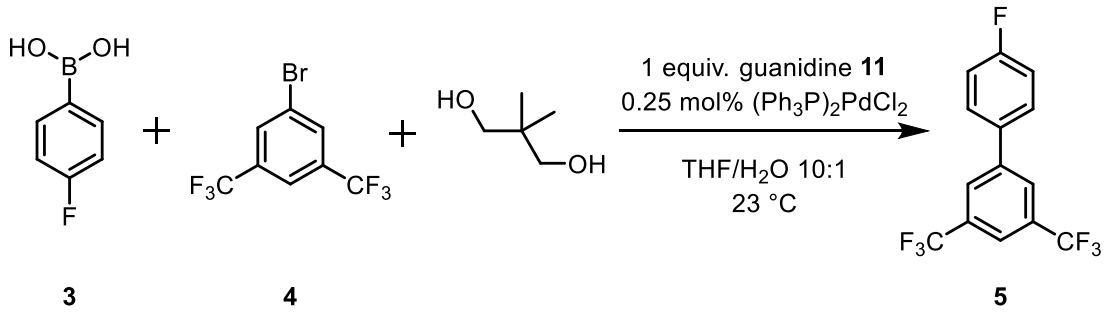

3 **4** **5**

Scheme 4.4.4 – SM cross-coupling of boronic acid **3**/ester **1**/**2** (1 equiv.) with 1,3-bis(trifluoromethyl)-5-bromobenzene **4** (1 equiv.) with addition of glycol, monitored by ^{19}F NMR with 1-fluoronaphthalene as an internal standard

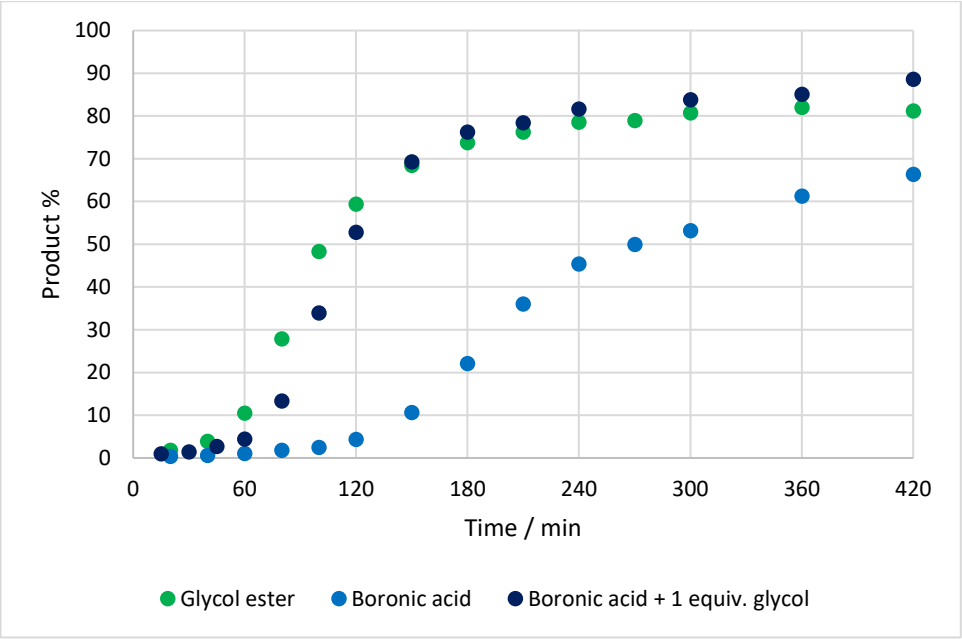

Graph 8.4.2.1 – Product **5** formation for the SM cross-coupling of boronic acid **3**/ester **1**/**2** (0.04 M) with 1,3-bis(trifluoromethyl)-5-bromobenzene **4** (0.04 M) with addition of glycol, monitored by ^{19}F NMR with 1-fluoronaphthalene as an internal standard

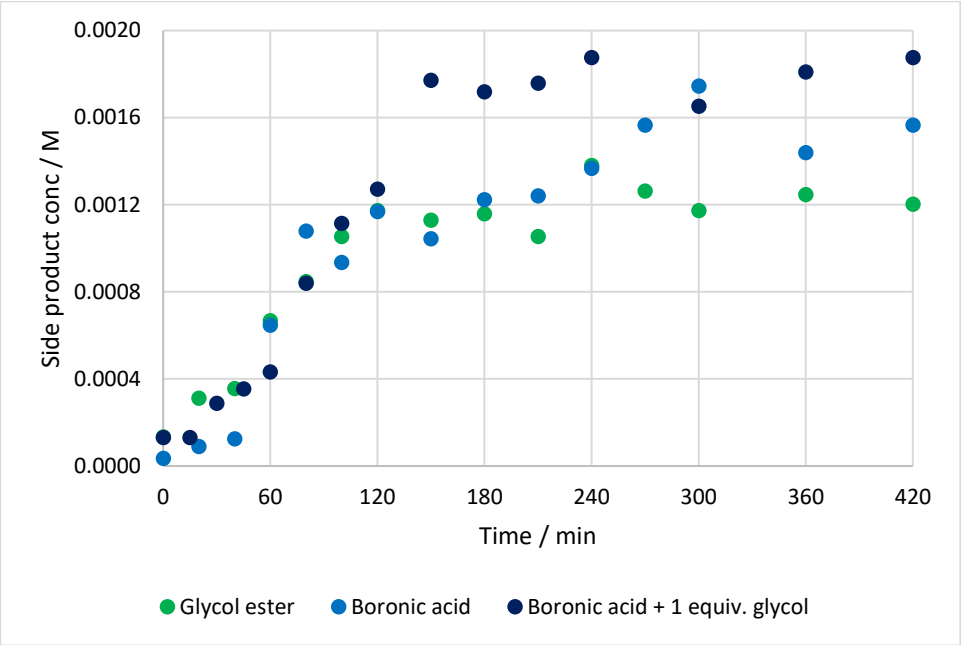

Graph 8.4.2.2 – Side product formation for the SM cross-coupling of boronic acid **3**/ester **1**/**2** (0.04 M) with 1,3-bis(trifluoromethyl)-5-bromobenzene **4** (0.04 M) with addition of glycol, monitored by ^{19}F NMR with 1-fluoronaphthalene as an internal standard

8.4.3. Varying equiv. 1,1,1-tris(hydroxymethyl)ethane

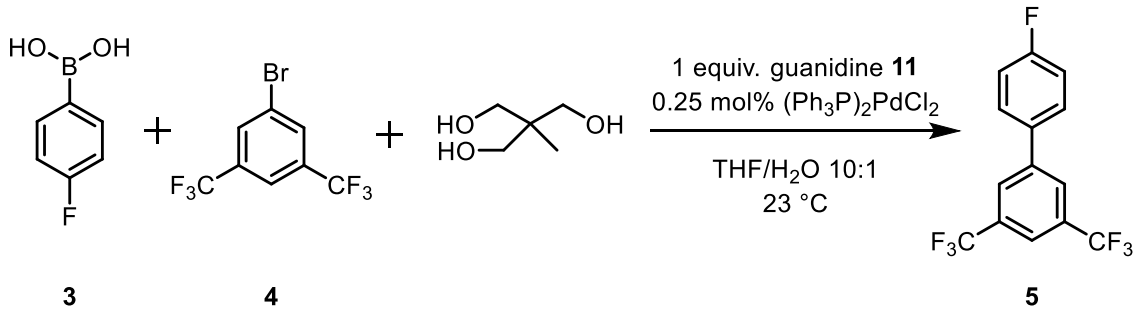

3 **4** **5**

Scheme 4.4.7 – SM cross-coupling of boronic acid **3** (1 equiv.) with 1,3-bis(trifluoromethyl)-5-bromobenzene **4** (1 equiv.) with addition of 1,1,1-tris(hydroxymethyl)ethane, monitored by ^{19}F NMR with 1-fluoronaphthalene as an internal standard

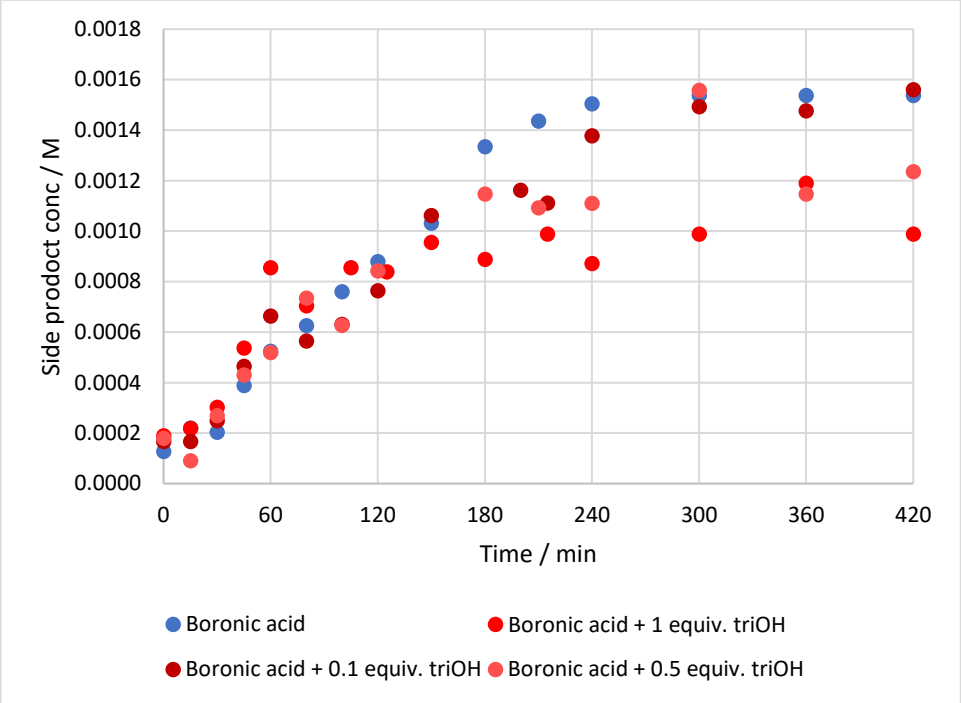

Graph 8.4.3.1 – Side product formation in the SM cross-coupling of boronic acid **3** (0.04 M) with 1,3-bis(trifluoromethyl)-5-bromobenzene **4** (0.04 M) with addition of 1,1,1-tris(hydroxymethyl)ethane, monitored by ^{19}F NMR with 1-fluoronaphthalene as an internal standard

8.4.4. Effect of cross-coupling under air

All reactions were performed under an inert nitrogen atmosphere, using standard Schlenk-line techniques. To see if the reaction needed to be kept under nitrogen, a reaction under air was set up in parallel to one under nitrogen, **Graph 8.4.4.1**. This showed that productive catalysis stalled under air, showing the need for the reaction to be conducted under nitrogen.

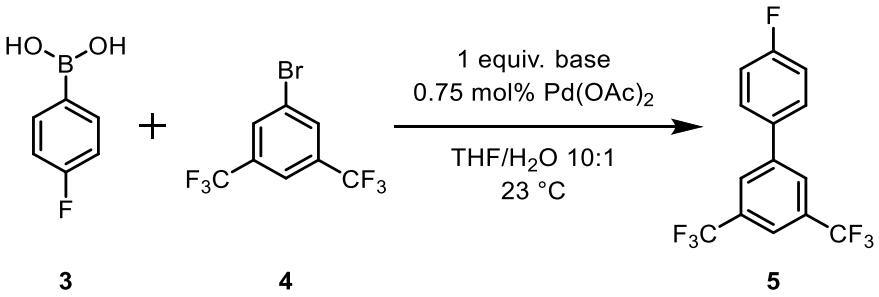

3 **4** **5**

Scheme 8.4.4.1 – SM cross-coupling of boronic acid **3** (1 equiv.) with 1,3-bis(trifluoromethyl)-5-bromobenzene **4** (1 equiv.) by ^{19}F NMR with 1-fluoronaphthalene as an internal standard

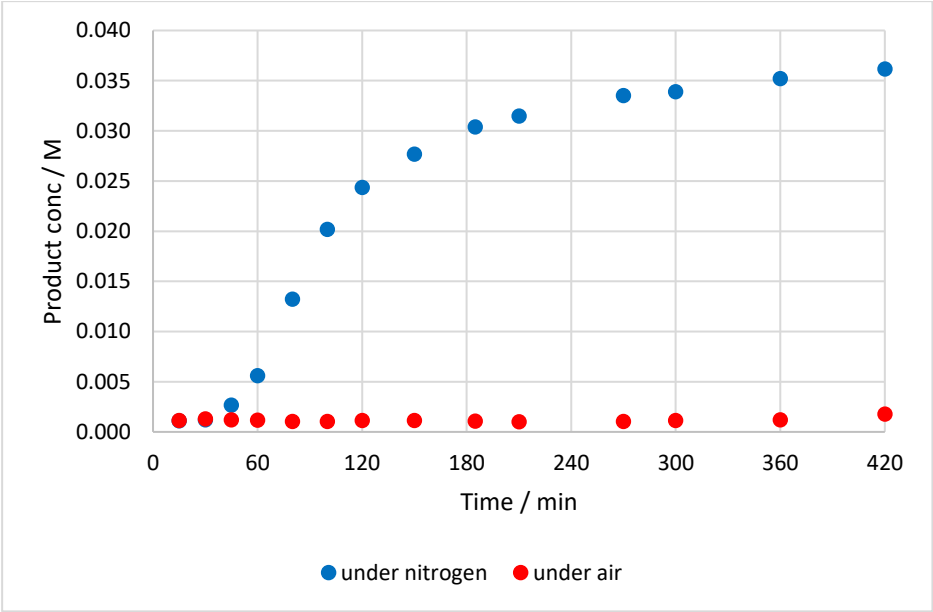

Graph 8.4.4.1 – Product formation in the SM cross-coupling of boronic acid (0.04 M) with 1,3-bis(trifluoromethyl)-5-bromobenzene (0.04 M) monitored by ^{19}F NMR with 1-fluoronaphthalene as an internal standard – reaction under nitrogen vs reaction under air

Chapter 5

8.5.1 Boronic acid + guanidine – to 1 equiv. guanidine

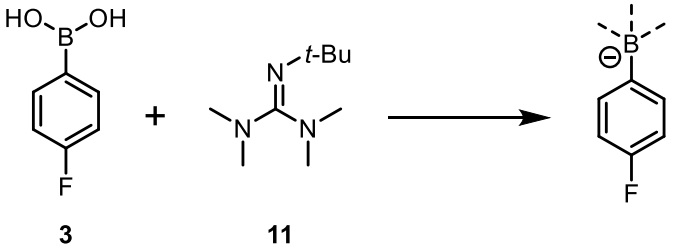

3 11

Scheme 5.2.1 – Boronic acid **3**/guanidine **11** adduct formation

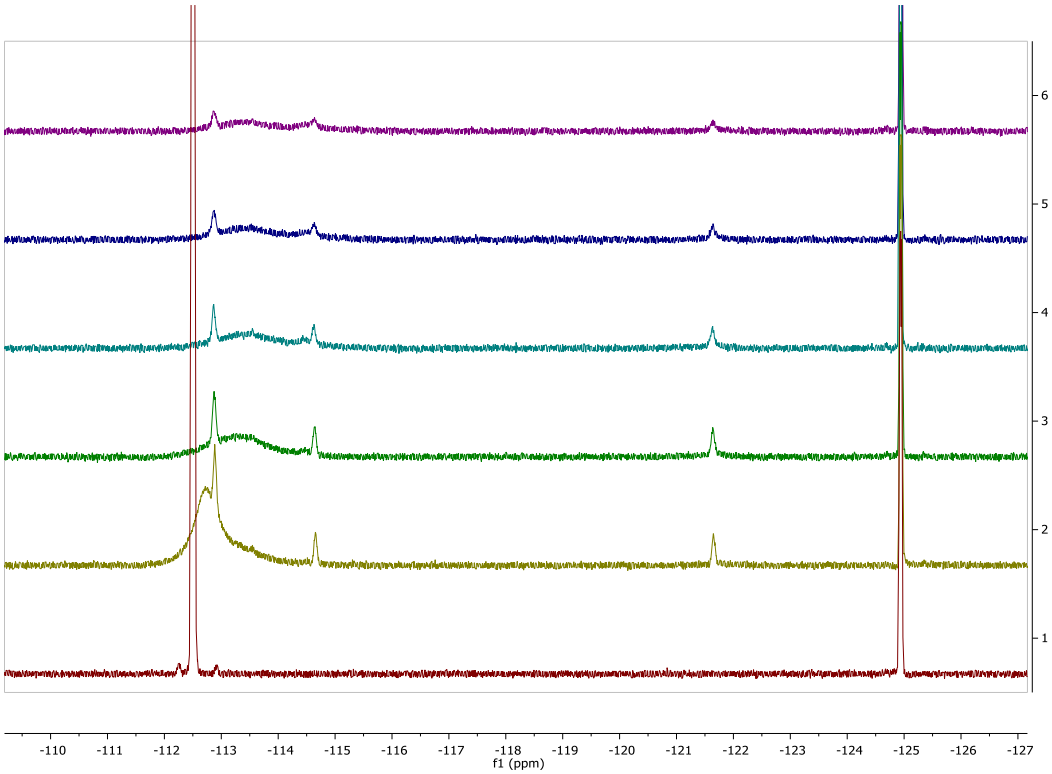

Fig 8.5.1.1 – Boronic acid **3** + guanidine **11** – to 1 equiv. guanidine **11** (top spectrum) in steps of 0.2. ^{19}F NMR, 300 K, 10:1 THF/water, with 1-fluoronaphthalene as an internal standard (−125 ppm)

8.5.2. NMR spectra for boronate formation using KOH

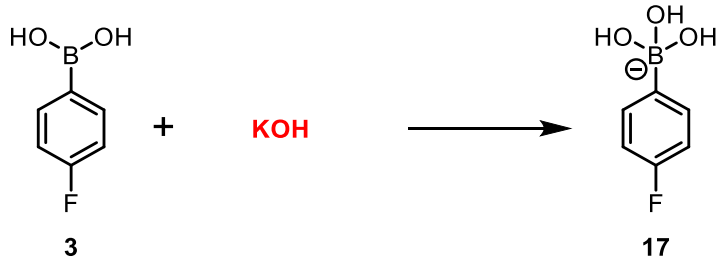

3 **17**

Scheme 5.3.1 – Boronate **17** formation using KOH

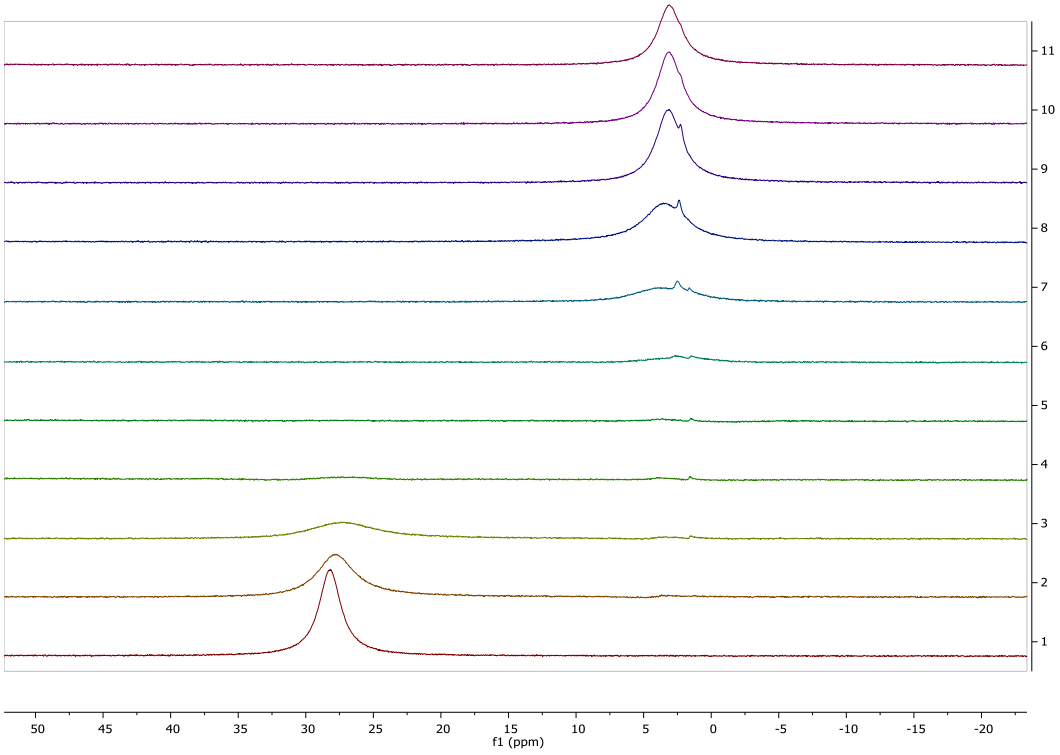

Fig 8.5.2.1 – Boronic acid **3** + KOH – to 2 equiv. KOH (top spectrum) in steps of 0.2. ^{11}B NMR. 300 K, 10:1 THF/water.

8.5.3. Glycol ester boronate formation

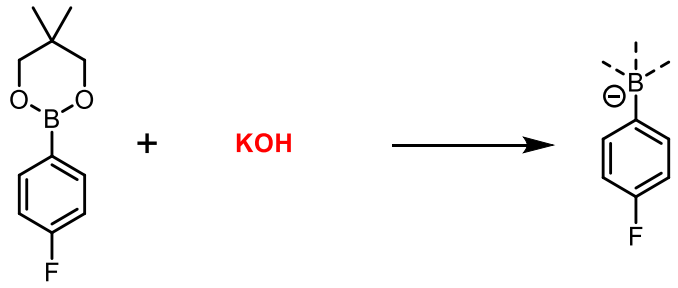

2

Scheme 8.5.3.1 – Glycol ester **2** + KOH

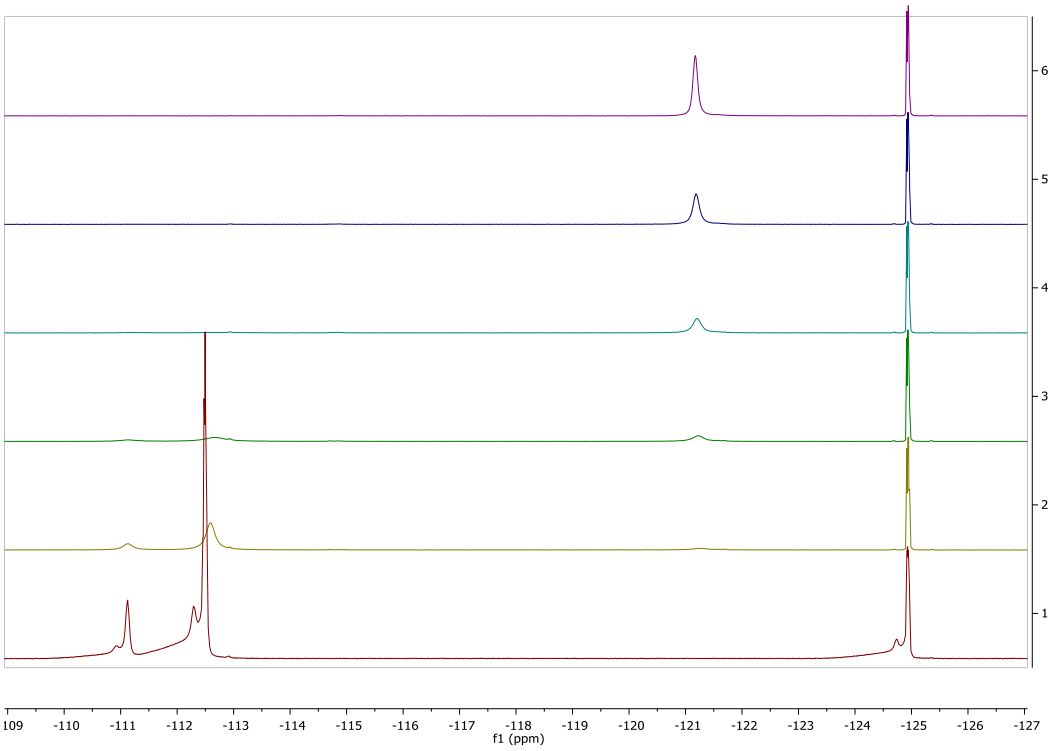

Fig 8.5.3.1 – Glycol ester **2** + KOH – to 1 equiv. KOH (top spectrum) in steps of 0.2. ^{19}F NMR, 300 K, 10:1 THF/water, with 1-fluoronaphthalene as an internal standard (−125 ppm)

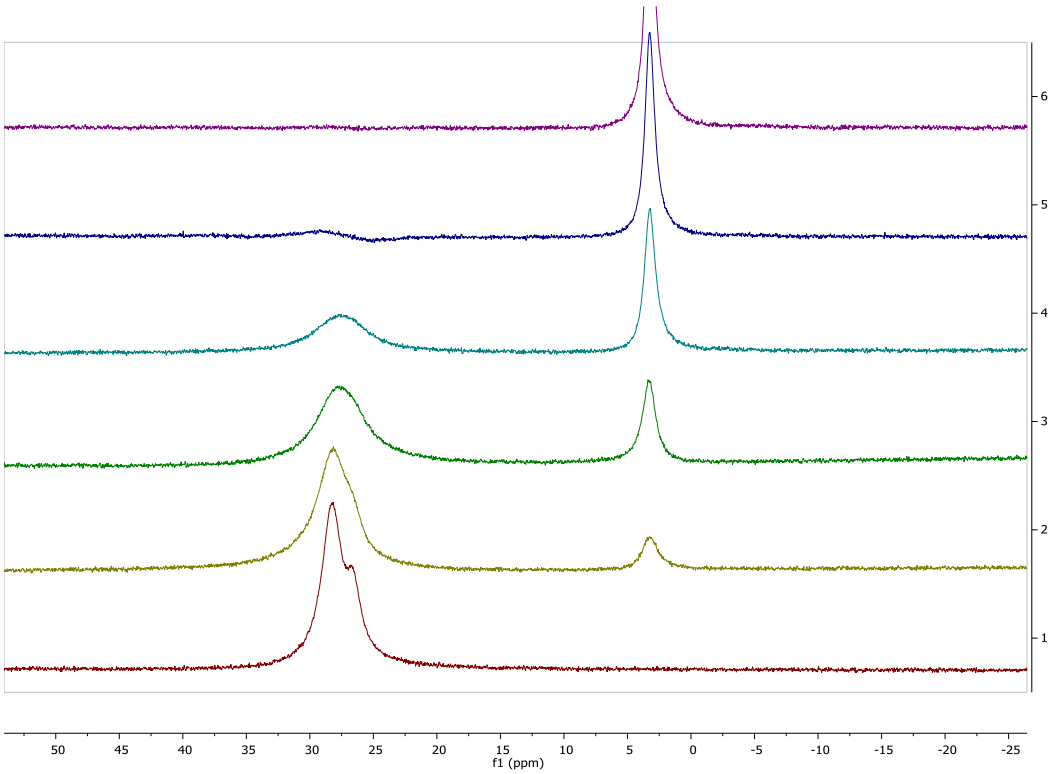

Fig 8.5.3.2 – Glycol ester + KOH – to 1 equiv. KOH (top spectrum) in steps of 0.2. ^{11}B NMR, 300 K, 10:1 THF/water

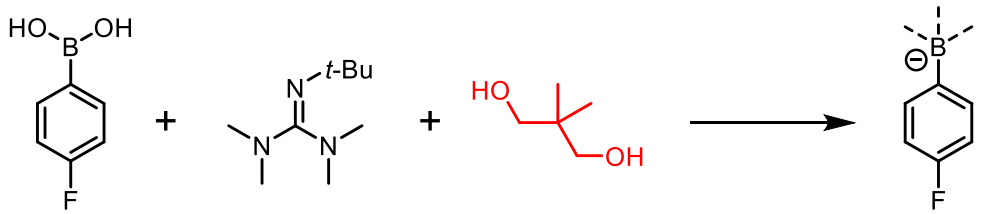

3 **11**

Scheme 5.4.3 – Boronic acid **3** + guanidine **11** – adding glycol

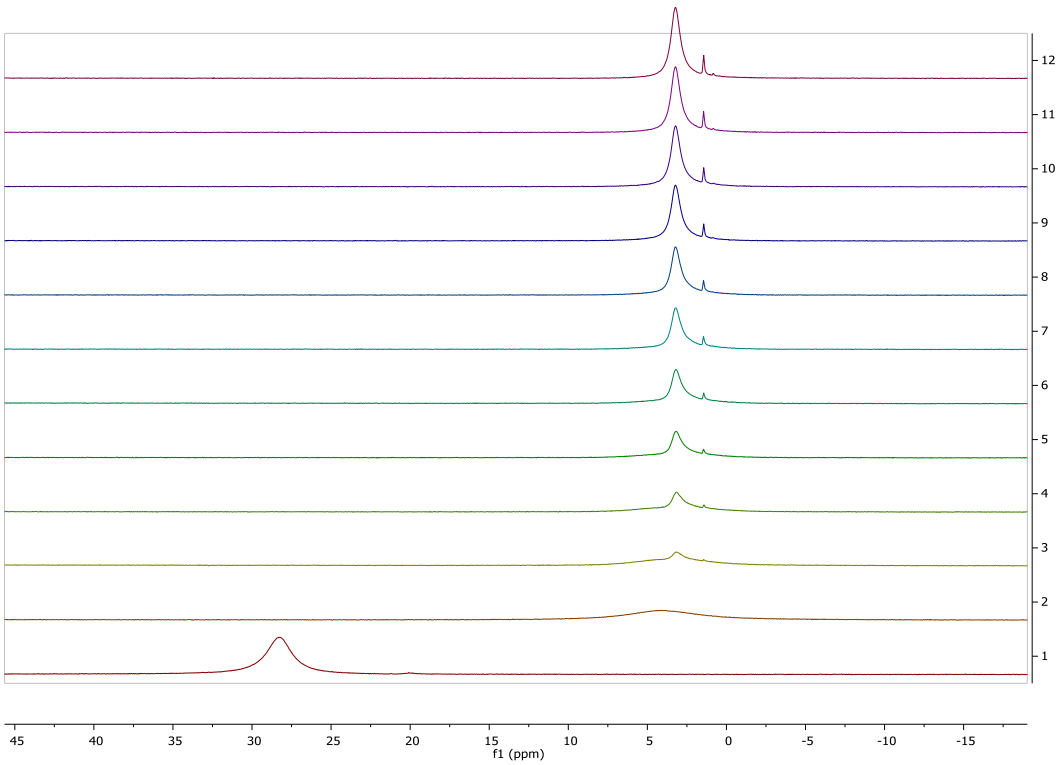

Fig 8.5.3.3 – Boronic acid **3** + 3 equiv. guanidine **11** + glycol – boronic acid **3**, no base (bottom spectrum), addition of 3 equiv. guanidine **11** (spectrum 2), then varying equiv. glycol to 1 equiv. (top spectrum) in steps of 0.1. ^{11}B NMR, 300 K, 10:1 THF/water

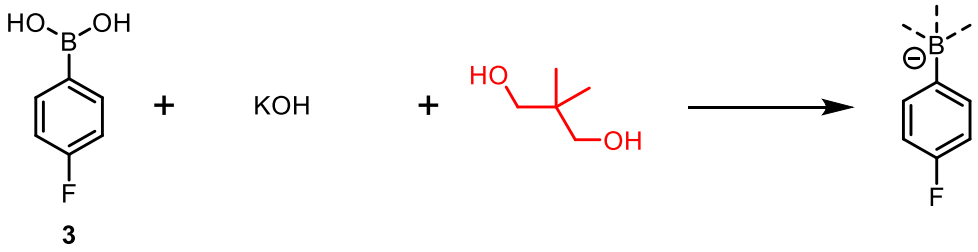

Scheme 8.5.3.2 – Boronic acid **3** + KOH – adding glycol

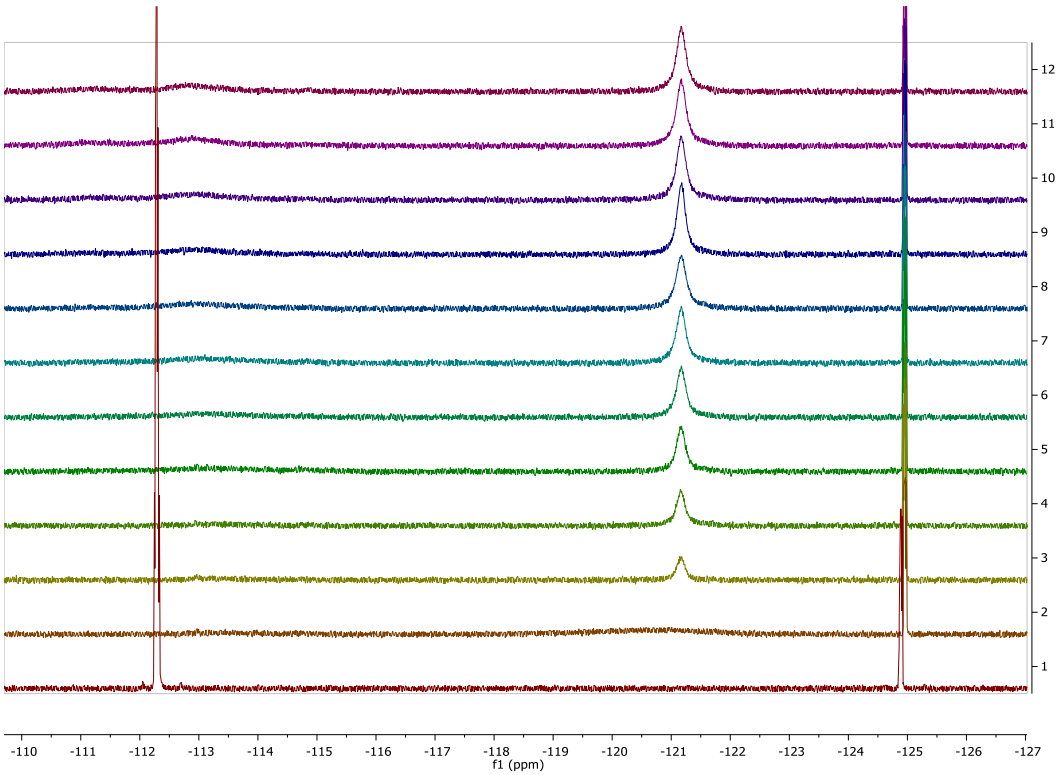

Fig 8.5.3.4 – Boronic acid **3** + 1 equiv. KOH + glycol – boronic acid **3**, no base (bottom spectrum), addition of KOH (spectrum 2), then varying equiv. glycol to 2 equiv. (top spectrum) in steps of 0.2. ^{19}F NMR, 300 K, 10:1 THF/water, with 1-fluoronaphthalene as an internal standard (−125 ppm)

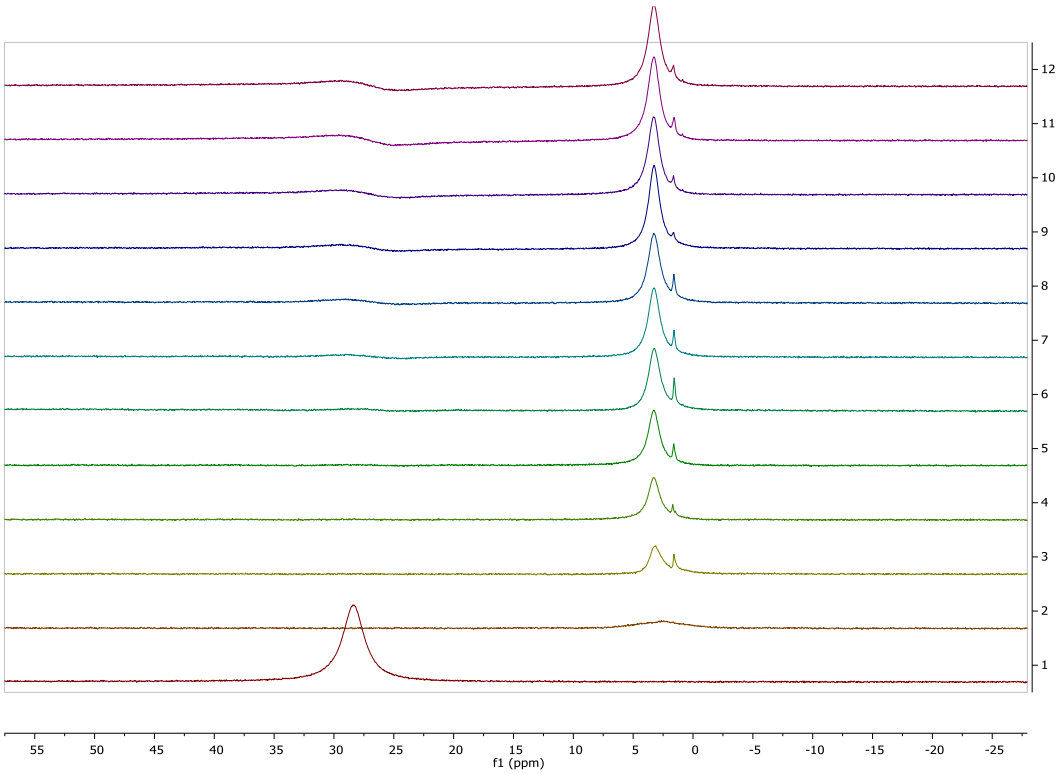

Fig 8.5.3.5 – Boronic acid **3** + 1 equiv. KOH + glycol – boronic acid **3**, no base (bottom spectrum), addition of KOH (spectrum 2), then varying equiv. glycol to 2 equiv. (top spectrum) in steps of 0.2. ^{11}B NMR, 300 K, 10:1 THF/water

8.5.4. Pinacol ester boronate formation

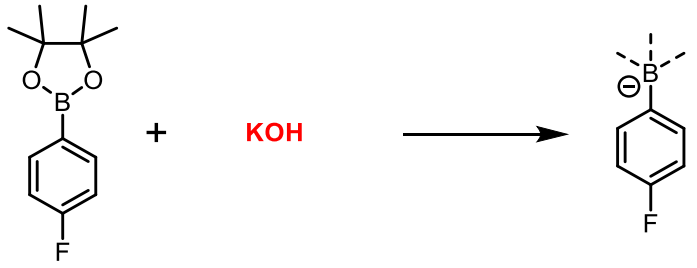

1

Scheme 8.5.4.1 – Pinacol ester **1** + KOH

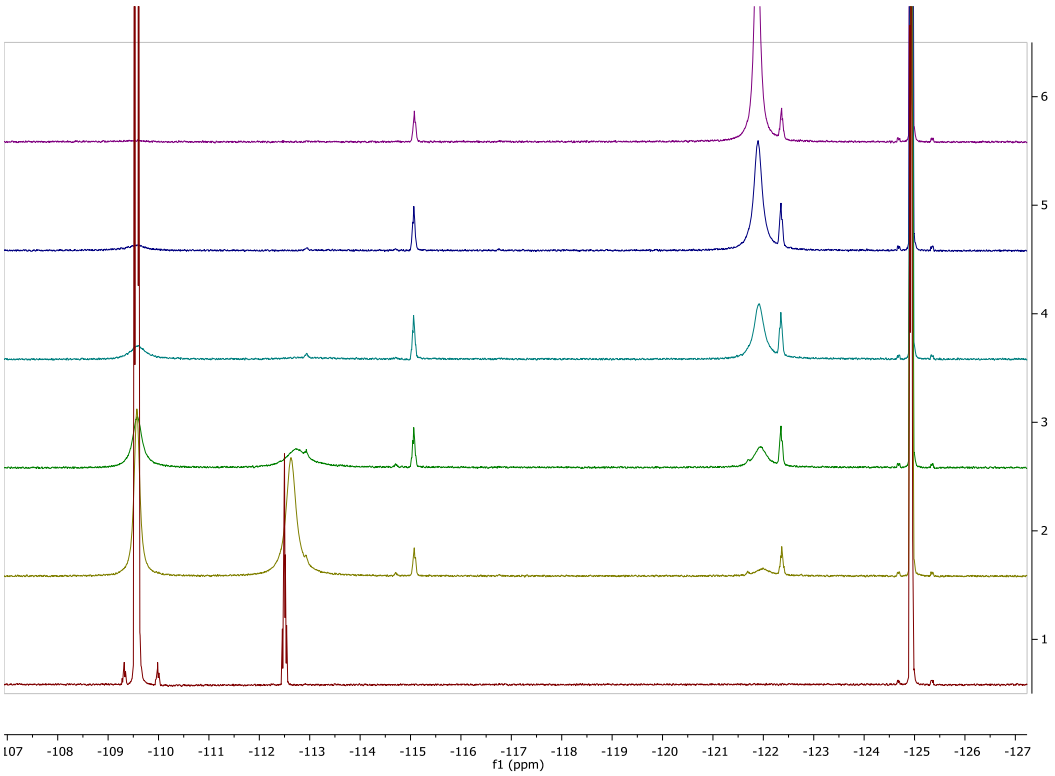

Fig 8.5.4.1 – Pinacol ester **1** + KOH – pinacol ester **1**, no base (bottom spectrum), then to 1 equiv. KOH (top spectrum) in steps of 0.2. ^{19}F NMR, 300 K, 10:1 THF/water, with 1-fluoronaphthalene as an internal standard (−125 ppm)

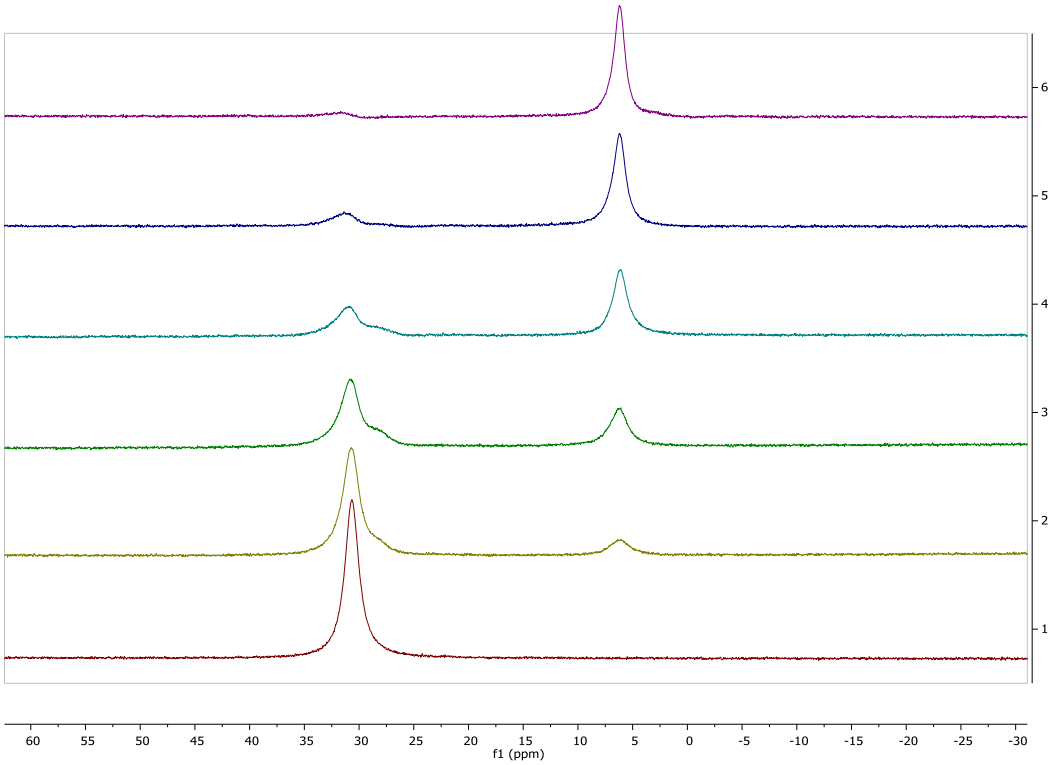

Fig 8.5.4.2 – Pinacol ester + KOH – pinacol ester **1**, no base (bottom spectrum), then to 1 equiv. KOH (top spectrum) in steps of 0.2. ^{11}B NMR, 300 K, 10:1 THF/water,

8.5.5. Boronic acid + K_2CO_3 in 1:1 THF/water

Changing the conditions from 10:1 THF/water to 1:1 THF/water did show more of a change of species with addition of potassium carbonate, **Fig 8.5.5.1**. This shows that potassium carbonate can form a boronate under different conditions where more water is present.

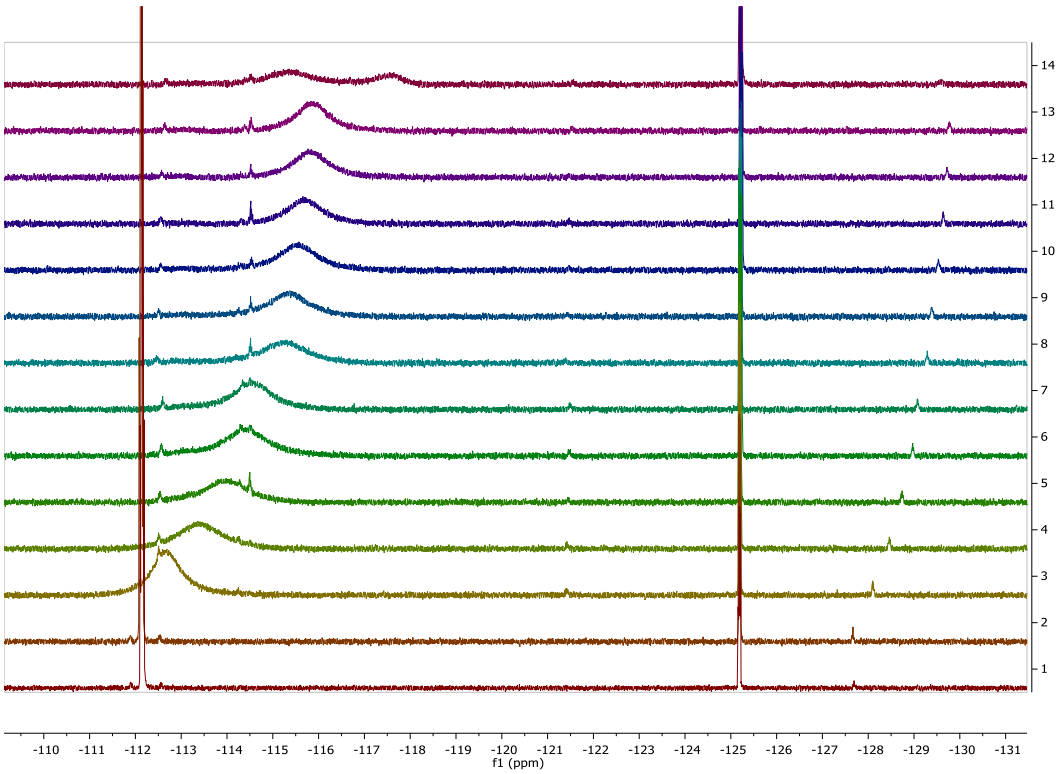

Fig 8.5.5.1 – Boronic acid **3** + K_2CO_3 – 0.2 to 2, 2.5, 3 equiv. K_2CO_3 – 1:1 THF/water. ^{19}F NMR, 300 K, 1:1 THF/water, with 1-fluoronaphthalene as an internal standard (−125 ppm). Small peak at −128 ppm is fluorophenol **8**

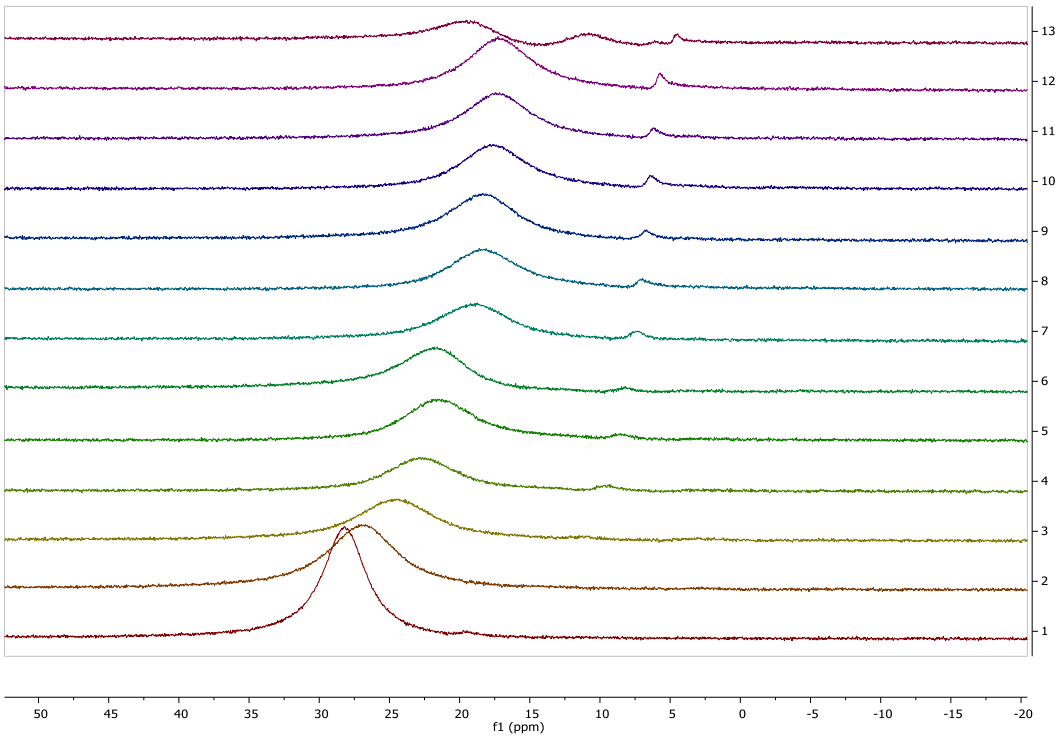

Fig 8.5.5.2 – Boronic acid + K_2CO_3 – 0.2 to 2, 2.5, 3 equiv. K_2CO_3 – 1:1 THF/water. ^{11}B NMR, 300 K, 1:1 THF/water

8.5.6. Boronate formation vary equivalents of different guanidines

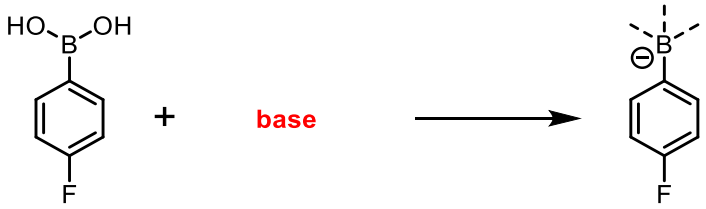

Scheme 5.6.1 – Boronate formation from boronic acid **3** + guanidine **11**/**13**/**14**

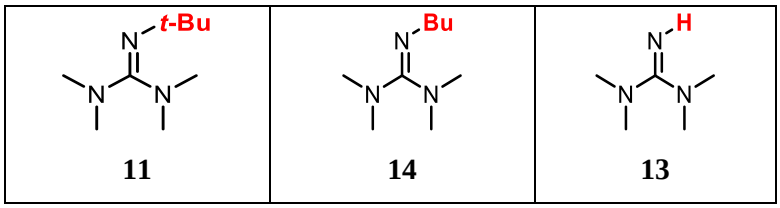

Fig 5.6.1 – Guanidine screening

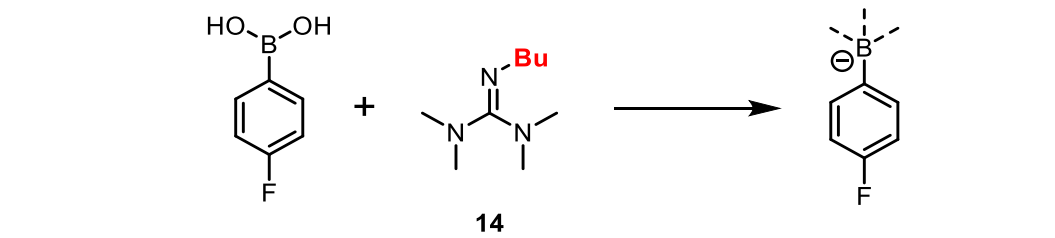

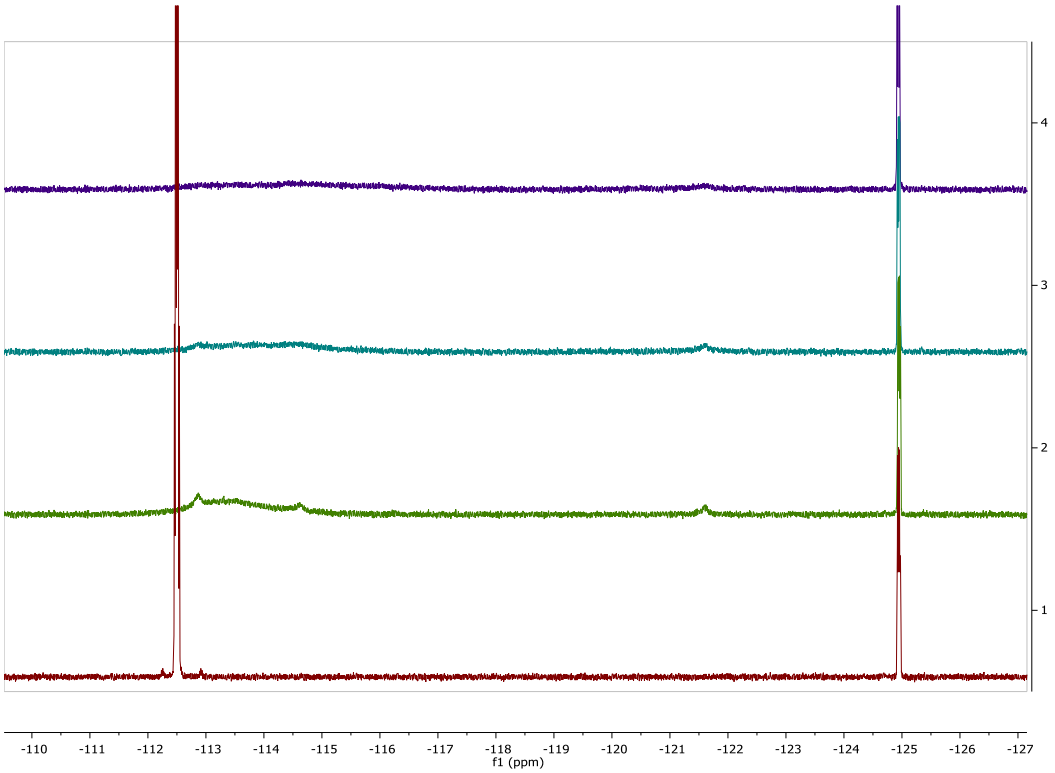

Fig 8.5.6.1 – Boronic acid + *n*-Bu guanidine **14** – 0, 1, 2, 3 equiv. *n*-Bu guanidine **14**. ^{19}F NMR, 300 K, 10:1 THF/water, with 1-fluoronaphthalene as an internal standard (−125 ppm)

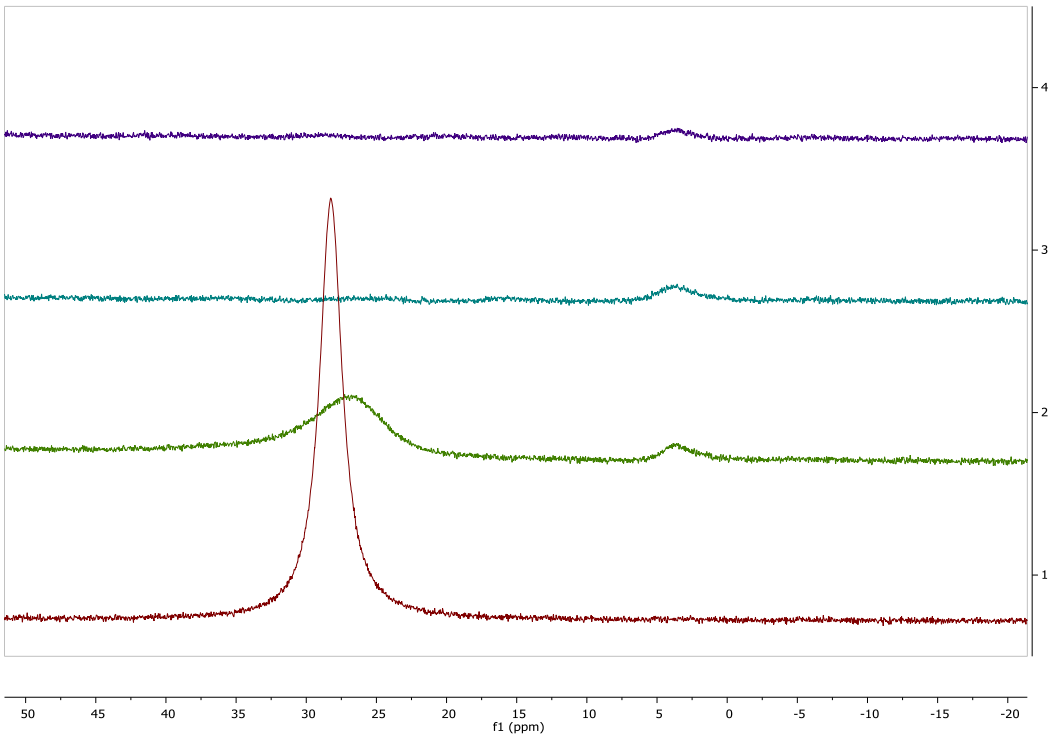

Fig 8.5.6.2 – Boronic acid + *n*-Bu guanidine **14** – 0, 1, 2, 3 equiv. *n*-Bu guanidine **14**. ^{11}B NMR, 300 K, 10:1 THF/water,

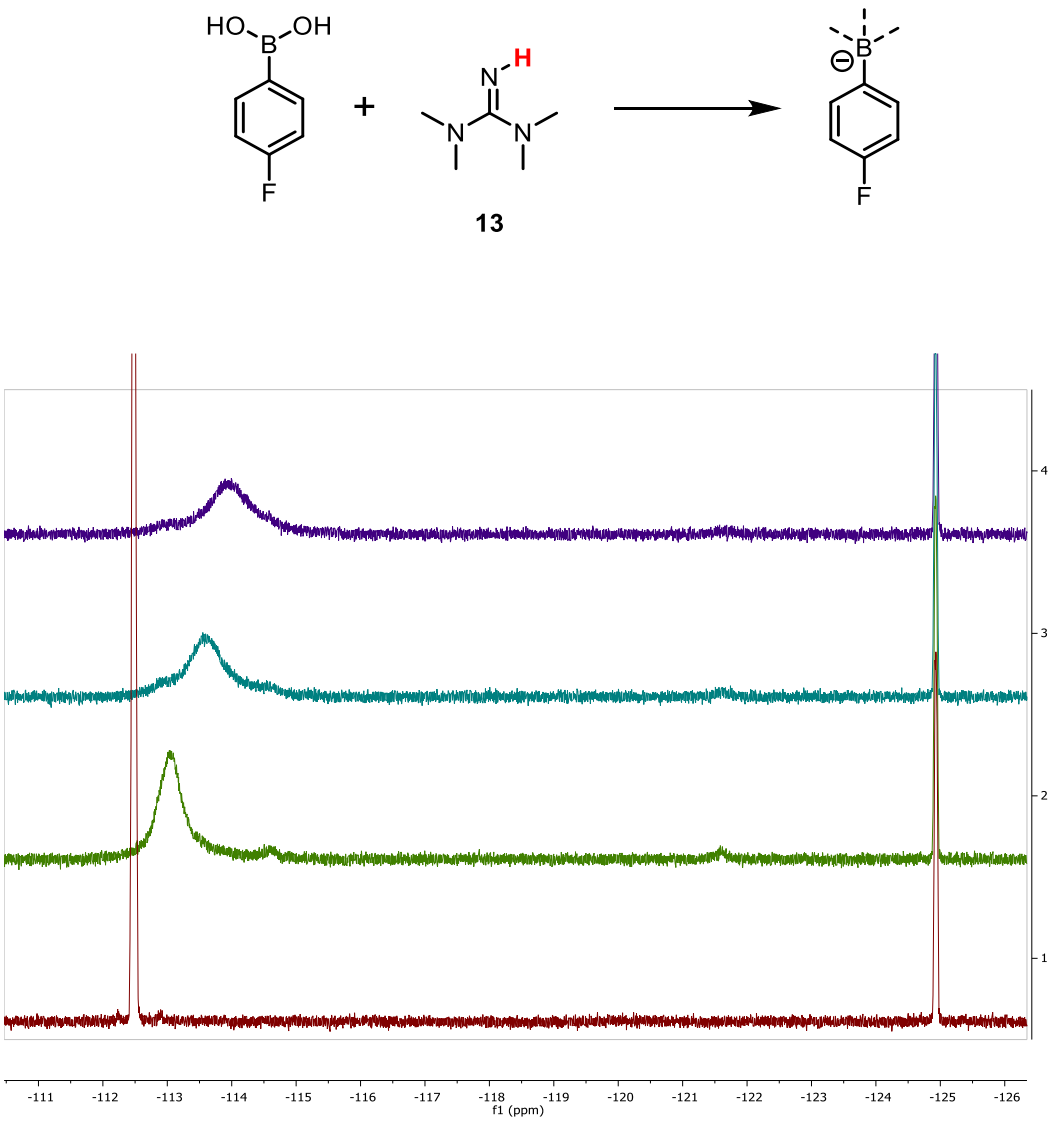

Fig 8.5.6.3 – Boronic acid + NH guanidine **13** – 0, 1, 2, 3 equiv. NH guanidine **13**. ^{19}F NMR, 300 K, 10:1 THF/water, with 1-fluoronaphthalene as an internal standard (−125 ppm)

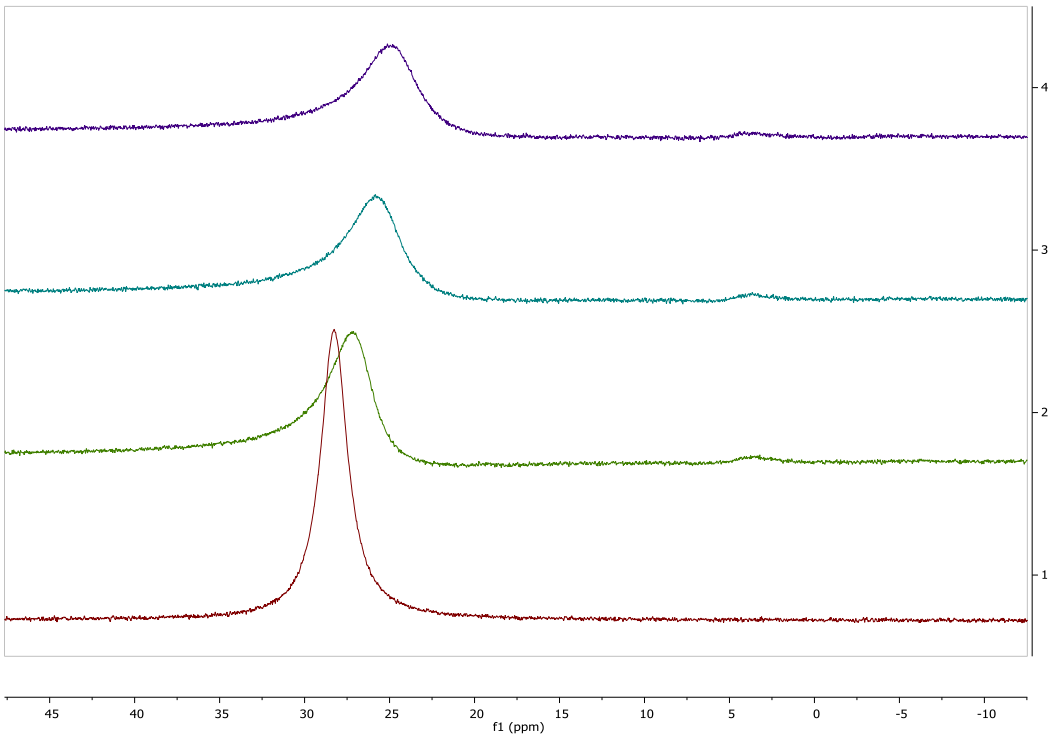

Fig 8.5.6.4 – Boronic acid + NH guanidine **13** – 0, 1, 2, 3 equiv. NH guanidine **13**. ^{11}B NMR, 300 K, 10:1 THF/water,

8.5.7. 2-Fluoroboronic acid boronate studies

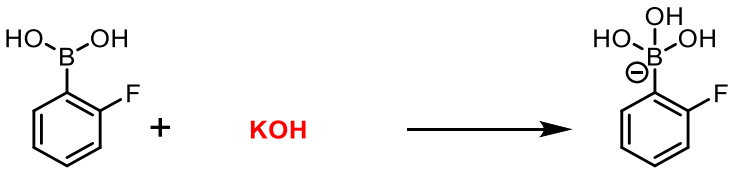

27 **28**

Scheme 5.7.2 – 2-Fluorophenyl boronic acid boronate **28** formation using KOH

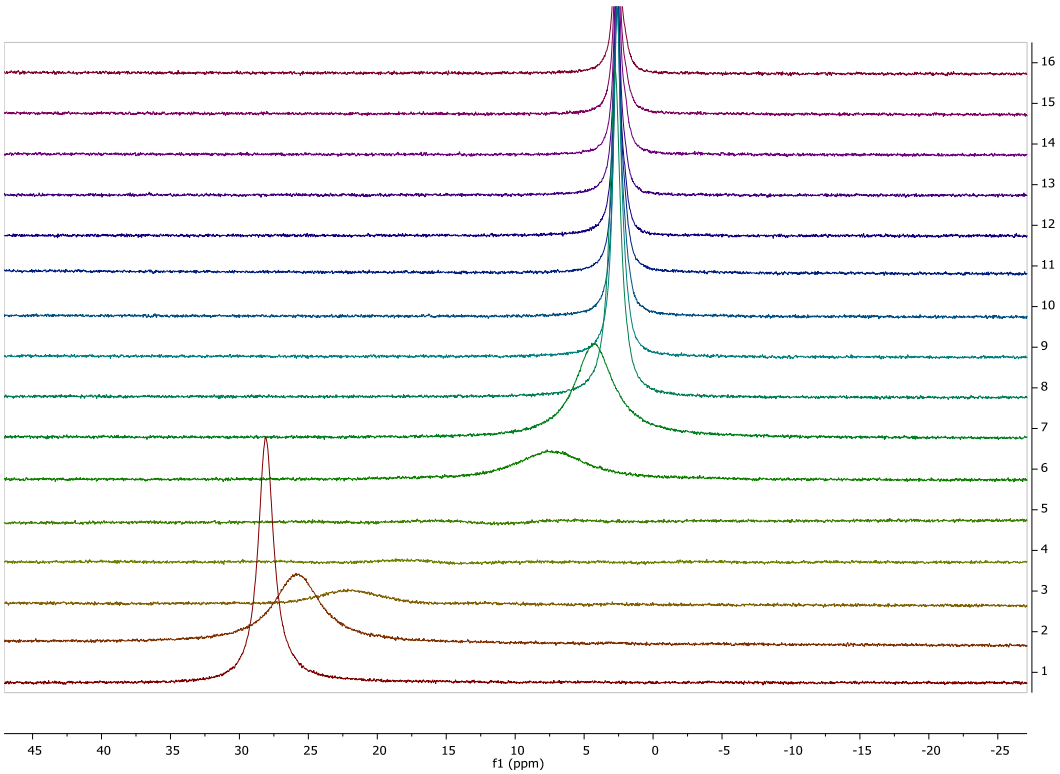

Fig 8.5.7.1 – 2-Fluorophenyl boronic acid **27** + KOH – to 3 equiv. KOH (top spectrum) in steps of 0.2. ^{11}B NMR, 300 K, 10:1 THF/water

8.5.8. 3-Fluoroboronic acid boronate studies

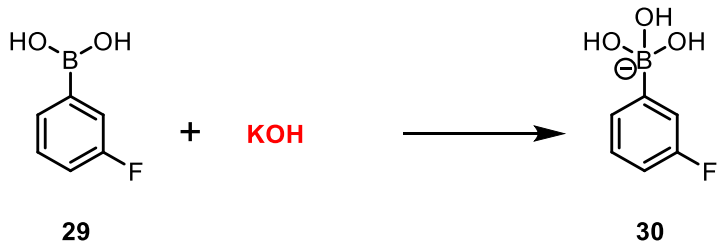

29 **30**

Scheme 5.7.3 – 3-Fluorophenyl boronic acid boronate **30** formation using KOH

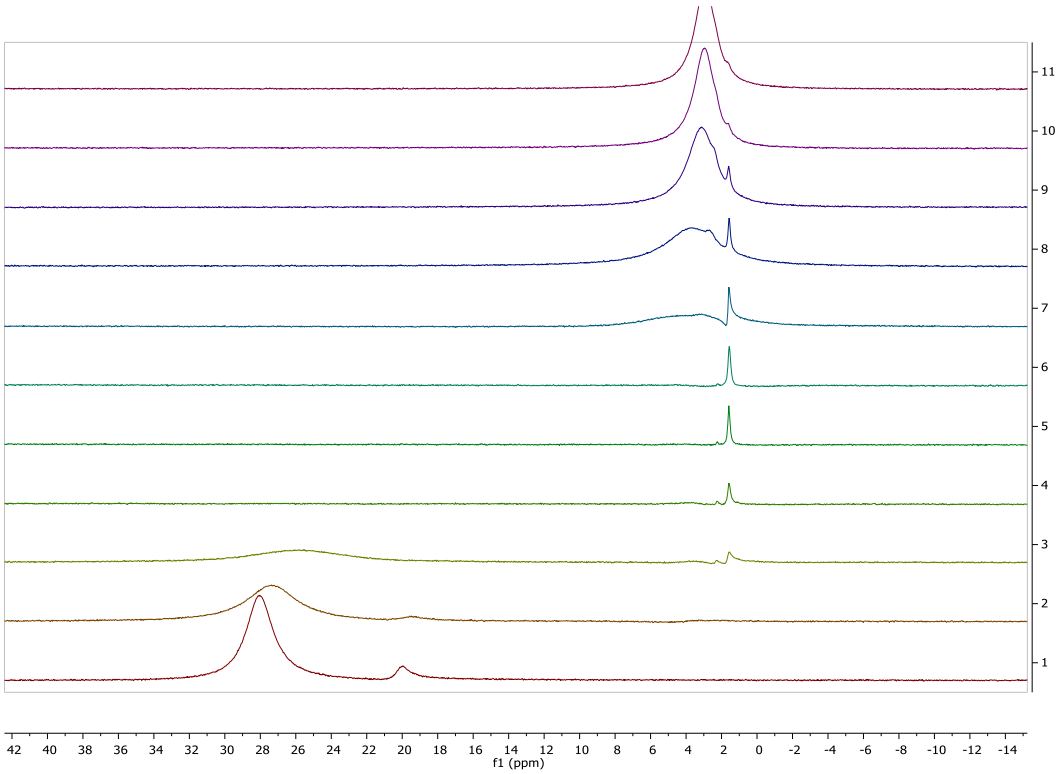

Fig 8.5.8.1 – 3-Fluorophenyl boronic acid **29** + KOH – to 2 equiv. KOH (top spectrum) in steps of 0.2. ^{11}B NMR, 300 K, 10:1 THF/water

8.5.9. Mixed boronic acid boronate studies

3F BA + 4F BA

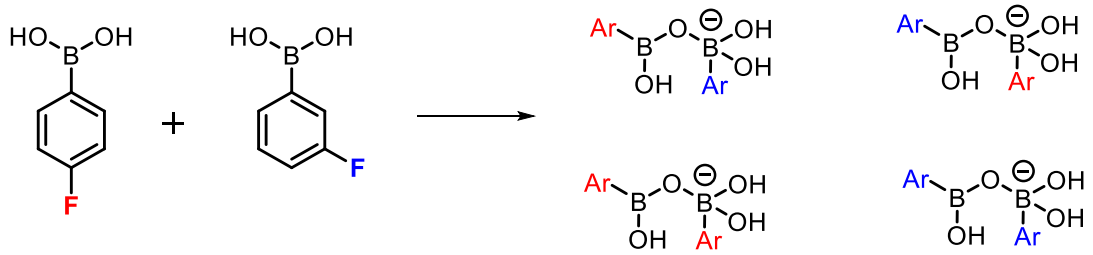

Fig 5.7.7 – Mixed boronic acid studies

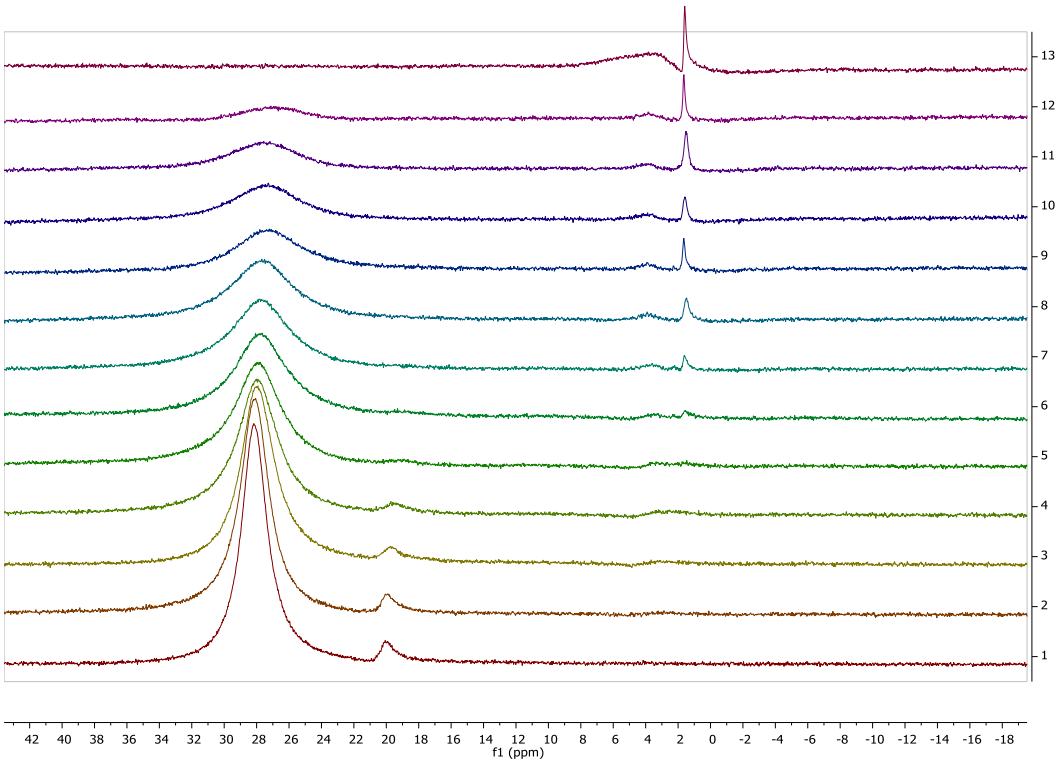

Fig 8.5.9.1 – 3-Fluorophenyl boronic acid **29** (0.02M) + 4-fluorophenyl boronic acid **3** (0.02M) + KOH – vary KOH equiv. to 0.55 in steps of 0.05. Top spectrum = 1 equiv. KOH. ^{11}B NMR, 300 K, 10:1 THF/water

Phenyl BA + 4F

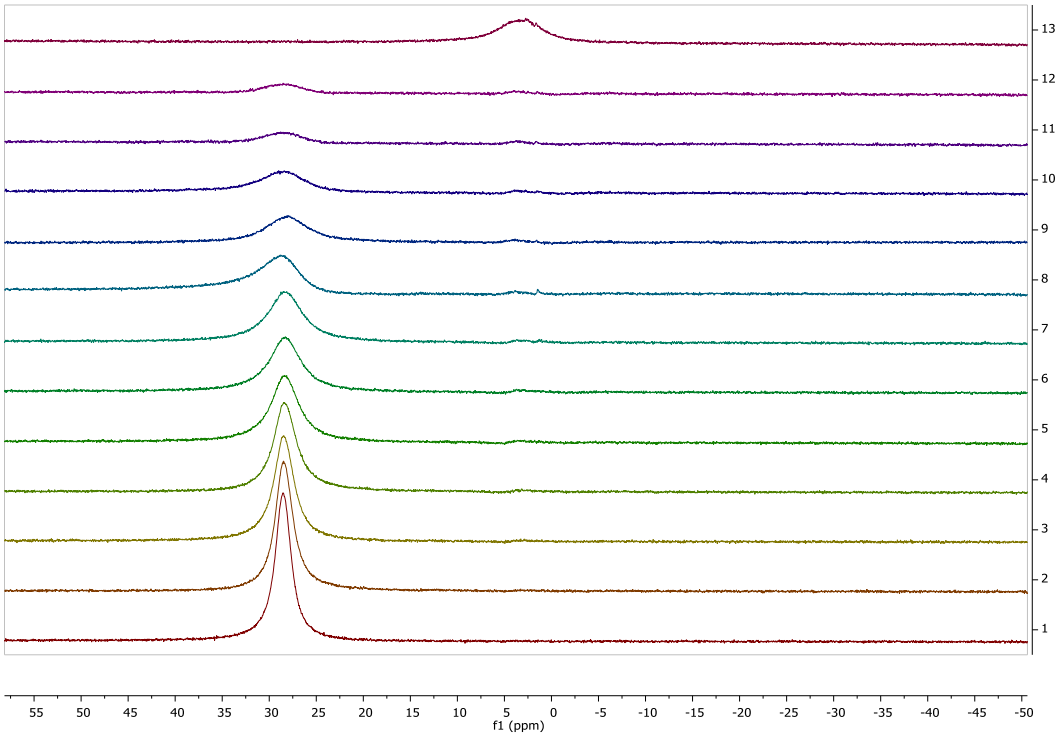

Fig 8.5.9.2 – Phenyl boronic acid **31** (0.02M) + 4-fluorophenyl boronic acid **3** (0.02M) + KOH – vary KOH equiv. to 0.55 in steps of 0.05. Top spectrum = 1 equiv. KOH. ^{11}B NMR, 300 K, 10:1 THF/water